

Studies on the Binding Specificity of Intelectin

by

Amira Ibrahim Aly Khalil

A thesis submitted in partial fulfillment of the requirements for the degree of

Doctor of Philosophy

Department of Chemistry
University of Alberta

© Amira Ibrahim Aly Khalil, 2015

Abstract

Our primary goal of this study was to obtain a better understanding for the carbohydrates binding interactions with human intelectin (hIntL). Studying the binding specificity of hIntL could help in discovering its natural substrate and might give us a clue about its role in the innate immune response as well as its pathophysiological action in various diseases.

In this project, recombinant expression of intelectins was successfully done using HeLa cells and H5V cells. Yeast (*Pachia pastoris*) did not prove to be a promising expression system for hIntL. Using chemical synthesis, compounds (**3.1–3.9**) were obtained to be screened as ligands for hIntL. Herein, we used surface plasmon resonance (SPR) as our analytical tool to study hIntL binding specificity towards various synthesized Gal β -containing oligosaccharides. Staudinger ligation chemistry as well as amine coupling were used to immobilize the carbohydrate epitopes to the SPR biosensor surface. Both hIntL-1 and hIntL-2 were screened against the derivatized surface.

To the soul of my father.

To my mother.

To Amgad, Omar and Habiba.

Acknowledgement

I want to show my gratitude to many people who supported me to achieve my goal and helped me throughout my Ph.D. First I want to thank my supervisor Professor Dr. Todd Lowary for being always supportive and helpful. He guided me a lot during my project through his suggestions and advices. I was really fortunate to be a member in his research group in the past five years.

I want to thank my supervisory committee; Professor Drs. West and Campbell for their support and guidance. Many thanks goes also to Dr. Christopher Cairo for his great help and advices during the binding studies using surface plasmon resonance.

I should not forget also to show my abberiation to Ruixiang Blake, Chun Xia Zou and Gareth Lambkin for teaching me many biological and molecular biology techniques and methods. I want to thank our collaborators in complex carbohydrate research center (University of Georgia, USA) for providing us with the cell line for the protein expression.

I can't forget to thank Dr. Jing Li (a former Ph.D. student in Lowary group). She was very supportive and encouraging when I first started my Ph.D and joined the group. Many thanks to all Lowary group members including former members (Dr. Myles Poulin, Dr. Hashem Taha, and Dr. Michele Richards).

I want also to thank Dr. Maju Joe for his chemistry tips and advices. Dr. Joe was always there to help, advice, and support. I really learned a lot from his

experience as an excellent chemist. Thanks to my friends Claude, Anushka and Dr. Kamar.

I could not have my dream come true without the support I had from my family and friends. Thanks my husband Dr. Amgad Albohy for being always nice, kind, caring, supportive and most of all a great father. Many thanks to my kids Omar and Habiba for their patience and smiles which gave me the energy and motivation to fulfill my goal.

Finally, I want to express my deep appreciation and gratitude to my mother who always meant everything for me. Thanks a lot my mother for your care, advices, support and encouraging. I wish I could be a great mother like my mom. Thanks to all my friends, family members and colleagues, I wish I could mention all the names here.

Table of contents

1. Introduction	1
1.1. Galactofuranose occurrence in natural oligosaccharide structures	2
1.1.1. Mycobacteria.....	3
1.1.2. Bacteria	4
1.1.3. Protozoa	6
1.1.4. Fungi	6
1.2. Galactose-binding lectins.....	8
1.2.1. Galectins	9
1.2.2. Biological function of the dendritic cell-specific intercellular adhesion molecule-3-grabbing non-integrin (DC-SIGN)	11
1.2.3. Discovery of human intelectins.....	14
1.3. Clinical significance of hIntL	32
1.3.1. Infection	32
1.3.2. Cancer	33
1.4. Project objectives	35
1.5. References.....	37
2. Expression and Characterization of Intelectins	58
2.1. Introduction	59

2.1.1.	Recombinant protein expression systems	59
2.2.	Results and discussion.....	60
2.2.1.	Attempts to express intelectin in <i>Pichia pastoris</i>	60
2.2.2.	Intelectin expression in HeLa cells	67
2.2.3.	Intelectin expression in mouse endothelial H5V cell line.....	69
2.2.4.	Characterization of hIntL-1 and hIntL-2.....	69
2.3.	Experimental procedures.....	71
2.3.1.	Preparation of pPIC9/hIntL construct.....	71
2.3.2.	mIntL-2 expression in HeLa cells.....	71
2.3.2.1	Maintenance of HeLa cell line	74
2.3.3.	Intelectin expression in mouse endothelial cells (H5V)	77
ii)	hIntL-1 expression.....	77
iii)	hIntL-1 purification using affinity sepharose 6B column	78
2.4.	Conclusion.....	81
2.5.	References	83
3.	Synthesis of the target oligosaccharides.....	89
3.1.	Introduction	90
3.1.1.	General methods used to obtain Gal β derivatives.....	91
3.2.	Synthetic strategies for the synthesis of the target compound (3.1–3.9).	96

3.2.1.	Synthetic strategy for oligosaccharides containing β -D-Galp-(1 \rightarrow 5)- β -D-Galp and β -D-Galp-(1 \rightarrow 6)- β -D-Galp linkages (3.1–3.4)	97
3.2.2.	Synthesis of compound containing β -D-Galp-(1 \rightarrow 6)- β -D-Glcp (3.7) and β -D-Galp-(1 \rightarrow 6)- α -D-Manp linkages (3.8)	116
3.2.3.	Rationale for the synthesis of compound 3.9 containing α -L-Araf119	
3.3.	Conclusion.....	123
3.4.	General methods.....	123
3.4.1.	General procedure for the deprotection of benzoylated products using Zémpfen conditions	124
3.4.2.	General procedure for the removal of levulinoyl protecting groups	125
3.5.	Experimental procedures.....	125
3.6.	References	178
4.	Binding specificity of intelectins using surface plasmon resonance	187
4.1.	Introduction	188
4.2.	Results and discussion.....	191
4.2.1.	Choice of the biosensor chip and surface functionalization method	191
4.2.2.	Staudinger ligation	193
4.2.3.	Synthesis of NHS-activated phosphine reagent 4.8	196
4.2.4.	Lectin binding	198

4.2.5.	hIntL-1 binding data from Consortium for Functional Glycomics (CFG)	212
4.2.6.	Conclusion	216
4.3.	General Methods	218
4.3.1.	Synthetic procedures	218
4.3.2.	Biosensor surface preparation using amine coupling	224
4.3.3.	Biosensor surface preparation using Staudinger ligation	225
4.3.4.	Detection of lectin binding specificity	225
4.3.5.	Competitive binding experiment with hIntL-1 using SPR	226
4.3.6.	Surface regeneration	227
4.3.7.	Fluorescent labelling of hIntL-1	227
4.3.8.	hIntL-1 screening against pathogen glycan array through CFG	229
4.4.	References	230
5.	Summary and future directions	240
5.1.	Summary	241
5.2.	Future directions	244
5.2.1.	Completion of the binding experiments	244
5.2.2.	Studying the binding interactions using other analytical methods	244
5.2.3.	Expansion of the carbohydrate library and synthesis of more ligands	245

5.2.4. Study structure–activity relationships (SAR) between ligands with high affinity and intelectins	246
5.2.5. Conducting <i>in vitro</i> assays with live bacteria	247
5.3. References.....	248
6. Appendix.....	250
6.1. SPR sensograms for different lectins.	251
Bibliography.....	258

List of Tables

1.1: Structural differences and binding activity of hIntL-1 and mIntL-1.	21
2.1: Eluent gradient and flow rates used in the LC–MS/MS analysis.....	81
4.1: Structure of the carbohydrate ligands immobilized on the corresponding flow channels using Staudinger ligation.....	195
4.2: Lectins used in the study of binding specificities	199
4.3: Binding affinities (K_D) of ConA towards compounds 3.1 , 3.2 , and 4.4	202
4.4: Binding affinities (K_D) of WGA towards compounds 3.1 , 3.2 , and 4.4	204
4.5: IC_{50} of D-ribose and 2-deoxy-D-ribose.	213
4.6: Names and structures from a 48-member glycan array of bacterial LPS molecules that exhibited binding with hIntL-1.	216

List of Figures

1.1: Equilibration between open chain D-galactose, D-galactopyranose (Galp), and D-galactofuranose (Galf).....	3
1.2: Schematic diagram of the mycobacterial cell wall.....	4
1.3: Linkages of the galactan fragment of the arabinogalactan chain.....	4
1.4: Galf-containing LPS of: a. Escherichia coli K-12, b. Klebsiella pneumoniae.....	5
1.5: Sulfated trisaccharide repeating unit of <i>Arthrobacter sp.</i>	5
1.6: LPG oligosaccharide myo-inositol structure of <i>Leishmania sp.</i>	6
1.7: Galf-containing glycosylinositol phosphorylceramide in <i>Paracoccidioides sp.</i>	7
1.8: Galactomannan fragment of EPS found in <i>Aspergillus fumigatus</i>	8
1.9: Types of galectins and formation of galectin/carbohydrate lattices.....	10
1.10: Schematic diagram of DC-SIGN structure.	12
1.11: Recognition of Galf–GNPs by both the EB-A2 antibody and DC-SIGN, which elicits inflammatory response.	14
1.12: Amino acid sequence alignment between hIntL-1, hIntL-2, mIntL-1, and mIntL-2.....	22
1.13: Schematic diagram showing the cellular localization of hIntL in the villi of the small intestine.	28
1.14: Protection of cellular surface glycans by intelectin shield in the innate immune system.....	30
1.15: Complement pathways: classical, lectin and alternative pathways... ..	31

2.1: Structural details of the pPIC9 vector.....	60
2.2: Primers used for hIntL-1 gene subcloning into pPIC9 vector.....	61
2.3: hIntL-1 gene.....	61
2.4: (i): DNA gel of PCR products for 1 ng DNA, (ii): 5 ng DNA a, c: IntL-H ₆ , b, d: H ₆ -IntL.....	62
2.5: (i); PCR products before enzyme digestion, a, b: IntL-H ₆ , c, d: H ₆ -IntL, (ii); e: pPIC9, f: digestion with EcoRI, g: NotI, h: EcoRI, NotI, and SAP...	63
2.6: a: Double digested template DNA, b: circular vector.....	64
2.7: Map of pJET1.2/blunt cloning vector (MBI Fermentas).....	65
2.8: (i); IntL-H ₆ (ii); H ₆ -IntL.....	66
2.9: SDS-PAGE of mIntL-2 after purification using Ni-NTA column.....	68
2.10: SDS-PAGE for hIntL-1 and hIntL-2.....	70
2.11: Human intestinal lactoferrin receptor amino acid sequences with matched peptides shown in bold red.....	71
3.1: Structures of the target compounds (3.1–3.9).....	90
3.2: Structures of azido-octyl acceptors 3.41 and 3.42.....	102
3.3: Linkages of galactan chain in the mycobacterial cell wall.....	104
3.4: Structure of disaccharides 3.1 and 3.2.....	105
3.5: Structures of disaccharides 3.5 and 3.6.....	110
3.6: Structures of disaccharides 3.7 and 3.8.....	115
3.7: Structure of compound 3.9.....	118

3.8: Structural similarity between D-galactose and L-arabinose.....	118
3.9: a: model of major allergen Art V 1, b: compound 3.73	119
3.10: Compound 3.4 as an example for the assignment of protons and carbons in each residue.....	123
4.1: Schematic diagram illustrating SPR spectroscopy.....	188
4.2: SPR sensogram showing the association, dissociation and regeneration phases.....	189
4.3: The structures of amine-containing carbohydrate epitopes 4.1 , 4.2 and 4.3	192
4.4: Immobilization of the amine carbohydrate epitopes to the CMD surface using amine coupling.....	193
4.5: Biosensor surface modification using Staudinger ligation.....	194
4.6: Structure of α -D-Manp. Hydroxyl groups that are essential for binding to ConA are shown in bold.....	198
4.7: Structural features of furanosyl sugars that interact with ConA.....	198
4.8: ConA (serial concentrations) over FC-1.....	200
4.9: SPR sensogram of ConA after subtraction RU of FC-1 from the RU of the reference (FC-4).....	200
4.10: Binding isotherm of ConA (0-100 μ g/mL) using C1 carbohydrate- derivatized biosensor chip.....	201
4.11: WGA (serial concentrations) over FC-1 (compound 3.1: (1 \rightarrow 5)-linked-Galf disaccharide).....	202

4.12: SPR sensogram of WGA after subtraction RU of FC-1 from the RU of the reference (FC-4).....	203
4.13: Binding isotherm of WGA using C1 carbohydrate-derivatized biosensor chip.....	204
4.14: PNA (serial concentrations) over FC-3 (4.4, lactose).....	205
4.15: SPR sensogram of hIntL-1 after subtraction RU of FC-1 from the RU of the reference (FC-4), showing maximum response units (RU _{max}) and response units at equilibrium (RU _{equilibrium}).....	207
4.16: Binding isotherm of hIntL-1 using C1 chip when single site binding model was applied (Equation 4.1).....	208
4.17: Binding isotherm of hIntL-1 using C1 chip when equation 4.2 was applied.....	209
4.18: IC ₅₀ curve of D-ribose.....	212
4.19: IC ₅₀ curve of 2-deoxy-D-ribose.....	212
4.20: Structures of compounds 3.4 and 3.7	214
4.21: Structure of Cy5-NHS dye.....	215
4.22: Binding between fluorescently labelled IntL-1 (72 µg/mL) and the corresponding bacterial LPS printed on CFG pathogen array.....	217
5.1: The structures of the synthesized compounds (3.1–3.9).....	241
5.2: Structures of essential building blocks 3.26 and 3.54	242
5.3: Azido-octyl acceptors 3.41 and 3.42	242
5.4: Structure of the proposed compounds 5.1–5.6	246
6.1: SPR sensogram of ConA (serial dilutions) injected over	

FC-2 of C1 carbohydrate-derivatized biosensor chip.....	250
6.2: SPR sensogram of ConA after subtraction RU of FC-2 from the RU of the reference (FC-4).....	250
6.3: SPR sensogram of ConA (serial dilutions) injected over FC-3 of C1 carbohydrate-derivatized biosensor chip.....	251
6.4: SPR sensogram of ConA after subtraction RU of FC-3 from the RU of the reference (FC-4).....	251
6.5: SPR sensogram of WGA (serial dilutions) injected over FC-2 of C1 carbohydrate-derivatized biosensor chip.....	252
6.6: SPR sensogram of WGA after subtraction RU of FC-2 from the RU of the reference (FC-4).....	252
6.7: SPR sensogram of WGA (serial dilutions) injected over FC-3 of C1 carbohydrate-derivatized biosensor chip.....	253
6.8: SPR sensogram of WGA after subtraction RU of FC-3 from the RU of the reference (FC-4).....	253
6.9: SPR sensogram of PNA (serial dilutions) injected over FC-1 of C1 carbohydrate-derivatized biosensor chip.....	254
6.10: SPR sensogram of PNA (serial dilutions) injected over carbohydrate-derivatized biosensor chip.....	254
6.11: SPR sensogram of hIntL-1 (serial dilutions) injected over FC-1 of C1 carbohydrate-derivatized biosensor chip.....	255
6.12: SPR sensogram of hIntL-1 (serial dilutions) injected over FC-2 of C1 carbohydrate-derivatized biosensor chip.....	255

6.13: SPR sensogram of hIntL-1 (serial dilutions) injected over FC-3
of C1 carbohydrate-derivatized biosensor chip.....256

List of Schemes

3.1: Fischer glycosylation reaction.....	91
3.2: Using long chain alcohol in the glycosylation of D-galacturonic acid	92
3.3: Perbenzoylation of galactose under high temperature.....	93
3.4: Base-catalyzed glycosylation of D-galactose.	94
3.5: Synthesis of galactofuranoside 3.19 by iodine-catalyzed cyclization of dithioacetal.....	94
3.6: Reduction of galactonolactone using disiamylborane.	95
3.7: Retrosynthetic route for the synthesis of oligosaccharides (3.1–3.4).....	98
3.8: Synthesis of thioglycoside 3.26 through cyclization of galactose dithioacetal 3.23	99
3.9: Preparation of thioglycoside donors 3.32 and 3.33	101
3.10: Synthesis of 8-azido-1-octanol 3.36	102
3.11: Synthesis of azido-octyl acceptors 3.41 and 3.42	103
3.12: Synthesis of disaccharides 3.1 and 3.2	106
3.13: Synthesis of trisaccharide 3.3	107
3.14: Synthesis of tetrasaccharide 3.4	109
3.15: Retrosynthetic route for the synthesis of 3.5 and 3.6	111
3.16: Synthesis of acceptors 3.55 and 3.57	112
3.17: Synthesis of disaccharides 3.58 and 3.59	113
3.18: Deprotection of disaccharides 3.58 and 3.59 and synthesis of disaccharides 3.5 and 3.6	114
3.19: Synthesis of acceptors 3.66 and 3.70	116

3.20: Synthesis of disaccharides 3.7 and 3.8	117
3.21: Synthesis of L-arabinofuranosyl donor 3.77	120
3.22: Synthesis of acceptor 3.79	120
3.23: Synthesis of compound 3.9	121
4.1: Synthesis of NHS-activated phosphine reagent 4.8	197

List of Abbreviations

AG	Arabinogalactan
BCG	Bacillus Calmette-Guerin
CMD	Carboxymethyl dextran
ConA	Concanavalin A
CRD	Carbohydrate-recognition domain
DCC	Dicyclohexylcarbodiimide
DC-SIGN	Dendritic cell-specific intercellular adhesion molecule-3-grabbing non- integrin
DIAD	Diisopropylazodicarboxylate
DMAP	(dimethylamino)pyridine
DMEM	Dulbecco's modified Eagle's medium
DMPU	Dimethylpropyleneurea
DTT	Dithiothreitol
ECM	Extracellular matrix
EDC	<i>N</i> -ethyl- <i>N'</i> -(3-diethylaminopropyl)- carbodiimide
EPS	Exopolysaccharides
FBS	Fetal bovine serum
FACS	Fluorescence-activated cell sorting
Gal f	Galactofuranose
GFP	Green fluorescent protein

GNP	Gold nanoparticles
hIntL	Human intelectin
HL-1	Human lectin-1
Hyp	Hydroxy-proline
ITC	Isothermal titration calorimetry
LB	Lysogeny broth
Lf	Lactoferrin
LPG	Lipophosphoglycan
LPS	Lipopolysaccharide
MASP	MBL-associated serine proteases
MBL	Mannose-binding lectin
MPM	Malignant pleural mesothelioma
NHS	<i>N</i> -hydroxysuccinimide
NIS	<i>N</i> -iodosuccinimide
NK	Natural killer
PAMP	Pathogen-associated molecular pattern
PBS	Phosphate buffered saline
PCR	Polymerase chain reaction
PG	Peptidoglycan
PNA	Peanut agglutinin
PPh ₃	Triphenylphosphine
RU	Response units
SAP	Shrimp alkaline phosphatase
SBA	Soybean agglutinin

SPR

Surface plasmon resonance

TNF- α

Tumor necrosis factor α

WGA

Wheat germ agglutinin

1. Introduction

1.1. Galactofuranose occurrence in natural oligosaccharide structures

Glycoconjugates are spread widely in many microorganisms as well as mammalian cells. Glycoconjugates play important roles in different biological events¹ including cellular growth,³ differentiation and adhesion.⁴ Glycoconjugates are unique molecules in terms of their structural diversity and complexity.¹

Monosaccharides in the hexopyranosyl form are the main building block of most glycoconjugates. However, the presence of hexofuranosides as a part of glycoconjugates is also known.⁵ The importance of these hexofuranosyl structures comes from their presence in many microorganisms including pathogenic ones, while they are absent in mammals. Many research groups have tried to gain a better understanding of hexofuranose biosynthesis, metabolism, biological importance and their role in pathogenicity.⁶ Hexofuranosides are important constituents in many microorganisms, including bacteria,⁷ protozoa⁸ and fungi.⁹

Galactofuranosyl (Gal_f) residues are the most widely spread hexofuranoses in naturally occurring glycoconjugates (**Figure 1.1**).¹⁰ Herein, my main focus will be directed towards Gal_f oligosaccharides and I will briefly review a few examples of microorganisms containing Gal_f as important constituents in their cell wall architecture.

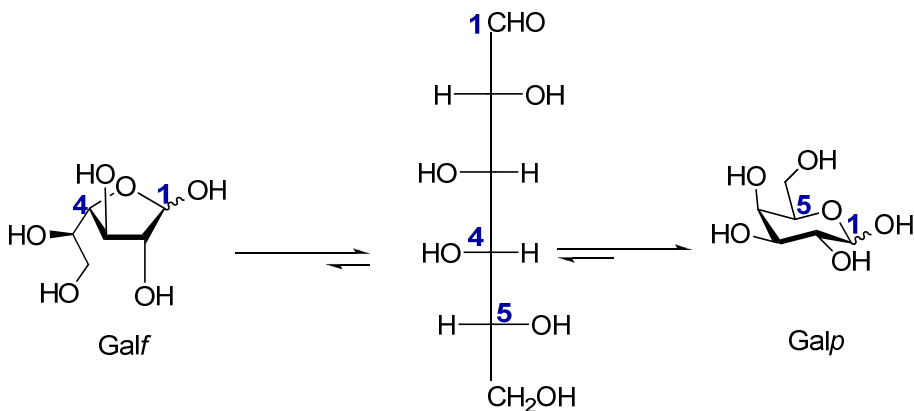


Figure 1.1: Equilibration between open chain D-galactose, D-galactopyranose (Galp), and D-galactofuranose (Galf).

1.1.1. Mycobacteria

Mycobacteria are the causative agent of tuberculosis (TB) and other diseases.^{11, 12} The cell wall architecture of mycobacterial species is very complex and is one of its virulence factors.¹³ The mycobacterial cell wall is composed mainly of mycolic acid and peptidoglycan (PG) layers. The mycolic acids and PG are connected together through an arabinogalactan (AG, **Figure 1.2**). The AG layer is composed of galactose and arabinose sugars both existing in the furanose form.^{7, 14} The AG portion consists of about 30 repeating Galf units, which exist in alternating β -(1 \rightarrow 5) and β -(1 \rightarrow 6) linkages as shown in **Figure 1**. There are three arabinan chains connected to the galactan via an *O*-linkage to the 5 position of a Galf moiety. It is believed that alteration or inhibition of the biosynthetic pathways that are involved in the synthesis of the mycobacterial cell wall could be a target in drug development against infections caused by these organisms.¹⁵

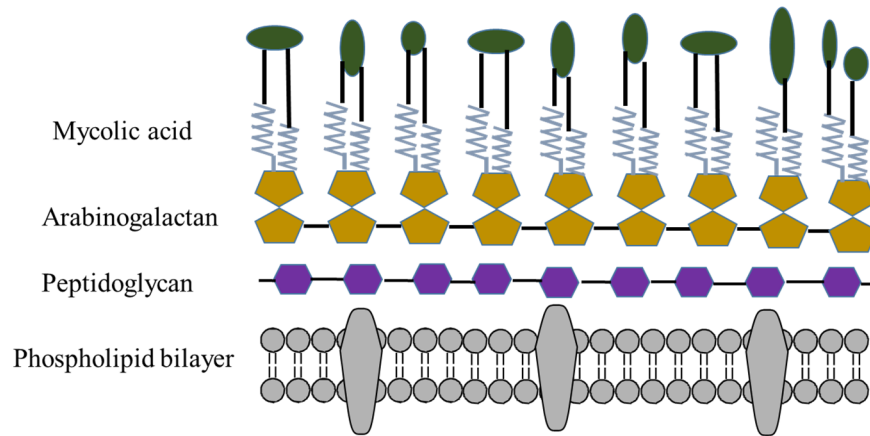


Figure 1.2: Schematic diagram of the mycobacterial cell wall.

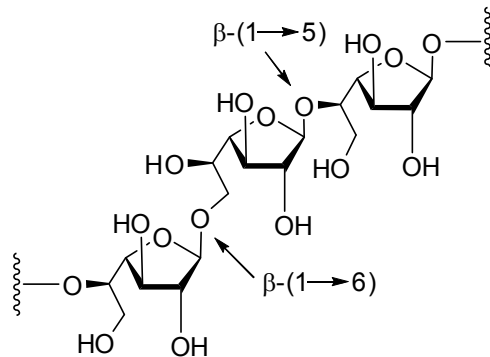
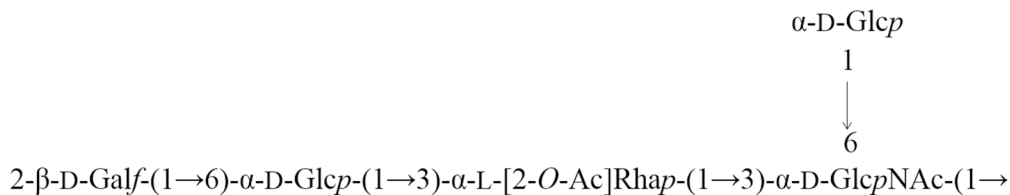


Figure 1.3: Linkages of the galactan fragment of the arabinogalactan chain.¹⁶

1.1.2. Bacteria

Galf units are also found in different glycoconjugates of many bacteria including pathogenic ones and are sometimes important for their virulence.⁵ For example the lipopolysaccharide (LPS) of many Gram-negative bacteria contain Galf units.^{17, 18} Examples are the O-antigens of *Escherichia coli* K-12¹⁹ and *Klebsiella pneumoniae*²⁰ (Figure 1.).

a.



b.



Figure 1.4: Galf-containing LPS of: a. *Escherichia coli* K-12,¹⁹ b. *Klebsiella pneumoniae*.²¹

Another unique Galf-containing structure was isolated from *Arthrobacter sp.* The peptidoglycan–polysaccharide complex isolated from this bacterium was found to contain a sulfated polysaccharide structure. This polysaccharide motif is composed of a repeating trisaccharide unit $[6\text{-}\beta\text{-D-Galf-(1}\rightarrow\text{6)-}\beta\text{-D-Galf-(1)]_n$, which has a $\beta\text{-D-Glcp}$ residue attached to one of the Galf via a $(1\rightarrow2)$ linkage²² (**Figure 1.**). This sulfated trisaccharide was reported previously to have antitumor effects through inhibition of angiogenesis.²³

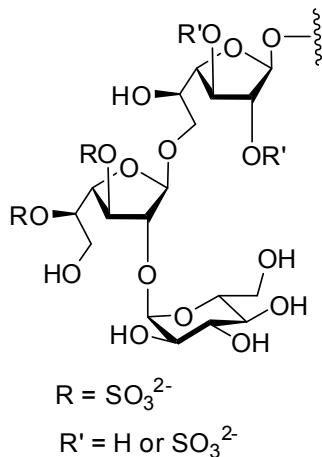


Figure 1.5: Sulfated trisaccharide repeating unit of *Arthrobacter sp.*²²

1.1.3. Protozoa

The most famous Gal β -containing protozoa are *Trypanosoma cruzi*⁸ and *Leishmania major*.²⁴ Both organisms contain an oligosaccharide lipophosphoglycan (LPG), which has a Gal β residue linked to a mannopyranoside residue via a β -(1 \rightarrow 3) linkage²⁵ (**Figure 1**). This LPG was found to be a virulence factor for these protozoa.²⁶

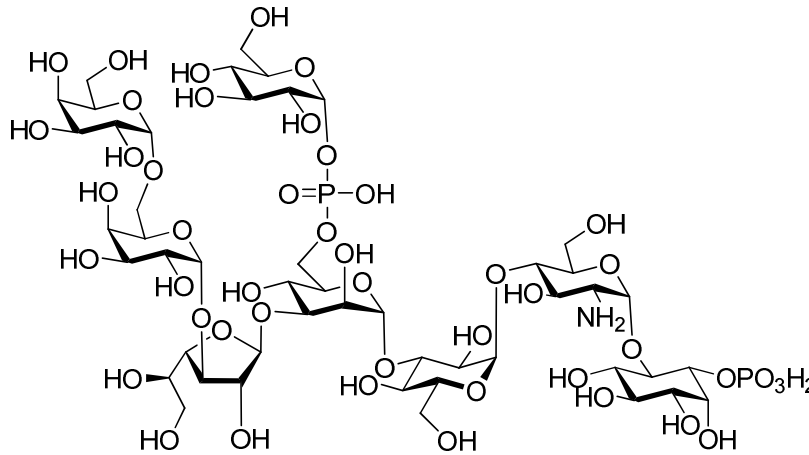


Figure 1.6: LPG oligosaccharide myo-inositol structure of *Leishmania sp.*²⁷

1.1.4. Fungi

An interesting example of a Gal β -containing fungus is *Paracoccidioides brasiliensis*. This fungus is responsible for many fungal infections in South and Central America.¹⁰ It contains a unique glycosylinositol phosphorylceramide moiety that contains Gal β in its structure (**Figure 1**). Due to the antigenic character of this Gal β -containing ceramide derivative, it could be used in various serological tests and is a promising diagnostic marker.²⁸

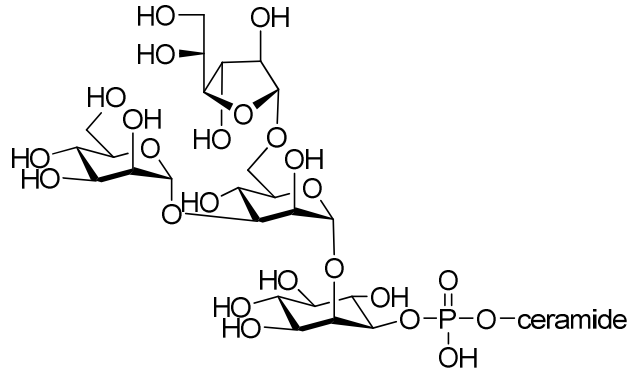


Figure 1.7: Galf-containing glycosylinositol phosphorylceramide in *Paracoccidioides sp.*²⁸

Another Galf-containing fungus is *Aspergillus fumigatus* and related species. The galactomannan structure of its mycelial cell wall was found to contain β -Galf-(1 \rightarrow 5)- β -Galf linkages. Those Galf units are immunodominant epitopes and may play an important role in the antigenicity of this fungus.² It worth mentioning here that the exopolysaccharides (EPS) produced by many fungi including *Aspergillus* and *Penicillium* contain repeating Galf units. The structure of the EPS is composed of (1 \rightarrow 2) and (1 \rightarrow 6) linked α -D-mannopyranosides. This mannopyranoside core chain contains side chains consisting of 5–10 (1 \rightarrow 5) linked β -D-Galf units²⁹ (**Figure 1.**).

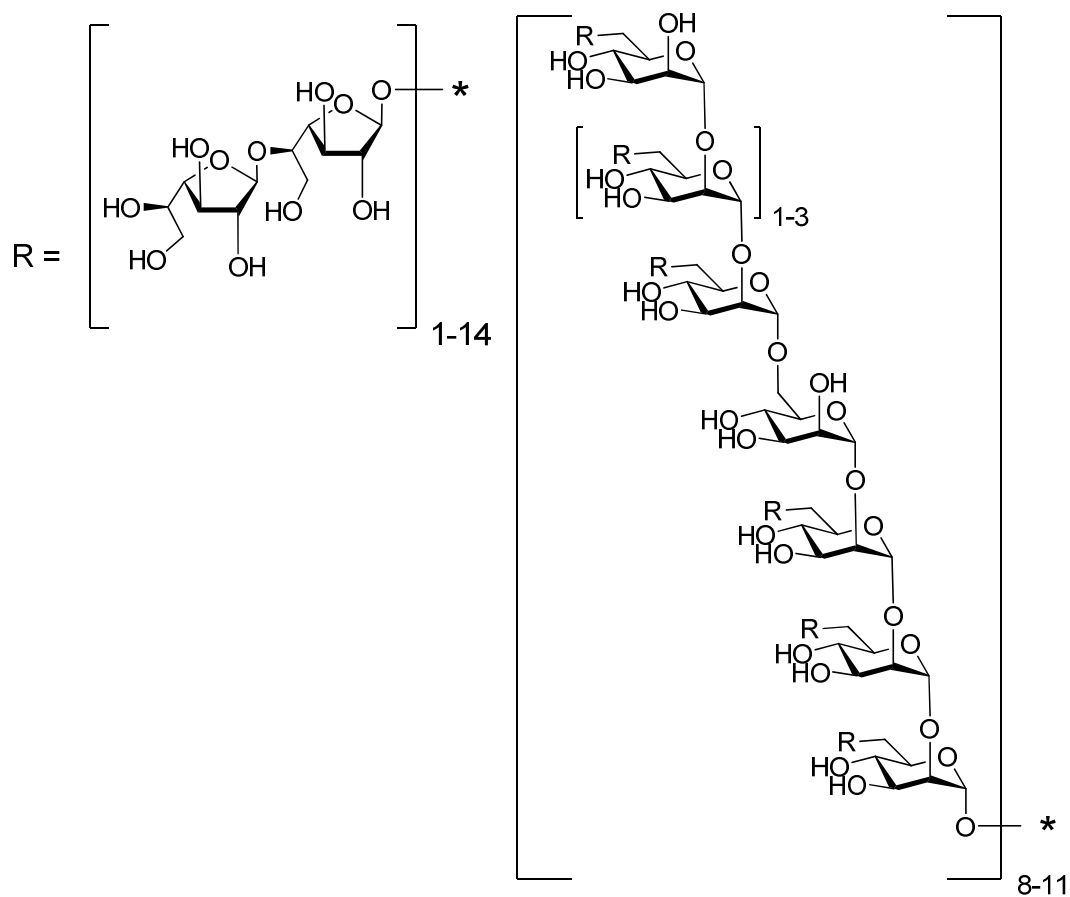


Figure 1.8: Galactomannan fragment of EPS found in *Aspergillus fumigatus*.²

1.2. Galactose-binding lectins

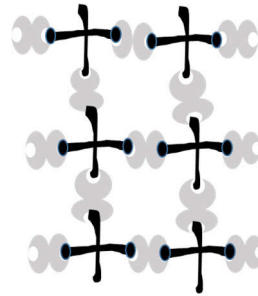
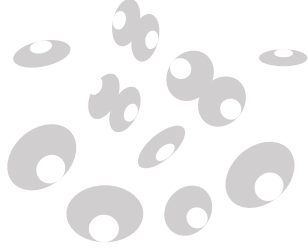
Lectins are carbohydrate-binding proteins that are widespread in plants and animals.³⁰ These proteins play an important role in various biological events including inflammation, cellular growth, cancer and fertilization.³¹⁻³³ Lectins can be classified into different families based on their structure, glycan affinity, function and other factors. Herein, I will briefly highlight lectins with known affinity to galactose in either its pyranose form (Galp) or its furanose form (Galf). In particular, the focus here will be on the galectins, dendritic cell-specific intercellular adhesion molecule-3-grabbing non-integrin (DC-SIGN) and

intelectins. Galectins are a family of lectins with known affinity towards β -Galp.³⁴ Recently, it was shown that human dendritic cells (DC) recognize the other galactose form, galactofuranose (Gal_f) through DC-SIGN lectin.³⁵ In 2001, a human lectin named intelectin was discovered and was reported to show binding affinity towards Gal_f.³⁶

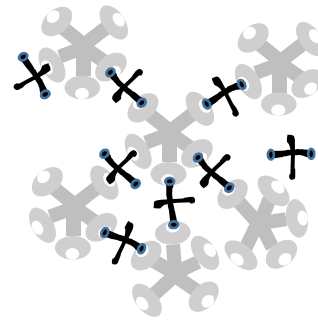
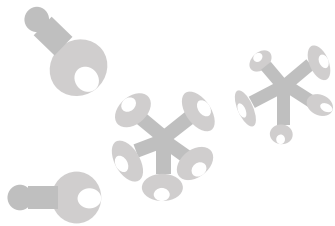
1.2.1. Galectins

Galectins are glycan binding proteins with affinity towards β -galactopyranosides.³⁷ These proteins are defined by the presence of at least one conserved carbohydrate-recognition domain (CRD), which is responsible for glycan binding.³⁸ The galectin family is large, containing 15 members found in mammals as well as microorganisms. Galectins are divided into three main categories, according to the number of CRDs, including: prototypical, chimeric, and tandem type galectins.³⁹ The prototypical galectins (galectin-1, 2, 5, 7, 10, 11, 13, 14 and 15) contain one CRD and hence they are monovalent lectins (**Figure 1.a**). The only chimeric galectin is galectin-3, which contains one CRD (C-terminal domain), an extended domain composed of glycine/proline repeats, and a short N-terminal end⁴⁰ (**Figure 1.b**). The three-dimensional structure of galactin-3 enables it to act as a multivalent lectin. The third type of galectin is the tandem-repeat-type (galectin-4, 6, 8, 9 and 12), which contain two homologous CRDs separated by an amino acid linker (up to 70 amino acids) and therefore they are divalent lectins^{41, 42} (**Figure 1.c**). Galectins are capable of forming higher order structures via non-covalent interactions with glycans.³⁷

a. Prototypical galectins



b. Chimeric type galectin



c. Tandem-repeat-type galectins

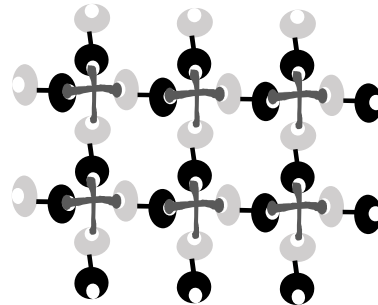
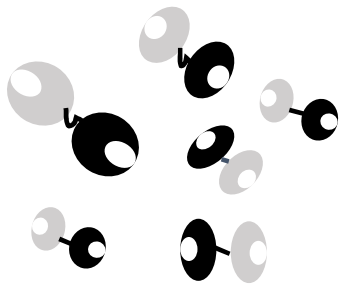


Figure 1.9: Types of galectins and formation of galectin/carbohydrate lattices.

1.2.1.1. Biological function of galectins

Rabinovich *et al*^{43, 44} published two interesting reviews that discuss, in detail, the biological function of the galectin family. Galectins have preferential binding affinity towards the β -Galp-(1 \rightarrow 4)-GlcNAc (LacNAc) motifs that are found in N-

or *O*-linked glycans.⁴⁵ The biological function of galectins can be subdivided according whether they act intracellularly or extracellularly.

Galectins play an important role in the regulation of intracellular processes including cell cycle progression, pre-messenger RNA (mRNA) splicing, apoptosis as well as cellular proliferation.⁴⁶ Galectins exhibit these functions via binding to their ligands inside the cell and initiating protein–protein interactions.⁴⁶ Extracellularly, galectins are important regulators of many cell–cell and cell–matrix interactions.⁴⁷ They bind to β -galactopyranoside containing glycoconjugates in the extracellular matrix (ECM) and molecules responsible for cellular adhesion. Due to this crosslinking function, galectins can regulate different cellular interactions.⁴⁸ Collectively, galectins are important regulators in cellular adhesion, migration and spreading.⁴⁰ Inspired by these important biological effects, researchers have studied galectins as potential targets for the treatment of different pathological disorders including inflammation,⁴⁹ cancer,⁵⁰ and autoimmune diseases.⁵¹

1.2.2. Biological function of the dendritic cell-specific intercellular adhesion molecule-3-grabbing non-integrin (DC-SIGN)

Dendritic cells are potent antigen presenting cells and play a very important role in generating strong immune responses and in maintaining immune homeostasis.⁵² DC-SIGN is a C-type transmembrane lectin receptor, which is mainly expressed on immature DCs found in peripheral tissues as well as on activated mature DCs in the lymph nodes, spleen and tonsils.⁵³ DC-SIGN has gained great attention in the past few years due to its important function as pathogen scavenger receptor.⁵⁴ Besides

acting as an antigen receptor, DC-SIGN also acts as an adhesion and signalling receptor. DC-SIGN is also capable of binding to some endogenous molecules including intracellular adhesion molecules (ICAM)-2, which are found on endothelial cells and ICAM-3 on T lymphocytes, thus playing a role in the migration of DCs across endothelial cells.⁵⁵ It was reported also that DC-SIGN can capture human immunodeficiency virus (HIV-1) and transport it into lymphoid tissues.⁵⁶

The DC-SIGN structure consists of a carbohydrate recognition domain (CRD), a neck-repeat region, a transmembrane domain and a cytoplasmic domain⁵³ (**Figure 1.2**). Tetramerization of DC-SIGN via the neck-repeat domain has a great influence on its binding affinity.⁵⁷

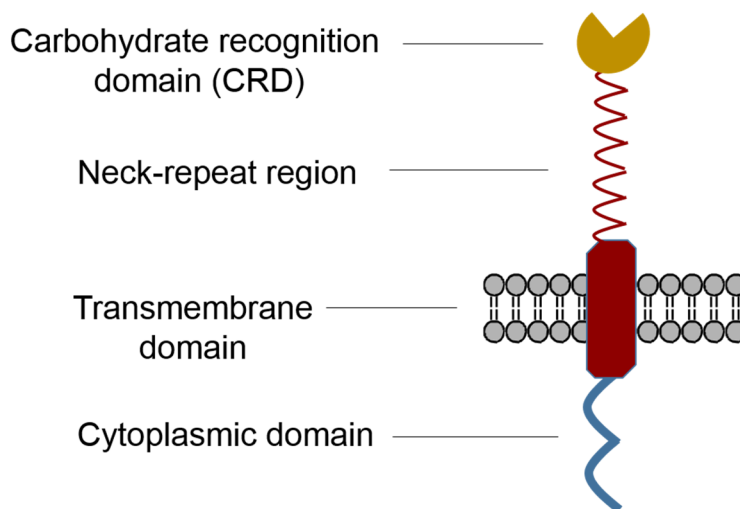


Figure 1.20: Schematic diagram of DC-SIGN structure.

DC-SIGN exhibits binding preferences towards high mannose-type oligosaccharides, but not single terminal mannose residues.⁵³ The minimum number of mannose residues that can be recognized by DC-SIGN is three, usually

located internally in the glycan structure.⁵⁸ Furthermore, DC-SIGN shows high binding affinity for Lewis blood group antigens that contain fucose residues in their structures.⁵⁹ DC-SIGN interacts with either mannose or fucose containing glycans that are found on pathogen surfaces. DC-SIGN shows strong binding ability to *Helicobacter pylori* lipopolysaccharide (LPS) as well as the lipophosphoglycan (LPG) of *Leishmania* sp. Additionally, DC-SIGN binds to the lipoarabinomannan (LAM) of the *Mycobacterium tuberculosis* cell wall. This interaction is found to be mediated through the dimeric and trimeric mannose residues found in the mannose cap of the LAM structure.⁶⁰

Inspired by all these findings, scientists wanted to explore any potential interaction between DC-SIGN and Gal β , which is found in many pathogens. This was the main objective for a study published recently by Tefsen and coworkers.³⁵ To study the role of Gal β in modulating host–pathogen interactions, they synthesized multivalent gold nanoparticles carrying Gal β (Gal β -GNPs) residues on their surface. Interestingly, the authors demonstrated that human DCs recognize Gal β -GNPs through interaction with the lectin DC-SIGN³⁵ (**Figure 1.3**). It was also shown that these Gal β -GNPs were recognized by the EB-A2 antibody, which is used for the diagnosis of Aspergillosis patients. This antibody detects Gal β -containing glycans in patient sera.³⁵

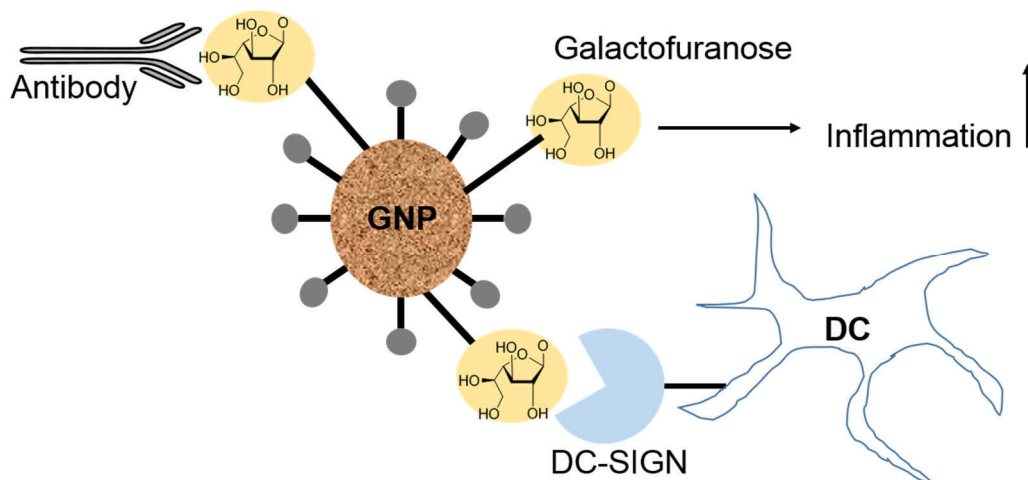


Figure 1.31: Recognition of Galf–GNPs by both the EB-A2 antibody and DC-SIGN, which elicits inflammatory response.

1.2.3. Discovery of human intelectins

As mentioned earlier, Galf residues present in many microorganisms but are absent in mammals. Therefore, Galf residues could play an important role in the virulence of these microorganisms and could initiate an immune response in the host cells.

In 2001, Tsuji *et al*⁶⁶ reported the discovery of a novel human lectin named intelectin (hIntL), also known as the lactoferrin receptor⁶¹ and omentin-1.⁶² The authors proposed that this protein exhibited binding preferences towards Galf residues found in bacterial cell walls. This was the first report of an animal lectin that is able to recognize Galf residues. Also in 2001, another two homologous human lectins were identified by another group,⁶³ which the authors named human lectin-1 (HL-1) and human lectin-2 (HL-2). The degree of similarity between HL-1 and *Xenopus laevis* lectin (XL-35) is 74%.⁶³ HL-1 and HL-2 show 80% identity to each other at the amino acid level. Interestingly, hIntL, which was cloned and

purified by Tsuji *et al.*,³⁶ showed the same amino acid sequence as that of HL-1. According to the authors,⁶³ the mRNA of HL-1 is expressed in heart, colon, small intestine and thymus. Other human tissues showing HL-1 expression are placenta, spleen and skeletal muscle, but at lower levels.

1.2.3.1. Structural features of human intelectins

In their initial study, Tsuji and coworkers³⁶ identified a novel lectin sequence in human placental tissue. They were able to express the protein in a secreted form from the rabbit kidney cell line RK-13. The unknown lectin was sequenced and the full length sequence was obtained. The sequence of this protein showed a considerable degree of homology with the mouse intelectin and that is why the authors named this protein human intelectin.³⁶ According to the authors³⁶ human intelectin (hIntL) is 120 kDa and 40 kDa protein under non-reducing and reducing conditions, respectively. So, they concluded that hIntL is a homotrimeric protein linked by disulfide bonds. Furthermore, they explained that the mature hIntL in its monomeric structure was calculated to be about 33 kDa, but under reducing conditions the actual size of monomeric hIntL was found to be 40 kDa. The authors attributed this difference in mass to potential glycosylation of the protein. There are two potential sites for *N*-glycosylation, Asn 154 and Asn 163. To confirm the presence of *N*-linked oligosaccharides, the authors treated both recombinant and placental hIntL with *N*-glycanase (an enzyme responsible for cleavage of *N*-linked glycans).⁶⁴ The molecular size of the *N*-glycanase treated hINT was 34 kDa, which is almost the same as the predicted mass of monomeric hINT.

1.2.3.2. Activity of human intelectin and its binding to bacterial glycans

The carbohydrate binding activity of hIntL was first explored by Tsuji *et al.*³⁶ In this work, the authors used various mono and disaccharides to elute hIntL from a galactopyranose–Sephacryl column. All the binding experiments were done in the presence of Ca^{2+} . The results could be summarized as follows: 1) complete elution of the absorbed hIntL from the column was observed using buffers containing 100 mM D-xylose, D-ribose, or 2-deoxy-D-ribose. This means that hIntL has an affinity of less than 100 mM towards those pentose sugars. 2) Elution with 100 mM β -D-galactofuranosyl-(1→4)-2-acetamido-2-deoxy-D-glucopyranose (Gal^f-GlcNAc) resulted in complete elution of the absorbed hIntL, a result similar to that obtained when pentoses were used. On the other hand, only 30% elution occurs when the galactopyranoside analogue of Gal^f-GlcNAc (β -D-galactopyranosyl-(1→4)-2-acetamido-2-deoxy-D-glucopyranose) was used. 3) When 100 mM solutions of galactose, N-acetylgalactosamine or fructose were used, 50% elution occurs. 4) When other hexoses (D-glucose, D-mannose, N-acetylmannosamine, N-acetylmannosamine, L-fucose, D-sorbose and L-rhamnose) were used at the same concentration, hIntL was hardly eluted. Thus, it was predicted that hIntL showed less affinity for those hexopyranoses. 5) No elution of hIntL was observed when melibiose or lactose were used. 6) When 10 mM EDTA was used, hIntL was completely eluted from the column.

The authors concluded from this binding study that hIntL showed the highest binding affinity towards Gal^f-GlcNAc and pentoses, medium affinity to hexopyranoses and Gal^p-GlcNAc, and no affinity to melibiose and lactose.

Furthermore, Ca^{2+} was shown to be essential for hIntL to exert its binding activity towards different sugars. C-type lectins are a family of proteins whose members share homology in their carbohydrate recognition domain (CRDs), e.g. collectins and selectins.⁶⁵ Although the binding activity of hIntL was shown to be Ca^{2+} dependent, this lectin is not considered to be a C-type lectin, due to the lack of a classical CRD. The only functional binding domain in the structure of hIntL is the region from Pro 38 to Val 82, which shares a high degree of similarity with the fibrinogen domain.³⁶

Inspired by the data obtained by Tsuji *et al*,³⁶ which suggested better affinity of hIntL towards Gal β -containing molecules, more efforts were made to explore the specificity of the protein. In particular, the ability of hIntL to bind to different naturally occurring Gal β -containing oligosaccharides was investigated as this binding event might play a role in the host defence mechanism against organisms containing these structural motifs.⁶⁶

Galactofuranosides, which are not present in mammalian tissues, are important antigens.^{2, 67} As outlined above, glycoconjugates containing Gal β residues are present in different microorganisms including pathogenic ones e.g., *Mycobacterium tuberculosis*,⁶⁸ *Streptococcus oralis*,⁶⁹ *Nocardia rubra*,⁶⁷ *Leishmania major*,⁷⁰ *Trypanosoma cruzi*,⁷⁰ *Aspergillus fumigatus*² and *Cladosporium resinae*.⁷¹

The cell wall architecture of both *Nocardia* and *Mycobacteria* contains a unique arabinogalactan structure (**Figure 1.**, above), which is rich in Gal α residues. This molecule could therefore play a role in the initiation of an immune response in the host.^{72, 73} In 2001, it was reported that hIntL has affinity to *Nocardia* arabinogalactan.³⁶ Furthermore, in 2009 it was shown that human intelectin-1 (hIntL-1) could bind to *Mycobacterium bovis* Bacillus Calmette-Guerin (BCG).⁶⁶

1.2.3.3. Human intelectin (hIntL) homologues (X-Lectin family)

Intelectins belong to a family of lectins known as the X-lectins. X-lectins were named after the first discovered member of the family, *Xenopus laevis* oocyte granule lectin (XL-35). X-lectin family members come from various origins including frog, human, mouse, sheep and lamprey.⁷⁴ These lectins exhibit a high degree of amino acid sequence homology and share what is known as a fibrinogen-like motif, which is thought to be involved in carbohydrate recognition.⁷⁵ The exact binding specificities and biological function of X-lectins are not fully understood. In general, the X-lectin family might play a role in pathogen recognition and participate in the innate immune system of the host.

1.2.3.3.a. *Xenopus laevis* oocyte granule lectin (XL-35)

The first characterized lectin member belonging to the X-lectin family was *Xenopus laevis* oocyte granule lectin XL-35. In 1997, Lee *et al*⁷⁶ cloned and expressed the cDNA of XL-35. The lectin binds to various monovalent and polyvalent glycans containing D-galactopyranosides; the binding was Ca²⁺ dependent.⁷⁷ Although,

carbohydrate binding by XL-35 requires Ca^{2+} , the predicted amino acid sequence does not contain the C-type lectin motif.⁷⁶ Under non-reducing conditions, the molecular weight of XL-35 is 500 kDa.⁷⁸ It was suggested that XL-35's native structure consisted of a dodecamer, as under reducing conditions the mass of the XL-35 monomer was 45 kDa.⁷⁹ Because the XL-35 lectin was the first identified lectin among its homologs, Lee *et al*⁷⁴ proposed the name X-lectin for those proteins homologous to XL-35. A characteristic feature of the X-lectin family is the presence of a fibrinogen-like domain. This domain is found in a region that shares the highest degree of sequence homology among the members of X-lectin family.⁷⁴

The ficolin/opsonin family⁷⁵ is another lectin family that contains this fibrinogen-like domain. Ficolins activate the complement pathway and play an important role in host innate immunity. Ficolins recognize pathogen-associated molecular patterns (PAMP), which are carbohydrate motifs found on the surface of pathogens, tumors or apoptotic cells.⁸⁰ Because X-lectins have the fibrinogen-like domain found in the ficolin family, it has been suggested that X-lectins could have similar biological roles to those of the ficolin family.⁷⁴

1.2.3.3.b. Mouse intelectin

In 1998, Komiya *et al*⁸¹ isolated a murine cDNA that showed about 61% homology with XL-35. They named this protein intelectin. The expression was mainly found to be specific to the Paneth cells of the small intestine.⁸¹ Because it is expressed in the small intestine, the authors concluded that this protein is an ortholog of hIntL-

2. Furthermore, another mouse cDNA sequence was identified by Pemberton and coworkers.⁸² The later protein was named intelectin-2. Both mouse intelectins (mIntL-1 and mIntL-2) had 92% similarity in their amino acid sequences. It was shown that there was up-regulation of mIntL-2 levels in the jejunum following infection with *Trichinella spiralis*.⁸² The authors concluded that mIntL-2 could play a role in the innate immune response in the mouse against parasitic infections.⁸² In 2007, Tsuji and coworkers⁸³ explored structural differences as well as the activity of human and mouse intelectins. The main results of this study⁸³ are summarized in **Table 1.1**.

Although, hIntL and mIntL are homologous lectins (**Figure 1.4**), they exhibit many differences in their structure and activity. From **Table 1.1**, we can see a difference in the oligomeric structure; whereas hIntL-1 is a homotrimeric lectin, mIntL-1 is monomeric. Also, there are differences in terms of the presence of glycosylation and disulfide linkages. Furthermore, the saccharide binding specificities of both lectins are not same, probably due to structural differences. However, both lectins require Ca^{2+} to bind to various saccharides.⁸³

Table 1.1: Structural differences and binding activity of hIntL-1 and mIntL-1.

	Human intelectin-1 (hIntL-1)	Mouse intelectin-1 (mIntL-1)
Molecular mass	106 kDa homotrimer	34 kDa Monomer
Disulfide linkage	Present (Cys31–Cys48)	Absent
N-linked oligosaccharide	One (Asn163)	Absent
Saccharide binding activity ^a		
1) Galactose	Partially eluted	< 30%
2) 2-deoxygalactose	100% eluted	< 30%
3) 6-deoxygalactose, lactose, melibiose, Galp-GlcNAc ^b	No elution	No elution
4) Galf-GlcNAc ^c	100% eluted	33% eluted
5) Pentoses ^d	> 50% elution	< 30%
Ca²⁺ requirements	Yes	Yes

^a Elution from galactose/sepharose column

^b 2-acetamido-2-deoxy-4-*O*-β-D-galactopyranosyl-D-glucopyranose

^c 2-acetamido-2-deoxy-4-*O*-β-D-galactofuranosyl-D-glucopyranose

^d D-ribose, L-ribose and D-xylose

```

sp|Q8WWA0|ITLN1_HUMAN -----MNQLSFLFLFIATRIGWSTDEAN-----TYFKEWTCSSSPSL 37
sp|Q8WWU7|ITLN2_HUMAN MLMLRLTMTRLCFLFFSVATSGCSAAAASLEMLSRFETCAFSFS-SL 49
sp|Q80ZA0|ITL1B_MOUSE -----MTQLGFLLFIMIATRVCSAAEEN-----LDTNRWGNSEFFSSL 37
sp|O88310|ITL1A_MOUSE -----MTQLGFLLFIMVATRGCSAAEEN-----LDTNRWGNSEFFSSL 37
          *.:* ****: .* *: . : * **

sp|Q8WWA0|ITLN1_HUMAN PRSCKEIKDECPSAFDGLYFLRTENGVIYQTFCDMTSGGGGWTLVASVHE 87
sp|Q8WWU7|ITLN2_HUMAN PRSCKEIKERCHSAGDGLYFLRTKNGVVYQTFCDMTSGGGGWTLVASVHE 99
sp|Q80ZA0|ITL1B_MOUSE PRSCKEIKQEDTKAQDGLYFLRTENGVIYQTFCDMTAGGGGWTLVASVHE 87
sp|O88310|ITL1A_MOUSE PRSCKEIKQEHTKAQDGLYFLRTKNGVIYQTFCDMTAGGGGWTLVASVHE 87
*****: . * *****:***:*****: . *****

sp|Q8WWA0|ITLN1_HUMAN NDMRGKCTVGDWRWSSQQGSKAVYPEGDGNWANYNFTFGSAEAATSDDYKNP 137
sp|Q8WWU7|ITLN2_HUMAN NDMRGKCTVGDWRWSSQQGNKADYPEGDGNWANYNFTFGSAEAATSDDYKNP 149
sp|Q80ZA0|ITL1B_MOUSE NNLGRCTVGDWRWSSQQGNRADYPEGDGNWANYNFTFGSAEATSDDYKNP 137
sp|O88310|ITL1A_MOUSE NDMRGKCTVGDWRWSSQQGNRADYPEGDGNWANYNFTFGSAEAATSDDYKNP 137
*.:**:* *****: . * *****:*****:*****:*****

sp|Q8WWA0|ITLN1_HUMAN GYYDIQAKDLGIWHVPNKSPMQHWRNSLLRYRTDTGFLQTLGHNLFGLIY 187
sp|Q8WWU7|ITLN2_HUMAN GYYDIQAKDLGIWHVPNKSPMQHWRNSALLRYRTNTGFLQRLGHNLFGLIY 199
sp|Q80ZA0|ITL1B_MOUSE GYFDIQAENLGIWHVPNNSPLHTWRNSLLRYRTFTGFLQRLGHNLFGLY 187
sp|O88310|ITL1A_MOUSE GYFDIQAENLGIWHVPNKSPLHNWRKSLLRYRTFTGFLQHLGHNLFGLY 187
**:* **:* *****:***: . **:* ***** ***** *****:.*

sp|Q8WWA0|ITLN1_HUMAN QKYPVKYGEKGCWTDNGPVI PVVYDFGDAQKTASYSPYQGREFTAGFVQ 237
sp|Q8WWU7|ITLN2_HUMAN QKYPVKYRSGKCNWDNGPAIPVVYDFGDAKKTASYSPYQGREFVAGFVQ 249
sp|Q80ZA0|ITL1B_MOUSE QKYPVKYGEKGCWTDNGPAFPVVYDFGDAQKTASYSPSGRNEFTAGYVQ 237
sp|O88310|ITL1A_MOUSE KKYPVKYGEKGCWTDNGPALPVVYDFGDARKTASYSPSGQREFTAGYVQ 237
:***** .****.****:*****:***** *:.**.*:**

sp|Q8WWA0|ITLN1_HUMAN FRVFNNERAANALCAGMRVTGCNTEHHCIGGGGFPEASPQQCGDFSGFD 287
sp|Q8WWU7|ITLN2_HUMAN FRVFNNERAANALCAGIKVTGCNTEHHCIGGGGFFPQGKPRQCGDFSAFD 299
sp|Q80ZA0|ITL1B_MOUSE FRVFNNERAASALCAGVRVTGCNTEHHCIGGGGFFPEFDPEECGDFAAFD 287
sp|O88310|ITL1A_MOUSE FRVFNNERAASALCAGVRVTGCNTEHHCIGGGGFFPEGNPVQCGDFASFD 287
*****:*****:*****:***: . * :***:.*

sp|Q8WWA0|ITLN1_HUMAN WSGYGTHVGYSSSREITEAAVLLFYR 313
sp|Q8WWU7|ITLN2_HUMAN WDGYGTHVKSSCSREITEAAVLLFYR 325
sp|Q80ZA0|ITL1B_MOUSE ANGYGTHIRYSNSREITEAAVLLFYR 313
sp|O88310|ITL1A_MOUSE WDGYGTHNGYSSSRKITEAAVLLFYR 313
.***** * **:* *****

```

Figure 1.42: Amino acid sequence alignment between *hIntL-1*, *hIntL-2*, *mIntL-1*, and *mIntL-2*.

1.2.3.3.c. Ascidian lectin

Yokosawa and coworkers⁸⁴ isolated a galactose-specific lectin from plasma and hemocytes of the ascidian *Halocynthia roretzi*. The lectin was found to contain 348 amino acids, the sequence of which represented ~40% identity (70% similarity) to XL-35. This lectin could play a role in stimulating phagocytosis.⁸⁵ The authors suggested that it could bind to foreign microorganisms via galactose residues causing agglutination and thus enhancing phagocytosis.⁷⁴

1.2.3.3.d. Lamprey serum lectin

As a result of infection by a pathogenic microorganism, Bayne and coworkers were able to detect an immune-related lectin in *Oncorhynchus mykiss* (rainbow trout).⁸⁶ They named this lectin Lamprey serum lectin, which showed about 73% similarity to the C-terminal region of XL-35.⁷⁴

1.2.3.3.e. Alligator lectin

In 2012, a new lectin was discovered in the American alligator (*Alligator mississippiensis*).⁸⁷ This lectin exhibited 58% and 59% sequence similarity to both human and mIntL-1, respectively. Unlike human intelectins, this alligator lectin lacks *N*-glycosylation sites, but its sequence suggested the potential presence of *O*-linked glycans. When the authors tested the carbohydrate binding affinities of the protein, they found that it showed high binding preferences toward mannose and mannan.⁸⁷ Furthermore, the authors found that alligator lectin lacks a cysteine at position 42. This cysteine is conserved in certain intelectin homologs. The absence

of this cysteine could affect the tertiary structure of the alligator lectin and hence its binding activity and thermal stability.⁸⁷

1.2.3.3.f. Sheep intelectins

Two sheep intelectins (sIntL-1 and sIntL-2) were discovered in 2007.^{88, 89} Both lectins are up-regulated as a result of parasitic infection. In 2009, a new sheep intelectin (sIntL-3) was identified.⁹⁰ French and coworkers⁹⁰ wanted to examine the expression levels of these three sheep intelectins in response to two nematode infections. These infections are known to be mediated through T helper cell type 2 (Th2) pathways. These infection models were *Teladorsagia circumcincta* challenge and *Dictyocaulus filaria* natural infection.⁹⁰ They found that the three sIntLs were absent in the control sheep and were expressed in the mucosa of both the challenged and the control unchallenged animals. From these results, it was concluded that intelectins play an important role in the innate immune response of sheep infected with nematodes.⁹⁰

1.2.3.3.g. Lactoferrin receptor

Lactoferrin (Lf) is an iron-binding glycoprotein that is 80 kDa in size and composed of two globular domains. Lf was first discovered and identified in bovine milk.⁹¹⁻⁹⁴ Recently, Lf was also discovered in various body fluids including intestinal fluids and saliva. Lf is released from granules in neutrophils during infection and inflammation.⁹⁵ Numerous studies have demonstrated that Lf plays an important role in different biological events, for example: immunomodulation,^{96, 97} iron

absorption, activation of cellular proliferation, and antimicrobial effects.⁹⁸ In many studies, scientists have tried to understand the relation between human lactoferrin receptor (LfR) and human intelectins.⁶¹

In 2001, Suzuki et al⁹⁹ cloned and sequenced the human small intestinal lactoferrin receptor. Interestingly, the authors showed that the structure of the cloned LfR revealed 100% structural identity with human intelectin, except that LfR has an extra transmembrane domain which is lacking in human intelectin.⁹⁹ The proposed biological function of small intestinal LfR is to facilitate iron absorption. Physiological iron levels affects the expression levels of the small intestinal LfR, the protein was up-regulated in association with iron depletion.¹⁰⁰

Scientists have investigated if LfR could play a role in enhancing the immune system. It has been shown that orally administered bovine lactoferrin (bLf) increases intestinal CD4+, CD8+ T cells and natural killer (NK) cells.¹⁰¹ Furthermore, it has been reported that bLf could have anti-metastatic action.¹⁰² Thus, orally taken bLf could bind to bLfR enhancing intestinal immunological responses and exerting anti-metastatic effects. Furthermore, the synthesis of interleukin-18 (IL-18) was stimulated upon ingestion of bLf.¹⁰³ IL-18 regulates the expression of other genes including interferon- γ in T and NK cells, and tumor necrosis factor α (TNF- α).¹⁰⁴ IL-18 also stimulates responses mediated by T helper cell type 1 (Th1) and NK cells¹⁰⁵ as well as angiogenesis inhibition.¹⁰⁶ Therefore,

hLf could participate in similar immunological effects mediated by its receptor hLFR.

1.2.3.3.h. Omentin-1

Schäffler *et al*⁶² first reported the genomic sequence of omentin-1. Omentin-1 is an adipocytokine present in adipose tissue and interestingly, omentin-1 structure and human intelectin-1 are splicing variants proteins.³⁶ In Crohn's disease, ulcerative colitis, and inflammatory bowel disease, intestinal bacteria play a very important role in the onset and progression of the disease.¹⁰⁷ For example, patients suffering from Crohn's disease showed low or no omentin-1 expression levels. Thus, omentin/intelectin-1 could be a promising candidate for further studies towards better understanding the course of these diseases.

In 2012 scientists studied the effect of omentin-1 on bone metabolism.¹⁰⁸ It was shown that omentin-1 has bone-sparing effect in estrogen-deficient mice. In another interesting study, it was discovered that there is a relation between obesity and circulating levels of omentin in plasma.¹⁰⁹ It is well known that obese individuals are more susceptible to hypertension as well as other cardiovascular disorders.¹¹⁰ Inspired by this fact, scientists investigated the effect of omentin on isolated blood vessels.¹¹¹ Omentin showed a nitrogen oxide (NO)-mediated vasodilataion effect on blood vessels. According to Yang *et al*,¹¹² omentin affects insulin-mediated glucose transport and hence could be implicated in obesity. From all these investigations, it could be concluded that an important role might be played by omentin/intelectin in metabolism as well as other disorders.

1.2.3.4. Proposed physiological function of human intelectin (hIntL)

The proposed main function of hIntL has been attributed to two main effects. The first effect is direct, through hIntL mucosal protection due to its location and disposition in the human tissues. The second effect is an indirect one that occurs via its involvement in the activation of the complement–lectin pathway.

The principal function of hIntL could be attributed primarily to its localization in human tissues. As mentioned earlier, the main location of hIntL is the small intestine.³⁶ It was important to locate exactly where intelectins could be found in the small intestine and thus gain more detail about the cellular and subcellular distribution of human intelectins in the small intestine. This was the main objective of a study done by Wrackmeyer and coworkers.¹¹³ Using immunofluorescence and immunogold electron microscopy, the authors localized hIntL to Paneth cells in the bottom of the crypts¹¹³(

Figure 1.5). Furthermore, hIntL was shown to be localized in goblet cells along the crypt–villus axis.¹¹³

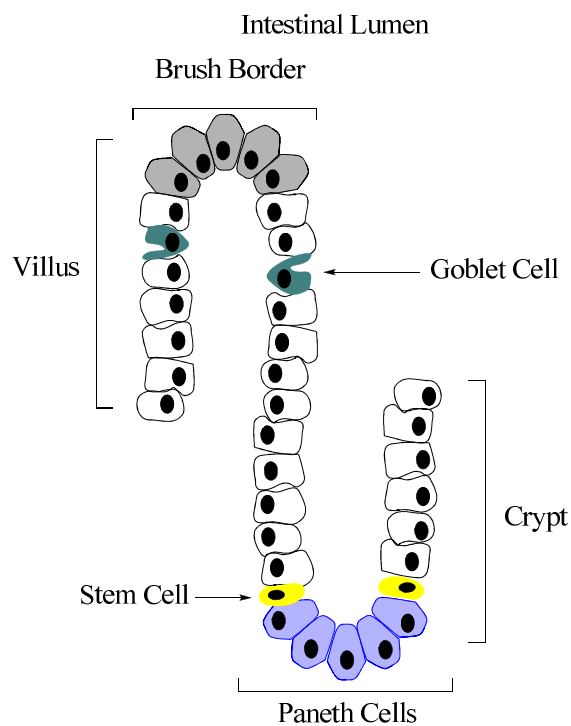


Figure 1.53: Schematic diagram showing the cells (Paneth, Goblet and brush border) which secrete hIntL in the villi of the small intestine.

More interestingly, the authors showed that the major constituent of both microvillar lipid rafts and super-rafts was hIntL.¹¹³ The lipid raft model is defined as a dynamic nanoscale sterol and sphingolipid-enriched ordered structures of certain proteins within the lipid bilayer. These structures can be activated and transformed from the resting state to the dynamic state by certain protein–protein, lipid–lipid and lipid–protein interactions.¹¹⁴

Knowing the exact location of hIntL in the small intestine enabled the authors to predict the main physiological role of the protein. It was proposed that hIntL plays a role in mucosal protection against different pathogenic parasites and

microorganisms, which could be found in the intestinal lumen.¹¹³ Human intelectins are not known to function by an agglutination effect, probably due to their inability to form noncovalent multimers.³⁶ Therefore, the antimicrobial effect of hIntL could not be attributed to agglutination of microorganisms in the intestinal lumen. Alternatively, hIntL could exert their protective role via binding to glycolipids that are found in the brush border microvilli.¹¹³ The luminal brush border is known to be rich in various glycolipids with terminal galactose moieties (lactosylceramides, galactosylceramides and GM1).¹¹⁵ Thus, the main protective role of hIntL could be attributed to inhibition of glycolipids from acting as pathogen receptors¹¹³ (**Figure 1.6**). Also, hIntL could act as protective shield through forming cross linkages between its trivalent structure together with the lipids and the glycoconjugates forming what are known as super-rafts. Furthermore, locally secreted antiglycosyl antibodies IgG, IgM and IgA could protect the intestinal brush border in a similar mechanism through binding to various glycoconjugates.¹¹⁶ These assemblies play an important role in the protection of the gut lumen through minimizing the loss of the digestive enzymes.¹¹⁵

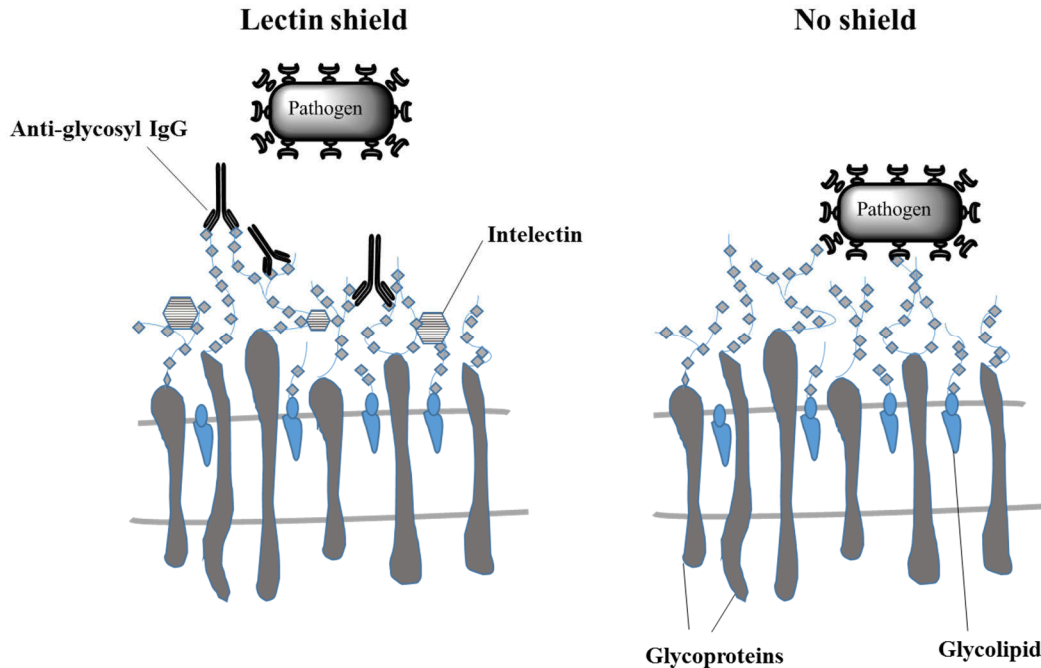


Figure 1.6: Protection of cellular surface glycans by intelectin shield in the innate immune system (figure adapted from the literature¹¹⁷).

It is worth mentioning that in addition to the mucosal protective role played by hIntL, it could participate in the innate immune response indirectly through activation of the complement pathway in a similar fashion to mannose-binding lectin (MBL) and ficolins.¹¹⁸ Complement activation pathways are classified into three main categories: classical,¹¹⁹ alternative,^{120, 121} and lectin pathways¹²²

Figure 1.7). MBL and ficolins act as recognition molecules where they recognize the pathogen through their microbial carbohydrate motifs.¹²³ This lectin–carbohydrate binding initiates complement activation, which is an important key step in both the innate and adaptive pathways.^{120, 121} As mentioned earlier, hIntL binds to the arabinogalactan of *Nocardia*³⁶ and also binds to *Mycobacterium bovis*⁶⁶ (BCG), presumably, through recognition of GalF residues present in the cell wall

of both pathogens. Thus, hIntL could also be an activator of the complement system via the lectin pathway; therefore, hIntL might enhance phagocytosis.

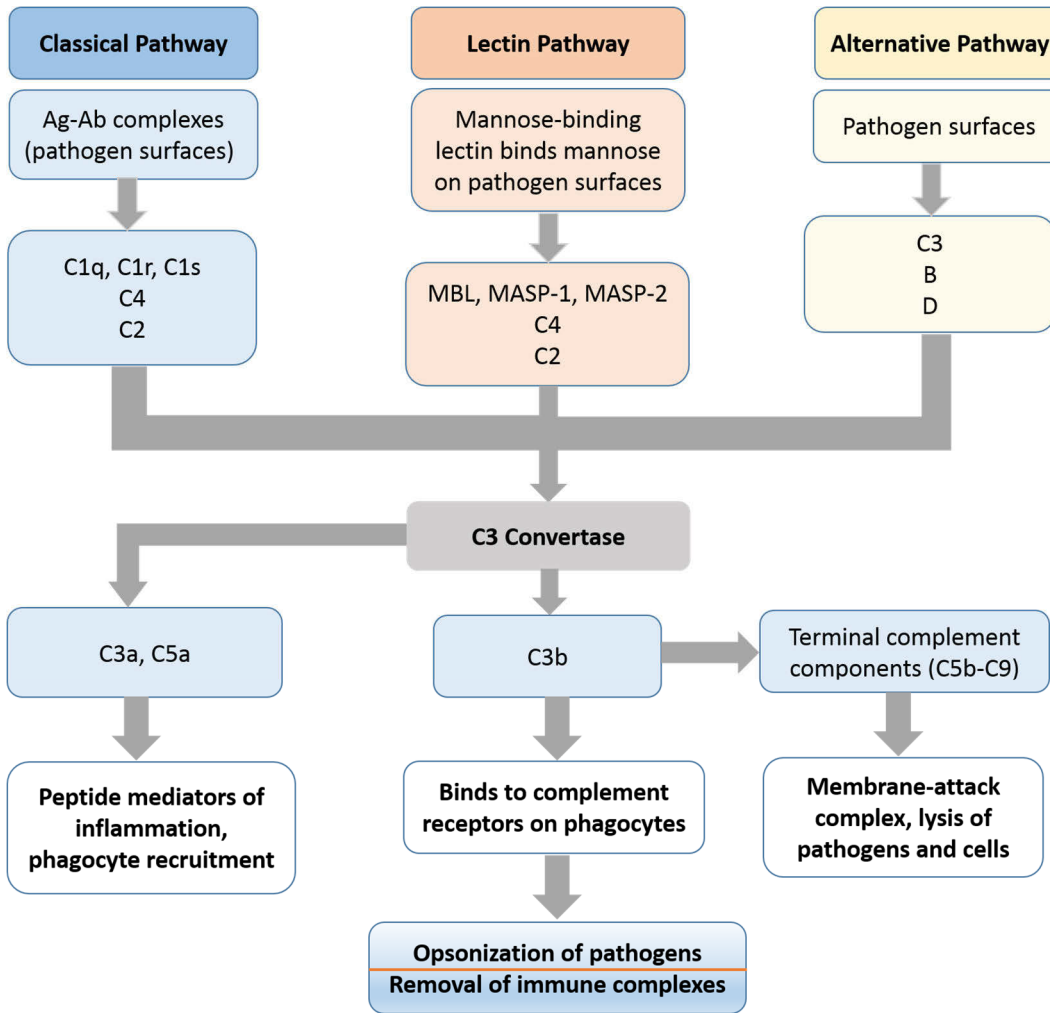


Figure 1.7: Complement pathways: classical, lectin and alternative pathways, Ag: antigen; Ab: antibody; MBL: mannose binding lectin; MASP: MBL-associated serine proteases; C1q, C1r, C1s, C2, C3, C3a, C4, C5a, C5b, B, D, and C9: complement components.

1.3. Clinical significance of hIntL

I will review briefly the link between intelectins and various infections and diseases and highlight the potential role of intelectins in the pathophysiology of those diseases.

1.3.1. Infection

There are many reports that reveal the relationship between expression levels of intelectin and microbial or parasitic infections. Among those reports is a study by Datta *et al* in 2005, which identified the up-regulation of several antimicrobial genes, including intelectin, in mice after infection with the intestinal nematode *Trichuris muris*.¹²⁴ Furthermore, Pemberton and coworkers⁸² showed that the expression level of mouse intelectin-2 was significantly increased in both Paneth and goblet cells as a result of *Trichinella spiralis* infection.

Many research groups have tried to understand if intelectins could be a contributor to allergic inflammation. An important study by Kuperman and coworkers¹²⁵ demonstrated that intelectin gene expression was twofold increased in the lung epithelium. This analysis was done in IL-13-overexpressing mice as well as in an ovalbumin model of allergic inflammation. Another study done on sheep showed that there was an IL-4 dependent increase in intelectin expression in an allergic model compared to the control non allergic ones.⁸⁸ Both IL-13 and IL-4 are important cytokines in lung allergy and inflammation, and this could highlight the possible role that intelectins could play as allergic mediators, the expression of

which is controlled by both cytokines. Furthermore, Voehringer and coworkers reported¹²⁶ that both intelectin-1 and intelectin-2 expression in transgenic mice is induced during infection with the helminth parasite *Nippostrongylus brasiliensis*. The expression of both intelectins was found to be STAT6-dependent. STAT6 is a transcription factor that is activated in response to different cytokines (IL-4 or IL-13). Once STAT6 is activated, it is translocated into the nucleus where it induces the expression of various genes including intelectins-1 and 2.

Another interesting study revealed the decreased expression levels of hIntL-1 in smokers compared to non-smokers.¹²⁷ It is known that hIntL-1 plays an important role in the host defence mechanism against bacteria.¹²⁸ Therefore, the down regulation of intelectin levels, which occurred as a result of cigarette smoking, could be an example of the immunomodulatory effects of smoking and might be the cause of increased infection rates in smokers compared to non-smokers.¹²⁷

1.3.2. Cancer

Gastric cancer is among the most widespread cancers worldwide.¹²⁹ Because hIntL is localized in the goblet cells of the colon,³⁶ a study investigating the potential role of hIntL in gastric cancer was carried out.¹³⁰ For the first time, it was demonstrated that hIntL is absent from normal gastric mucosa using immunohistochemical staining. On the other hand, gastric cancer specimens showed aberrant expression levels of hIntL, suggesting that hIntL could be a key factor in the carcinogenic processes in gastric mucosa.¹³⁰

Furthermore, it has been shown that hIntL could be involved in lung cancer. Malignant pleural mesothelioma (MPM) is a fatal disease with a very poor prognosis.¹³¹ In 2005, Wali *et al*¹³² reported the high expression of hIntL mRNA in MPM cells. Using western blots, immunohistochemistry and enzyme-linked immunosorbent assays, Tsuji *et al*¹³³ demonstrated that only epithelioid-type MPMs showed abundant hIntL levels. In contrast, the protein was absent from both pleura-invading lung cancer and reactive cancer cells near the lung. This result suggested the potential use of hIntL for differential diagnosis of MPM and also the possible use of hIntL as a clinical marker for the diagnosis of MPM as it is overexpressed in the pleural effusions.¹³³

In 2012, a study done by Park *et al*¹³⁴ investigated the expression levels of hIntL-1 in nasal polyps. Using real time PCR and Western blot analysis, the authors reported an increase of hIntL-1 expression in nasal polyps compared to the levels found in normal nasal tissues.¹³⁴ That result was confirmed by immunofluorescent staining. Intelectin-1 found in the epithelium and submucosa of nasal polyps was stained strongly while decreased staining levels were observed in the case of normal nasal mucosa.¹³⁴ These results could open the door for more extensive research to be done to understand the role of hIntL-1 in the progression and pathophysiology of nasal polyps.

1.4. Project objectives

Although it was reported previously that human intelectins bind to Gal β -containing glycans in microorganisms,^{36, 66} there is no information about the detailed binding specificity or affinity of the Gal β -intelectin interaction. The first and only qualitative measurement of the hIntL binding preferences was done by Tsuji and coworkers in 2001.³⁶ In that study, the authors showed that hIntL was preferentially eluted from a galactopyranose–Sepharose column by a Gal β -containing disaccharide (see above), which led the authors to hypothesize that hIntL recognizes Gal β -containing residues. Obviously, we need a better understanding of the nature of the interaction between the lectin and its ligand, which could serve as the starting point to study the biological role of hIntL. This project was designed to address a number of different questions about the interaction of intelectin and its ligands, including:

- Does hIntL indeed bind to Gal β -containing glycans?
- Does hIntL bind to other glycans?
- Does hIntL recognise different Gal β -containing glycans with the same affinity?
- Do hIntL-1 and hIntL-2 have the same binding preferences?
- Does the difference in the linkages in the glycan (either α or β) affect the binding affinity and specificity between hIntL-1 and hIntL-2?
- Does hIntL have binding affinity towards the structurally-related L-arabinofuranosides?

Our main objective of this project is to find answers to the proposed questions. These questions were addressed through hIntL expression (Chapter 2), the chemical synthesis of a *Galf*-containing library (Chapter 3), testing the binding specificity of hIntL using surface plasmon resonance (SPR, Chapter 4).

1.5. References

1. Holeman, A.; Seeberger, P. H., Carbohydrate diversity: synthesis of glycoconjugates and complex carbohydrates. *Curr. Opin. Biotech.* **2004**, *15*, 615-622.
2. Leitao, E. A.; Bittencourt, V. C. B.; Haido, R. M. T.; Valente, A. P.; Peter-Katalinic, J.; Letzel, M.; de Souza, L. M.; Barreto-Bergter, E., beta-Galactofuranose-containing O-linked oligosaccharides present in the cell wall peptidogalactomannan of *Aspergillus fumigatus* contain immunodominant epitopes. *Glycobiology* **2003**, *13*, 681-692.
3. Wiederschain, G. Y., Glycobiology: Progress, problems, and perspectives. *Biochemistry-Moscow* **2013**, *78*, 679-696.
4. Dawson, H.; Andre, S.; Karamitopoulou, E.; Zlobec, I.; Gabius, H.-J., The Growing Galectin Network in Colon Cancer and Clinical Relevance of Cytoplasmic Galectin-3 Reactivity. *Anticancer Res.* **2013**, *33*, 3053-3059.
5. Tefsen, B.; Ram, A. F. J.; van Die, I.; Routier, F. H., Galactofuranose in eukaryotes: aspects of biosynthesis and functional impact. *Glycobiology* **2012**, *22*, 456-469.
6. Richards, M. R.; Lowary, T. L., Chemistry and Biology of Galactofuranose-Containing Polysaccharides. *Chembiochem* **2009**, *10*, 1920-1938.
7. Brennan, P. J.; Nikaido, H., The envelope of Mycobacteria. *Annu. Rev. Biochem.* **1995**, *64*, 29-63.
8. Delederkremer, R. M.; Colli, W., Galactofuranose-containing glycoconjugates in trypanosomatids. *Glycobiology* **1995**, *5*, 547-552.

9. Ahrazem, O.; Prieto, A.; Leal, J. A.; Jimenez-Barbero, J.; Bernabe, M., Fungal cell wall galactomannan isolated from *Apodus deciduus*. *Carbohydr. Res.* **2002**, *337*, 1503-1506.
10. Peltier, P.; Euzen, R.; Daniellou, R.; Nugier-Chauvin, C.; Ferrieres, V., Recent knowledge and innovations related to hexofuranosides: structure, synthesis and applications. *Carbohydr. Res.* **2008**, *343*, 1897-1923.
11. Dashti, Y.; Grkovic, T.; Quinn, R. J., Predicting natural product value, an exploration of anti-TB drug space. *Nat. Prod. Rep.* **2014**, *31*.
12. Duthie, M. S.; Raychaudhuri, R.; Tutterrow, Y. L.; Misquith, A.; Bowman, J.; Casey, A.; Balagon, M. F.; Maghanoy, A.; Beltran-Alzate, J. C.; Romero-Alzate, M.; Cardona-Castro, N.; Reed, S. G., A rapid ELISA for the diagnosis of MB leprosy based on complementary detection of antibodies against a novel protein-glycolipid conjugate. *Diagn. Micr. Infec. Dis.* **2014**, *79*, 233-239.
13. Bloom, B. R.; Murray, C. J. L., Tuberculosis - commentary on a reemergent killer. *Science* **1992**, *257*, 1055-1064.
14. Besra, G. S.; Khoo, K. H.; McNeil, M. R.; Dell, A.; Morris, H. R.; Brennan, P. J., A new interpretation of the structure of the mycolyl arabinogalactan complex of *Mycobacterium tuberculosis* as revealed through characterization of oligoglycosylalditol fragments by fast-atom-bombardment mass-spectrometry and H1 nuclear magnetic resonance spectroscopy. *Biochemistry* **1995**, *34*, 4257-4266.

15. Pan, F.; Jackson, M.; Ma, Y. F.; McNeil, M., Cell wall core galactofuran synthesis is essential for growth of mycobacteria (vol 183, pg 3991, 2001). *J. Bacteriol.* **2001**, *183*, 6971-6971.
16. Pathak, A. K.; Pathak, V.; Seitz, L.; Maddry, J. A.; Gurcha, S. S.; Besra, G. S.; Suling, W. J.; Reynolds, R. C., Studies on (beta,1 -> 5) and (beta,1 -> 6) linked octyl Gal(f) disaccharides as substrates for mycobacterial galactosyltransferase activity. *Bioorg. Med. Chem.* **2001**, *9*, 3129-3143.
17. Jann, B.; Shashkov, A. A.; Kochanowski, H.; Jann, K., Structural comparison of the O6 specific polysaccharides from *Escherichia coli* O6-K2-H1, *Escherichia coli* O6-K13-H1, and *Escherichia coli* O6-K54-H10. *Carbohydr. Res.* **1994**, *263*, 217-225.
18. Kol, O.; Wieruszkeski, J. M.; Strecker, G.; Montreuil, J.; Fournet, B.; Zalisz, R.; Smets, P., Structure of the O-specific polysaccharide chain from *Klebsiella pneumoniae* O1K2 (NCTC-5055) lipopolysaccharide. *Carbohydr. Res.* **1991**, *217*, 117-125.
19. Whitfield, C., Biosynthesis of lipopolysaccharide O-antigens. *Trends Microbiol.* **1995**, *3*, 178-185.
20. Clarke, B. R.; Bronner, D.; Keenleyside, W. J.; Severn, W. B.; Richards, J. C.; Whitfield, C., Role of RFE and RFBF in the initiation of biosynthesis of D-galactan-i, the lipopolysaccharide O-antigen from *Klebsiella pneumoniae* serotype-O1. *J. Bacteriol.* **1995**, *177*, 5411-5418.
21. Clarke, B. R.; Bronner, D.; Keenleyside, W. J.; Severn, W. B.; Richards, J. C.; Whitfield, C., Role of RFE and Rfbf in the initiation of biosynthesis of

- D-galactan-I, the lipopolysaccharide O-antigen from *klebsiella-pneumoniae* serotype-O1. *J. Bacteriol.* **1995**, *177*, 5411-5418.
22. Yamazaki, K.; Suzuki, M.; Inukai, K.; Kuga, H.; Korenaga, H., Structural study on a sulfated polysaccharide-peptidoglycan complex produced by *Arthrobacter sp.* *Biosci. Biotech. Bioch.* **1998**, *62*, 2138-2144.
23. Inoue, K.; Korenaga, H.; Tanaka, N. G.; Sakamoto, N.; Kadoya, S., The sulfated polysaccharide-peptidoglycan complex potently inhibits embryonic angiogenesis and tumor growth in the presence of cortisone acetate. *Carbohydr. Res.* **1988**, *181*, 135-142.
24. McConville, M. J.; Homans, S. W.; Thomasoates, J. E.; Dell, A.; Bacic, A., Structures of the glycoinositolphospholipids from *Leishmania major* - a family of novel galactofuranose-containing glycolipids. *J. Biol. Chem.* **1990**, *265*, 7385-7394.
25. Turco, S. J.; Descoteaux, A., The lipophosphoglycan of leishmania parasites. *Annu. Rev. Microbiol.* **1992**, *46*, 65-94.
26. McConville, M. J.; Ferguson, M. A. J., The structure, biosynthesis and function of glycosylated phosphatidylinositols in the parasitic protozoa and higher eukaryotes. *Biochem. J.* **1993**, *294*, 305-324.
27. Moody, S. F.; Handman, E.; McConville, M. J.; Bacic, A., The structure of *Leishmania major* amastigote lipophosphoglycan. *J. Biol. Chem.* **1993**, *268*, 18457-18466.
28. Levery, S. B.; Toledo, M. S.; Straus, A. H.; Takahashi, H. K., Structure elucidation of sphingolipids from the mycopathogen *Paracoccidioides*

- brasiliensis*: An immunodominant beta-galactofuranose residue is carried by a novel glycosylinositol phosphorylceramide antigen. *Biochemistry* **1998**, *37*, 8764-8775.
29. Leal, J. A.; GomezMiranda, B.; Prieto, A.; Domenech, J.; Ahrazem, O.; Bernabe, M., Possible chemotypes from cell wall polysaccharides, as an aid in the systematics of *Penicillium* and its teleomorphic states *Eupenicillium* and *Talaromyces*. *Mycol. Res.* **1997**, *101*, 1259-1264.
30. Sharon, N., Lectins: past, present and future. *Biochem. Soc. T.* **2008**, *36*, 1457-1460.
31. Hernandez, J. D.; Baum, L. G., Ah, sweet mystery of death! Galectins and control of cell fate. *Glycobiology* **2002**, *12*, 127R-136R.
32. Dube, D. H.; Bertozzi, C. R., Glycans in cancer and inflammation. Potential for therapeutics and diagnostics. *Nat. Rev. Drug Discov.* **2005**, *4*, 477-488.
33. Dwek, R. A., Glycobiology: Toward understanding the function of sugars. *Chem. Rev.* **1996**, *96*, 683-720.
34. Demetter, P.; Nagy, N.; Martin, B.; Mathieu, A.; Dumont, P.; Decaestecker, C.; Salmon, I., The galectin family and digestive disease. *J. Pathol.* **2008**, *215*, 1-12.
35. Chiodo, F.; Marradi, M.; Park, J.; Ram, A. F. J.; Penades, S.; van Die, I.; Tefsen, B., Galactofuranose-Coated Gold Nanoparticles Elicit a Pro-inflammatory Response in Human Monocyte-Derived Dendritic Cells and Are Recognized by DC-SIGN. *ACS Chem. Biol.* **2014**, *9*, 383-389.

36. Tsuji, S.; Uehori, J.; Matsumoto, M.; Suzuki, Y.; Matsuhisa, A.; Toyoshima, K.; Seya, T., Human intelectin is a novel soluble lectin that recognizes galactofuranose in carbohydrate chains of bacterial cell wall. *J. Biol. Chem.* **2001**, *276*, 23456-23463.
37. Yang, R.-Y.; Rabinovich, G. A.; Liu, F.-T., Galectins: structure, function and therapeutic potential. *Expert Rev. Mol. Med.* **2008**, *10*, 1-24.
38. Cooper, D. N. W., Galectinomics: finding themes in complexity. *BBA-Gen. Subjects* **2002**, *1572*, 209-231.
39. Hirabayashi, J.; Kasai, K., The family of metazoan metal-independent beta galactoside binding lectins - structure, function and molecular evolution. *Glycobiology* **1993**, *3*, 297-304.
40. Elola, M. T.; Wolfenstein-Todel, C.; Troncoso, M. F.; Vasta, G. R.; Rabinovich, G. A., Galectins: matricellular glycan-binding proteins linking cell adhesion, migration, and survival. *Cell Mol. Life Sci.* **2007**, *64*, 1679-1700.
41. Brewer, C. F., Binding and cross-linking properties of galectins. *BBA-Gen. Subjects* **2002**, *1572*, 255-262.
42. Sacchettini, J. C.; Baum, L. G.; Brewer, C. F., Multivalent protein-carbohydrate interactions. A new paradigm for supermolecular assembly and signal transduction. *Biochemistry* **2001**, *40*, 3009-3015.
43. Lichtenstein, R. G.; Rabinovich, G. A., Glycobiology of cell death: when glycans and lectins govern cell fate. *Cell Death Differ.* **2013**, *20*, 976-986.

44. Cerliani, J. P.; Stowell, S. R.; Mascanfroni, I. D.; Arthur, C. M.; Cummings, R. D.; Rabinovich, G. A., Expanding the Universe of Cytokines and Pattern Recognition Receptors: Galectins and Glycans in Innate Immunity. *J. Clin. Immunol.* **2011**, *31*, 10-21.
45. Nakahara, S.; Oka, N.; Raz, A., On the role of galectin-3 in cancer apoptosis. *Apoptosis* **2005**, *10*, 267-275.
46. Liu, F. T.; Patterson, R. J.; Wang, J. L., Intracellular functions of galectins. *BBA-Gen. Subjects* **2002**, *1572*, 263-273.
47. Bornstein, P.; Sage, E. H., Matricellular proteins: extracellular modulators of cell function. *Curr. Opin. Cell Biol.* **2002**, *14*, 608-616.
48. Murphy-Ullrich, J. E., The de-adhesive activity of matricellular proteins: is intermediate cell adhesion an adaptive state? *J. Clin. Invest.* **2001**, *107*, 785-790.
49. Zuberi, R. I.; Hsu, D. K.; Kalayci, O.; Chen, H. Y.; Sheldon, H. K.; Yu, L.; Apgar, J. R.; Kawakami, T.; Lilly, C. M.; Liu, F. T., Critical role for galectin-3 in airway inflammation and bronchial hyperresponsiveness in a murine model of asthma. *Am. J. Pathol.* **2004**, *165*, 2045-2053.
50. Kasamatsu, A.; Uzawa, K.; Nakashima, D.; Koike, H.; Shiiba, M.; Bukawa, H.; Yokoe, H.; Tanzawa, H., Galectin-9 as a regulator of cellular adhesion in human oral squamous cell carcinoma cell lines. *Int. J. Mol. Med.* **2005**, *16*, 269-273.
51. Seki, M.; Sakata, K.-m.; Oomizu, S.; Arikawa, T.; Sakata, A.; Ueno, M.; Nobumoto, A.; Niki, T.; Saita, N.; Ito, K.; Dai, S.-Y.; Katoh, S.; Nishi, N.;

- Tsukano, M.; Ishikawa, K.; Yamauchi, A.; Kuchroo, V.; Hirashima, M., Beneficial effect of galectin 9 on rheumatoid arthritis by induction of apoptosis of synovial fibroblasts. *Arthritis Rheum.* **2007**, *56*, 3968-3976.
52. Banchereau, J.; Briere, F.; Caux, C.; Davoust, J.; Lebecque, S.; Liu, Y.-J.; Pulendran, B.; Palucka, K., Immunobiology of dendritic cells. In *Annu. Rev. Immunol.*, Paul, W. E.; Fathman, C. G.; Glimcher, L. H., Eds. 2000; Vol. 18, pp 767-811.
53. Geijtenbeek, T. B. H.; Torensma, R.; van Vliet, S. J.; van Duijnhoven, G. C. F.; Adema, G. J.; van Kooyk, Y.; Figdor, C. G., Identification of DC-SIGN, a novel dendritic cell-specific ICAM-3 receptor that supports primary immune responses. *Cell* **2000**, *100*, 575-585.
54. Figdor, C. G.; van Kooyk, Y.; Adema, G. J., C-type lectin receptors on dendritic cells and Langerhans cells (vol 2, pg 77, 2002). *Nat. Rev. Immunol.* **2002**, *2*, 377-377.
55. Geijtenbeek, T. B. H.; Kwon, D. S.; Torensma, R.; van Vliet, S. J.; van Duijnhoven, G. C. F.; Middel, J.; Cornelissen, I.; Nottet, H.; KewalRamani, V. N.; Littman, D. R.; Figdor, C. G.; van Kooyk, Y., DC-SIGN, a dendritic cell-specific HIV-1-binding protein that enhances trans-infection of T cells. *Cell* **2000**, *100*, 587-597.
56. Gringhuis, S. I.; van der Vlist, M.; van den Berg, L. M.; den Dunnen, J.; Litjens, M.; Geijtenbeek, T. B. H., HIV-1 exploits innate signaling by TLR8 and DC-SIGN for productive infection of dendritic cells. *Nat. Immunol.* **2010**, *11*, 419-U81.

57. Mitchell, D. A.; Fadden, A. J.; Drickamer, K., A novel mechanism of carbohydrate recognition by the C-type lectins DC-SIGN and DC-SIGNR - Subunit organization and binding to multivalent ligands. *J. Biol. Chem.* **2001**, *276*, 28939-28945.
58. Feinberg, H.; Mitchell, D. A.; Drickamer, K.; Weis, W. I., Structural basis for selective recognition of oligosaccharides by DC-SIGN and DC-SIGNR. *Science* **2001**, *294*, 2163-2166.
59. Guo, Y.; Feinberg, H.; Conroy, E.; Mitchell, D. A.; Alvarez, R.; Blixt, O.; Taylor, M. E.; Weis, W. I.; Drickamer, K., Structural basis for distinct ligand-binding and targeting properties of the receptors DC-SIGN and DC-SIGNR. *Nat. Struct. Mol. Biol.* **2004**, *11*, 591-598.
60. Maeda, N.; Nigou, J.; Herrmann, J. L.; Jackson, M.; Amara, A.; Lagrange, P. H.; Puzo, G.; Gicquel, B.; Neyrolles, O., The cell surface receptor DC-SIGN discriminates between Mycobacterium species through selective recognition of the mannose caps on lipoarabinomannan. *J. Biol. Chem.* **2003**, *278*, 5513-5516.
61. Suzuki, Y. A.; Lopez, V.; Lonnerdal, B., Mammalian lactoferrin receptors: structure and function. *Cell Mol. Life Sci.* **2005**, *62*, 2560-2575.
62. Schaffler, A.; Neumeier, A.; Herfarth, H.; Furst, A.; Scholmerich, J.; Buchler, C., Genomic structure of human omentin, a new adipocytokine expressed in omental adipose tissue. *BBA-Gene struct. Expr.* **2005**, *1732*, 96-102.

63. Lee, J. K.; Schnee, J.; Pang, M.; Wolfert, M.; Baum, L. G.; Moremen, K. W.; Pierce, M., Human homologs of the *Xenopus* oocyte cortical granule lectin XL35. *Glycobiology* **2001**, *11*, 65-73.
64. Hirsch, C.; Blom, D.; Ploegh, H. L., A role for N-glycanase in the cytosolic turnover of glycoproteins. *EMBO J.* **2003**, *22*, 1036-1046.
65. Weis, W. I.; Taylor, M. E.; Drickamer, K., The C-type lectin superfamily in the immune system. *Immunol. Rev.* **1998**, *163*, 19-34.
66. Tsuji, S.; Yamashita, M.; Hoffman, D. R.; Nishiyama, A.; Shinohara, T.; Ohtsu, T.; Shibata, Y., Capture of heat-killed *Mycobacterium bovis* bacillus Calmette-Guerin by intelectin-1 deposited on cell surfaces. *Glycobiology* **2009**, *19*, 518-526.
67. Daffe, M.; McNeil, M.; Brennan, P. J., Major structural features of the cell-wall arabinogalactans of *Mycobacterium*, *Rhodococcus*, and *Nocardia* spp. *Carbohydr. Res.* **1993**, *249*, 383-398.
68. Pedersen, L. L.; Turco, S. J., Galactofuranose metabolism: a potential target for antimicrobial chemotherapy. *Cell Mol. Life Sci.* **2003**, *60*, 259-266.
69. Abeygunawardana, C.; Bush, C. A.; Cisar, J. O., Complete structure of the cell surface polysaccharide of *Streptococcus oralis*-C104 - a 600-MHz NMR-study. *Biochemistry* **1991**, *30*, 8568-8577.
70. Suzuki, E.; Toledo, M. S.; Takahashi, H. K.; Straus, A. H., A monoclonal antibody directed to terminal residue of beta-galactofuranose of a glycolipid antigen isolated from *Paracoccidioides brasiliensis*; Cross-reactivity with *Leishmania major* and *Trypanosoma cruzi*. *Glycobiology* **1997**, *7*, 463-468.

71. Calixto, R.; Mattos, B.; Bittencourt, V.; Lopes, L.; Souza, L.; Sasaki, G.; Cipriani, T.; Silva, M.; Barreto-Bergter, E., beta-Galactofuranose-containing structures present in the cell wall of the saprophytic fungus *Cladosporium (Hormoconis) resinae*. *Res. Microbiol.* **2010**, *161*, 720-728.
72. Tsuji, S.; Matsumoto, M.; Takeuchi, O.; Akira, S.; Azuma, I.; Hayashi, A.; Toyoshima, K.; Seya, T., Maturation of human dendritic cells by cell wall skeleton of *Mycobacterium bovis* bacillus Calmette-Guerin: Involvement of Toll-like receptors. *Infect. Immun.* **2000**, *68*, 6883-6890.
73. Izumi, S.; Hirai, O.; Hayashi, K.; Konishi, Y.; Okuhara, M.; Kohsaka, M.; Aoki, H.; Yamamura, Y., Induction of a tumor necrosis factor-like activity by *Nocardia rubra* cell-wall skeleton. *Cancer Res.* **1987**, *47*, 1785-1792.
74. Lee, J. K.; Baum, L. G.; Moremen, K.; Pierce, M., The X-lectins: A new family with homology to the *Xenopus laevis* oocyte lectin XL-35. *Glycoconjugate J.* **2004**, *21*, 443-450.
75. Kilpatrick, D. C.; Fujita, T.; Matsushita, M., P35, an opsonic lectin of the ficolin family, in human blood from neonates, normal adults, and recurrent miscarriage patients. *Immunol. Lett.* **1999**, *67*, 109-112.
76. Lee, J. K.; Buckhaults, P.; Wilkes, C.; Teilhet, M.; King, M. L.; Moremen, K. W.; Pierce, M., Cloning and expression of a *Xenopus laevis* oocyte lectin and characterization of its mRNA levels during early development. *Glycobiology* **1997**, *7*, 367-372.

77. Arranz-Plaza, E.; Tracy, A. S.; Siriwardena, A.; Pierce, J. M.; Boons, G. J., High-avidity, low-affinity multivalent interactions and the block to polyspermy in *Xenopus laevis*. *J. Am. Chem. Soc.* **2002**, *124*, 13035-13046.
78. Roberson, M. M.; Barondes, S. H., Lectin from embryos and oocytes of *Xenopus laevis* - purification and properties. *J. Biol. Chem.* **1982**, *257*, 7520-7524.
79. Outenreath, R. L.; Roberson, M. M.; Barondes, S. H., Endogenous lectin secretion into the extracellular matrix of early embryos of *Xenopus laevis*. *Dev. Biol.* **1988**, *125*, 187-194.
80. Ren, Y.; Ding, Q.; Zhang, X., Ficolins and infectious diseases. *Virologica Sinica* **2014**, *29*, 25-32.
81. Komiya, T.; Tanigawa, Y.; Hirohashi, S., Cloning of the novel gene intelectin, which is expressed in intestinal paneth cells in mice. *Biochem. Biophys. Res. Commun.* **1998**, *251*, 759-762.
82. Pemberton, A. D.; Knight, P. A.; Wright, S. H.; Miller, H. R. P., Proteomic analysis of mouse jejunal epithelium and its response to infection with the intestinal nematode, *Trichinella spiralis*. *Proteomics* **2004**, *4*, 1101-1108.
83. Tsuji, S.; Yamashita, M.; Nishiyama, A.; Shinohara, T.; Zhongwei, U.; Myrvik, Q. N.; Hoffman, D. R.; Henriksen, R. A.; Shibata, Y., Differential structure and activity between human and mouse intelectin-1: Human intelectin-1 is a disulfide-linked trimer, whereas mouse homologue is a monomer. *Glycobiology* **2007**, *17*, 1045-1051.

84. Yokosawa, H.; Harada, K.; Igarashi, K.; Abe, Y.; Takahashi, K.; Ishii, S., Galactose-specific lectin in the hemolymph of solitary ascidian, *Halocynthia roretzi* - molecular, binding and functional properties. *Biochim. Biophys. Acta.* **1986**, *870*, 242-247.
85. Abe, Y.; Tokuda, M.; Ishimoto, R.; Azumi, K.; Yokosawa, H., A unique primary structure, cDNA cloning and function of a galactose-specific lectin from ascidian plasma. *Eur. J. Biochem.* **1999**, *261*, 33-39.
86. Bayne, C. J.; Gerwick, L.; Fujiki, K.; Nakao, M.; Yano, T., Immune-relevant (including acute phase) genes identified in the livers of rainbow trout, *Oncorhynchus mykiss*, by means of suppression subtractive hybridization. *Dev. Comp. Immunol.* **2001**, *25*, 205-217.
87. Darville, L. N. F.; Merchant, M. E.; Maccha, V.; Siddavarapu, V. R.; Hasan, A.; Murray, K. K., Isolation and determination of the primary structure of a lectin protein from the serum of the American alligator (*Alligator mississippiensis*). *Comp. Biochem. Phys. B* **2012**, *161*, 161-169.
88. French, A. T.; Bethune, J. A.; Knight, P. A.; McNeilly, T. N.; Wattedegera, S.; Rhind, S.; Miller, H. R. P.; Pemberton, A. D., The expression of intelectin in sheep goblet cells and upregulation by interleukin-4. *Vet. Immunol. Immunop.* **2007**, *120*, 41-46.
89. French, A. T.; Knight, P. A.; Smith, W. D.; Brown, J. K.; Craig, N. M.; Pate, J. A.; Miller, H. R. P.; Pemberton, A. D., Up-regulation of intelectin in sheep after infection with *Teladorsagia circumcincta*. *Int. J. Parasitol.* **2008**, *38*, 467-475.

90. French, A. T.; Knight, P. A.; Smith, W. D.; Pate, J. A.; Miller, H. R. P.; Pemberton, A. D., Expression of three intelectins in sheep and response to a Th2 environment. *Vet. Res.* **2009**, *40*.
91. Lonnerdal, B.; Iyer, S., Lactoferrin - molecular structure and biological function. *Annu. Rev. Nutr.* **1995**, *15*, 93-110.
92. Lash, J. A.; Coates, T. D.; Baehner, R. L.; Boxer, L. A., Plasma lactoferrin reflects granulocyte activation in-vivo. *Pediatr. Res.* **1982**, *16*, 208A-208A.
93. He, J. L.; Furmanski, P., Sequence specificity and transcriptional activation in the binding of lactoferrin to DNA. *Nature* **1995**, *373*, 721-724.
94. Brock, J., Lactoferrin - a multifunctional immunoregulatory protein. *Immunol. Today* **1995**, *16*, 417-419.
95. Lonnerdal, B.; Iyer, S., Lactoferrin: Molecular structure and biological function. In *Annu. Rev. Nutr.*, McCormick, D. B., Ed. 1995; Vol. 15, pp 93-110.
96. Kuhara, T.; Yamauchi, K.; Tamura, Y.; Okamura, H., Oral administration of lactoferrin increases NK cell activity in mice via increased production of IL-18 and type IIFN in the small intestine. *J. Interf. Cytok. Res.* **2006**, *26*, 489-499.
97. Ward, P. P.; Uribe-Luna, S.; Conneely, O. M., Lactoferrin and host defense. *Biochem. Cell Biol.* **2002**, *80*, 95-102.
98. Brock, J. H., The physiology of lactoferrin. *Biochem. Cell Biol.* **2002**, *80*, 1-6.

99. Suzuki, Y. A.; Shin, K.; Lonnerdal, B., Molecular cloning and functional expression of a human intestinal lactoferrin receptor. *Biochemistry* **2001**, *40*, 15771-15779.
100. Mikogami, T.; Marianne, T.; Spik, G., Effect of intracellular iron depletion by picolinic acid on expression of the lactoferrin receptor in the human colon carcinoma cell subclone HT29-18-C-1. *Biochem. J.* **1995**, *308*, 391-397.
101. Wang, W. P., Activation of intestinal mucosal immunity in tumor-bearing mice by lactoferrin. *Jpn. J. Cancer Res.* **2000**, *91*, 1359-1359.
102. Iigo, M.; Kuhara, T.; Ushida, Y.; Sekine, K.; Moore, M. A.; Tsuda, H., Inhibitory effects of bovine lactoferrin on colon carcinoma 26 lung metastasis in mice. *Clin. Exp. Metastas.* **1999**, *17*, 35-40.
103. Kuhara, T.; Iigo, M.; Itoh, T.; Ushida, Y.; Sekine, K.; Terada, N.; Okamura, H.; Tsuda, H., Orally administered lactoferrin exerts an antimetastatic effect and enhances production of IL-18 in the intestinal epithelium. *Nutr. Cancer* **2000**, *38*, 192-199.
104. Puren, A. J.; Razeghi, P.; Fantuzzi, G.; Dinarello, C. A., Interleukin-18 enhances lipopolysaccharide-induced interferon-gamma production in human whole blood cultures. *J. Infect. Dis.* **1998**, *178*, 1830-1834.
105. Okamoto, I.; Kohno, K.; Tanimoto, T.; Ikegami, H.; Kurimoto, M., Development of CD8(+) effector T cells is differentially regulated by IL-18 and IL-12. *J. Immunol.* **1999**, *162*, 3202-3211.

106. Cao, R. H.; Farnebo, J.; Kurimoto, M.; Cao, Y. H., Interleukin-18 acts as an angiogenesis and tumor suppressor. *FASEB J.* **1999**, *13*, 2195-2202.
107. Schaffler, A.; Herfarth, H., Creeping fat in Crohn's disease: travelling in a creeper lane of research? *Gut* **2005**, *54*, 742-744.
108. Xie, H.; Xie, P. L.; Luo, X. H.; Wu, X. P.; Zhou, H. D.; Tang, S. Y.; Liao, E. Y., Omentin-1 exerts bone-sparing effect in ovariectomized mice. *Osteoporosis Int.* **2012**, *23*, 1425-1436.
109. Batista, C. M. d. S.; Yang, R.-Z.; Lee, M.-J.; Glynn, N. M.; Yu, D.-Z.; Pray, J.; Ndubuizu, K.; Patil, S.; Schwartz, A.; Kligman, M.; Fried, S. K.; Gong, D.-W.; Shuldiner, A. R.; Pollin, T. I.; McLenithan, J. C., Omentin plasma levels and gene expression are decreased in obesity. *Diabetes* **2007**, *56*, 1655-1661.
110. Shuger, S. L.; Sui, X.; Church, T. S.; Meriwether, R. A.; Blair, S. N., Body mass index as a predictor of hypertension incidence among initially healthy normotensive women. *Am. J. Hypertens.* **2008**, *21*, 613-619.
111. Yamawaki, H.; Tsubaki, N.; Mukohda, M.; Okada, M.; Hara, Y., Omentin, a novel adipokine, induces vasodilation in rat isolated blood vessels. *Biochem. Biophys. Res. Commun.* **2010**, *393*, 668-672.
112. Yang, R. Z.; Lee, M. J.; Hu, H.; Pray, J.; Wu, H. B.; Hansen, B. C.; Shuldiner, A. R.; Fried, S. K.; McLenithan, J. C.; Gong, D. W., Identification of omentin as a novel depot-specific adipokine in human adipose tissue: possible role in modulating insulin action. *Am. J. Physiol-Endoc. M.* **2006**, *290*, E1253-E1261.

113. Wrackmeyer, U.; Hansen, G. H.; Seya, T.; Danielsen, E. M., Intelectin: A novel lipid raft-associated protein in the enterocyte brush border. *Biochemistry* **2006**, *45*, 9188-9197.
114. Simons, K.; Gerl, M. J., Revitalizing membrane rafts: new tools and insights. *Nat. Rev. Mol. Cell Bio.* **2010**, *11*, 688-699.
115. Braccia, A.; Villani, M.; Immerdal, L.; Niels-Christiansen, L. L.; Nystrom, B. T.; Hansen, G. H.; Danielsen, E. M., Microvillar membrane Microdomains exist at physiological temperature - Role of galectin-4 as lipid raft stabilizer revealed by "superrafts". *J. Biol. Chem.* **2003**, *278*, 15679-15684.
116. Hansen, G. H.; Niels-Christiansen, L. L.; Immerdal, L.; Danielsen, E. M., Antibodies in the small intestine: mucosal synthesis and deposition of anti-glycosyl IgA, IgM, and IgG in the enterocyte brush border. *Am. J. Physiol-Gastr. L.* **2006**, *291*, G82-G90.
117. Dann, S. M.; Eckmann, L., Innate immune defenses in the intestinal tract. *Curr. Opin. Gastroen.* **2007**, *23*, 115-120.
118. Endo, Y.; Takahashi, M.; Fujita, T., Lectin complement system and pattern recognition. *Immunobiology* **2006**, *211*, 283-293.
119. Law, S. K.; Lichtenberg, N. A.; Levine, R. P., Covalent binding and hemolytic activity of complement proteins. *Proc. Natl. Acad. Sci-Biol.* **1980**, *77*, 7194-7198.
120. Walport, M. J., Advances in immunology: Complement (First of two parts). *New Engl. J. Med.* **2001**, *344*, 1058-1066.

121. Walport, M. J., Advances in immunology: Complement (Second of two parts). *New England Journal of Medicine* **2001**, *344*, 1140-1144.
122. Fujita, T.; Matsushita, M.; Endo, Y., The lectin-complement pathway - its role in innate immunity and evolution. *Immunol. Rev.* **2004**, *198*, 185-202.
123. Holmskov, U.; Malhotra, R.; Sim, R. B.; Jensenius, J. C., Collectins - collagenous C-type lectins of the innate immune defense system. *Immunol. Today* **1994**, *15*, 67-74.
124. Datta, R.; deSchoolmeester, M. L.; Hedeler, C.; Paton, N. W.; Brass, A. M.; Else, K. J., Identification of novel genes in intestinal tissue that are regulated after infection with an intestinal nematode parasite. *Infect. Immun.* **2005**, *73*, 4025-4033.
125. Kuperman, D. A.; Lewis, C. C.; Woodruff, P. G.; Rodriguez, M. W.; Yang, Y. H.; Dolganov, G. M.; Fahy, J. V.; Erle, D. J., Dissecting asthma using focused transgenic modeling and functional genomics. *J. Allergy Clin. Immun.* **2005**, *116*, 305-311.
126. Voehringer, D.; Stanley, S. A.; Cox, J. S.; Completo, G. C.; Lowary, T. L.; Locksley, R. M., *Nippostrongylus brasiliensis*: Identification of intelectin-1 and -2 as Stat6-dependent genes expressed in lung and intestine during infection. *Exp. Parasitol.* **2007**, *116*, 458-466.
127. Carolan, B. J.; Harvey, B. G.; De, B. P.; Vanni, H.; Crystal, R. G., Decreased expression of intelectin 1 in the human airway epithelium of smokers compared to nonsmokers. *J. Immunol.* **2008**, *181*, 5760-5767.

128. Peebles, R. S., Jr., The intelectins: a new link between the immune response to parasitic infections and allergic inflammation? *Am. J. Physiol-Lung C.* **2010**, 298, L288-L289.
129. Shah, M. A.; Kelsen, D. P., Gastric Cancer: A Primer on the Epidemiology and Biology of the Disease and an Overview of the Medical Management of Advanced Disease. *Journal of the National Comprehensive Cancer Network* **2010**, 8, 437-447.
130. Zheng, L. D.; Weng, M. X.; Qi, M.; Qi, T.; Tong, L.; Hou, X. H.; Tong, Q. S., Aberrant expression of intelectin-1 in gastric cancer: its relationship with clinicopathological features and prognosis. *J. Cancer Res. Clin.* **2012**, 138, 163-172.
131. Ruffie, P.; Feld, R.; Minkin, S.; Cormier, Y.; Boutanlaroze, A.; Ginsberg, R.; Ayoub, J.; Shepherd, F. A.; Evans, W. K.; Figueredo, A.; Pater, J. L.; Pringle, J. F.; Kreisman, H., Diffuse malignant mesothelioma of the pleura in Ontario and Quebec - a retrospective study of 332 patients. *J. Clin. Oncol.* **1989**, 7, 1157-1168.
132. Wali, A.; Morin, P. J.; Hough, C. D.; Lonardo, F.; Seya, T.; Carbone, M.; Pass, H. I., Identification of intelectin overexpression in malignant pleural mesothelioma by serial analysis of gene expression (SAGE). *Lung Cancer-J Iaslc* **2005**, 48, 19-29.
133. Tsuji, S.; Tsuura, Y.; Morohoshi, T.; Shinohara, T.; Oshita, F.; Yamada, K.; Kameda, Y.; Ohtsu, T.; Nakamura, Y.; Miyagi, Y., Secretion of intelectin-

1 from malignant pleural mesothelioma into pleural effusion. *Brit. J. Cancer* **2010**, *103*, 517-523.

134. Park, I.-H.; Park, S.-J.; Cho, J.-S.; Moon, Y.-M.; Kim, T. H.; Lee, S. H.; Lee, H.-M., Increased expression of intelectin-1 in nasal polyps. *Am. J. Rhinol. Allergy* **2012**, *26*, 274-277.

2. Expression and Characterization of Intelectins

2.1. Introduction

2.1.1. Recombinant protein expression systems

In the past few years, the biotechnology industry has grown and expanded very fast and the expression of a wide range of recombinant proteins in different systems has become an important area of research.¹ The most common expression systems for recombinant proteins are *Escherichia coli*, yeasts (*Saccharomyces cerevisiae*, *Pichia pastoris*) and mammalian cells.² There are various aims for the production of recombinant proteins including therapeutic applications,³ as well as molecular biology research.⁴ Today, the production of recombinant proteins for pharmaceutical uses has attracted significant attention. The first organism used for the production of recombinant human proteins was the gram negative bacterium *E. coli*. In 2009 the commercial biotechnology products from *E. coli* contributed about \$50 billion to the pharmaceutical protein market.⁶ Through many years scientists gained significant knowledge about *E. coli* biochemistry and molecular biology.⁷⁻⁹ In 2011, 211 biopharmaceuticals were approved for use as therapeutic agents; 31% of those biopharmaceutical agents were produced in *E. coli*, 15% in yeast and 43% in mammalian cells.⁵

The choice of a suitable expression system depends on the protein of interest. The major goal of this project was to obtain a better understanding of the binding specificity of intelectins, which necessitated access to reasonable quantities of these proteins to conduct the binding assays. It was known from the literature that hIntL is a glycosylated, homotrimeric, secreted protein.¹⁰⁻¹² Despite being simple, cheap,

and generally producing a high yield of protein,² *E. coli* was not the expression system of choice for intelectins, due to problems associated with protein folding and lack of post-translational modification, i.e., glycosylation.² Furthermore, due to the reducing environment of the cytoplasm in *E. coli*,¹³ any native disulfide bonds will be reduced and this could affect the tertiary protein structure and hence the activity. Due to all these problems, we excluded *E. coli* from being an expression system for intelectins and focused on other expression systems including yeast and mammalian cells.

Yeast are simple eukaryotes and are capable of most complex post-translational modifications.¹⁴ Despite the fact that mammalian cells are the most expensive and complex systems, they are the hosts of choice for heterologous proteins due to the protein quality and the highest extent of post-translational modifications.^{2, 15} This chapter will highlight the different attempts I carried out to express the intelectins in both yeast and mammalian cells.

2.2. Results and discussion

Yeast (*Pichia pastoris*) and mammalian cells (HeLa cells and mouse endothelial H5V cells) were the two expression systems I used to express the intelectins. This work is detailed below.

2.2.1. Attempts to express intelectin in *Pichia pastoris*

Yeast is a common expression system for the production of recombinant proteins. The most widely used yeast species are *Pichia pastoris* and *Saccharomyces*.^{16, 17} Recently, *Pichia pastoris* has gained attention in both industry and academic research laboratories as an attractive host for the production of different proteins including complex membrane proteins,¹⁸ heterologous proteins and secreted proteins.^{19, 20} Using *Pichia pastoris* as an expression system has many advantages including a high yield of protein production ranging from milligrams to multiple grams protein per litre of culture.^{21, 22} Furthermore, the factors controlling protein production and scaling up, such as pH, feed rate and aeration, can be easily controlled.²³ When *Pichia pastoris* is compared to mammalian cells as an expression system, *Pichia pastoris* is generally more convenient as it requires simpler growth media and culture conditions.^{24, 25} There are a number of factors that make *Pichia pastoris* the host of choice when one wants to express heterologous proteins. Among those factors are the ability of *Pichia pastoris* to promote protein folding as well as post-translational modifications such as protein glycosylation and disulfide bond formation.¹⁴ Another advantage of *Pichia pastoris* is the availability of simple purification techniques for the secreted proteins due to the presence of low levels of contamination from other native secreted proteins.²⁶ Inspired by these advantages, I aimed to express hIntL using *Pichia pastoris*.

I initially chose pPIC9 as the vector for hIntL-1 expression in *Pichia pastoris*. For the structural details of the pPIC9 vector see **Figure 2.1**. The most significant region

in this vector is the AOX1 promoter site, as *Pichia pastoris* has two alcohol oxygenase enzymes (AOX1 and AOX2) that are²⁷ These enzymes allow *Pichia pastoris* to use methanol as its carbon source and drives protein expression.²⁸ In addition to the promoter site, there is the secretion signal site, which is required for protein secretion, and the ampicillin resistance gene, which is used for the selection of the colonies after transformation.²⁹

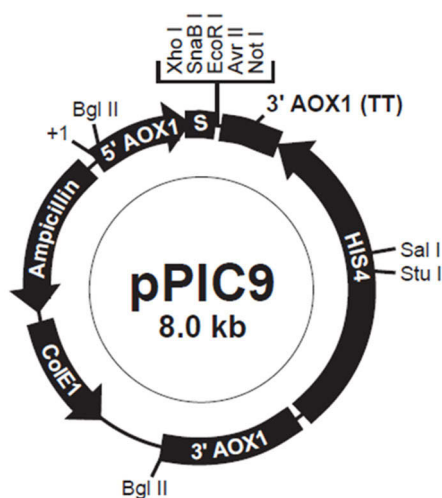


Figure 2.1: Structural details of the pPIC9 vector (adapted from Life Technologies).³⁰

The primers were designed and used to amplify the hIntL-1 (**Figure 2.2**) gene with 5' *EcoRI* site and 3' *NotI* sites for subcloning into pPIC9. The primers are as follows; **DssInt-E5'**: ATA TAT GAA TTC GCT GAA GAG AAC CTG GAC ACC, **DssInt-EH5'**: ATG CTA GAA TTC CAC CAT CAT CAT CAC CAC GCT GAA GAG AAC CTG GAC ACC, **Int-HSN3'**: ATA TAT GCG GCC GCT CAG TGA TGG TGA TGG TGG TGG CGA TAA AAC AGA AGC ACG GC, **Int-N3'**: ATA TAT GCG GCC GCT CAG CGA TAA AAC AGA AGC ACG G.

Oligos DssInt-E5' and Int-HSN3' were used to amplify DNA that codes hIntL-1 with a C-terminal His₆ tag (hIntL-H₆). Oligos DssInt-EH5' and Int-N3' were used to amplify the hIntL-1 gene with an N-terminal His₆ tag (H₆-hIntL). Both versions of hIntL-1 lack the mammalian signal sequence but contain the yeast secretory signal. Polymerase chain reaction (PCR) was used for hIntL-1 gene amplification. For the PCR reaction, I chose two different quantities of template DNA (1 ng and 5 ng) and explored the DNA quantity that worked best in terms of amplification levels.

```

ATGAACCAACTCAGCTTCCCTGCTGTTTCTCATAGCGACCACCAGAGGATGGAGTACAGAT
GAGGCTAATACTTACTTCAAGGAATGGACCTGTTCTTCGTCTCCATCTCTGCCAGAAGC
TGCAAGGAAATCAAAGACGAATGTCCTAGTGCATTTGATGGCCTGTATTTTCTCCGCACT
GAGAATGGTGTATCTACCAGACCTTCTGTGACATGACCTCTGGGGGTGGCGGCTGGACC
CTGGTGGCCAGCGTGCATGAGAATGACATGCGTGGGAAGTGCACGGTGGGCGATCGCTGG
TCCAGTCAGCAGGGCAGCAAAGCAGACTACCCAGAGGGGGACGGCAACTGGGCCAACTAC
AACACCTTTGGATCTGCAGAGGCGGCCACGAGCGATGACTACAAGAACCCTGGCTACTAC
GACATCCAGGCCAAGGACCTGGGCATCTGGCACGTGCCAATAAGTCCCCCATGCAGCAC
TGGAGAAACAGCTCCCTGCTGAGGTACCGCACGGACACTGGCTTCCCTCCAGACACTGGGA
CATAATCTGTTTGGCATCTACCAGAAATATCCAGTCAAATATGGAGAAGGAAAGTGTGG
ACTGACAACGGCCCCGGTGATCCCTGTGGTCTATGATTTTGGCGACGCCAGAAAACAGCA
TCTTATTACTCACCTATGGCCAGCGGGAATTCAGTGCAGGATTTGTTTCAGTTCAGGGTA
TTTAATAACGAGAGAGCAGCCAACGCCTTGTGTGCTGGAATGAGGGTCACCGGATGTAAC
ACTGAGCACCAGTGCATTGGTGGAGGAGGATACTTCCAGAGGCCAGTCCCCAGCAGTGT
GGAGATTTTCTGGTTTTGATTGGAGTGGATATGGAACATGTTGGTTACAGCAGCAGC
CGTGAGATAACTGAGGCAGCTGTGCTTCTATTCTATCGTTGA

```

Figure 2.2: hIntL-1 gene.

To purify the PCR products, agarose gel electrophoresis was used. A gel of the PCR products using 1 ng of the hIntL-1 template DNA is shown in **Figure 2.3i**. **Figure 2.3ii** shows the gel of the PCR products when 5 ng template DNA was tried using both hIntL-H₆ and H₆-hIntL. Both template DNA quantities (1 and 5 ng) exhibited the expected gene length at about 10 kb.

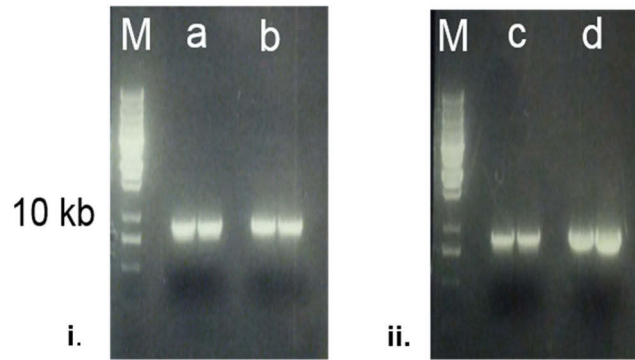


Figure 2.3: (i): DNA gel of PCR products for 1 ng DNA, (ii): 5 ng DNA
a, c: IntL-H₆, b, d: H₆-IntL.

The DNA in the corresponding bands was extracted from the gel and double digested using EcoRI and NotI restriction enzymes. The pPIC9 vector was subjected to the same digestion protocol. In addition to the restriction enzymes, shrimp alkaline phosphatase (SAP) enzyme was added to inhibit vector self-ligation. Then, agarose gel electrophoresis was used to separate the digested products. As illustrated in **Figure 2.4i**, the gel shows the PCR products before enzyme digestion, while **Figure 2.4ii** shows the enzyme digestion products of the circular pPIC9 vector (**e**), digested fragments using EcoRI (**f**), digested fragments using NotI (**g**) and double digestion using EcoRI and NotI in the presence of SAP (**h**).

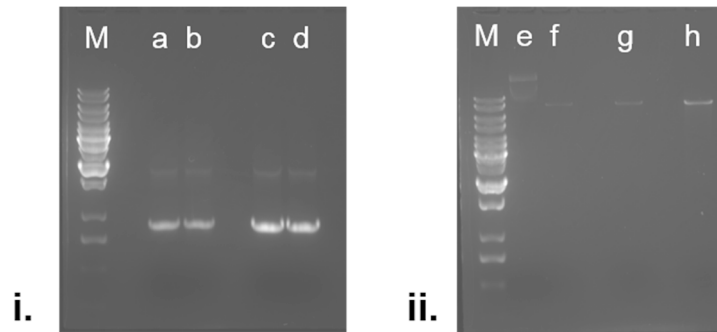


Figure 2.4: (i); PCR products before enzyme digestion, a, b: IntL-H₆, c, d: H₆-IntL, (ii); e: pPIC9, f: digestion with EcoRI, g: NotI, h: EcoRI, NotI, and SAP.

The gel bands corresponding to H₆-IntL, IntL-H₆, and pPIC9 were cut out and the DNA was extracted. The concentration of the DNA was measured and was shown to be 41.8 µg/mL, 62.7 µg/mL and 4.2 µg/mL for IntL-H₆, H₆-IntL, and the vector, respectively.

Then, ligation of the inserts, either H₆-IntL or IntL-H₆, with the vector was done. The ligation was carried out using T4 DNA ligase at both a 3:1 (H₆-IntL and IntL-H₆) and 1:1 (H₆-IntL and IntL-H₆) insert-to-vector ratio. The double digested vector with or without the addition of SAP was used as a positive control (no inserts were added). The ligated products were then transformed into competent DH5α cells. Unfortunately, after incubation overnight at 37 °C, there was no growth on the plates. One possible explanation for the lack of growth could be that the inserts were not digested properly using the EcoRI/NotI restriction enzymes, which made the insert fragments lack the complementary sites to ligate with the vector.

Because there could be a problem in the digestion, all the above steps including digestion, ligation and transformation were repeated. Surprisingly, only one agar plate showed one colony corresponding to IntL-H₆ insert. I thought that the amount of the used DNA was insufficient; therefore, I subjected all of the ligation reactions to DNA concentration and precipitation using sodium acetate and ethanol. Using this concentration protocol I hoped to ensure that I obtained enough DNA for the transformation. After DNA concentration, the ligated products were then transformed into DH5 α cells, which resulted in the growth of two colonies (IntL-H₆). I took a streak from these colonies and prepared liquid culture and another streak over a lysogeny broth (LB)/ampicillin plate. After incubation of the liquid culture at 37 °C overnight, the DNA was extracted using a miniprep protocol (QIAGEN). The DNA inserts were subjected to double digestion again with EcoRI and NotI restriction enzymes. The digested products were run over an agarose gel to determine their size (**Figure 2.5**).

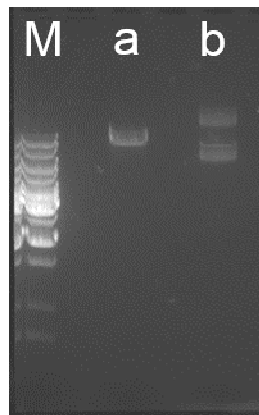


Figure 2.5: *a: Double digested DNA template (IntL-H₆), b: circular vector.*

To confirm that the pPIC9 vector was subcloned with the proper construct, I prepared a DNA sample for sequencing. Unfortunately, the results were not promising and revealed only the sequence of the vector without the insertion of the hIntL-1 construct. After many failed trials aimed to prepare the pPIC9 vector with the desired construct, I decided to use another vector, pJET1.2.

The pJET1.2 vector was used to facilitate the incorporation of hIntL-1 gene into pPIC9 using a sticky-end cloning protocol. Any DNA fragment, either with blunt or sticky ends, can be cloned using this vector. The pJET1.2 vector (**Figure 2.6**) contains a lethal gene, which, upon insertion of the gene for the protein to be expressed, is disrupted, so that only cells that have the recombinant vector can grow. This lethal gene is used as the selection parameter.

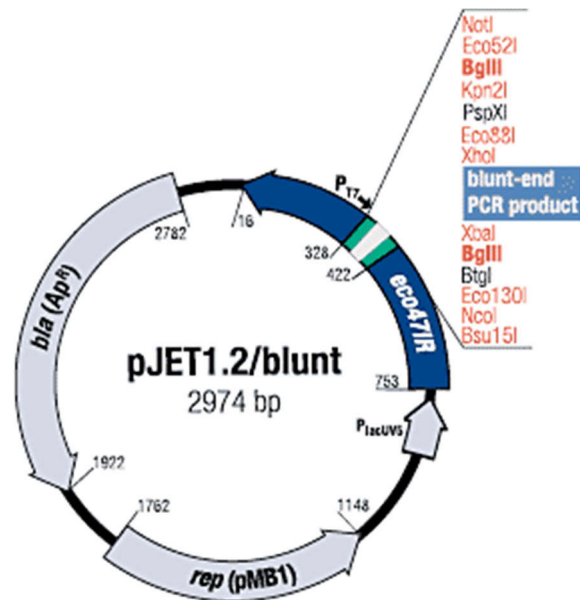


Figure 2.6: Map of pJET1.2/blunt cloning vector (MBI Fermentas).³¹

The purified hIntL-1 gene PCR products obtained previously were used to set up the sticky-end cloning protocol.³² The T4 DNA ligase was used for the ligation reactions. Then, the ligated products were transformed into DH5 α cells, where the positive control contained only the vector (no hIntL-1 gene added) and the negative control was wild-type cells.

Two agar plates, one with IntL-H₆ insert and the other with H₆-IntL insert, were incubated at 37 °C overnight. Many colonies grew on the two plates, which suggested that the cloning was successful. From each plate, six colonies were chosen randomly to culture on new plates and to prepare LB liquid cultures that would be used eventually for the DNA extraction. The pJET1.2/IntL vector was double digested using EcoRI/NotI, followed by agarose gel analysis (**Figure 2.7i and ii**).

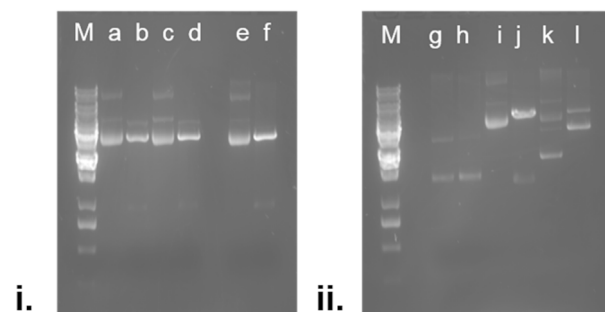


Figure 2.7: (i); *IntL-H₆*, a, c, e: inserts without digestion, b, d, f: double digested inserts, (ii); *H₆-IntL*, g, i, k: inserts without digestion, h, j, l: double digested inserts.

From the gel shown in **Figure 2.7i**, I wanted to check the DNA sequences from three colonies from IntL-H₆ (lanes a, c, e in the gel). On the other hand, the gel

resulting from the DNA isolated from colonies corresponded to H₆-IntL was not promising and showed possible contamination (**Figure 2.7ii**). Six sequencing reactions (representing the three colonies from IntL-H₆) were prepared; two reactions for each using either forward or reverse primers. The sequencing data showed that the DNA sequence of pJET1.2/IntL-H₆ (from colony **a** shown in **Figure 2.7i**) was as expected, which confirmed that the plasmid contained the desired construct. At this point, I tried to cut out the IntL-H₆ insert from the pJET1.2 vector to install it back to the pPIC9 vector, but I faced many problems. None of these experiments met my desired goal to clone the IntL gene into the pPIC9 vector. Due to all those challenges and limited time, I decided to focus on another expression system for hIntL-1 expression.

2.2.2. Intelectin expression in HeLa cells

HeLa cells were my next choice as an expression system for the intelectins. I first tried to express mouse intelectin instead of the human one. The mouse intelectin-2 (mIntL-2) gene was inserted into the pcDNA3.1 vector.¹ The gene includes a His₆ tag to facilitate protein purification. I followed the known reported protocols for the maintenance and growth of the HeLa cell line. I used Lipofectamine 2000 as the transfecting agent. After cell harvesting and purification of the cell lysate using a Ni-NTA column, the column eluate was evaluated by SDS-PAGE (**Figure 2.8**) to confirm protein purity as well as molecular weight. SDS-PAGE of mIntL showed

¹ The gene was prepared previously by Professor Christopher W. Cairo's group (University of Alberta).

one main band at 37 kDa. The protein yield was low, around 100 µg per 3 T75 flasks (45 mL).

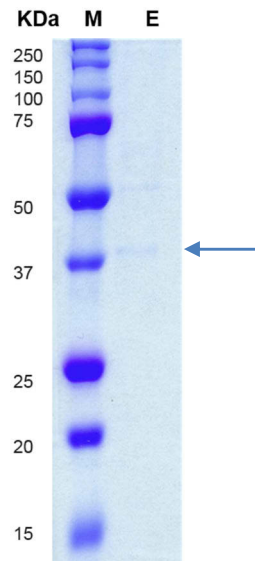


Figure 2.8: Coomassie stained 10% SDS-PAGE of mIntL-2 after purification using Ni-NTA column; M: Protein marker, E: mIntL-2 elution.

2.2.3. Intelectin expression in mouse endothelial H5V cell line

In late 2011, we were fortunate to have discussions with Professor Michael Pierce at the University of Georgia, whose group had successfully expressed the intelectins in the mouse endothelial H5V cell line. Professor Pierce was kind enough to share the recombinant cell line with us, which allowed me to express the protein. In my hands, the H5V cell line proved to be an effective expression system for both hIntL-1 and hIntL-2. Despite being effective at producing the protein, the expression was not straightforward as I had to optimize many conditions to produce a stable, active protein, which could be expressed in reasonable yield. The same protocols used for the maintenance and growth of HeLa cells were applied here for the H5V cells. Because hIntLs are secreted proteins, the media was used as the source of protein.

To facilitate later protein purification, I used low serum media (Optimem media), which contains low amount of proteins required for cellular growth. The desired protein was purified from the media using a Sepharose 6B column and SDS-PAGE was used to check the protein identity and purity. The protein yield was around 100 µg per 10 mL media, significantly higher than the amount of mIntL-2 that was produced in HeLa cells.

2.2.4. Characterization of hIntL-1 and hIntL-2

After obtaining pure protein as indicated by SDS-PAGE (**Figure 2.9**), it was necessary to confirm the protein identity and molecular weight. This was done by in-gel protein digestion followed by characterization of the protein band using LC/MS-MS. Protein reduction followed by alkylation were carried out before running the in-gel digestion protocol. Reduction, alkylation and in-gel digestion protocols were adapted from literature.³³

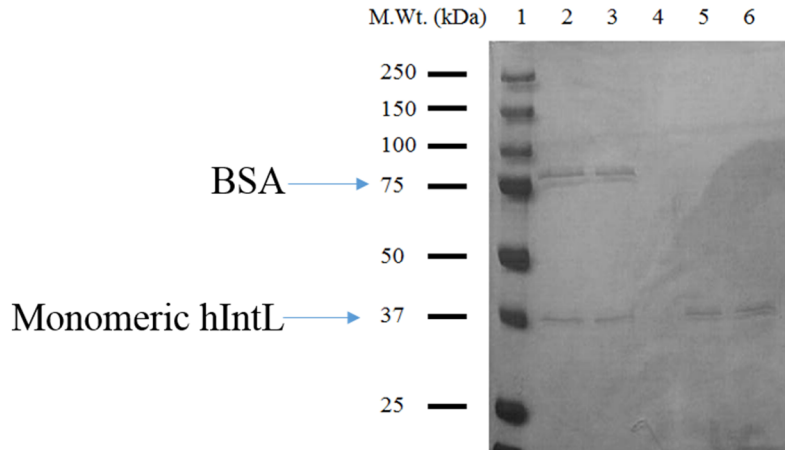


Figure 2.9: Coomassie stained 10% SDS-PAGE for hIntL-1 and hIntL-2; 1: ladder, 2: hIntL-1 wash, 3: hIntL-2 wash, 4: empty lane, 5: pure hIntL-1, 6: pure hIntL-2, BSA: bovine serum albumin

The digested gel bands for both hIntL-1 and 2 were characterized using LC/tandem mass at the mass spectrometry lab at the University of Alberta using Mascot search results. The band corresponding to 37 kDa in the SDS-PAGE (the predicted size of the protein) revealed a molecular weight of 35525 Da and showed 22% coverage (**Figure 2.10**) with human intestinal lactoferrin receptor (100% sequence similarity with hIntL-1).

1 MNQLSFLFL IATTRGWSTD EANTYFKEWI CSSSPSLPRS CK**EIKDECPS**
 51 **AFDGLYFLRT** ENGVIIYQTFI DMTSGGGGWT LVASVHENDM RGKCTVGDRW
 101 SSQQGSKADY PEGDGNWANY NTFGSAAEAT SDDYKNPGYY DIQAKDLGIW
 151 HVPNKSPMQH WRNSSLLRYR **TDTGFLQTLG HNLFGIYQKY** PVKYGEGKCW
 201 TDNGPVIPIV YDFGDAQK**TA SYSPYQRE FTAGFVQFRV** FNNERAANAL
 251 CAGMRVTGCN TEHHCIGGGG YFPEASPPQC GDFSGFDWSG YGTHVGYSSS
 301 **REITEAAVLL FYR**

Figure 2.10: Human intestinal lactoferrin receptor amino acid sequences with matched peptides shown in bold red.

To summarize, different expression systems were used to express either human or mouse intelectins. I was not able to clone hIntL gene in the *Pichia pastoris* vector and hence was not able to express hIntL in *Pichia pastoris*. On the other hand, both HeLa and H5V cells worked well as expression systems for mIntL-2 and hIntLs (hIntL-1 and hIntL-2), respectively. The mIntL-2 obtained from HeLa cells was expressed as the His-tagged protein and hence was purified using a Ni-NTA column. On the other hand, both hIntL-1 and 2 expressed in H5V cells were purified using Sepharose 6B column, and the protein purity and identity were confirmed through SDS-PAGE as well as LC-MS.

2.3. Experimental procedures

2.3.1. Preparation of pPIC9/hIntL construct

2.3.1.1. Polymerase Chain Reaction (PCR) for hIntL-1 gene

The hIntL-1 gene was prepared and the primers were designed for the PCR reactions. Two PCR reactions (each using two different amounts of DNA) were done using the above primers to amplify the hIntL-1 gene; one with the His tag on the C-terminus (IntL-H₆) and the other with the His tag on the N-terminus (H₆-

IntL). PCR was done using the following temperature gradient, where the cycle started at 94 °C for 2.5 min, followed by 52 °C for 30 sec and then 68 °C for 54 sec followed by 5 min at 68 °C. The cycle was held at 4 °C for 2 h at the end. This cycle was repeated 30 times.

2.3.1.2. DNA extraction

Bands were cut from the gel and the DNA was extracted using the QIAquick (Thermo Scientific) DNA extraction protocol. DNA fragments were placed in clean Eppendorf tube and weighed. QG buffer (300 µL 5.5 M guanidine thiocyanate, 20 mM Tris HCl pH 6.6) were added at three times the measured volume (100 µL) of the gel. The Eppendorf tubes were placed in the heat block and incubated at 50 °C for 10 min to dissolve the gel. After the gel was dissolved, 100 µL isopropanol were added to each tube. This last step was essential to increase the yield of the extracted DNA. Then, the DNA sample was placed in the QIAquick spin column and was centrifuged for 1 min. The flow-through was discarded and the spin column was washed with 0.5 mL QG buffer and centrifuged for another 1 min. Wash buffer (0.75 mL, 1.0 M NaCl, 50 mM MOPS pH 7.0, 15% isopropanol) was added followed by centrifugation for 1 min. The flow-through was discarded. The spin column was centrifuged for 1 min to ensure that all traces of the wash buffer were removed. Then, the QIAquick column was placed in a clean tube and of elution buffer (50 µL, 1.25 M NaCl, 50 mM Tris-HCl pH 8.5, 15% isopropanol) were added. The column was then centrifuged at maximum speed for 1 min to elute the DNA (H₆-IntL and IntL-H₆) into Eppendorf collecting tubes.

2.3.1.3. DNA transformation into DH5 α competent cells

DH5 α competent cells were thawed in an ice–water mixture. Ten empty tubes were placed on ice (8 tubes for the ligation reactions, as well as positive and negative controls). Into each tube DH5 α cells (50 μ L) were added. In the positive control tube, pPIC9 vector (1 μ L of a 1 ng/ μ L solution) was added. The negative control tube only contained the DH5 α cells (no DNA added). In the remaining tubes, an aliquot (5 μ L) from each ligation reaction was added. The tubes were mixed thoroughly and then kept on ice for 30 min. The tubes were then subjected to heat shock at 42 °C for 90 sec in the water bath, followed by cooling in ice water for 2 min. In an aseptic area, LB media (950 μ L) was transferred into each tube. The tubes were then incubated at 37 °C for 45 min with shaking and then centrifuged at 16000 x g for 1 min to pellet the cells. A portion of the LB media was discarded leaving behind about 200 μ L. The cells were re-suspended by pipetting up and down until a homogenous mixture was obtained. Agar–ampicillin plates were used for the transformation, which was started by transferring an aliquot of the cell suspension (50 μ L) into each agar plate. Then, the agar plates were incubated at 37 °C overnight and checked for colonies growth the next day.

2.3.1.4. DNA concentration using sodium acetate and ethanol

In each ligation tube, 3 M sodium acetate (20 μ L) was added followed by the addition of 95% ethanol (450 μ L). The tubes were cooled on ice for 15 min and then centrifuged for 15 min at 4 °C. The supernatant was aspirated using a glass pipette. Into each tube 70% ethanol (1 mL) was added and the mixture was

centrifuged again for 5 min at 4 °C. The ethanol was aspirated and the pellets were allowed to air dry. Finally, water (5 µL) was added into each tube followed by heat shock at 65 °C for 5 min.

2.3.2. mIntL-2 expression in HeLa cells

2.3.2.1 Maintenance of HeLa cell line

i) Thawing of HeLa cells

One vial containing HeLa cells was thawed in a water bath at 37 °C for 2 min. The cells were then transferred into a 15 mL centrifuge tube, and Dulbecco's modified Eagle's medium (DMEM, 10 mL) with 10% fetal bovine serum (Hyclone) was added and the mixture mixed well by a glass pipette. Then, the cell mixture was centrifuged for 2 min at 1200 rpm at room temperature. After centrifugation, the old media was discarded using a glass pipette and fresh DMEM (2 mL) was added and the solution was mixed gently. Into two T75 flasks, fresh DMEM (20 mL) was added and the cell mixture (1 mL, cells and media) was added into each flask. The cells were then checked under a microscope to ensure that there was minimal aggregation and that most of the cells were present as single cells. The flasks were left in the incubator at 37 °C and were checked for proper growth within 1–2 days. Usually, the cells were ready for passage after 2–3 days of incubation.

ii) Passage of HeLa cells:

DMEM enriched with 10% FBS, 0.25% Trypsin/EDTA (T/E) (Life Technologies), 10 mM phosphate buffered saline (PBS, 137 mM NaCl, 2.7 mM KCl, 10 mM Na₂HPO₄, 2 mM KH₂PO₄, pH 7.4) (Sigma) were pre-warmed in a water bath at 37

°C. New T75 flasks were prepared for the new cell passage by adding fresh DMEM (15 mL) containing 10% FBS. The old media was aspirated by glass pipette using vacuum. PBS (5 mL) was used to wash each flask and make sure that no old media remained. The PBS wash was discarded. In each flask, T/E solution (3 mL) were added and the flask was incubated at 37 °C for 3 min. Fresh DMEM media containing 10% FBS (10 mL) was added to the flask and the solution was mixed well with the detached cells. The cell suspension was then transferred into a 15 mL centrifuge tube and was centrifuged at 1200 rpm for 2 min. After centrifugation, the cells were pelleted and the media was discarded. To the cell pellet, DMEM media (2 mL) was added and mixed gently by pipetting up and down until a homogenous cell suspension was obtained. The cell suspension (1 mL) was added into the new T75 flask and mixed gently. The passaged cells were checked under microscope to check that the cell suspension was well dispersed. The flasks were then incubated at 37 °C for growth prior to mIntL-2 gene transfection.

2.3.2.5. Mouse intelectin (mIntL-2) gene transfection

The mIntL-2 gene was transfected into HeLa cells using Lipofectamine 2000 (Invitrogen). Passage of the HeLa cells was done one day before transfection. Cells were checked for high confluency before transfection took place. A 90% confluency level was reached, which was recommended by the Invitrogen protocol. HeLa cells were pre-incubated with DMEM (no FBS added) at 37 °C for 30 min. The mIntL-2 DNA plasmid (5 mL) was diluted using serum free medium (DMEM) where the total volume was about 50 µL. Lipofectamine 2000 (7.5 µL) was diluted

with DMEM (42.5 μ L) to reach a total volume of 50 μ L. Both the plasmid and the Lipofectamine solutions were left at room temperature for 5 min. The two mixtures were mixed gently and allowed to stand for 20 min at room temperature. Then, the DNA and Lipofectamine 2000 mixture was added into the pre-incubated HeLa cells in DMEM. The cells were then incubated at 37 °C and after 2.5 h, the medium was changed into complete growth medium (DMEM with 10% FBS). The cells were imaged under a microscope 24–48 h later after transfection to check for dispersion of the cell suspension cell viability.

2.3.2.6. Harvesting HeLa cells

After transfection, old media was removed in a centrifuge tube and the T75 flasks were washed with PBS and the PBS wash was collected with the old media. For each T75 flask, 2 mL lysis buffer (50 mM NaH_2PO_4 , 300 mM NaCl, 10 mM imidazole and 0.05% Tween) were added. The cellular lysates were collected from all the flasks and were sonicated for 4 min using a cell sonicator followed by centrifugation of the mixture at 13800 rpm. The lysates were concentrated using spin column (MWCO 10 kD) and centrifuged at 13800 rpm for 30 min. The concentrated lysate was dialyzed overnight in HEPES buffer (10 mM HEPES, 1 mM CaCl_2 , 150 mM NaCl, 0.005% surfactant P20, pH 7.4). The His-tagged mIntL-2 protein was isolated and purified from the cellular lysate using Ni-NTA agarose bead suspension (Qiagen).

2.3.3. Intelectin expression in mouse endothelial cells (H5V)

i) Construction of pTracer/hIntLs expression plasmid²

cDNA encoding the open reading frame of hIntLs was cloned by reverse transcription-polymerase chain reaction (PCR). Primers were designed on the basis of a reported hIntL-1 sequence,³⁴ as follows: (5'-CCACTAGTATTACAATGAACCAACTCAGCTTCC-3' and (5'-CCTCTAGACTCTCAACGATAGAATAGAAGCACA-3'). cDNA was synthesized using previously isolated hIntL-1 clone from human small intestinal total RNA.³⁴ A single band was amplified by PCR using these primers, cDNA, and Platinum Polymerase High Fidelity (Invitrogen Inc.) (35 cycles, 94 °C for 30 s, 60 °C for 30 s, and 72 °C for 60 s). The PCR product was digested with enzymes, SpeI and XbaI and cloned into the pTracer vector. The DNA sequence was confirmed by the University of Georgia Molecular Genetics Instrumentation Facility.

ii) hIntL-1 expression

The pTracer/ hIntL-1 expression plasmid cDNA was transfected into H5V cells, polyoma middle T transformed mouse heart endothelial cell line, using Lipofectamine 2000 (Invirogen, Inc.). Stable cells expressing hIntL-1 were isolated by using green fluorescent protein (GFP) which was sorted by applying fluorescence-activated cell sorting (FACS) technique. The stable cells were cultured in 15 mL Dulbecco's modified Eagle's medium (DMEM) with 10% fetal

² The preparation of both intelectin genes and transformation into the H5V cell line were done by Dr. Michael Pierce's group, Complex Carbohydrate Research Center, University of Georgia.

bovine serum (Hyclone) for 2 days and then cells were incubated in 15 mL Optimem (Invitrogen, Inc.) for 3 days at 37 °C. During the first 1–2 days, the cells were checked under a microscope for proper growth and confluency. After 3–4 days, the media-containing the protein were collected and then either purified by affinity column or stored at –80 °C for later purification.

iii) hIntL-1 purification using affinity sepharose 6B column

First, a column (75 mL) was loaded with 50 mL Sepharose 6B resin (Sigma) and then equilibrated using equilibration buffer (150 mL, 20 mM Tris, 10 mM CaCl₂, 0.05% Tween 20 and pH 7.4) at a flow rate 2 mL/min. Equilibration was followed by loading the column with culture media after adding 10 mM CaCl₂, 0.05% Tween 20 and 150 µL protease inhibitor (Thermo Scientific) into the media. The flow through was collected at a flow rate 1 mL/min, followed by column washing with 150 mL of washing buffer (the same buffer composition as the equilibration buffer). Protein elution was started by eluting with 50 mL of the elution buffer (20 mM Tris, 100 mM ribose 0.05% Tween 20 and pH 7.4). The eluted fractions (5 mL each) were collected at a flow rate 1 mL/min and the A₂₈₀ was measured for each fraction.

The required gel bands were cut and placed in 2 mL Eppendorf tubes. A fresh solution of 20 mM dithiothreitol (DTT) in 100 mM ammonium bicarbonate was prepared. From the later solution, 100 µL were added on the gel bands and was incubated at 60 °C for 1 h. The DTT solution was discarded and 55 mM iodoacetamide (IAM, 100 µL) in 100 mM ammonium bicarbonate. The tubes were

incubated at room temperature for 45 min in the dark. The IAM solution was removed and the gels were rinsed with 100 mM ammonium bicarbonate for 10 min, followed by rinsing with acetonitrile for another 10 min. The later rinsing procedure was repeated twice and then the gels were dried for 30 min using the speed vac.

After drying the gel bands on a speed vac under vacuum, in-gel digestion was carried out. First, a trypsin solution was prepared by adding Promega sequencing grade trypsin (20 µg) to 50 mM ammonium bicarbonate solution (1 mL). An aliquot of this trypsin (50 µL, enough to cover the gel slices) was added to each gel slice and the mixture was incubated for 45 min on ice. The tubes were placed in a shaker and incubated at room temperature overnight. The solution was removed from each tube and placed in a low binding microcentrifuge tubes (Sigma) to minimize peptide binding to the surface of the tube. Into the tubes containing the gel slices an aqueous solution of 5% acetonitrile–0.1% TFA (50 µL) were added and the tubes were shaken at room temperature for 15 min. The last step was repeated twice and the solutions were pooled into the overnight digestion solutions. Finally, an aqueous solution of 50% acetonitrile/0.1% TFA (50 µL) was added to the gel slices with shaking for 15 min and the solutions were collected with the previous eluates. The eluates were dried to about 10 µL on a speed vac, transferred to an autosampler vial and stored at –80 °C.

iv) Checking the protein molecular weight and purity using SDS–PAGE
Denaturing SDS–PAGE and Coomassie staining were done according to the Mini-

protein 3 cell instruction manual from BioRad.³⁵ 10% SDS-PAGE gel was used. The gels ran at 200 V (constant V) for about 40 min, followed by staining in 100 mL Coomassie stain solution in a plastic container. Then, the container was placed in the microwave on high power for 1 min. The gels were shaken gently for 5 min and then the stain was poured off and 100 mL destain solution (7.5% acetic acid 10% ethanol) were added. The gels were left in the destaining solution overnight until the desired level of destaining was reached.

v) LC-MS/MS

The digested peptides were dissolved in water with 0.1% formic acid and then subjected to LC-MS/MS analysis on a UPLC (Waters, Milford, MA) coupled with q-ToF premier mass spectrometer (Waters, Milford, MA). **Table 2.1** shows the eluent gradient as well as the flow rate.

Table 2.1: Eluent gradient and flow rates used in the LC–MS/MS analysis, A: water with 0.1% formic acid, B: acetonitrile with 0.1% formic acid.

Time (min)	Flow rate (µL/min)	A%	B%
0.00	0.350	98.0	2.0
2.00	0.350	94.0	6.0
25.00	0.350	75.0	25.0
40.00	0.350	55.0	45.0
45.00	0.350	25.0	75.0
50.00	0.350	5.0	95.0
55.00	0.500	5.0	95.0

MS/MS data were analyzed through proteomic software called Mascot (version 2.2, Matrix Science).

2.4. Conclusion

In this chapter, the different expression systems I attempted to use for the recombinant intelectin expression were discussed. As outlined above, I did not investigate the use of *E. coli* as I did not consider it to be a suitable expression system for intelectins. During my attempts to express hIntL in *Pachia pastoris*, I initially used pPIC9 as the cloning vector. Later, the pJET1.2 vector was used as an alternate way to clone hIntL. Unfortunately, after significant effort was made to optimize the conditions and procedures, I was unable to clone the desired gene into the pPIC9 vector and turned to using alternative hosts.

The two mammalian expression systems (HeLa and H5V cells) proved to be effective. mIntL and hIntL were expressed in HeLa cells and H5V, respectively. Comparing HeLa cells and H5V for intelectin expression, I found that H5V was better and afforded higher protein yield. A Sepharose 6B column was used for hIntLs purification and the proteins were eluted from the column upon treatment with buffer containing 100 mM ribose. SDS-PAGE as well as LC-MS spectrometry were used for hIntL-1 and hIntL-2 characterization.

2.5. References

1. Chu, L.; Robinson, D. K., Industrial choices for protein production by large-scale cell culture. *Current Opinion in Biotechnology* **2001**, *12*, 180-187.
2. Berlec, A.; Strukelj, B., Current state and recent advances in biopharmaceutical production in *Escherichia coli*, yeasts and mammalian cells. *Journal of Industrial Microbiology & Biotechnology* **2013**, *40*, 257-274.
3. Chadd, H. E.; Chamow, S. M., Therapeutic antibody expression technology. *Current Opinion in Biotechnology* **2001**, *12*, 188-194.
4. Prazeres, D. M. F.; Ferreira, G. N. M.; Monteiro, G. A.; Cooney, C. L.; Cabral, J. M. S., Large-scale production of pharmaceutical-grade plasmid DNA for gene therapy: problems and bottlenecks. *Trends in Biotechnology* **1999**, *17*, 169-174.
5. Walsh, G., Biopharmaceutical benchmarks 2010. *Nature Biotechnology* **2010**, *28*, 917-924.
6. Goodman, M., MARKET WATCH Sales of biologics to show robust growth through to 2013. *Nature Reviews Drug Discovery* **2009**, *8*, 837-837.
7. Baneyx, F., Recombinant protein expression in *Escherichia coli*. *Current Opinion in Biotechnology* **1999**, *10*, 411-421.
8. Swartz, J. R., Advances in *Escherichia coli* production of therapeutic proteins. *Current Opinion in Biotechnology* **2001**, *12*, 195-201.
9. Demain, A. L., Small bugs, big business: The economic power of the microbe. *Biotechnology Advances* **2000**, *18*, 499-514.

10. Tsuji, S.; Uehori, J.; Matsumoto, M.; Suzuki, Y.; Matsuhisa, A.; Toyoshima, K.; Seya, T., Human intelectin is a novel soluble lectin that recognizes galactofuranose in carbohydrate chains of bacterial cell wall. *J. Biol. Chem.* **2001**, *276*, 23456-23463.
11. Lee, J. K.; Baum, L. G.; Moremen, K.; Pierce, M., The X-lectins: A new family with homology to the *Xenopus laevis* oocyte lectin XL-35. *Glycoconjugate Journal* **2004**, *21*, 443-450.
12. Wrackmeyer, U.; Hansen, G. H.; Seya, T.; Danielsen, E. M., Intelectin: A novel lipid raft-associated protein in the enterocyte brush border. *Biochemistry* **2006**, *45*, 9188-9197.
13. Singh, S. M.; Panda, A. K., Solubilization and refolding of bacterial inclusion body proteins. *Journal of Bioscience and Bioengineering* **2005**, *99*, 303-310.
14. Lin Cereghino, G. P.; Sunga, A. J.; Lin Cereghino, J.; Cregg, J. M., Expression of foreign genes in the yeast *Pichia pastoris*. *Genetic engineering* **2001**, *23*, 157-69.
15. Knappskog, S.; Ravneberg, H.; Gjerdrum, C.; Trosse, C.; Stern, B.; Pryme, I. F., The level of synthesis and secretion of *Gaussia princeps* luciferase in transfected CHO cells is heavily dependent on the choice of signal peptide. *Journal of Biotechnology* **2007**, *128*, 705-715.
16. Bill, R. M., Yeast - a panacea for the structure-function analysis of membrane proteins? *Current Genetics* **2001**, *40*, 157-171.

17. Gelperin, D. M.; White, M. A.; Wilkinson, M. L.; Kon, Y.; Kung, L. A.; Wise, K. J.; Lopez-Hoyo, N.; Jiang, L. X.; Piccirillo, S.; Yu, H. Y.; Gerstein, M.; Dumont, M. E.; Phizicky, E. M.; Snyder, M.; Grayhack, E. J., Biochemical and genetic analysis of the yeast proteome with a movable ORF collection. *Genes & Development* **2005**, *19*, 2816-2826.
18. Freigassner, M.; Pichler, H.; Glieder, A., Tuning microbial hosts for membrane protein production. *Microbial Cell Factories* **2009**, *8*.
19. Reilander, H.; Weiss, H. M., Production of G-protein-coupled receptors in yeast. *Current Opinion in Biotechnology* **1998**, *9*, 510-517.
20. Sarramegna, V.; Talmont, R.; Demange, P.; Milon, A., Heterologous expression of G-protein-coupled receptors: comparison of expression systems from the standpoint of large-scale production and purification. *Cellular and Molecular Life Sciences* **2003**, *60*, 1529-1546.
21. Macauley-Patrick, S.; Fazenda, M. L.; McNeil, B.; Harvey, L. M., Heterologous protein production using the *Pichia pastoris* expression system. *Yeast* **2005**, *22*, 249-270.
22. Wegner, G. H., Emerging applications of the methylotrophic yeasts. *Fems Microbiology Letters* **1990**, *87*, 279-283.
23. Higgins, D. R.; Cregg, J. M., Introduction to *Pichia pastoris*. In *Methods in Molecular Biology; Pichia protocols*, Higgins, D. R.; Cregg, J. M., Eds. 1998; Vol. 103, pp 1-15.
24. de Jong, L. A. A.; Grunewald, S.; Franke, J. P.; Uges, D. R. A.; Bischoff, R., Purification and characterization of the recombinant human dopamine

- D2S receptor from *Pichia pastoris*. *Protein Expression and Purification* **2004**, *33*, 176-184.
25. Cereghino, G. P. L.; Cereghino, J. L.; Ilgen, C.; Cregg, J. M., Production of recombinant proteins in fermenter cultures of the yeast *Pichia pastoris*. *Current Opinion in Biotechnology* **2002**, *13*, 329-332.
 26. White, J. F.; Trinh, L. B.; Shiloach, J.; Grisshammer, R., Automated large-scale purification of a G protein-coupled receptor for neurotensin. *Febs Letters* **2004**, *564*, 289-293.
 27. Cereghino, G. P. L.; Cereghino, J. L.; Sunga, A. J.; Johnson, M. A.; Lim, M.; Gleeson, M. A. G.; Cregg, J. M., New selectable marker/auxotrophic host strain combinations for molecular genetic manipulation of *Pichia pastoris*. *Gene* **2001**, *263*, 159-169.
 28. Ahmad, M.; Hirz, M.; Pichler, H.; Schwab, H., Protein expression in *Pichia pastoris*: recent achievements and perspectives for heterologous protein production. *Appl. Microbiol. Biotechnol.* **2014**, *98*, 5301-5317.
 29. Cereghino, J. L.; Cregg, J. M., Heterologous protein expression in the methylotrophic yeast *Pichia pastoris*. *Fems Microbiology Reviews* **2000**, *24*, 45-66.
 30. http://tools.lifetechnologies.com/content/sfs/manuals/pich_man.pdf,
Accessed on October 5, 2011.
 31. <http://www.thermoscientificbio.com/fermentas/>, *Accessed on May 7, 2014.*
 32. <http://www.thermoscientificbio.com/>, *Accessed on May 10, 2014.*
 33. <http://www.piercenet.com/instructions/>, *Accessed on April 28, 2014.*

34. Lee, J. K.; Schnee, J.; Pang, M.; Wolfert, M.; Baum, L. G.; Moremen, K. W.; Pierce, M., Human homologs of the *Xenopus* oocyte cortical granule lectin XL35. *Glycobiology* **2001**, *11*, 65-73.
35. <http://www.bio-rad.com/>, Accessed on April 5, 2014.

3. Synthesis of the Target Oligosaccharides

3.1. Introduction

Although there are reports showing that human intelectin has a binding preference for Gal β -containing oligosaccharides,¹ to date there is no detailed quantitative information about the nature of this interaction or the affinity of this lectin for different ligands. Inspired by this fact, we decided to obtain better understanding about the binding specificity and affinity of intelectin, which could help to identify its biological role. To gain this information it was critical to get access to Gal β -containing oligosaccharides to be used as potential ligands for intelectin. Obtaining these oligosaccharides from natural sources (bacteria, fungi, or protozoa) was not an ideal method, due to many challenges including difficulties in obtaining pure fragments in milligram quantities, and the requirement to work with microorganisms that, in some cases, are highly pathogenic. Alternatively, we could obtain these oligosaccharides via chemical synthesis in pure form and in the amount needed for the desired biochemical studies.

Before going through the detailed synthetic procedures used to obtain my target compounds **3.1–3.9 (Figure 3.1)**, I will discuss briefly the different routes reported in the literature to synthesize furanosyl glycosides with special focus on Gal β -containing molecules.

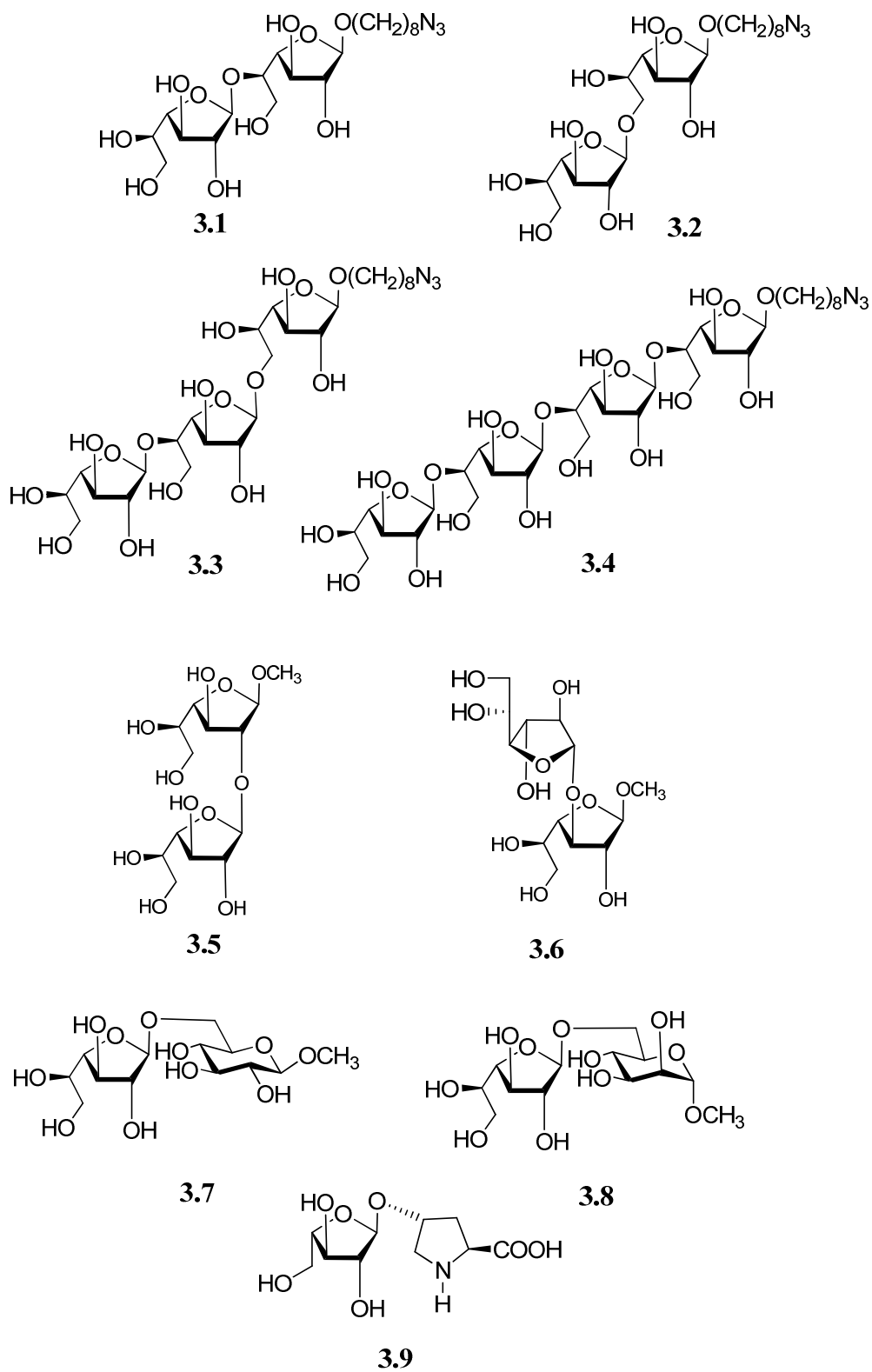
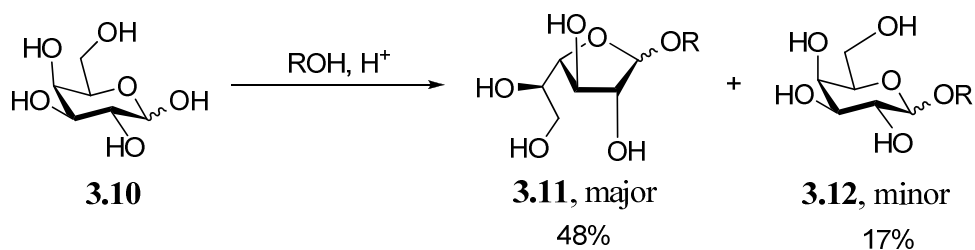


Figure 3.1: Structures of the target Compounds (3.1–3.9).

3.1.1. General methods used to obtain Galf derivatives

3.1.1.1. Fischer glycosylation

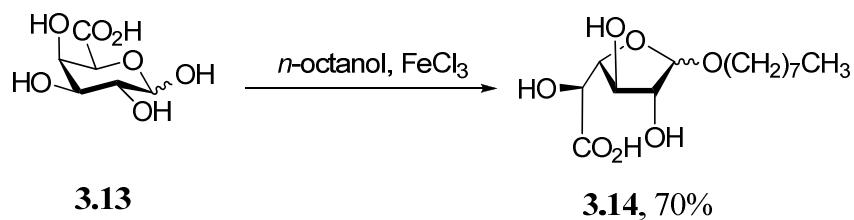
Fischer glycosylation is the most widely used method to obtain furanosides as the major sugar isomer. This method involves reacting an unprotected reducing sugar with an alcohol in an acid catalyzed reaction²⁻⁵ (**Scheme 3.1**). When galactose (**3.10**) is subjected to these conditions under kinetic conditions,⁶ galactofuranosides (e.g., **3.11**) can be isolated as the major product (48%, **Scheme 3.1**) from this reaction. However, reaction conditions need to be optimized in order to obtain furanosides in high yields with minimum pyranoside (e.g., **3.12**) formation. Although Fischer glycosylation is a simple method pyranoside by-products (**3.12**, 17%, **Scheme 3.1**) are formed which reduces the yield and can complicate purification.^{7, 8}



Scheme 3.1: Fischer glycosylation reaction.

Furthermore, Ferrières *et al*⁷ reported that when uronic acids e.g., D-galacturonic acid **3.13** was glycosylated with long chain alcohols (*n*-octanol, *n*-dodecanol or 10-undecen-1-ol), the products were mainly in the furanose form. The production of this alkyl D-galactofuranosiduronic acid **3.14** was catalyzed by Lewis acids including FeCl₃ or BF₃·OEt₂, (**Scheme 3.2**). The authors also found that the use of

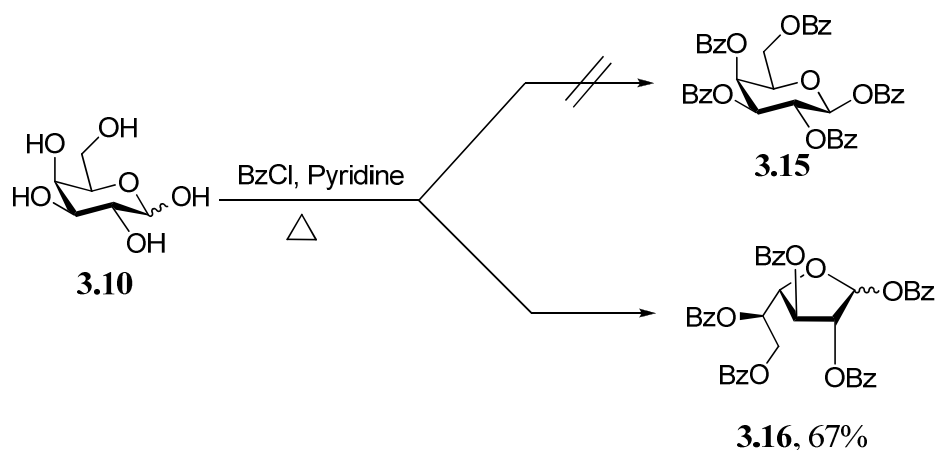
complexing agents such as CaCl₂ could affect both chemoselectivity and anomeric stereoselectivity of these products.



Scheme 3.2: Using long chain alcohol in the glycosylation of D-galacturonic acid.

3.1.1.2. Peracylation at high temperature

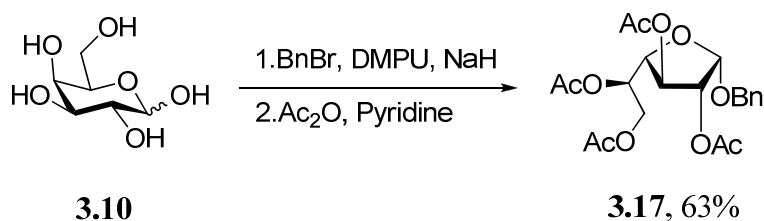
In a work done by D'Accorso *et al.*,⁹ they intended to synthesize 1,2,3,4,6-penta-*O*-benzoyl-β-D-galactopyranose (**3.15**, **Scheme 3.3**) upon treating D-galactose with benzoyl chloride in pyridine at high temperature. Instead, surprisingly, the main product was 1,2,3,5,6-penta-*O*-benzoyl-α/β-D-galactofuranose (**3.16**). The furanose ring structure was confirmed by both ¹H NMR and ¹³C NMR spectroscopy. A disadvantage of this method is the moderate yield of the produced Gal_f derivative. The main advantage is the synthesis of a protected Gal_f derivative in one step.



Scheme 3.3: Perbenzoylation of galactose under high temperature.

3.1.1.3. Base-catalyzed glycosylations

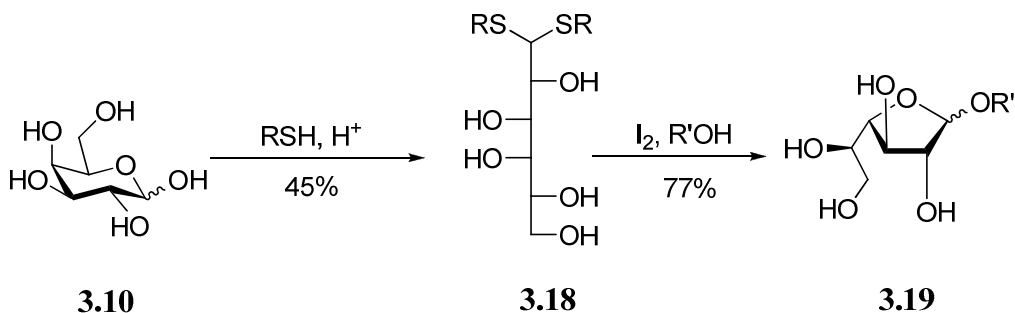
Schmidt and coworkers¹⁰ have shown that alkyl hexosides can be synthesized starting from free hexoses, using an electrophilic reagent and strong base in *N,N'*-dimethylpropyleneurea (DMPU) as the solvent. This method was efficient in obtaining α -D-galactofuranoside **3.17** in 63% yield without any contamination with the β -anomer, (**Scheme 3.4**). The preparation of *n*-pentenyl hexofuranosides could be also achieved if the alkyl chain is replaced by a pentenyl chain.⁸ This method offers the synthesis of a Galf derivative selectively protected at the anomeric position, which made these building blocks important starting materials in many oligosaccharide syntheses. Also, the anomeric control is an important advantage of this method. However, the moderate yield limits the widespread use of this method.



Scheme 3.4: Base-catalyzed glycosylation of D-galactose.

3.1.1.4. Cyclization of dithioacetals

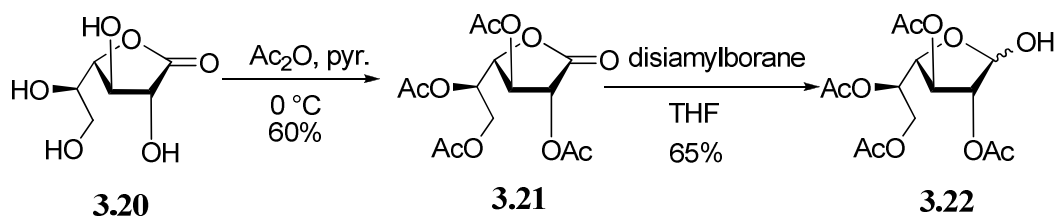
This method (**Scheme 3.5**) involves treating a reducing sugar with a thiol in the presence of an acid¹¹ to generate a dithioacetal (e.g., **3.18**). Next, cyclization of the dithioacetal with either mercuric salts¹² or iodine in the presence of an alcohol leads to the glycoside.^{13, 14} The main advantage of this method is that the glycoside could be obtained exclusively in the furanoside form¹⁵ in reasonable yield (77%) as shown is **Scheme 3.5**. The advantage of using iodine over the mercuric salts is the avoidance of toxic heavy metals.¹⁵



Scheme 3.5: Synthesis of galactofuranoside 3.19 by iodine-catalyzed cyclization of dithioacetal.

3.1.1.5. Reduction of galactonolactones

Kohn and coworkers¹⁶ explored the use of D-galactolactone as a potential starting material for the synthesis of Galf units. Acetylation of the commercially available D-galactonolactone (**3.20**, **Scheme 3.6**) afforded the tetracetylated intermediate **3.21** in 60% yield. The later compound was subjected to reduction conditions using disiamylborane to afford Galf derivative **3.22** in 65% yield. The main disadvantages of this method are the use of expensive starting materials: D-galactolactone and disiamylborane. Furthermore, the Galf derivative **3.22** was obtained in moderate yield (65%), which could be a limitation for large scale reactions.



Scheme 3.6: Reduction of galactonolactone using disiamylborane.

3.2. Synthetic strategies for the synthesis of the target compound (3.1–3.9)

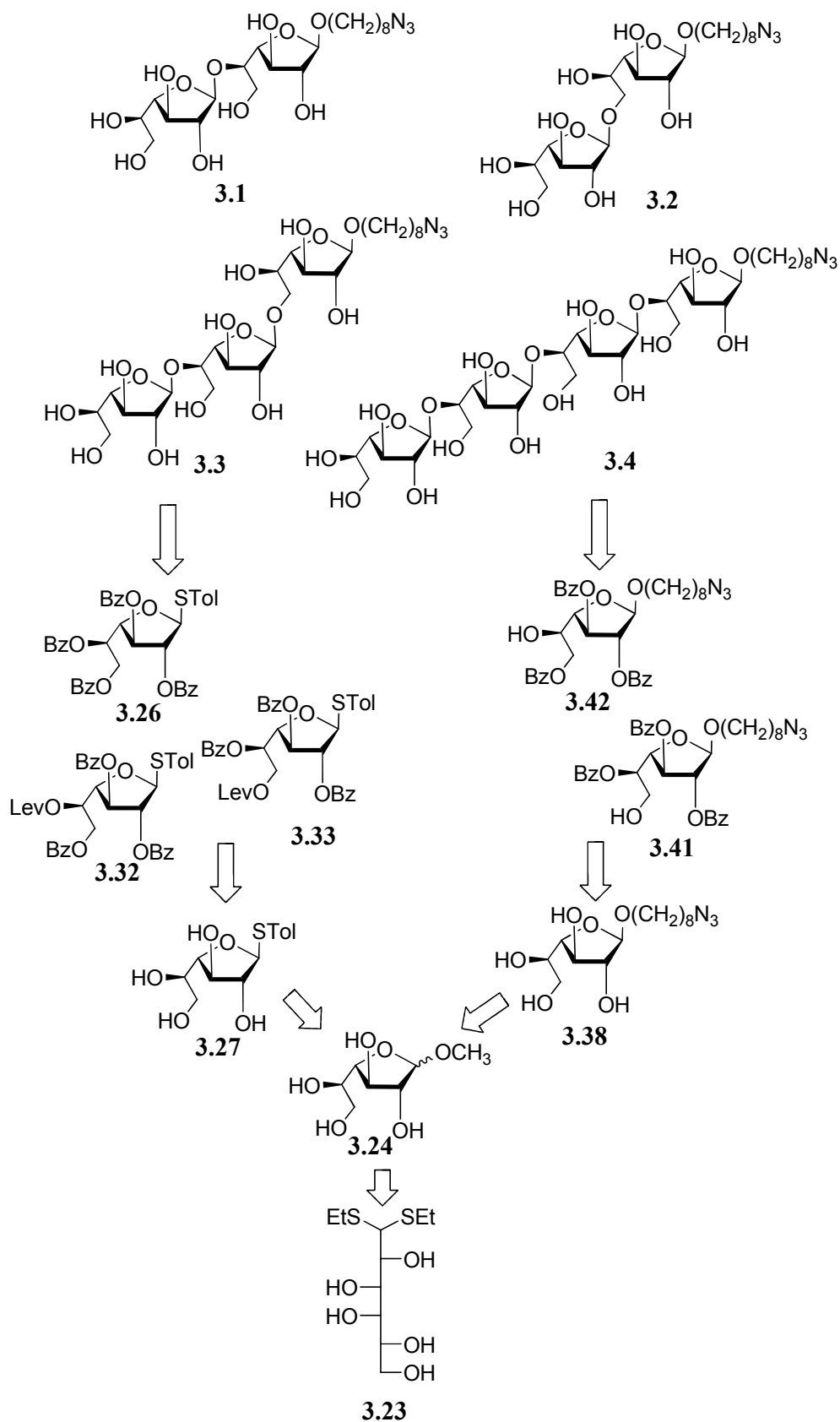
As highlighted in the introduction chapter, the main aim of this project is to study the binding specificity of intelectin, and to achieve this aim I needed to synthesize a number of Gal f -containing oligosaccharides (**Figure 3.1**) that differ in their types of linkages and the number of Gal f units. It was important to design compounds that are analogues of naturally occurring molecules in microorganisms (bacteria, fungi or protozoa) to obtain a better idea about the biological role of intelectin towards those different motifs.

To facilitate the discussion of the different strategies used for the synthesis of the target oligosaccharides, the work is organized into four main synthetic routes according to the target structures. The four strategies are shown below:

- Strategy for the synthesis of compounds containing β -D-Gal f -(1 \rightarrow 5)- β -D-Gal f and β -D-Gal f -(1 \rightarrow 6)- β -D-Gal f linkages (**3.1–3.4**)
- Strategy for the synthesis of compounds containing β -D-Gal f -(1 \rightarrow 2)- β -D-Gal f (**3.5**) and β -D-Gal f -(1 \rightarrow 3)- β -D-Gal f linkages (**3.6**)
- Strategy for the synthesis of compounds containing β -D-Gal f -(1 \rightarrow 6)- β -D-Glc p (**3.7**) and β -D-Gal f -(1 \rightarrow 6)- α -D-Man p linkages (**3.8**)
- Strategy for the synthesis of compound containing β -L-Araf (**3.9**)

3.2.1. Synthetic strategy for oligosaccharides containing β -D-Galf-(1 \rightarrow 5)- β -D-Galf and β -D-Galf-(1 \rightarrow 6)- β -D-Galf linkages (3.1–3.4)

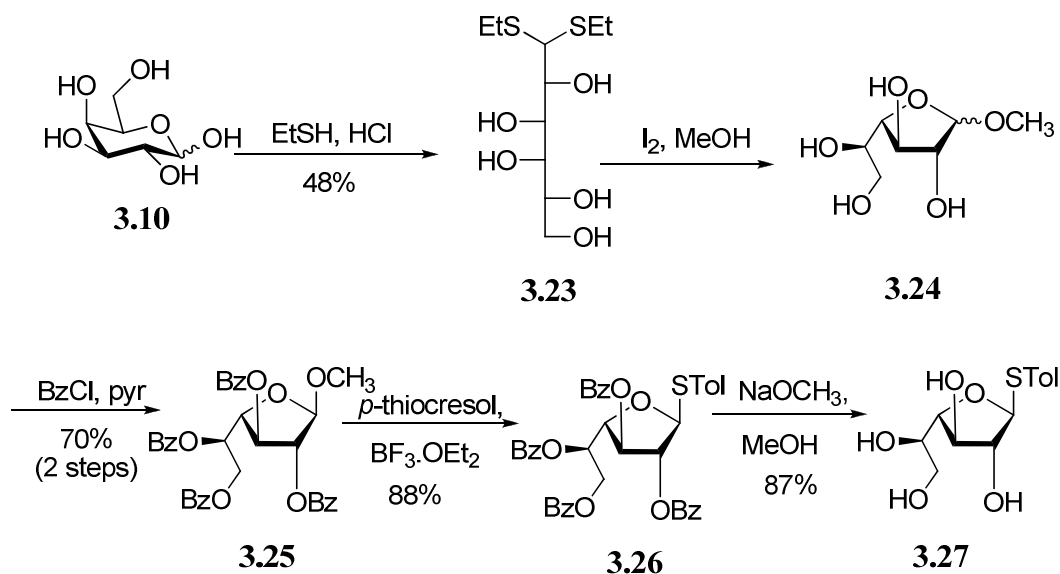
To obtain target oligosaccharides **3.1–3.4**, I followed a strategy reported earlier by our group (**Scheme 3.7**).¹³ In that approach, galactose dithioacetal **3.23**¹³ was used as the precursor for the synthesis of the galactofuranose building blocks. Methyl galactofuranoside **3.24**¹³ was obtained through iodine cyclization of thioacetal **3.23** in the presence of methanol. Starting from the methyl glycoside **3.25**¹³, thioglycoside donor **3.26** was obtained and used as the precursor to synthesize other thioglycoside donors **3.32** and **3.33**, as well as for the synthesis of the azido octyl glycoside acceptors **3.41** and **3.42**. In the literature, there are many reagents to activate thioglycosides,¹⁷⁻²¹ in this work I chose *N*-iodosuccinimide–silver triflate (NIS–AgOTf)¹⁹ as the activating agents. The incorporation of the azido-octyl linker at the reducing end was done to facilitate the binding studies with intelectin, which will be discussed in more detail in **Chapter 4**.



Scheme 3.7: Retrosynthetic route for the synthesis of oligosaccharides (3.1–3.4).

3.2.1.1. Synthesis of the thioglycoside donor

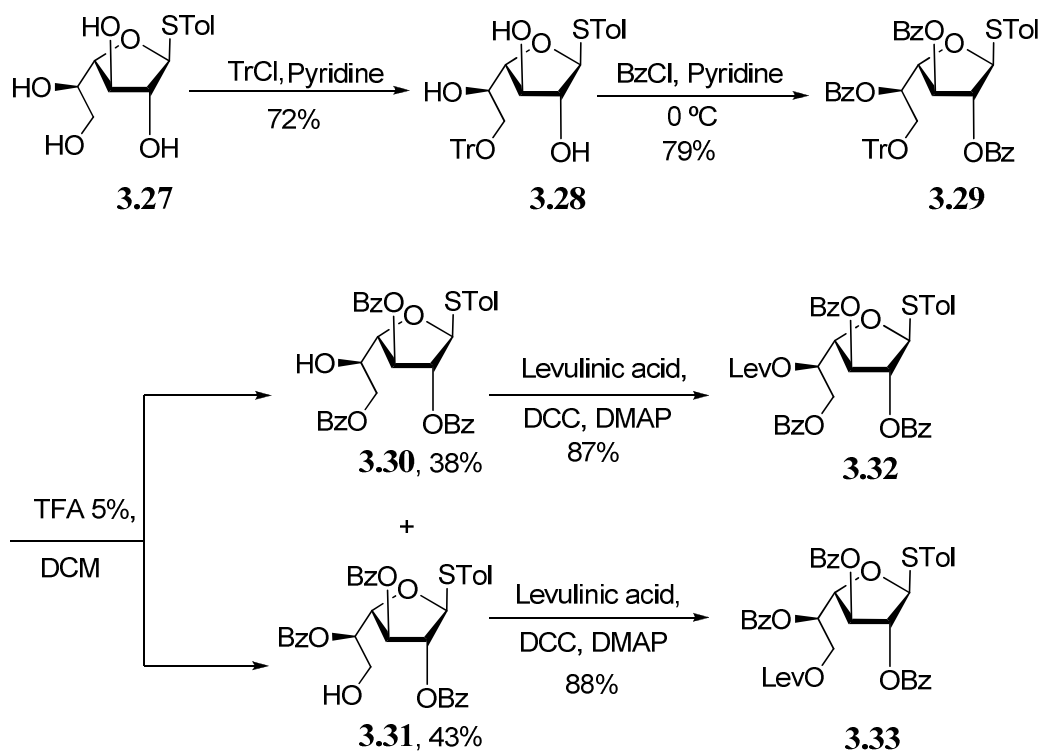
Thioglycoside synthesis was achieved using galactose dithioacetal **3.23** as the precursor. As shown in **Scheme 3.8**, D-galactose was reacted with ethanethiol in the presence of HCl to yield galactose diethyl dithioacetal **3.23**¹³ in 48% yield. The next step was the formation of galactofuranoside **3.24** through iodine-promoted cyclization of the dithioacetal in the presence of methanol. The reaction was stopped through the addition of sodium thiosulfate until a colorless solution was obtained followed by neutralization using sodium bicarbonate. With no further workup, the organic phase was evaporated *in vacuo* and the resulting crude product was subjected to the next step, protection by per-*O*-benzoylation. The crude methyl galactofuranoside **3.24**¹³ was dissolved in pyridine and allowed to cool to 0 °C. Then, benzoyl chloride was added dropwise to give the benzoylated product **3.25**¹³ in 70% yield over the two steps.



Scheme 3.8: Synthesis of thioglycoside **3.26** through cyclization of galactose dithioacetal **3.23**.

Next, the perbenzoylated methyl glycoside **3.25** was treated with *p*-thiocresol in the presence of boron trifluoride diethyl etherate ($\text{BF}_3 \cdot \text{OEt}_2$) to give the desired β -thioglycoside donor **3.26** in 88% yield. Thioglycoside donor **3.26** is a very valuable building block in my synthetic plan to the target compounds. Having donor **3.26** in hand allowed me to synthesize the other required thioglycoside donors **3.32** and **3.33**, as well as the azido-octyl acceptors **3.41** and **3.42**. To proceed further in my synthetic procedures, the perbenzoylated thioglycoside **3.26** was subjected to Zémpfen debenzoylation conditions using sodium methoxide in methanol (**Scheme 3.8**) to produce compound **3.27** in 87% yield as a white amorphous powder.

As outlined in **Scheme 3.9**, selective protection of the 6-hydroxyl group of compound **3.27** was successfully achieved when it was treated with trityl chloride in pyridine to give the 6-*O*-tritylated compound **3.28** in 72% yield. Benzoylation of compound **3.28** gave the fully protected sugar **3.29** in 79% yield.

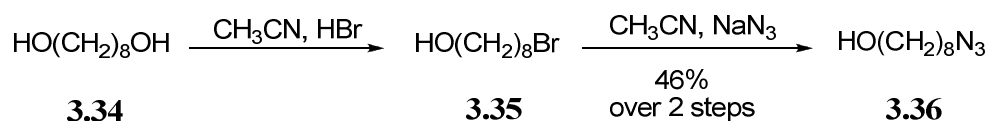


Scheme 3.9: Preparation of thioglycoside donors 3.32 and 3.33.

Treatment of compound **3.29** with 5% trifluoroacetic acid in dichloromethane¹³ resulted in the removal of the trityl group and the formation of **3.30** and **3.31** in 38% and 43% yield, respectively. The structure assignment of both compounds **3.30** and **3.31** was made feasible through the difference in the H-5 chemical shift, so in case of **3.30**, H-5 appeared more upfield compared to the H-5 when 5-OH is benzoylated (**3.31**). Both compounds were required in my synthetic plan, so this acyl migration from O5 to O6 was a desired step in my case. Subsequently, compounds **3.30** and **3.31** were treated with levulinic acid in the presence of DCC and DMAP to yield donors **3.32** and **3.33** in 87% and 88% yield, respectively, (Scheme 3.9).

3.2.1.2. Synthesis of 8-azido-1-octanol

To synthesize the required target compounds with the octyl-azido linker at the reducing end, it was necessary to prepare 8-azido-1-octanol, **3.36**. The reported procedure²² was modified to synthesize the target. First, 1,8-octandiol **3.34** was treated with HBr to yield 8-bromo-1-octanol, **3.35**. Subsequent reaction of **3.35** with sodium azide, yielded **3.36** in 46% yield over the two steps (**Scheme 3.10**).



Scheme 3.10: Synthesis of 8-azido-1-octanol 3.36.

3.2.1.3. Preparation of azido octyl glycoside acceptors

Target compounds **3.1–3.4** were designed such that the reducing end has an azido-octyl linker. The incorporation of that linker will play an important role in the binding studies with intelectin using surface plasmon resonance spectroscopy. The required acceptors are **3.41** and **3.42** (**Figure 3.2**).

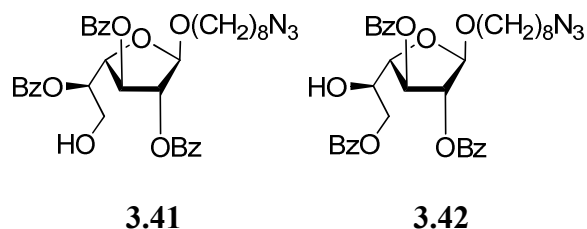
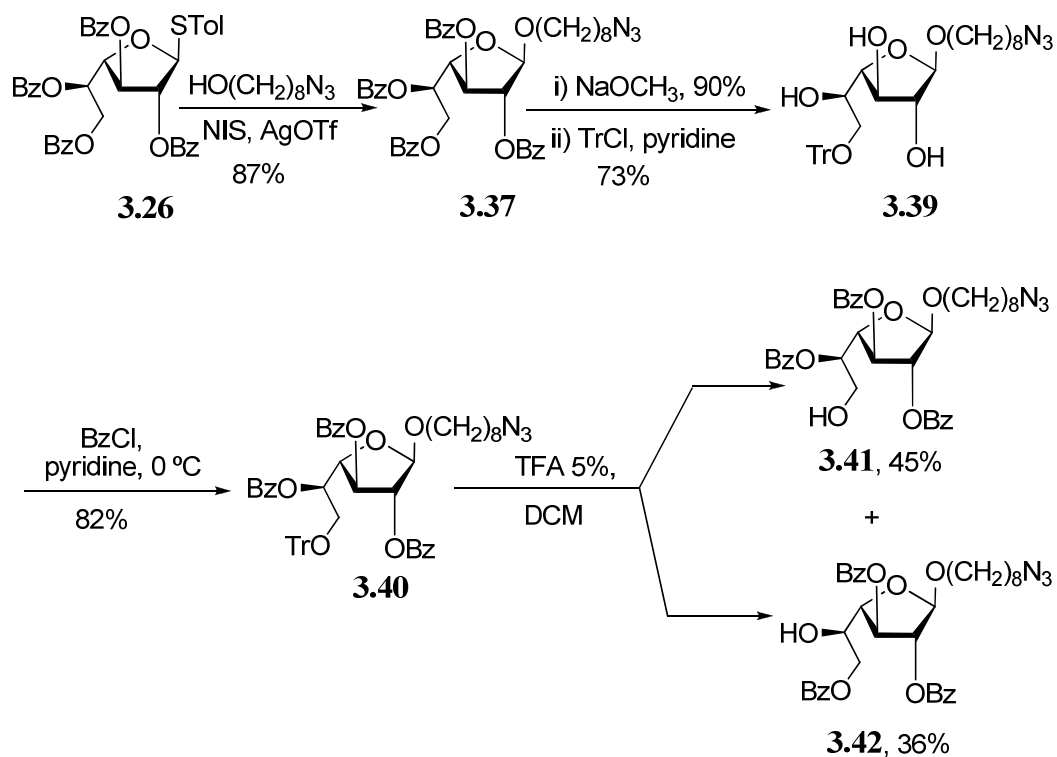


Figure 3.2: Structures of azido-octyl acceptors 3.41 and 3.42.

The azido octyl acceptors **3.41** and **3.42** were synthesized from thioglycoside donor **3.26** as illustrated in **Scheme 3.11**. When thioglycoside donor **3.26** was reacted with **3.36** in the presence of NIS and AgOTf, compound **3.37** was produced in 87% yield. Using Zémpfen conditions for debenzoylation, compound **3.38** was produced in 90% yield. An approach similar to that used for the synthesis of thioglycoside donors **3.32** and **3.33** was applied here for the synthesis of **3.41** and **3.42**. This involved protection of the 6-hydroxyl group of **3.38** using the bulky trityl group resulting in the formation of the tritylated compound **3.39** in 73% yield. Compound **3.39** was fully protected using benzoyl chloride in pyridine to give compound **3.40** in 82% yield. Using trifluoroacetic acid in dichloromethane, cleavage of the trityl group took place with the formation of acceptors **3.41** and **3.42** in 45% and 36% yield, respectively. Having these acceptors in hand enabled me to start the synthesis of the target oligosaccharides **3.1–3.4**, which will be discussed below.



Scheme 3.11: Synthesis of azido-octyl acceptors 3.41 and 3.42.

3.2.1.4. Synthesis of oligosaccharides

The main goal of my synthetic work is to gain access to oligosaccharide molecules that will be used as ligands to test the binding affinity of intelectin. Having this in mind, I wanted to design my molecules such that they represent a wide range of naturally occurring oligosaccharides found in the glycoconjugates in many microorganisms. Oligosaccharides **3.1–3.3** were designed as analogues of the galactan chain found in mycobacteria, which is composed of Galf repeating units connected via alternating (1→5) and (1→6) linkages¹³ (**Figure 3.3**).

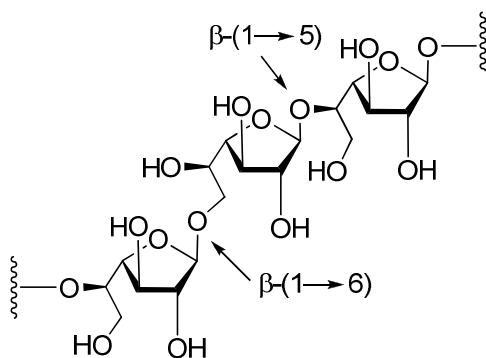


Figure 3.3: Linkages of galactan chain in the mycobacterial cell wall.

Tetrasaccharide **3.4** has four Galf units linked via (1→5) linkages, which corresponds to the Galf-containing side chain found in different *Aspergillus* species.²³ This motif in *Aspergillus fumigatus* was found to be immunogenic in humans,²³ but whether this tetrasaccharide can play a role in the innate immune response against *A. fumigatus* via human intelectin binding remains to be studied. Therefore, obtaining information about the recognition of the tetrasaccharide **3.4** by human intelectins could be useful.

3.2.1.5. Synthesis of disaccharides **3.1** and **3.2**

The synthesis of disaccharides **3.1** and **3.2** (**Figure 3.4**) was achieved through NIS–AgOTf activation of thioglycoside **3.26** and coupling with either acceptors **3.41** or **3.42** as shown in **Scheme 3.12**.

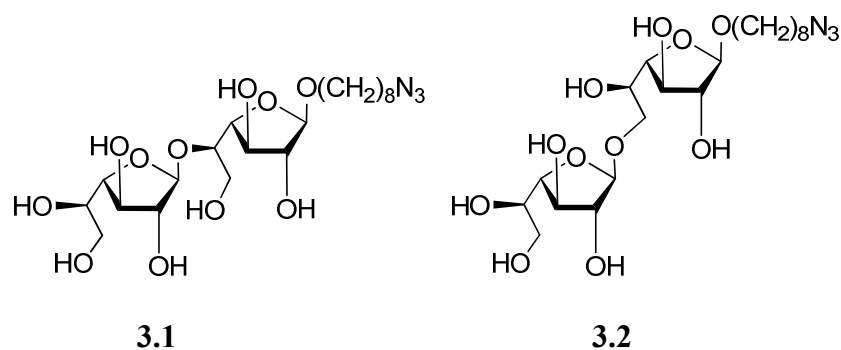
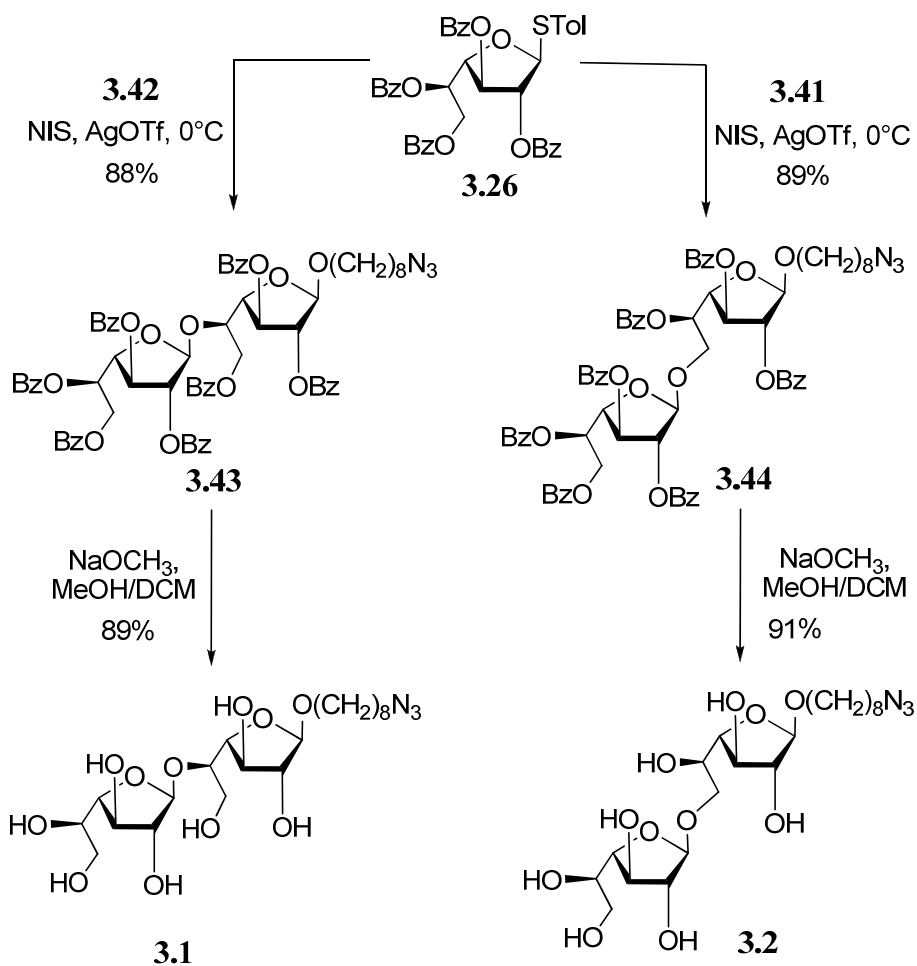


Figure 3.4: Structure of disaccharides 3.1 and 3.2.

For the synthesis of **3.1**, thioglycoside **3.26** was coupled with the azido-octyl acceptor **3.42** in the presence of NIS and a catalytic amount of AgOTf. This resulted in the formation of the fully protected disaccharide **3.43** in 88% yield. The same coupling procedure was used to obtain disaccharide **3.2**. Thus, thioglycoside **3.26** was reacted with acceptor **3.41** to form disaccharide **3.44**. The final step in the synthesis of **3.1** and **3.2** was deprotection, where both **3.43** and **3.44** were subjected to Zémlen deacylation conditions for debenzoylation to afford disaccharides **3.1** and **3.2** in 89% and 91% yield, respectively.

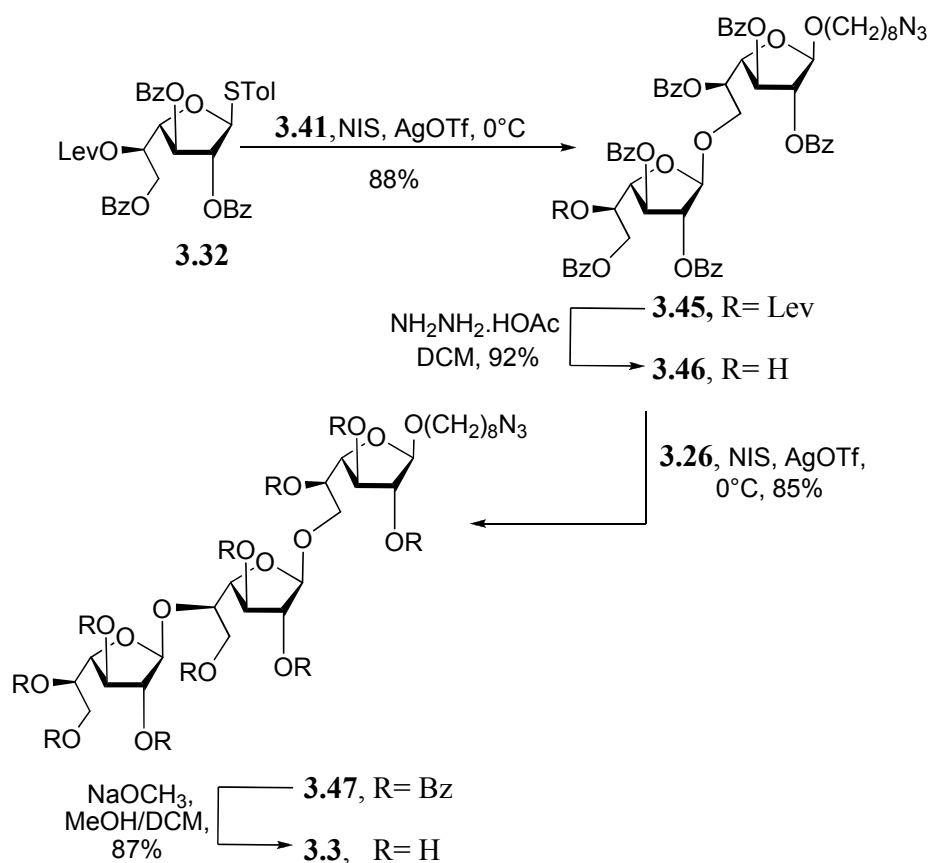


Scheme 3.12: Synthesis of disaccharides 3.1 and 3.2.

3.2.1.6. Synthesis of trisaccharide 3.3 and tetrasaccharide 3.4

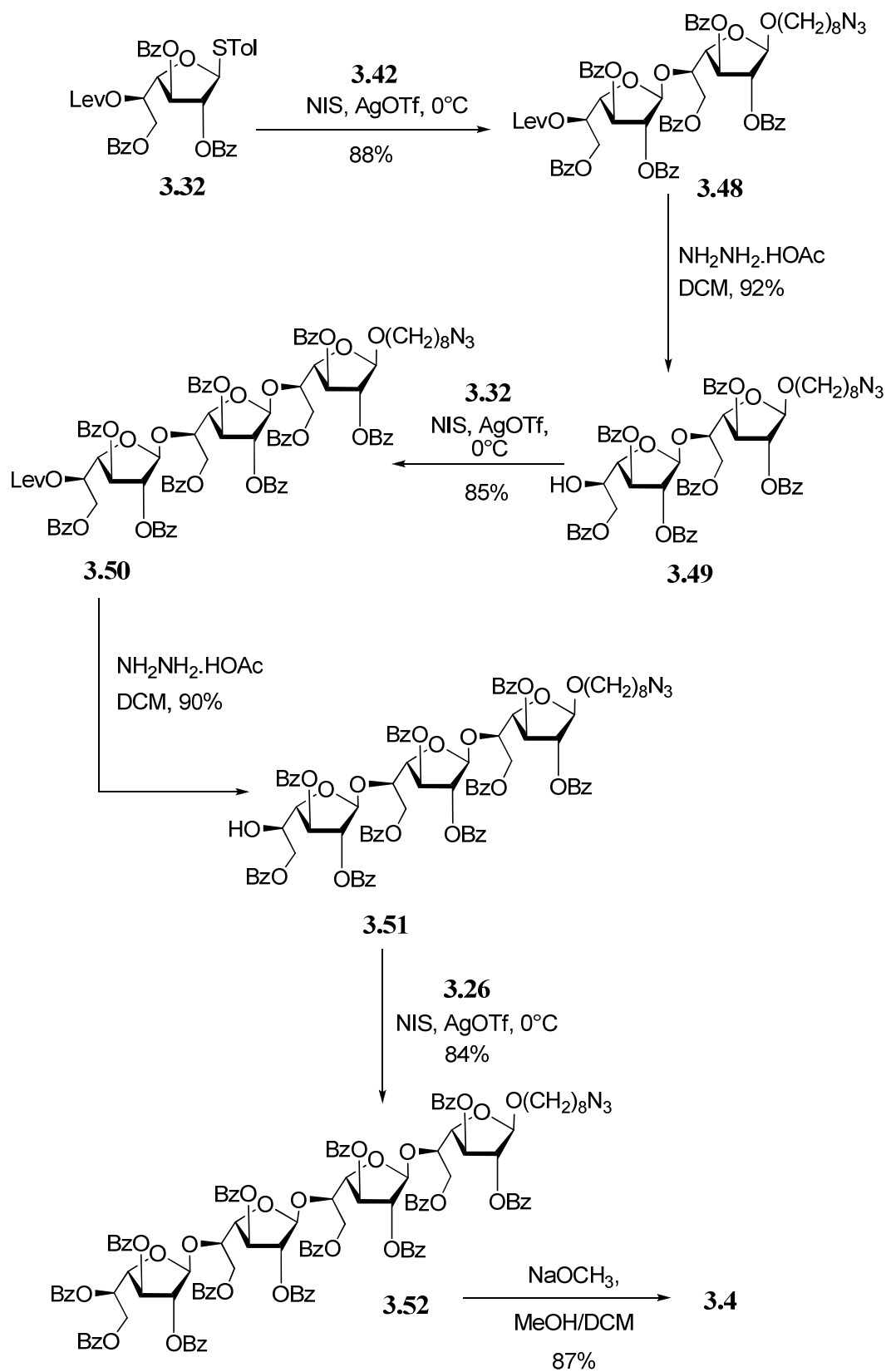
To synthesize trisaccharide 3.3 and tetrasaccharide 3.4, I followed the approach described in **Schemes 3.13** and **3.14**, where both the target molecules were built starting from the reducing end and then the chain was extended towards the non-reducing end. As shown in **Scheme 3.13** for the synthesis of trisaccharide 3.3, the required building blocks were the azido-octyl acceptor 4.41 and the thioglycoside donors 3.32 and 3.26. The first step towards the synthesis of 3.3 was coupling the

azido-octyl glycoside **3.41**, which has a free hydroxyl group at C-6, with the thioglycoside donor **3.32** using NIS–AgOTf activation. This reaction afforded the 5'-*O*-levulinoyl protected disaccharide **3.45** in 88% yield. Using hydrazine acetate, the levulinoyl protecting group was removed selectively to give the disaccharide acceptor **3.46** in 92% yield. The synthesis of trisaccharide **3.47** was achieved upon coupling of the disaccharide acceptor **3.46** and the fully protected thioglycoside donor **3.26** to give **3.47** in 85% yield. To obtain the final trisaccharide **3.3**, compound **3.47** was deprotected using sodium methoxide in methanol to give **3.3** in 87% yield.



Scheme 3.13: Synthesis of trisaccharide 3.3.

The same synthetic approach was used to synthesize tetrasaccharide **3.4** according to **Scheme 3.14**. The synthesis of **3.4** involved azido-octyl acceptor **3.42** and thioglycoside donors **3.32** and **3.26**. The chain extension started with the synthesis of disaccharide **3.48**, which was obtained in 88% yield when acceptor **3.42** was coupled with 5'-*O*-levulinoyl protected thioglycoside donor **3.32**. With the selective removal of the levulinoyl protecting group, disaccharide alcohol **3.49** was obtained in 92% yield. The 5'-OH containing-disaccharide was taken further towards the synthesis of the 5'-*O*-levulinoyl protected trisaccharide **3.50** in 85% yield. Repeating the step for the removal of the levulinoyl group in **3.50** afforded the trisaccharide acceptor **3.51** in 90% yield. The final glycosylation step between the later acceptor **3.51** and the thioglycoside donor **3.26** afforded the fully protected tetrasaccharide **3.52** in 84% yield. Similar to the synthesis of the final trisaccharide **3.3**, tetrasaccharide **3.52** was fully debenzoylated to give the target tetrasaccharide **3.4** in 87% yield.



Scheme 3.14: Synthesis of tetrasaccharide 3.4.

3.2.1.7. Synthesis of compounds containing β -D-Galf-(1 \rightarrow 2)- β -D-Galf linkage (3.5) and β -D-Galf-(1 \rightarrow 3)- β -D-Galf linkage (3.6)

Among my target Galf oligosaccharides are compounds **3.5** and **3.6** (**Figure 3.5**). These two disaccharides contain unique linkages. Disaccharide **3.5** contains two Galf moieties linked via a β -(1 \rightarrow 2) linkage, whereas in disaccharide **3.6** the two Galf residues are linked via a β -(1 \rightarrow 3) linkage. The rationale behind designing these two oligosaccharides is that they are fragments of naturally occurring molecules in bacteria and fungi. It was reported that β -D-Galf-(1 \rightarrow 2)- β -D-Galf glycosidic linkages are present in various microorganisms including *Penicillium*,²⁴ *Talaromyces*,²⁵ and the pathogenic protozoa *Trypanosoma cruzi*.²⁶ Furthermore, it was found that *Aspergillus*,²⁷ *Chaetosartorya*,²⁸ *Renibacterium salmoninarum*²⁹ as well as *Penicillium*²⁴ contain β -D-Galf-(1 \rightarrow 3)- β -D-Galf linkages as part of their components, especially the cell wall.

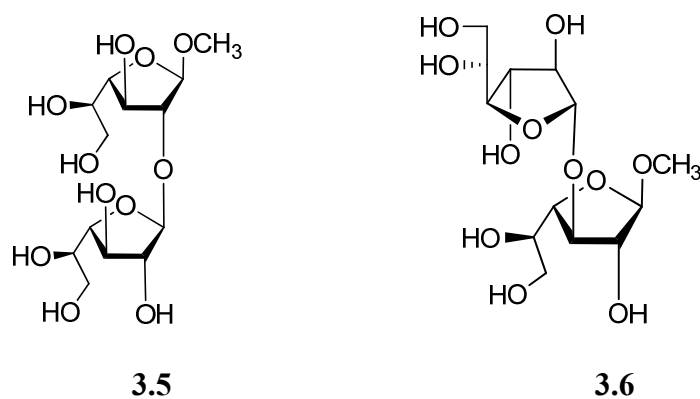
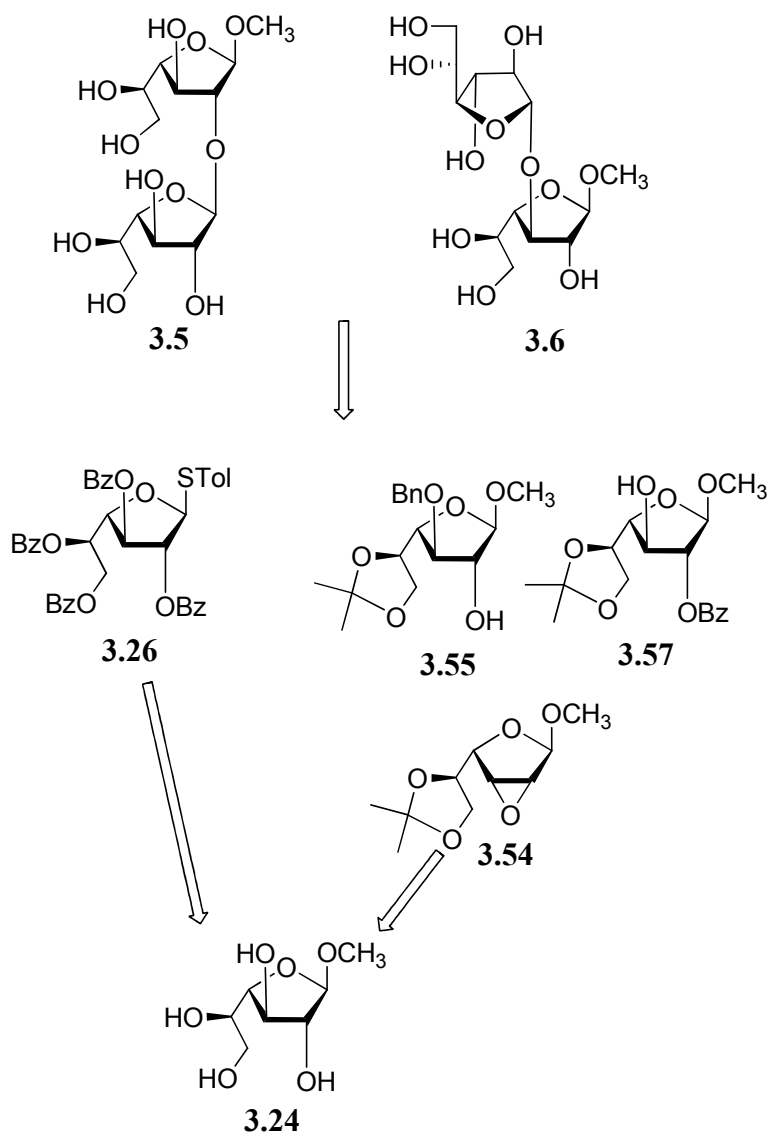


Figure 3.5: Structures of disaccharides 3.5 and 3.6

To synthesize disaccharides **3.5** and **3.6**, I designed a retrosynthetic route as shown in **Scheme 3.15**. Because I already had the thioglycoside donor **3.26** in hand, my

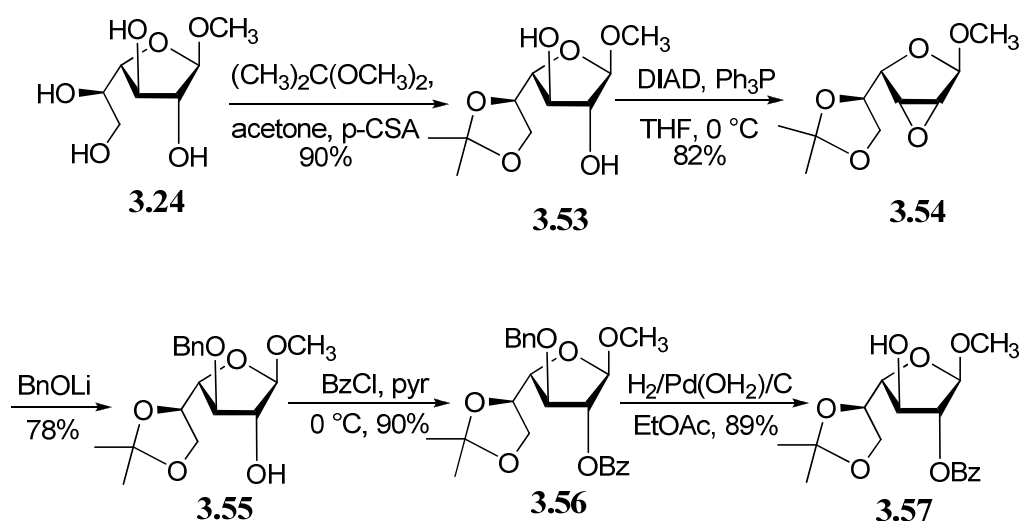
attention turned towards the preparation of the required acceptors. The key intermediate for the synthesis of both acceptors **3.55** and **3.57** was the 2,3-anhydro sugar derivative **3.54**.



Scheme 3.15: Retrosynthetic route for the synthesis of 3.5 and 3.6.

Starting with methyl β -D-galactofuranoside **3.24**, selective protection of O-5 and O-6 as an isopropylidene acetal afforded compound **3.53** in 90% yield. To obtain the 2,3-anhydro-sugar derivative, **3.53** was reacted with

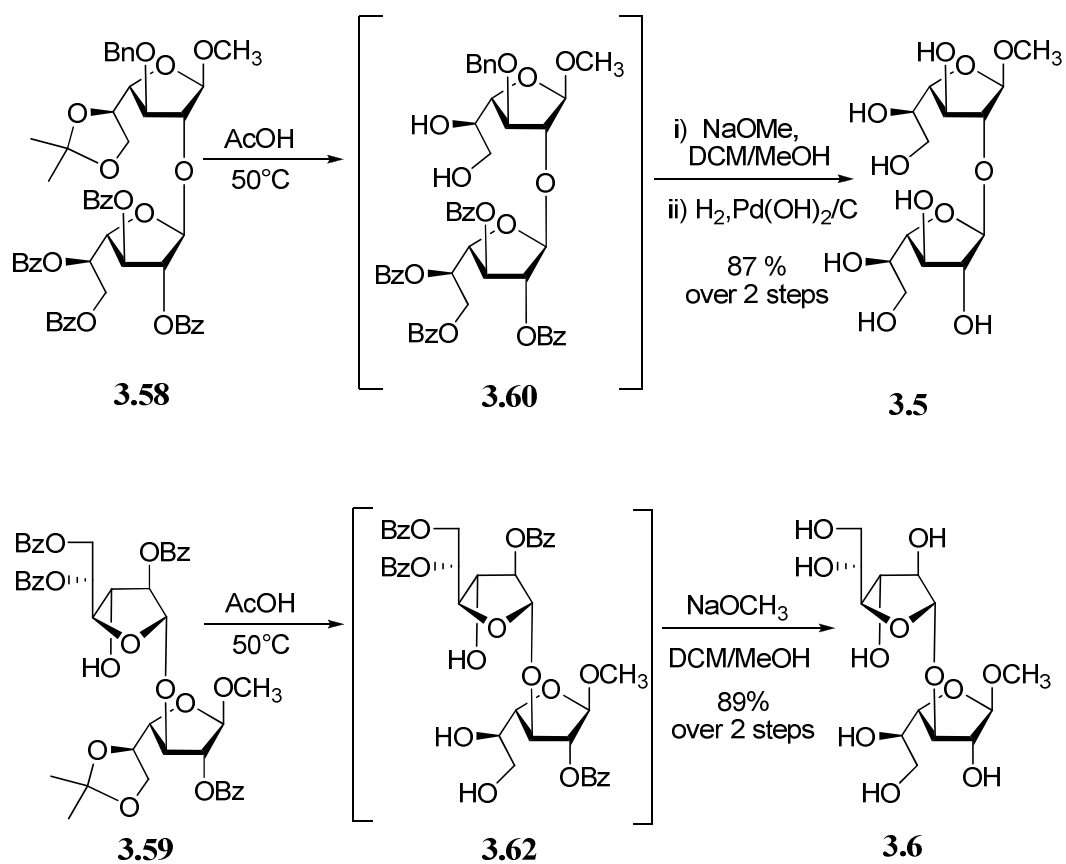
diisopropylazodicarboxylate (DIAD) and triphenylphosphine (PPh₃) to give the epoxide **3.54** in 82% yield. It was critical to obtain this important key intermediate **3.54** in good yield as it was the precursor for both acceptors **3.55** and **3.57**. Inspired by previous work done in our group,³⁰ I focused my attention on the next step, which was the regioselective opening of the epoxide. This was achieved upon treating the epoxide with BnOLi in benzyl alcohol, where acceptor **3.55** was obtained in 78% yield. Through successive steps of benzylation and debenylation of **3.55**, the other acceptor **3.57** was obtained in good yield.



Scheme 3.16: Synthesis of acceptors 3.55 and 3.57.

3.2.1.8. Synthesis of disaccharides 3.5 and 3.6

Having both acceptors **3.55** and **3.57** in hand enabled me to do the glycosylation between donor **3.26** and either acceptor **3.55** or **3.57** to give the desired β -(1 \rightarrow 2)



Scheme 3.18: Deprotection of disaccharides 3.58 and 3.59 and synthesis of disaccharides 3.5 and 3.6.

3.2.2. Synthesis of compound containing β -D-Galf-(1 \rightarrow 6)- β -D-Glcp (3.7) and β -D-Galf-(1 \rightarrow 6)- α -D-Manp linkages (3.8)

My interest in the synthesis of disaccharides **3.7** and **3.8**, which contain a β -D-Galf-(1 \rightarrow 6)- β -D-Glcp linkage and a β -D-Galf-(1 \rightarrow 6)- α -D-Manp linkage, respectively, came from the fact that they are part of different glyconjugates in various microorganisms. For example, the β -D-Galf-(1 \rightarrow 6)-D-Glcp motif was reported to be a part of the lipopolysaccharide (LPS) in *Escherichia coli* K-12.³¹ On the other hand the β -D-Galf-(1 \rightarrow 6)-D-Manp disaccharide was shown to be present in *Microsporium*,³² *Paraccidioides brasiliensis*,³³ *Trichophyton*³² and the exopolysaccharide (EPS) of *Aspergillus*.^{27, 34-36}

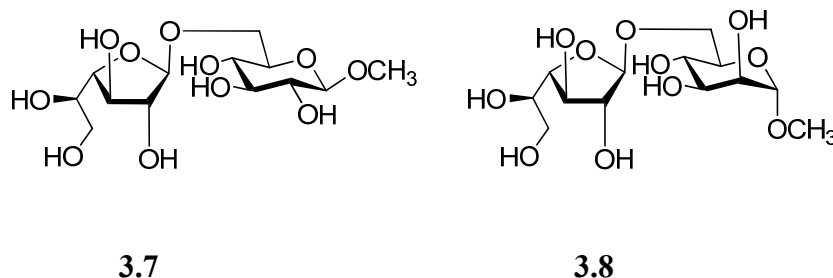
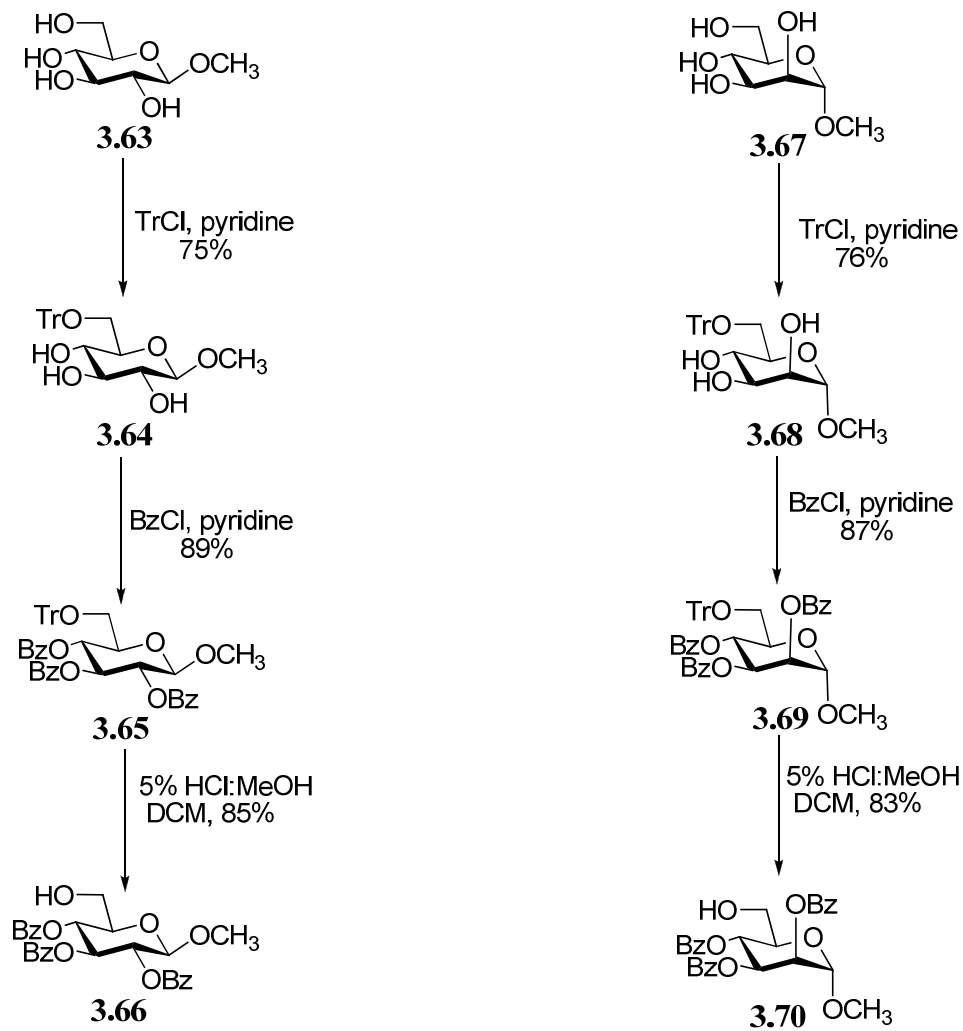


Figure 3.6: Structures of disaccharides 3.7 and 3.8

The sugar donor used for the synthesis of disaccharides **3.7** and **3.8** was thioglycoside **3.26**, which was used previously as a donor for the synthesis of oligosaccharides **3.1–3.6**. To obtain the acceptors **3.66** and **3.70**, I followed the strategy shown in **Scheme 3.19**, which started with the selective protection of the C-6 hydroxyl groups by tritylation of both methyl β -D-glucopyranoside **3.63** and methyl α -D-mannopyranoside **3.67** to give compounds **3.64** and **3.68**, respectively. Full protection was achieved by treating **3.64** and **3.68** with benzoyl chloride in

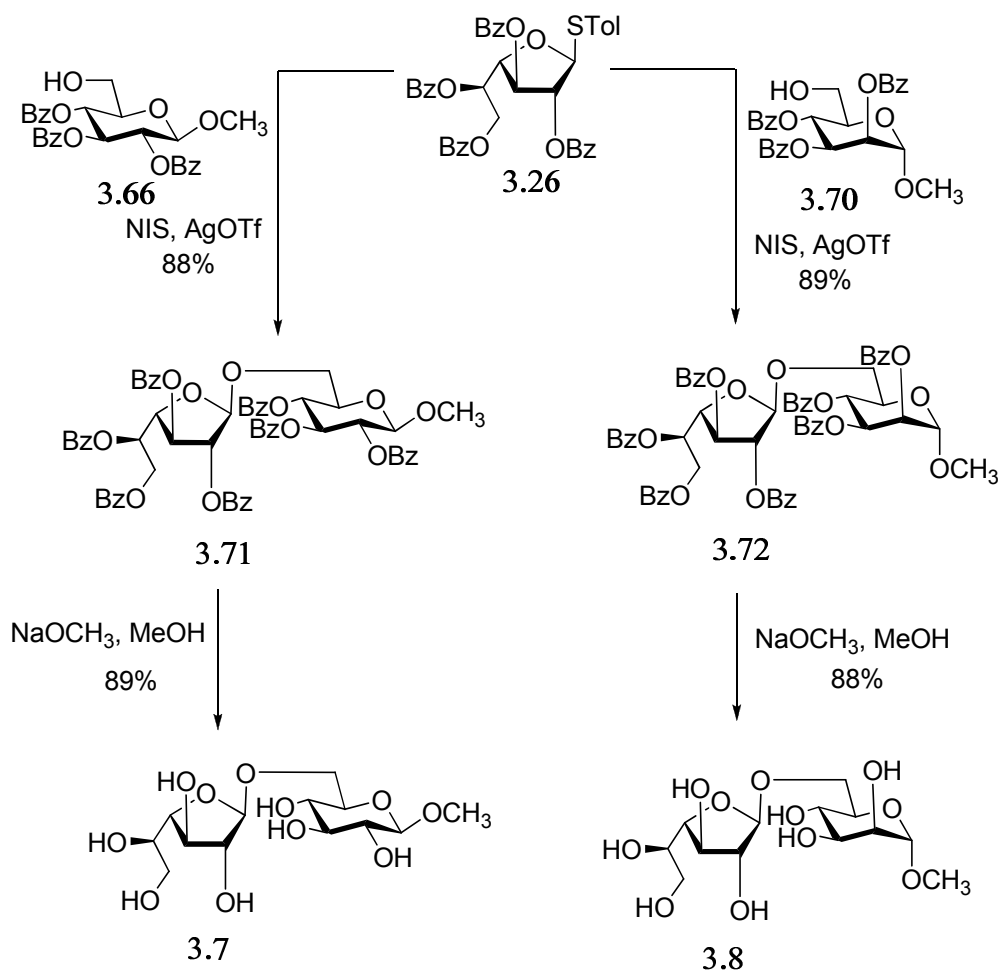
pyridine at 0 °C to give the fully protected monosaccharides **3.65** and **3.69**, respectively. The final step towards obtaining the acceptors **3.66** and **3.70** was the deprotection of the trityl group using mild acidic conditions (5% HCl in methanol) to give acceptor **3.64** (85%) and acceptor **3.70** (83%).



Scheme 3.19: Synthesis of acceptors 3.66 and 3.70.

3.2.2.1. Synthesis of disaccharides 3.7 and 3.8

To prepare the disaccharides, thioglycoside donor **3.26** was coupled with acceptors **3.66** and **3.70** under NIS–AgOTf activating conditions to give disaccharides **3.71** and **3.72** in 88% and 89% yield, respectively. Debenzoylation of both disaccharides afforded the fully deprotected disaccharide targets **3.7** and **3.8** in 89% and 88% yield, respectively, (Scheme 3.20).



Scheme 3.20: Synthesis of disaccharides 3.7 and 3.8.

3.2.3. Rationale for the synthesis of compound 3.9 containing α -L-Araf

Compound 3.9 shown in **Figure 3.7** was designed based on the structural similarity between D-galactose and L-arabinose as illustrated in **Figure 3.8**. Compound 3.9 was synthesized to be tested in the binding studies with human intelectin.

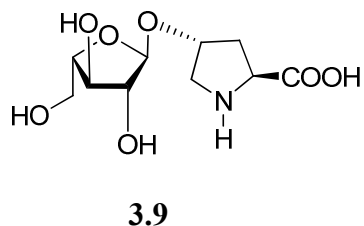


Figure 3.7: Structure of compound 3.9.

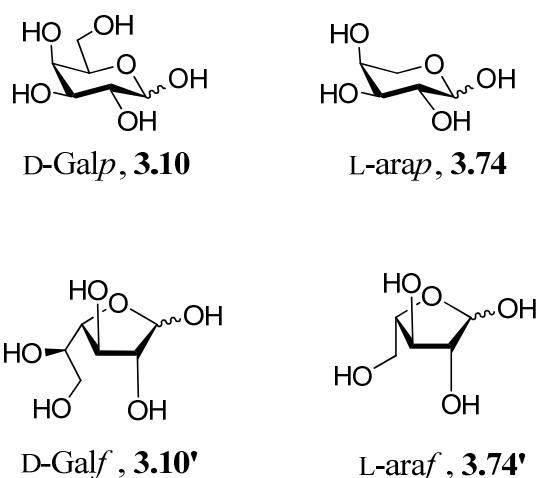


Figure 3.8: Structural similarity between D-galactose and L-arabinose.

Mugwort (*Artemisa vulgaris*) pollen is an important allergen in hay fever.³⁷ Significant work has been done to determine the structure of the major allergen (Art v 1) of this pollen. Using molecular modelling through analyses of the electrostatic surface potential of three-dimensionally similar proteins³⁷ and structural

characterization via NMR and mass spectrometry,³⁸ researchers were able to develop a model for Art v 1, (**Figure 3.9a**). The allergen is proposed to be a glycoprotein with two *O*-linked glycosides, which are linked to the protein via *trans*-4-hydroxy-proline (Hyp). As shown in **Figure 3.9a**, one can notice the presence of clusters made up of repeating units of β -L-arabinofuranosides of Hyp. These repeating motifs were found to be responsible for the antibody production when the whole glycoprotein was tested for its antigenicity.³⁹

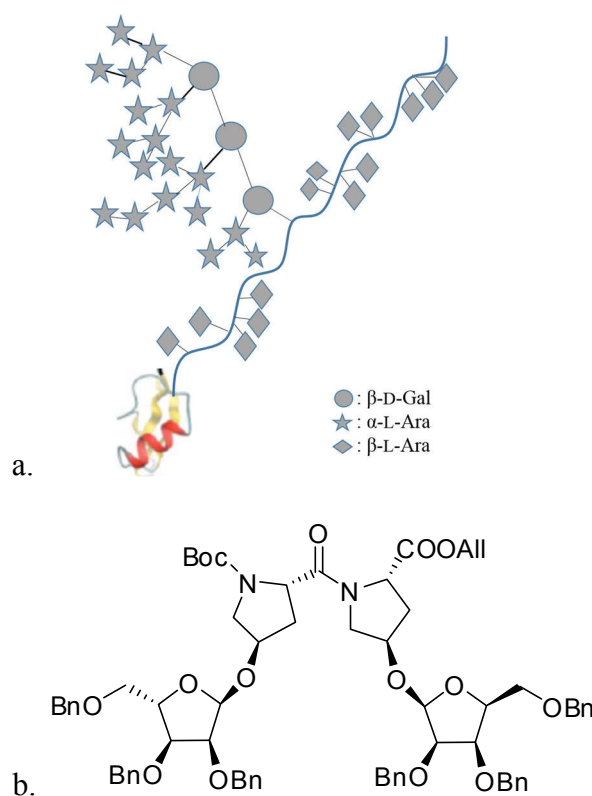


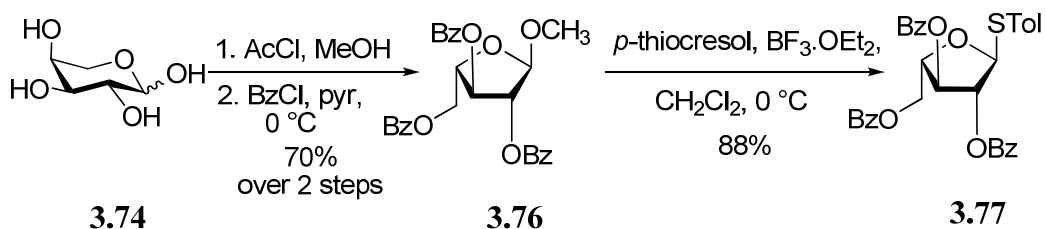
Figure 3.9: a: model of major allergen Art V 1, b: compound 3.73.⁴⁰

In 2010, Xie *et al*⁴⁰ synthesized compound **3.73**, (**Figure 3.9b**), which they thought to be the minimum epitope of the major allergen of Mugwort. As mentioned in the introduction chapter, human intelectin may play an important role in allergy and

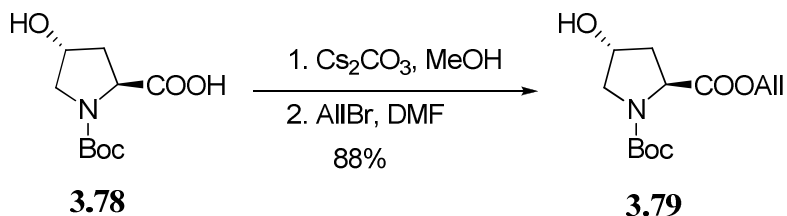
asthma.⁴¹⁻⁴³ Having that in mind, I decided to synthesize compound **3.9**, which has the minimum structure responsible for the potential allergic effects.

To start the synthesis of compound **3.9**, L-arabinose (**3.74**) was allowed to react with a methanolic solution of acetyl chloride to yield methyl glycoside **3.75**. Without separating the product, it was reacted with benzoyl chloride in pyridine at 0 °C, to give the fully protected methyl β-L-arabinofuranoside **3.76** in 70% yield over two steps. To obtain the thioglycoside donor **3.77**, methyl glycoside **3.76** was reacted with *p*-thiocresol in the presence of BF₃·OEt₂, resulting in the formation of the desired thioglycoside in 88% yield (**Scheme 3.21**).

For the synthesis of acceptor **3.79**, the commercially available *N*-Boc hydroxyproline **3.78** was protected via the formation of the allyl ester (**Scheme 3.22**) in 88% yield.

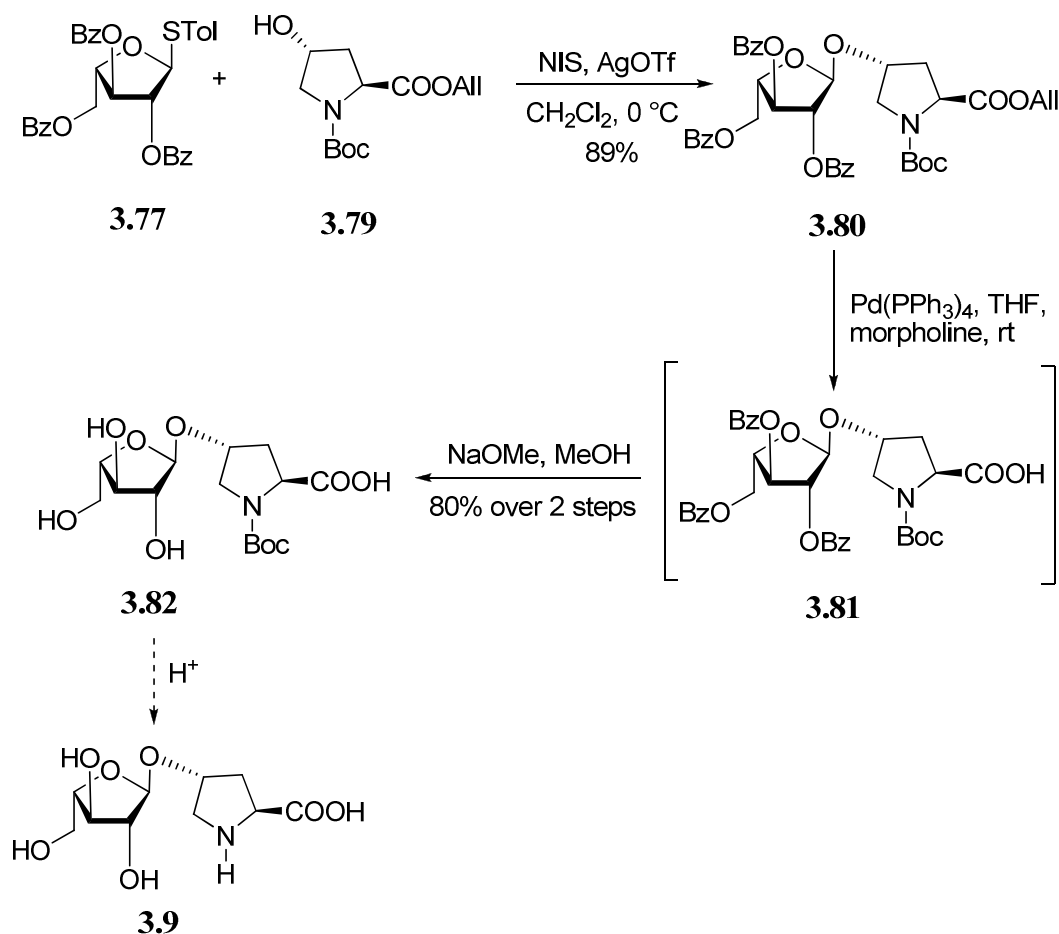


Scheme 3.21: Synthesis of L-arabinofuranosyl donor 3.77.



Scheme 3.22: Synthesis of acceptor 3.79.

Glycosylation between L-arabinofuranosyl thioglycoside donor **3.77** and hydroxyproline acceptor **3.79** in the presence of NIS–AgOTf afforded compound **3.80** in 89% yield as shown in **Scheme 3.23**. Deprotection of the allyl group was achieved by using tetrakis(triphenylphosphine)palladium Pd(PPh₃)₄ to give compound **3.81**, which was not separated. Instead, it was subjected to Zémlen conditions for deprotection of the benzoyl groups, which afforded **3.82** in 80% yield over two steps. The final deprotection of compound **3.82** will furnish compound **3.9**.



Scheme 3.23: Synthesis of compound 3.9.

3.3. Conclusion

The synthesis of the target compounds (3.1–3.8) was achieved successfully. The structures of the synthesized oligosaccharides represent examples of molecules from a wide range of microorganisms including bacteria, fungi and protozoa. The main glycoside donor used in the synthesis was the thioglycoside donor 3.26, which was synthesized using the dithioacetal cyclization approach. Thioglycoside donors were coupled with the synthesized acceptors under NIS–AgOTf activation conditions. The synthesized compounds were used as ligands to screen the binding affinity of hIntL-1 and 2, which will be discussed in detail in Chapter 4.

3.4. General methods

All reagents were purchased from commercial sources and used without further purification. Oven-dried glassware was used for all reactions. Reaction solvents were dried by passage through columns of alumina and copper under nitrogen. All reactions, unless stated otherwise, were carried out at room temperature under positive pressure of argon. Organic solutions were concentrated under vacuum below 40 °C. Reaction progress was monitored by TLC on Silica Gel 60 F₂₅₄ (0.25 mm, E. Merck). Visualization of the TLC spots was done either under UV light or charring the TLC plates with acidified *p*-anisaldehyde solution in ethanol or phosphomolybdic acid stain. Most of the purification methods were done using column chromatography (Silica Gel 40–60 μM). Optical rotations $[\alpha]_D$ measurement were carried out at 22 °C and reported in deg·cm² dm⁻¹·g⁻¹. ¹H NMR spectra were recorded using 500 MHz or 400 MHz instruments, and the data are reported as if they were first order. ¹³C NMR (APT) spectra were recorded at

125 MHz. Assignments of data were made using ^1H - ^1H COSY and HMQC experiments. In the experimental section, the assigned protons and carbons of the first residue will be reported as such (without any primes), where the subsequent rings were assigned as 1', 1'' and 1''' as shown in **Figure 3.10**. Electrospray mass spectra were recorded on samples suspended in THF/MeOH mixture with added NaCl.

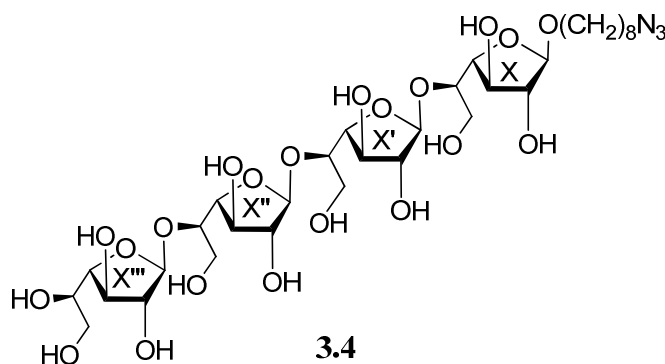


Figure 3.10: *Compound 3.4 as an example for the assignment of protons and carbons in each residue.*

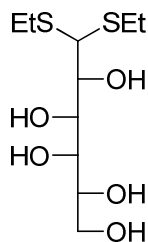
3.4.1. General procedure for the deprotection of benzoylated products using Zémlen conditions

The benzoylated compound was dissolved in 3:1 MeOH-CH₂Cl₂ (20–50 mL). To that solution NaOMe in MeOH (0.1 M) was added dropwise until the solution reached pH 12 as determined by using universal pH paper. The reaction mixture was allowed to stir from 4–8 h at room temperature followed by neutralization using either glacial acetic acid or prewashed Amberlite-15 (H⁺) cation exchange resin. After filtration and concentration of the solution, the crude residue was purified using column chromatography.

3.4.2. General procedure for the removal of levulinoyl protecting groups

The levulinoyl protected sugar (1 equivalent) was dissolved in 3:1 CH₂Cl₂-MeOH (10 mL) and hydrazine acetate (2 equivalents) was added. The solution was stirred for 2–4 h and the reaction was monitored by TLC to check the complete removal of the levulinoyl group. The solvent was concentrated under vacuum, and the residue was diluted with EtOAc. The organic solution was then washed with a saturated solution of NaHCO₃ and brine, and then dried over Na₂SO₄ anhydrous, filtered and concentrated. The crude residue was purified using column chromatography.

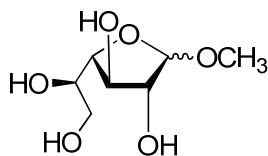
3.5. Experimental procedures



3.23

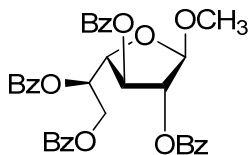
D-Galactose diethyl dithioacetal (3.23). D-Galactose **3.10** (40.00 g, 0.222 mol) was dissolved in 70 mL concentrated HCl. Ethanethiol (40 mL) was then added and the reaction mixture was vigorously shaken releasing the pressure from time to time. Within 5 min, the reaction temperature had increased and so 20 mL of an ice/water mixture were added, followed by more ice water to help crystallization of the product, which was filtered out and washed with ice water. For purification purposes, recrystallization of the product from absolute ethanol gave a pure

crystalline product **3.23** (30.47 g, 48%). The ^1H NMR and ^{13}C NMR spectra obtained for **3.23** agreed with those reported previously.¹³



3.24

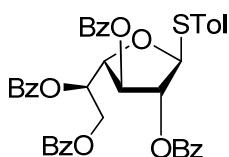
Methyl α/β -D-galactofuranoside (3.24). Diethyl dithioacetal **3.23** (5.0 g, 17.0 mmol) was dissolved in I_2 in MeOH (2% w/v, 250 mL) and the mixture was stirred overnight. To quench the excess I_2 , solid $\text{Na}_2\text{S}_2\text{O}_3$ was added until the brownish red color of I_2 disappeared. A saturated NaHCO_3 wash was done to ensure neutralization of the reaction mixture followed by concentration of the organic layer to give **3.24** (2.5 g, 75%) as a white solid (β/α mixture 9:1). Pure β -anomer was obtained by column chromatography using 7:1 CH_2Cl_2 -MeOH as the eluant. The ^1H NMR and ^{13}C NMR spectra obtained for **3.24** agreed with those reported previously.¹³



3.25

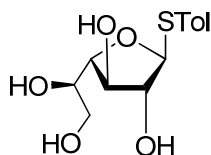
Methyl 2,3,5,6-tetra-O-benzoyl- β -D-galactofuranoside (3.25). Compound **3.24** (2.1 g, 10.3 mmol) was dissolved in pyridine (15 mL) and the solution was cooled to 0 °C before benzoyl chloride (6.2 mL, 89.7 mmol) was added dropwise. The

reaction mixture was stirred for 7 h followed by the addition of ice water to quench excess benzoyl chloride. The reaction mixture was diluted with CH₂Cl₂ (35 mL), washed with water, 1 M HCl and finally a saturated NaHCO₃ solution. The organic layer was then dried using anhydrous Na₂SO₄, filtered and concentrated. The crude residue was purified by column chromatography (4:1 hexanes–EtOAc) to give compound **3.25** (5.6 g, 90%) as a white amorphous solid. The ¹H NMR and ¹³C NMR spectra obtained for **3.25** agreed with those reported previously.¹³



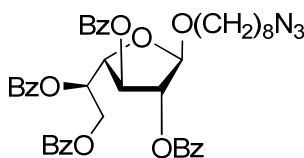
3.26

***p*-Tolyl 2,3,5,6-tetra-*O*-benzoyl-1-thio- β -D-galactofuranoside (3.26).** To a solution of methyl glycoside **3.25** (15.0 g, 24.5 mmol) in CH₂Cl₂ (150 mL) cooled to 0 °C, *p*-thiocresol (3.98 g, 32.2 mmol) was added. The reaction mixture was stirred for 15 min followed by the slow addition of BF₃·OEt₂ (20.25 mL, 159.5 mmol). The reaction mixture was then stirred overnight while warming to room temperature and then was neutralized with Et₃N. The organic layer was washed with a saturated solution of NaHCO₃ followed by water and brine. The organic layer was then dried over anhydrous Na₂SO₄, filtered and concentrated. The crude product was purified using column chromatography (4:1 hexanes–EtOAc) to give thioglycoside **3.26** (12.36 g, 87%) as a white solid. The ¹H NMR and ¹³C NMR spectra for **3.26** matched the data reported previously.¹³



3.27

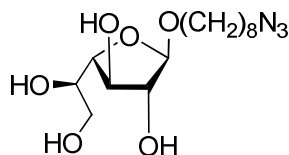
***p*-Tolyl 1-thio- β -D-galactofuranoside (3.27).** The perbenzoylated thioglycoside **3.26** (13.5 g, 19.2 mmol) was debenzoylated according to the procedure reported previously,⁴⁴ where it was dissolved in 3:1 MeOH-CH₂Cl₂, followed by the addition of NaOMe (0.1 M) in MeOH until the solution reacted pH 12 as determined by universal pH indicator. The reaction mixture was stirred overnight and then neutralized with glacial acetic acid. The solution was concentrated to give a crude yellow syrup that was purified by column chromatography (9:1 CH₂Cl₂-MeOH) to providing **3.27** (4.84 g, 88%) as a white amorphous powder. The ¹H NMR and ¹³C NMR spectra for compound **3.27** matched the previously reported data.¹³



3.37

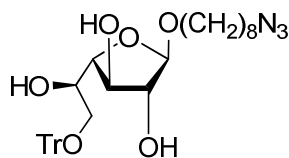
8-Azido-octyl 2,3,5,6-tetra-*O*-benzoyl- β -D-galactofuranoside (3.37). Thioglycoside **3.26** (β -anomer) (2.0 g, 2.84 mmol) and alcohol **3.36** (320 mg, 1.89 mmol) were dissolved in dry CH₂Cl₂ (20 mL) in the presence of 300 mg activated, powdered 4 Å molecular sieves and the mixture was cooled to 0 °C. The reaction mixture was stirred for 15 min followed by the addition of *N*-iodosuccinimide (NIS, 635 mg, 2.84 mmol), and AgOTf (120 mg, 0.47 mmol). The reaction mixture was stirred for another 30 min and then Et₃N was added. The reaction mixture was

diluted with CH₂Cl₂ and filtered through a Celite pad. The filtrate was washed with a saturated Na₂S₂O₃ solution followed by water, brine, and then dried over Na₂SO₄ anhydrous and filtered. The solvent was evaporated and the residue was purified using column chromatography (4:1 hexane–EtOAc) to give compound **3.67** (1.13 g, 85%) as a colorless syrup. *R_f* 0.32 (4:1 hexanes–EtOAc); [α]_D –119.7 (*c* 0.4, CH₂Cl₂); ¹H NMR (500 MHz, CDCl₃, δ _H): 8.20–7.85 (m, 6 H, Ar), 7.63–7.35 (m, 14 H, Ar), 6.14 (app dt, 1 H, *J* = 7.8, 3.4 Hz, H-5), 5.66 (d, 1 H, *J* = 5.2 Hz, H-3), 5.49 (d, 1 H, *J* = 1.2 Hz, H-2), 5.32 (s, 1 H, H-1), 4.84–4.72 (m, 2 H, H-6a,b), 4.66 (dd, 1 H, *J* = 5.3, 3.5 Hz, H-4), 3.78 (td, 1 H, *J* = 9.6, 6.7 Hz, octyl OCH₂), 3.56 (td, 1 H, *J* = 9.5, 6.3 Hz, octyl OCH₂), 3.25 (t, 2 H, *J* = 6.9 Hz, octyl CH₂N₃), 1.64–1.60 (m, 4 H, octyl CH₂), 1.44–1.29 (m, 8 H, octyl CH₂); ¹³C NMR (125 MHz, CDCl₃, δ _C): 166.1 (C=O), 165.7 (C=O), 165.6 (C=O), 165.5 (C=O), 133.4 (Ar), 133.3 (Ar), 133.2 (Ar), 133.1 (Ar), 129.9 (Ar), 129.9 (Ar), 129.8 (Ar), 129.7 (Ar), 129.6 (Ar), 129.5 (Ar), 129.1(Ar), 129.0 (Ar), 128.4 (Ar), 128.4 (Ar), 128.4 (Ar), 105.6 (C-1), 82.1 (C-2), 81.2 (C-4), 76.8 (C-3), 70.3(C-5), 67.6 (octyl OCH₂), 63.6 (C-6), 51.5 (octyl CH₂N₃), 29.5 (octyl CH₂), 29.3 (octyl CH₂), 29.1 (octyl CH₂), 28.8 (octyl CH₂), 26.7 (octyl CH₂), 26.1 (octyl CH₂). HR ESIMS: *m/z* [M+Na⁺] calcd for C₄₂H₄₃N₃NaO₁₀: 772.2841. Found: 772.2833.



3.38

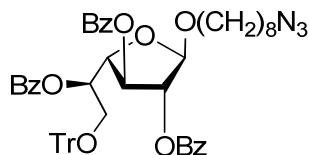
8-Azido-octyl β -D-galactofuranoside (3.38). Compound **3.37** (1.1 g, 1.5 mmol) was debenzoylated according to the general debenzoylation procedure described above. Removal of the solvent afforded an oily residue, which was purified by column chromatography (9:1 CH_2Cl_2 -MeOH) to give compound **3.38** (444 mg, 89%) as a colorless oil. R_f 0.4 (5:1 CH_2Cl_2 -MeOH); $[\alpha]_D -49.5$ (c 0.4, CH_2Cl_2); ^1H NMR (500 MHz, CDCl_3 , δ_{H}): 4.98 (s, 1 H, H-1), 4.13–3.97 (m, 4 H, H-2, H-3, H-4, H-5), 3.82–3.64 (m, 3 H, H-6a,b, octyl CH_2), 3.44 (dt, 1 H, $J = 9.6, 6.7$ Hz, octyl CH_2), 3.28 (t, $J = 6.9$ Hz, 2 H, octyl CH_2N_3), 1.62–1.58 (m, 4 H, octyl CH_2), 1.36–1.21 (m, 8 H, octyl CH_2); ^{13}C NMR (125 MHz, CDCl_3 , δ_{C}): 107.9 (C-1), 85.6 (C-4), 79.9 (C-3), 78.2 (C-5), 71.1 (C-2), 68.0 (octyl OCH_2), 64.2 (C-6), 51.5 (octyl CH_2N_3), 29.5 (octyl CH_2), 29.3 (octyl CH_2), 29.1 (octyl CH_2), 28.8 (octyl CH_2), 26.7 (octyl CH_2), 25.9 (octyl CH_2); HR ESIMS: m/z $[\text{M}+\text{Na}^+]$ calcd for $\text{C}_{14}\text{H}_{27}\text{N}_3\text{NaO}_6$: 356.1792. Found: 356.1790.



3.39

8-Azido-octyl 6-O-trityl- β -D-galactofuranoside (3.39). To a solution of compound **3.38** (1.2 g, 3.6 mmol) in pyridine (35 mL), trityl chloride (1.5 g, 5.31 mmol) was added. The reaction mixture was stirred at 50 °C for 48 h. After cooling,

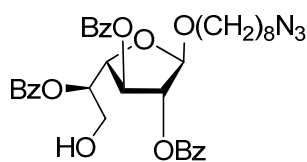
the solvent was evaporated; co-evaporation with toluene removed all traces of pyridine. The residue was then purified using column chromatography (19:1 CH₂Cl₂–MeOH) to give **3.39** (1.44 g, 70%) as a colorless oil. *R_f* 0.49 (19:1 CH₂Cl₂–MeOH); [α]_D –63.6 (*c* 0.5, CH₂Cl₂); ¹H NMR (500 MHz, CDCl₃, δ_H) 7.49–7.42 (m, 5 H, Ar), 7.37–7.25 (m, 10 H, Ar), 4.96 (s, 1 H, H-1), 4.10–4.01 (m, 2 H, H-2, H-3), 3.97–3.91 (m, 2 H, H-4, H-5), 3.68 (dt, 1 H, *J* = 9.6, 6.7 Hz, octyl OCH₂), 3.45–3.33 (m, 3 H, octyl CH₂, H-6a,b), 3.25 (t, 2 H, *J* = 7.0 Hz, octyl CH₂N₃), 1.57–1.52 (m, 5 H, octyl CH₂), 1.39–1.27 (m, 7 H, octyl CH₂); ¹³C NMR (125 MHz, CDCl₃, δ_C) 143.6 (Ar), 128.6 (Ar), 127.9 (Ar), 127.3 (Ar), 108.3 (C-1), 87.2 (Ph₃C) 86.9 (C-4), 79.1 (C-2), 78.3 (C-3), 70.8 (C-5), 67.6 (C-6), 64.7 (octyl OCH₂), 51.5 (octyl CH₂N₃), 29.4 (octyl CH₂), 29.2 (octyl CH₂), 29.0 (octyl CH₂), 28.8 (octyl CH₂), 26.6 (octyl CH₂), 26.0 (octyl CH₂); HR ESIMS: *m/z* [M+Na⁺] calcd for C₃₃H₄₁N₃NaO₆: 598.2888. Found: 598.2882.



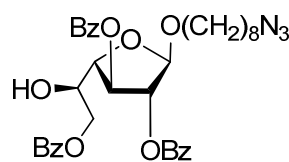
3.40

8-Azido-octyl 2,3,5-tri-*O*-benzoyl-6-*O*-trityl-β-D-galactofuranoside (3.40). A solution of **3.39** (1.2 g, 2.08 mmol) in pyridine (50 mL) was cooled to 0 °C. Benzoyl chloride (1.68 g, 12 mmol) was then added slowly. The reaction mixture was stirred overnight and was then poured over ice water mixture and extracted with CH₂Cl₂. The organic layer was washed with brine, dried over anhydrous Na₂SO₄, filtered and concentrated to give a crude residue that was purified using column chromatography (3:1 Hexane–EtOAc) to give **3.40** (1.45g, 82%) as a white solid,

R_f 0.39 (3:1 Hexane–EtOAc); $[\alpha]_D -51.2$ (c 0.5 CH_2Cl_2); $^1\text{H NMR}$ (500 MHz, CDCl_3 , δ_{H}) 8.22–8.10 (m, 2 H, Ar), 8.08 (d, 2 H, $J = 8.2$ Hz, Ar), 7.90 (d, 2 H, $J = 8.2$ Hz, Ar), 7.67–7.18 (m, 24 H, Ar), 5.89–5.77 (app dt, 1 H, $J = 10.0, 5.1$ Hz, H-5), 5.46 (d, 1 H, $J = 4.8$ Hz, H-3), 5.38 (s, 1 H, H-1), 5.27 (d, 1 H, $J = 4.9$ Hz, H-2), 4.74 (dd, 1 H, $J = 5.3, 4.8$ Hz, H-4), 3.82–3.71 (m, 2 H, H-6a,b), 3.62 (dd, 1 H, $J = 9.7, 6.0$ Hz, octyl OCH_2), 3.53 (ddt, 1 H, $J = 18.5, 9.8, 5.6$ Hz, octyl OCH_2), 3.23 (t, 3 H, $J = 7.0$ Hz, octyl CH_2N_3), 1.71–1.54 (m, 4 H, octyl CH_2), 1.37–1.28 (m, 8 H, octyl CH_2); $^{13}\text{C NMR}$ (125 MHz, CDCl_3 , δ_{C}) 165.7 (C=O), 165.5 (C=O), 165.5 (C=O), 143.6 (Ar), 133.4 (Ar), 133.2 (Ar), 133.1 (Ar), 130.0 (Ar), 129.9 (Ar), 129.9 (Ar), 129.8 (Ar), 129.3 (Ar), 129.1 (Ar), 128.6 (Ar), 128.4 (Ar), 128.3 (Ar), 127.8 (Ar), 127.0 (Ar), 105.4 (C-1), 86.9 (Ph_3C), 82.3 (C-4), 80.9 (C-2), 76.5 (C-3), 72.1 (C-5), 67.4 (C-6), 62.7 (octyl OCH_2), 51.4 (octyl CH_2N_3), 29.5 (octyl CH_2), 29.3 (octyl CH_2), 29.1 (octyl CH_2), 28.8 (octyl CH_2), 26.7 (octyl CH_2), 26.1 (octyl CH_2); HR ESIMS: m/z $[\text{M}+\text{Na}^+]$ calcd for $\text{C}_{54}\text{H}_{53}\text{N}_3\text{NaO}_9$: 910.3814. Found: 910.3815.



3.41

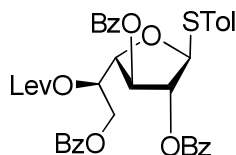


3.42

8-Azido-octyl 2,3,5-tri-*O*-benzoyl- β -D-galactofuranoside (3.41) and **8-azido-octyl 2,3,6-tri-*O*-benzoyl- β -D-galactofuranoside (3.42)**. A solution of compound **3.40** (1.3 g, 1.46 mmol) in CH_2Cl_2 (35 mL) was cooled to 0°C and 5% trifluoroacetic acid in CH_2Cl_2 (20 mL) was added dropwise. The reaction mixture was stirred for 24 h, concentrated, and then co-evaporated with toluene. The residue

was purified using column chromatography (4:1 Hexane–EtOAc) to give **3.41** (423 mg, 45%) and **3.42** (329 mg, 35%) both as colourless syrup. R_f 0.28 (**3.41**) and R_f 0.35 (**3.42**) (3:1 Hexane–EtOAc). Data for **3.41**: $[\alpha]_D -20.5$ (c 0.4, CH_2Cl_2); ^1H NMR (400 MHz, CDCl_3 , δ_{H}) 8.11–8.03 (m, 3 H, Ar), 8.02–7.95 (m, 2 H, Ar), 7.64–7.48 (m, 3 H, Ar), 7.50–7.26 (m, 7 H, Ar), 5.64 (app dt, 1 H, 7.2, $J = 4.9$ Hz, H-5), 5.60 (d, 1 H, $J = 5.1$ Hz, H-3), 5.48 (d, 1 H, $J = 1.0$ Hz, H-2), 5.31 (s, 1 H, H-1), 4.68–4.60 (m, 1 H, H-4), 4.08 (br s, 2 H, H-6a,b), 3.76–3.74 (m, 1 H, octyl OCH_2), 3.58–3.55 (m, 1 H, octyl OCH_2), 3.24 (t, 2 H, $J = 7.0$ Hz, octyl CH_2N_3), 1.56–1.48 (m, 4 H, octyl CH_2), 1.40–1.24 (m, 8 H, octyl CH_2); ^{13}C NMR (125 MHz, CDCl_3 , δ_{C}) 166.4 (C=O), 165.8 (C=O), 165.5 (C=O), 133.6 (Ar), 133.5 (Ar), 133.3 (Ar), 130 (Ar), 129.9 (Ar), 129.7 (Ar), 129.6 (Ar), 129.1 (Ar), 129.1 (Ar), 128.6 (Ar), 128.5 (Ar), 128.5 (Ar), 128.4 (Ar), 105.7 (C-1), 82.2 (C-2), 81.9 (C-4), 77.6 (C-5), 73.5 (C-3), 67.6 (octyl OCH_2), 62.7 (C-6), 51.0 (octyl CH_2N_3), 29.5 (octyl CH_2), 29.3 (octyl CH_2), 29.1 (octyl CH_2), 28.8 (octyl CH_2), 26.7 (octyl CH_2), 26.1 (octyl CH_2); HR ESIMS: m/z $[\text{M}+\text{Na}^+]$ calcd for $\text{C}_{35}\text{H}_{39}\text{N}_3\text{NaO}_9$: 668.2579. Found: 668.2575. Data for **3.42** $[\alpha]_D +2.9$ (c 0.4, CH_2Cl_2); ^1H NMR (400 MHz, CDCl_3 , δ_{H}) 8.11–8.02 (m, 6 H, Ar), 7.63–7.52 (m, 3 H, Ar), 7.49–7.39 (m, 6 H, Ar), 5.64 (d, 1 H, $J = 4.8$ Hz, H-3), 5.52 (d, 1 H, $J = 1.3$ Hz, H-2), 5.27 (s, 1 H, H-1), 4.60 (dd, 1 H, $J = 12.6, 8.0$ Hz, H-6a), 4.55–4.44 (m, 2 H, H-5, H-6a), 4.37 (dd, 1 H, $J = 4.8, 2.2$ Hz, H-4), 3.72 (dt, 1 H, $J = 9.5, 6.7$ Hz, octyl OCH_2), 3.51 (dt, 1 H, $J = 9.5, 6.2$ Hz, octyl OCH_2), 3.21 (t, 2 H, $J = 7.0$ Hz, octyl CH_2N_3), 2.40 (s, 1 H, OH), 1.68–1.43 (m, 4 H, octyl CH_2), 1.30–1.19 (m, 8 H, octyl CH_2); ^{13}C NMR (125 MHz, CDCl_3 , δ_{C}) 166.5 (C=O), 166.0 (C=O), 165.4 (C=O), 133.6 (Ar), 133.1 (Ar), 129.9

(Ar), 129.9 (Ar), 129.8 (Ar), 129.7 (Ar), 129.2 (Ar), 129.1 (Ar), 128.6 (Ar), 128.5 (Ar), 128.4 (Ar), 105.7 (C-1), 83.1 (C-4), 81.5 (C-2), 78.2 (C-3), 69.1 (C-5), 67.6 (C-6), 66.2 (octyl OCH₂), 51.4 (octyl CH₂N₃), 29.4 (octyl CH₂), 29.2 (octyl CH₂), 29.1 (octyl CH₂), 28.8 (octyl CH₂), 26.6 (octyl CH₂), 26.0 (octyl CH₂); HR ESIMS: *m/z* [M+Na⁺] calcd for C₃₅H₃₉N₃NaO₉: 668.2579. Found: 668.2563.

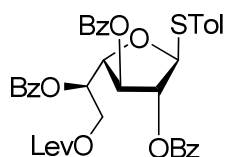


3.32

p-Tolyl 2,3,6-tri-*O*-benzoyl-5-*O*-levulinoyl-1-thio-β-*D*-galactofuranoside

(3.32). A mixture of **3.30**¹³ (840 mg, 1.4 mmol), levulinic acid (215 μL, 2.1 mmol), dicyclohexylcarbodiimide (DCC, 433 mg, 2.1 mmol) and 4-(dimethylamino)pyridine (DMAP, 86 mg, 0.7 mmol) in CH₂Cl₂ (30 mL) was stirred for 3 h. The reaction mixture was diluted with CH₂Cl₂, filtered through Celite and then the organic layer was washed with a saturated NaHCO₃ solution and brine. The organic layer was then dried over anhydrous Na₂SO₄, filtered, and concentrated to give a residue that was purified using column chromatography (3:1 Hexane–EtOAc) to give compound **3.32** (847 mg, 87%) as a colourless syrup, *R_f* 0.31 (2:1 Hexane–EtOAc); [α]_D –19.8 (*c* 9.0, CH₂Cl₂); ¹H NMR (400 MHz, CDCl₃, δ_H) 8.09 (ddd, 4 H, *J* = 8.3, 6.1, 1.2 Hz, Ar), 8.00 (dd, 2 H, *J* = 8.3, 1.3 Hz, Ar), 7.63–7.52 (m, 3 H, Ar), 7.50–7.38 (m, 8 H, Ar), 7.12 (d, 2 H, *J* = 7.9 Hz, Ar), 5.80 (app dt, 1 H, *J* = 7.0, 4.3 Hz, H-5), 5.74 (d, 1 H, *J* = 1.7 Hz, H-1), 5.69 (app t, 1 H, *J* = 1.8 Hz, H-2), 5.62 (dd, 1 H, *J* = 4.5, 2.1 Hz, H-3), 4.81 (app t, 1 H, *J* = 4.6 Hz, H-4), 4.68 (dd, 1 H, *J* = 11.9, 4.3 Hz, H-6a), 4.56 (dd, 1 H, *J* = 11.9, 7.0 Hz, H-6b), 2.71–2.57

(m, 4 H, Lev-(CH₂)₂), 2.33 (s, 3 H, Ar-CH₃), 2.08 (s, 3 H, Lev-CH₃); ¹³C NMR (125 MHz, CDCl₃, δ_C) 205.9 (C=O), 172.0 (C=O), 166.0 (C=O), 165.5 (C=O), 165.3 (C=O), 138.3 (Ar), 133.7 (Ar), 133.2 (Ar), 133.1 (Ar), 130.1 (Ar), 129.9 (Ar), 129.9 (Ar), 129.8 (Ar), 129.6 (Ar), 129.4 (Ar), 129.0 (Ar), 128.9 (Ar), 128.6 (Ar), 128.6 (Ar), 128.4 (Ar), 91.5 (C-1), 82.0 (C-2), 81.2 (C-4), 77.6 (C-3), 69.9 (C-5), 63.2 (C-6), 37.9 (Lev-CH₂), 29.7 (Lev-CH₂), 28.1 (Lev-CH₃), 21.2 (Ar-CH₃); HR ESIMS: *m/z* [M+Na⁺] calcd for C₃₉H₃₆NaO₁₀S: 719.1921. Found: 719.1912

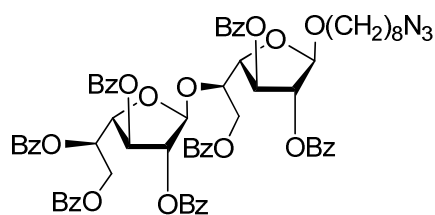


3.33

p-Tolyl 2,3,5-tri-*O*-benzoyl-6-*O*-levulinoyl-1-thio-β-*D*-galactofuranoside

(3.33). The same synthetic procedure employed to obtain **3.32**, was used to synthesize **3.33**, where a mixture of **3.31**¹³ (510 mg, 0.85 mmol), levulinic acid (130 μL, 1.27 mmol), dicyclohexylcarbodiimide (DCC, 262 mg, 1.27 mmol) and 4-(dimethylamino)pyridine (DMAP, 52 mg, 0.43 mmol) in CH₂Cl₂ (30 mL) was stirred for 3.5 h and the same work up for **3.32** was applied here to give compound **3.33** (520 mg, 88%) as a colourless syrup, *R_f* 0.28 (2:1 Hexane–EtOAc); [α]_D –74.0 (*c* 1.7, CH₂Cl₂), ¹H NMR (400 MHz, CDCl₃, δ_H) 8.09 (ddd, 4 H, *J* = 13.0, 8.2, 1.1 Hz, Ar), 7.90 (dd, 2 H, *J* = 8.3, 1.2 Hz, Ar), 7.64–7.43 (m, 7 H, Ar), 7.33 (dt, 4 H, *J* = 17.8, 7.9 Hz, Ar), 7.13 (d, 2 H, *J* = 8.0 Hz, Ar), 5.96 (app dt, 1 H, *J* = 8.1, 4.3 Hz, H-5), 5.78 (s, 1 H, H-1), 5.68–5.59 (m, 2 H, H-2, H-3), 4.93–4.81 (m, 1 H, H-4), 4.58 (dd, 1 H, *J* = 11.8, 4.5 Hz, H-6a), 4.49 (dd, 1 H, *J* = 11.8, 7.3 Hz, H-6b), 2.66 (t, 2 H, *J* = 6.7, Hz, Lev-CH₂), 2.54 (t, 2 H, *J* = 6.5, Hz, Lev-CH₂), 2.34 (s, 3

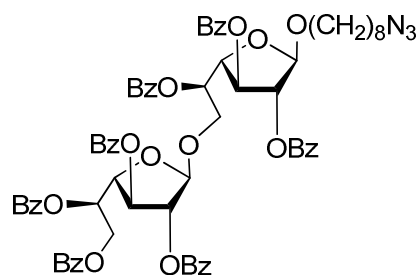
H, Ar-CH₃), 2.09 (s, 3 H, Lev-CH₃); ¹³C NMR (125 MHz, CDCl₃, δ_c) 206.2 (C=O), 172.2 (C=O), 165.7 (C=O), 165.5 (C=O), 165.3 (C=O), 138.3 (Ar), 133.6 (Ar), 133.5 (Ar), 133.4 (Ar), 133.2 (Ar), 130.1 (Ar), 130 (Ar), 129.9 (Ar), 129.9 (Ar), 129.5 (Ar), 129.3 (Ar), 128.9 (Ar), 128.8 (Ar), 128.6 (Ar), 128.5 (Ar), 91.6 (C-1), 82.3 (C-2), 81.4 (C-4), 77.9 (C-3), 70.2 (C-5), 63.0 (C-6), 37.8 (Lev-CH₂), 29.7 (Lev-CH₂), 27.8 (Ar-CH₃), 21.2 (Lev-CH₃); HR ESIMS: *m/z* [M+Na⁺] calcd for C₃₉H₃₆NaO₁₀S: 719.1921. Found: 719.1912



3.43

8-Azido-octyl 2,3,5,6-tetra-*O*-benzoyl-β-D-galactofuranosyl-(1→5)-2,3,6-tri-*O*-benzoyl-β-D-galactofuranoside (3.43). Acceptor **3.42** (110 mg, 0.17 mmol), donor **3.26** (176 mg, 0.26 mmol), and activated powdered 4 Å molecular sieves (425 mg) were added to CH₂Cl₂ (25 mL). The reaction mixture was cooled to 0 °C and stirred for 15 min before the addition of NIS (55 mg, 0.23 mmol) and AgOTf (10 mg, 0.042 mmol). After 30 min Et₃N was added. The mixture was then diluted with CH₂Cl₂ and filtered through Celite. The organic layer was washed with a saturated solution of Na₂S₂O₃ then brine, dried over Na₂SO₄, filtered, concentrated and purified by column chromatography afforded disaccharide **3.43** (182 mg, 88%) as a colourless oil (2:1 Hexanes–EtOAc). *R_f* 0.31 (2:1 Hexane–EtOAc); [α]_D –67.2 (*c* 1.5, CH₂Cl₂); ¹H NMR (400 MHz, CDCl₃, δ_H) 7.99–7.84 (m, 11 H, Ar), 7.83 (d, 4 H, *J* = 7.8 Hz, Ar), 7.65–7.01 (m, 20 H, Ar), 6.11 (app dt, 1 H, *J* = 7.0, 3.6

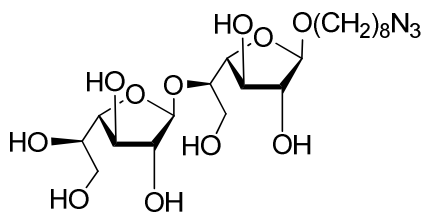
Hz, H-5'), 5.86 (dd, 1 H, $J = 5.1, 1.3$ Hz, H-3), 5.82 (s, 1 H, H-1'), 5.72 (s, 1 H, H-2'), 5.63 (dd, 1 H, $J = 5.1, 1.1$ Hz, H-3'), 5.51 (s, 1 H, H-2), 5.22 (s, 1 H, H-1), 5.08 (dd, 1 H, $J = 5.0, 3.5$ Hz, H-4'), 4.75–4.64 (m, 5 H, H-6a, H-6a', H-5, H-6b, H-6b'), 4.56–4.42 (dd, 1 H, $J = 5.1, 1.0$ Hz, H-4), 3.75 (ddd, 1 H, $J = 10.0, 6.0, 6.0$ Hz, octyl OCH₂), 3.51 (ddd, 1 H, $J = 10.0, 6.0, 6.0$ Hz, octyl OCH₂), 3.20 (t, 2 H, $J = 7.0$ Hz, octyl CH₂N₃), 1.57–1.50 (m, 4 H, octyl OCH₂), 1.37–1.22 (m, 8 H, octyl OCH₂); ¹³C NMR (125 MHz, CDCl₃, δ_C) 166.1 (C=O), 166.0 (C=O), 165.6 (C=O), 165.6 (C=O), 165.5 (C=O), 165.4 (C=O), 165.2 (C=O), 133.4 (Ar), 133.4 (Ar), 133.3 (Ar), 133.2 (Ar), 133.1 (Ar), 133.0 (Ar), 132.9 (Ar), 129.9 (Ar), 129.9 (Ar), 129.8 (Ar), 129.8 (Ar), 129.7 (Ar), 129.8 (Ar), 129.7 (Ar), 129.6 (Ar), 129.5 (Ar), 129.0 (Ar), 128.9 (Ar), 128.9 (Ar), 128.8 (Ar), 128.5 (Ar), 128.4 (Ar), 128.4 (Ar), 128.3 (Ar), 128.2 (Ar), 128.1 (Ar), 105.5 (C-1'), 105.2 (C-1), 82.4 (C-2'), 82.1 (C-2), 82.0 (C-4'), 81.7 (C-4), 77.9 (C-3), 77.5 (C-3'), 77.3 (C-5), 77.1 (C-5'), 70.5 (C-6'), 67.5 (octyl OCH₂), 64.6 (C-6), 51.4 (octyl CH₂N₃), 29.4 (octyl CH₂), 29.2 (octyl CH₂), 29.1 (octyl CH₂), 28.8 (octyl CH₂), 26.6 (octyl CH₂), 26.1 (octyl CH₂); HR ESIMS: m/z [M+Na⁺] calcd. for C₆₉H₆₅N₃O₁₈Na: 1246.4155. Found: 1246.4158.



3.44

8-Azido-octyl 2,3,5,6-tetra-O-benzoyl- β -D-galactofuranosyl-(1 \rightarrow 6)-2,3,5-tri-O-benzoyl- β -D-galactofuranoside (3.44). Acceptor **3.41** (100 mg, 0.15 mmol) and thioglycoside donor **3.26** (160 mg, 0.23 mmol) were dissolved in CH₂Cl₂ (25 mL) and activated powdered 4 Å molecular sieves (400 mg) were added. The reaction mixture was cooled to 0 °C and stirred for 15 min before the addition of NIS (80 mg, 0.16 mmol) and AgOTf (14.2 mg, 0.06 mmol). After 30 min, Et₃N was added. The mixture was then diluted with CH₂Cl₂ and filtered through Celite. The organic layer was washed with a saturated solution of Na₂S₂O₃ then brine, dried over Na₂SO₄, filtered, concentrated and purified by column chromatography (2:1 Hexanes–EtOAc) to give **3.44** (150 mg, 89%) as a colourless oil. *R*_f 0.29 (2:1 Hexane–EtOAc); [α]_D –67.2 (*c* 0.6, CH₂Cl₂); ¹H NMR (400 MHz, CDCl₃, δ _H) 8.09–7.99 (m, 8 H, Ar), 7.98–7.89 (m, 4 H, Ar), 7.80–7.76 (m, 2 H, Ar), 7.54–7.44 (m, 7 H, Ar), 7.39–7.25 (m, 14 H, Ar), 6.07 (app dt, 1 H, *J* = 5.0, 3.6 Hz, H-5'), 5.91 (app dt, 1 H, *J* = 5.0, 3.8 Hz, H-5), 5.62–5.58 (m, 2 H, H-3, H-3'), 5.44 (d, 1 H, *J* = 1.1 Hz, H-2'), 5.41 (d, 1 H, *J* = 1.1, H-2), 5.39 (s, 1 H, H-1'), 5.26 (br s, 1 H, H-1), 4.80–4.72 (m, 3 H, H-4, H-6a', H-6b'), 4.70 (dd, 1 H, *J* = 4.9, 3.8 Hz, H-4'), 4.20 (dd, 1 H, *J* = 10.5, 5.8 Hz, H-6a), 4.06 (dd, 1 H, *J* = 10.5, 5.8 Hz, H-6b), 3.75 (ddd, 1 H, *J* = 10.0, 6.0, 6.0 Hz, octyl OCH₂), 3.52 (ddd, 1 H, *J* = 10.0, 6.0, 6.0 Hz, octyl OCH₂), 3.20 (t, 2 H, *J* = 7.0 Hz, octyl CH₂N₃), 1.57–1.51 (m, 4 H, octyl OCH₂), 1.34–1.22 (m, 8 H, octyl OCH₂); ¹³C NMR (125 MHz, CDCl₃, δ _C) 166.1 (C=O), 165.8 (C=O), 165.7 (C=O), 165.6 (C=O), 165.6 (C=O), 165.4 (C=O), 165.2 (C=O), 137.4 (Ar), 133.9 (Ar), 133.4 (Ar), 133.3 (Ar), 133.2 (Ar), 133.2 (Ar), 133.1 (Ar), 132.9 (Ar), 129.9 (Ar), 129.8 (Ar), 129.7 (Ar), 129.6 (Ar), 129.4 (Ar), 129.1

(Ar), 129.0 (Ar), 128.9 (Ar), 128.8 (Ar), 128.5 (Ar), 128.4 (Ar), 128.4 (Ar), 128.3 (Ar), 128.3 (Ar), 106.1 (C-1'), 105.7 (C-1), 82.2 (C-2'), 81.9 (C-2), 81.8 (C-4'), 81.3 (C-4), 77.5 (C-3), 77.4 (C-3'), 77.30 (C-5), 77.1 (C-5'), 71.2 (C-6), 70.2 (C-6'), 67.7 (octyl OCH₂), 51.4 (octyl CH₂N₃), 29.4 (octyl CH₂), 29.2 (octyl CH₂), 29.1 (octyl CH₂), 28.8 (octyl CH₂), 26.6 (octyl CH₂), 26.0 (octyl CH₂), 21.1 (octyl CH₂); HR ESIMS: *m/z* [M+Na⁺] calcd. for C₆₉H₆₅N₃O₁₈Na: 1246.4155. Found: 1246.4148.

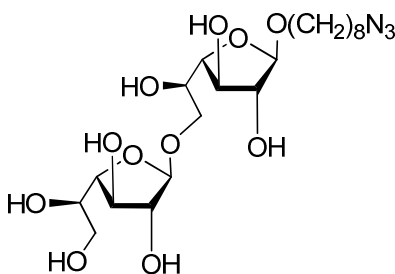


3.1

8-Azido-octyl β-D-galactofuranosyl-(1→5)-β-D-galactofuranoside (3.1).

Applying the general deprotection procedure using Zemplén conditions on disaccharide **3.43** (100 mg, 0.08 mmol) afforded, after purification, the final target compound **3.1** (35 mg, 89%) as a colourless syrup. Purification was done using column chromatography (5:1 CH₂Cl₂–MeOH) followed by further purification using C18 silica gel using H₂O–MeOH as the eluent. *R_f* 0.41 (4:1 CH₂Cl₂–MeOH); [α]_D –124.2 (*c* 0.5, MeOH); ¹H NMR (500 MHz, CD₃OD, δ_H) 5.17 (br s, 1 H, H-1'), 4.82 (br s, 1 H, H-1), 4.15 (dd, 1 H, *J* = 5.9, 3.7 Hz, H-3'), 4.12–3.97 (m, 3 H, H-2, H-2', H-3), 3.91–3.87 (m, 1 H, H-4'), 3.81–3.77 (m, 2 H, H-4', H-5'), 3.75–3.69 (m, 3 H, H-5, H-6a, H-6b), 3.70–3.61 (m, 3 H, H-6'a, H-6'b, octyl OCH₂), 3.40 (td, 1 H, *J* = 9.6, 6.5 Hz, octyl OCH₂), 3.27 (t, 2 H, *J* = 6.9 Hz, octyl CH₂N₃),

1.57–1.48 (m, 4 H, octyl CH_2), 1.40–1.32 (m, 8 H, octyl CH_2); ^{13}C NMR (125 MHz, CD_3OD , δ_C) 109.3 (C-1'), 109.1 (C-1), 84.8 (C-2'), 83.6 (C-2), 83.4 (C-4'), 82.7 (C-4), 78.7 (C-3), 78.6 (C-3'), 77.1 (C-5), 72.2 (C-5'), 68.9 (C-6), 64.2 (octyl OCH_2), 62.8 (C-6'), 52.4 (octyl CH_2N_3), 30.6 (octyl CH_2), 30.3 (octyl CH_2), 30.2 (octyl CH_2), 29.9 (octyl CH_2), 27.7 (octyl CH_2), 27.1 (octyl CH_2); HR ESIMS: m/z $[M+Na^+]$ calcd. for $C_{20}H_{37}N_3NaO_{11}$: 518.2320. Found: 518.2317.

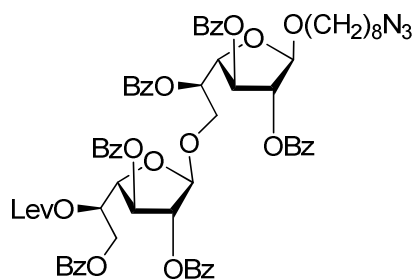


3.2

8-Azido-octyl β -D-galactofuranosyl-(1 \rightarrow 6)- β -D-galactofuranoside (3.2).

Applying the general deprotection procedure using Zémpfen conditions on disaccharide **3.44** (80 mg, 0.06 mmol) afforded, after purification, the final target compound **3.2** (27 mg, 91%) as a colourless syrup. Purification was done using column chromatography (5:1 CH_2Cl_2 -MeOH) followed by further purification using C18 silica gel using H_2O -MeOH as eluent, R_f 0.43 (4:1 CH_2Cl_2 -MeOH); $[\alpha]_D -98.3$ (c 1.1, MeOH); 1H NMR (500 MHz, CD_3OD , δ_H) 4.91 (d, 1 H, $J = 1.1$ Hz, H-1'), 4.83 (br s, 1 H, H-1), 4.02–3.99 (m, 1 H, H-3'), 3.99–3.96 (m, 3 H, H-2, H-2', H-3), 3.92 (dd, 1 H, $J = 3.8, 1.86$ Hz, H-4'), 3.86–3.80 (m, 2 H, H-4', H-5'), 3.80 (dd, 1 H, $J = 10.3, 4.33$ Hz, H-6a'), 3.74–3.67 (m, 3 H, H-6'b, H-6a,b), 3.64–3.59 (m, 1 H, H-5), 3.56–3.51 (m, 1 H, octyl OCH_2), 3.41 (td, 1 H, $J = 9.6, 6.6$ Hz,

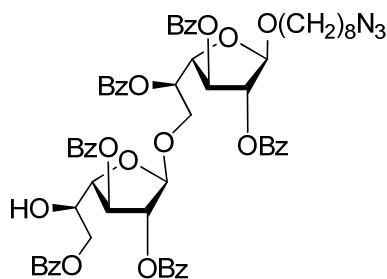
octyl OCH₂), 3.27 (t, 2 H, *J* = 6.9 Hz, octyl CH₂N₃), 1.63–1.54 (m, 4 H, octyl CH₂), 1.37–1.25 (m, 8 H, octyl CH₂); ¹³C NMR (125 MHz, CD₃OD, δ_C) 110.0 (C-1'), 109.3 (C-1), 84.9 (C-2'), 84.6 (C-2), 83.5 (C-4'), 82.9 (C-4), 78.8 (C-3), 72.5 (C-3'), 71.1 (C-5), 70.7 (C-5'), 68.9 (C-6), 64.5 (C-6'), 62.8 (octyl OCH₂), 52.5 (octyl CH₂N₃), 30.7 (octyl CH₂), 30.2 (octyl CH₂), 30.3 (octyl CH₂), 29.9 (octyl CH₂), 27.8 (octyl CH₂), 27.2 (octyl CH₂); HR ESIMS: *m/z* [M+Na⁺] calcd. for C₂₀H₃₇N₃NaO₁₁: 518.2320. Found: 518.2315.



3.45

8-Azido-octyl 2,3,6-tri-*O*-benzoyl-5-*O*-levulinoyl-β-D-galactofuranosyl-(1→6)-2,3,5-tri-*O*-benzoyl-β-D-galactofuranoside (3.45). Acceptor **3.41** (200 mg, 0.31 mmol), donor **3.32** (324 mg, 0.46 mmol), activated powdered 4 Å molecular sieves (425 mg) in CH₂Cl₂ (25 mL) were cooled to 0 °C. The reaction mixture was stirred for 15 min before the addition of NIS (104 mg, 0.46 mmol) and AgOTf (20 mg, 0.078 mmol). After 30 min Et₃N was added. The mixture was diluted with CH₂Cl₂ and filtered through Celite. The organic layer was washed with a saturated solution of Na₂S₂O₃ then brine, dried over Na₂SO₄, filtered, concentrated and purified by column chromatography (2:1 Hexane–EtOAc) to give **3.45** (317 mg, 87%) as a colorless oil, *R_f* 0.35 (2:1 Hexane–EtOAc); [α]_D –3.6 (*c* 0.5, CH₂Cl₂); ¹H

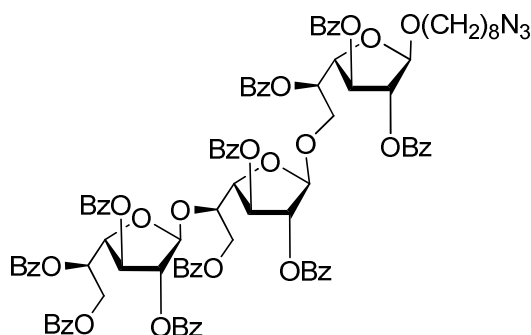
NMR (500 MHz, CDCl₃, δ_H) 8.11–7.97 (m, 10 H, Ar), 7.97–7.88 (m, 2 H, Ar), 7.61–7.27 (m, 18 H, Ar), 5.94 (app dt, 1 H, *J* = 5.9, 4.1 Hz, H-5), 5.80 (app dt, 1 H, *J* = 6.0, 3.8 Hz, H-5'), 5.62 (d, 1 H, *J* = 5.8 Hz, H-3), 5.51 (d, 1 H, *J* = 5.9 Hz, H-3'), 5.47 (d, 1 H, *J* = 1.0 Hz, H-2'), 5.45 (d, 1 H, *J* = 1.2 Hz, H-2), 5.39 (s, 1 H, H-1'), 5.30 (s, 1 H, H-1), 4.77–4.64 (m, 3 H, H-4, H-4', H-6'a), 4.60 (dd, 1 H, *J* = 12.0, 7.5 Hz, H-6'b), 4.22 (dd, 1 H, *J* = 10.6, 5.5 Hz, H-6a), 4.07 (dd, *J* = 10.6, 6.7 Hz, H-6b), 3.77 (dt, 1 H, *J* = 9.6, 6.6 Hz, octyl OCH₂), 3.55 (dt, 1 H, *J* = 9.6, 6.4 Hz, octyl OCH₂), 3.22 (t, 2 H, *J* = 7.0 Hz, octyl CH₂N₃), 2.72–2.33 (m, 4 H, Lev-(CH₂)₂), 2.06 (s, 3 H, Lev-CH₃), 1.69–1.44 (m, 4 H, octyl CH₂), 1.44–1.12 (m, 8 H, octyl CH₂); ¹³C NMR (125 MHz, CDCl₃, δ_C) 205.8 (Lev C=O), 171.9 (C=O), 166.0 (C=O), 165.8 (C=O), 165.7 (C=O), 165.5 (C=O), 165.5 (C=O), 165.1 (C=O), 133.5 (Ar), 133.4 (Ar), 133.4 (Ar), 133.4 (Ar), 133.1 (Ar), 133.1 (Ar), 129.9 (Ar), 129.9 (Ar), 129.9 (Ar), 129.8 (Ar), 129.8 (Ar), 129.7 (Ar), 129.7 (Ar), 129.2 (Ar), 129.1 (Ar), 129.1 (Ar), 128.9 (Ar), 128.5 (Ar), 128.5 (Ar), 128.4 (Ar), 128.4 (Ar), 128.4 (Ar), 128.4 (Ar), 106.1 (C-1'), 105.7 (C-1), 82.2 (C-2), 81.7 (C-2'), 81.6 (C-4), 81.4 (C-4'), 77.6 (C-3), 77.5 (C-3'), 71.3 (C-5), 70.0 (C-5'), 67.7 (octyl OCH₂), 66.2 (C-6), 63.5 (C-6'), 51.4 (octyl CH₂N₃), 37.9 (Lev-CH₂), 29.6 (Lev-CH₃), 29.4 (Lev-CH₂), 29.3 (octyl CH₂), 29.1 (octyl CH₂), 28.8 (octyl CH₂), 28.0 (octyl CH₂), 26.7 (octyl CH₂), 26.1 (octyl CH₂); HR ESIMS: *m/z* [M+Na⁺] calcd for C₆₇H₆₇N₃NaO₁₉: 1240.4261. Found: 1240.4251.



3.46

8-Azido-octyl 2,3,6-tri-*O*-benzoyl- β -D-galactofuranosyl-(1 \rightarrow 6)-2,3,5-tri-*O*-benzoyl- β -D-galactofuranoside (3.46). A solution of **3.45** (250 mg, 0.21 mmol) in 8 mL (3:1 CH₂Cl₂–MeOH) and hydrazine acetate (37 mg, 0.4 mmol) was stirred for 2.5 h. The solvent was removed and the residue was diluted with EtOAc. The organic layer was then washed with a saturated solution of NaHCO₃, brine, dried over anhydrous Na₂SO₄, filtered and concentrated. The crude residue was purified using column chromatography (2.5:1 Hexane–EtOAc) to give **3.46** (185 mg, 83%) as a colourless syrup, *R_f* 0.42 (2:1 Hexane–EtOAc); [α]_D –29.3 (*c* 0.5, CH₂Cl₂); ¹H NMR (500 MHz, CDCl₃, δ _H) 8.13–8.00 (m, 10 H, Ar), 7.59–7.26 (m, 20 H, Ar), 5.95–5.90 (m, 1 H, H-5'), 5.68–5.62 (m, 2 H, H-3, H-3'), 5.61 (d, 1 H, *J* = 1.6 Hz, H-2), 5.50–5.43 (br s, 2 H, H-1', H-2'), 5.39 (d, 1 H, *J* = 1.3 Hz, H-1), 4.69–4.65 (m, 1 H, H-5), 4.62 (ddd, 1 H, *J* = 11.2, 6.9, 2.8 Hz, H-4), 4.56–4.43 (m, 3 H, H-4', H-6'a,b), 4.19–4.13 (m, 1 H, H-6a), 4.07–4.01 (m, 1 H, H-6b), 3.76 (ddt, 1 H, *J* = 10.3, 6.5, 3.3 Hz, octyl OCH₂), 3.54 (ddt, 1 H, *J* = 10.1, 6.7, 3.2 Hz, octyl OCH₂), 3.22 (t, 1 H, *J* = 7.0 Hz, octyl CH₂N₃), 2.77 (br s, 1 H, OH), 1.69–1.42 (m, 4 H, octyl CH₂), 1.42–1.12 (m, 8 H, octyl CH₂); ¹³C NMR (125 MHz, CDCl₃, δ _C) 166.5 (C=O), 166.1 (C=O), 165.8 (C=O), 165.7 (C=O), 165.5 (C=O), 165.1 (C=O), 133.5 (Ar), 133.4 (Ar), 133.1 (Ar), 129.9 (Ar), 129.9 (Ar), 129.8 (Ar), 129.7 (Ar), 129.7

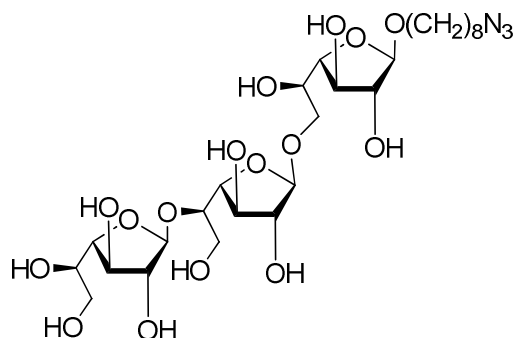
(Ar), 129.2 (Ar), 129.1 (Ar), 129.0 (Ar), 128.9 (Ar), 128.5 (Ar), 128.4 (Ar), 128.3 (Ar), 106.4 (C-1), 105.7 (C-1'), 83.6 (C-2), 82.2 (C-2'), 81.5 (C-4), 78.0 (C-4'), 77.6 (C-3'), 71.4 (C-3), 69.2 (C-5), 69.0 (C-5'), 67.7 (octyl OCH₂), 66.4 (C-6), 60.4 (C-6'), 51.4 (octyl CH₂N₃), 29.4 (octyl CH₂), 29.3 (octyl CH₂), 29.1 (octyl CH₂), 28.8 (octyl CH₂), 26.7 (octyl CH₂), 26.1 (octyl CH₂); HR ESIMS: *m/z* [M+Na⁺] calcd for C₆₂H₆₁N₃NaO₁₇: 1142.3893. Found: 1142.3884.



3.47

8-Azido-octyl 2,3,5,6-tetra-*O*-benzoyl- β -D-galactofuranosyl-(1 \rightarrow 5)-2,3,6-tri-*O*-benzoyl- β -D-galactofuranosyl-(1 \rightarrow 6)-2,3,5-tri-*O*-benzoyl- β -D-galactofuranoside (3.39). Acceptor **3.46** (180 mg, 0.16 mmol), donor **3.26** (170 mg, 0.24 mmol), and activated powdered 4 Å molecular sieves (410 mg) were added to CH₂Cl₂ (25 mL) and the reaction mixture was cooled to 0 °C. The reaction mixture was stirred for 15 min before the addition of NIS (85 mg, 0.37 mmol) and AgOTf (16 mg, 0.062 mmol). After 30 min Et₃N was added. The mixture was then diluted with CH₂Cl₂ and filtered through Celite. The organic layer was washed with a saturated solution of Na₂S₂O₃ then brine, dried over Na₂SO₄, filtered, and concentrated. The residue was purified using column chromatography (2:1 Hexane–EtOAc) to give **3.47** (230 mg, 85%) as a colorless syrup, *R_f* 0.23 (2:1

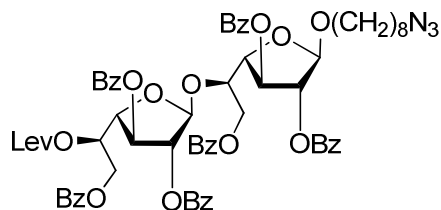
Hexane–EtOAc); $[\alpha]_D -14.1$ (c 0.5, CH_2Cl_2); ^1H NMR (498 MHz, CDCl_3 , δ_{H}) 8.07–7.80 (m, 20 H, Ar), 7.53–7.15 (m, 30 H, Ar), 6.06 (app dt, 1 H, $J = 6.2, 3.7$ Hz, H-5''), 5.93 (app dt, 1 H, $J = 6.1, 3.8$ Hz, H-5), 5.84 (d, 1 H, $J = 6.1$ Hz, H-3'), 5.82 (s, 1 H, H-1''), 5.69 (d, 1 H, $J = 1.3$ Hz, H-2''), 5.66 (d, 1 H, $J = 5.2$, H-3''), 5.61 (d, 1 H, $J = 5.0$ Hz, H-3), 5.47 (d, 1 H, $J = 1.3$ Hz, H-2'), 5.44 (d, 1 H, $J = 1.2$ Hz, H-2), 5.34 (s, 1 H, H-1'), 5.27 (s, 1 H, H-1), 5.06 (dd, 1 H, $J = 6.1, 5.1$ Hz, H-4''), 4.81–4.62 (m, 7 H, H-4, H-4', H-5', H6a',b', H6a'',b''), 4.19 (dd, 1 H, $J = 10.6, 5.6$ Hz, H-6a), 4.05 (dd, 1 H, $J = 10.6, 6.7$ Hz, H-6b), 3.74 (dt, 1 H, $J = 9.7, 6.6$ Hz, octyl OCH_2), 3.51 (dt, 1 H, $J = 9.7, 6.4$ Hz, octyl OCH_2), 3.18 (t, 2 H, $J = 7.0$ Hz, octyl CH_2N_3), 1.63–1.46 (m, 4 H, octyl CH_2), 1.39–1.23 (m, 8 H, octyl CH_2); ^{13}C NMR (125 MHz, CDCl_3 , δ_{C}) 166.1 (C=O), 165.9 (C=O), 165.8 (C=O), 165.7 (C=O), 165.7 (C=O), 165.6 (C=O), 165.5 (C=O), 165.5 (C=O), 165.2 (C=O), 165.2 (C=O), 133.3 (Ar), 133.3 (Ar), 133.2 (Ar), 133.1 (Ar), 132.9 (Ar), 132.9 (Ar), 129.9 (Ar), 129.8 (Ar), 129.7 (Ar), 129.7 (Ar), 129.6 (Ar), 129.6 (Ar), 129.2 (Ar), 129.1 (Ar), 128.9 (Ar), 128.9 (Ar), 128.8 (Ar), 128.8 (Ar), 128.5 (Ar), 128.3 (Ar), 128.2 (Ar), 128.2 (Ar), 106.1 (C-1), 105.6 (C-1''), 105.4 (C-1'), 83.0 (C-4'), 82.9 (C-4''), 82.1 (C-4), 82.0 (C-2'), 81.8 (C-2''), 81.4 (C-2), 77.8 (C-3'), 77.6 (C-3''), 77.3 (C-3), 72.8 (C-5), 71.2 (C-5'), 70.5 (C-5''), 67.8 (C-6), 66.1 (octyl OCH_2), 65.1 (C-6''), 63.8 (C-6'), 51.4 (octyl CH_2N_3), 29.4 (octyl CH_2), 29.3 (octyl CH_2), 29.1 (octyl CH_2), 28.8 (octyl CH_2), 26.6 (octyl CH_2), 26.0 (octyl CH_2); HR ESIMS: m/z $[\text{M}+\text{Na}^+]$ calcd for $\text{C}_9\text{H}_8\text{N}_3\text{NaO}_6$: 1720.5470. Found: 1720.5459.



3.3

8-Azido-octyl β -D-galactofuranosyl-(1 \rightarrow 5)- β -D-galactofuranosyl-(1 \rightarrow 6)- β -D-galactofuranoside (3.3). The trisaccharide **3.47** (200 mg, 0.13 mmol) was subjected to the general deprotection procedure for debenzoylation. The reaction mixture was stirred overnight and neutralized by glacial acetic acid. The solvents were evaporated and the residue was purified using column chromatography (2:1 CH₂Cl₂–MeOH) to give compound **3.3** (74 mg, 87%) as a colorless oil, *R_f* 0.24 (3:1 CH₂Cl₂–MeOH); [α]_D –113.1 (*c* 2.5, CH₂Cl₂); ¹H NMR (500 MHz, CD₃OD, δ _H) 5.16 (s, 1 H, H-1''), 4.90 (s, 1 H, H-1'), 4.83 (s, 1 H, H-1), 4.12 (app dt, 1 H, *J* = 5.4, 3.1 Hz, H-5''), 4.07 (dd, 1 H, *J* = 6.2, 3.3 Hz, H-5'), 4.05–3.95 (m, 5 H, H-2, H-2', H-2'', H-4', H-4''), 3.91–3.84 (m, 4 H, H-3'', H-3', H-5, H-4), 3.94–3.82 (m, 7 H, H-3, H6a,b, H-6'a,b, H-6''a,b), 3.51 (dd, 1 H, *J* = 10.3, 6.9 Hz, octyl OCH₂), 3.42–3.38 (m, 1 H, octyl OCH₂), 3.27 (t, 2 H, *J* = 6.9 Hz, octyl CH₂N₃), 1.58–1.50 (m, 4 H, octyl CH₂), 1.35–1.12 (m, 8 H, octyl CH₂); ¹³C NMR (126 MHz, CD₃OD δ _C) 109.8 (C-1'), 109.3 (C-1), 109.1 (C-1''), 84.9 (C-4'), 84.5 (C-4), 84.1 (C-4''), 83.5 (C-2''), 83.2 (C-2'), 82.7 (C-2), 78.8 (C-3'), 78.7 (C-3''), 78.6 (C-3), 77.2 (C-5'), 71.3 (C-5), 71.0 (C-5''), 70.6 (C-6'), 68.9 (octyl OCH₂), 64.2 (C-6''), 62.7 (C-6), 52.4 (octyl CH₂N₃), 30.6 (octyl CH₂), 30.4 (octyl CH₂), 30.2 (octyl CH₂), 29.9

(octyl CH₂), 27.8 (octyl CH₂), 27.1 (octyl CH₂); HR ESIMS: m/z [M+Na⁺] calcd for C₂₆H₄₇N₃NaO₁₆: 680.2849. Found: 680.2845.

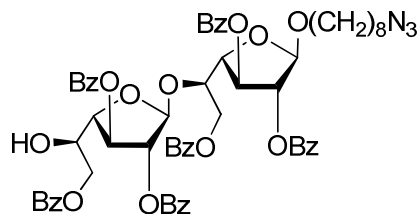


3.48

8-Azido-octyl 2,3,6-tri-O-benzoyl-5-O-levulinoyl- β -D-galactofuranosyl-(1 \rightarrow 5)-2,3,6-tri-O-benzoyl- β -D-galactofuranoside (3.48).

Acceptor **3.42** (100 mg, 0.15 mmol), donor **3.32** (160 mg, 0.23 mmol), activated powdered 4 Å molecular sieves (380 mg) were added to CH₂Cl₂ (30 mL) and the reaction mixture was cooled to 0 °C. The reaction mixture was stirred for 15 min before the addition of NIS (55 mg, 0.23 mmol) and AgOTf (10 mg, 0.034 mmol). After 30 min, Et₃N was added. The mixture was diluted with CH₂Cl₂ and filtered through Celite. The organic layer was washed with a saturated solution of Na₂S₂O₃ then brine, dried over Na₂SO₄, filtered, and concentrated. The obtained residue was purified using column chromatography (2:1 Hexane–EtOAc) to give **3.48** (160 mg, 88%) as a colorless oil R_f 0.28 (2:1 Hexane–EtOAc); $[\alpha]_D -0.7$ (c 0.4, CH₂Cl₂); ¹H NMR (500 MHz, CDCl₃, δ_H) 8.08–7.97 (m, 11 H, Ar), 7.90–7.86 (m, 2 H, Ar), 7.59–7.56 (m, 2 H, Ar), 7.53–7.40 (m, 11 H, Ar), 7.38–7.32 (m, 4 H, Ar), 5.84 (app dt, 1 H, $J = 7.1, 3.3$ Hz, H-5'), 5.81–5.76 (m, 2 H, H-1', H-3), 5.74 (dd, 1 H, $J = 1.8, 0.6$ Hz, H-2'), 5.56 (dd, 1 H, $J = 5.2, 1.6$ Hz, H-3'), 5.50 (d, 1 H, $J = 1.1$ Hz, H-2), 5.24 (s, 1 H, H-1), 4.91 (dd, 1 H, $J = 5.1, 4.2$ Hz, H-4'), 4.84–4.74 (m, 1 H,

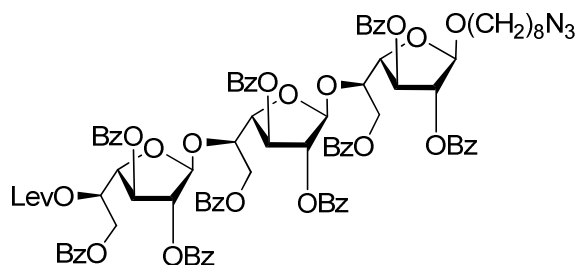
H-5), 4.76–4.66 (m, 3 H, H-4, H-6'a,b), 4.58–4.48 (m, 2 H, H-6a,b), 3.74 (td, 1 H, $J = 9.5, 6.7$ Hz, octyl OCH₂), 3.51 (td, 1 H, $J = 9.6, 6.3$ Hz, octyl OCH₂), 3.23 (t, 2 H, $J = 6.9$ Hz, octyl CH₂N₃), 2.67–2.55 (m, 1 H, Lev-CH₂) 2.52–2.45 (m, 1 H, Lev-CH₂), 2.04 (s, 3 H, Lev-CH₃), 1.65–1.54 (m, 4 H, octyl CH₂), 1.41–1.26 (m, 8 H, octyl CH₂); ¹³C NMR (125 MHz, CDCl₃, δ_C) 205.9 (Lev C=O), 171.9 (C=O), 166.1 (C=O), 165.9 (C=O), 165.7 (C=O), 165.5 (C=O), 165.4 (C=O), 165.2 (C=O), 133.5 (Ar), 133.3 (Ar), 133.1 (Ar), 129.8 (Ar), 129.1 (Ar), 128.9 (Ar), 128.4 (Ar), 105.5 (C-1'), 105.3 (C-1), 82.3 (C-2), 81.8 (C-2'), 77.4 (C-4), 77.1 (C-4'), 76.9 (C-3), 73.2 (C-3'), 70.1 (C-5'), 69.8 (C-5), 67.5 (octyl OCH₂), 64.6 (C-6), 63.5 (C-6'), 51.4 (octyl CH₂N₃), 37.9 (Lev-CH₂), 29.6 (Lev-CH₃), 29.3 (octyl CH₂), 29.1 (octyl CH₂), 28.8 (octyl CH₂), 27.9 (octyl CH₂), 26.7 (octyl CH₂), 26.1 (octyl CH₂); HR ESIMS: m/z [M+Na⁺] calcd for C₆₇H₆₇N₃NaO₁₉: 1240.4261. Found: 1240.4260.



3.49

8-Azido-octyl 2,3,6-tri-*O*-benzoyl-β-D-galactofuranosyl-(1→5)-2,3,6-tri-*O*-benzoyl-β-D-galactofuranoside (3.49). Disaccharide **3.48** (100 mg, 0.08 mmol) was subjected to the general procedure for the removal of the levulinoyl protecting group. After purification by column chromatography (2:1 Hexane–EtOAc) compound **3.49** (82 mg, 92%) was obtained as a colourless oil. R_f 0.34 (2:1 Hexane–EtOAc); $[\alpha]_D -0.5$ (c 0.4, CH₂Cl₂); ¹H NMR (500 MHz, CDCl₃, δ_H) 8.05–7.90 (m,

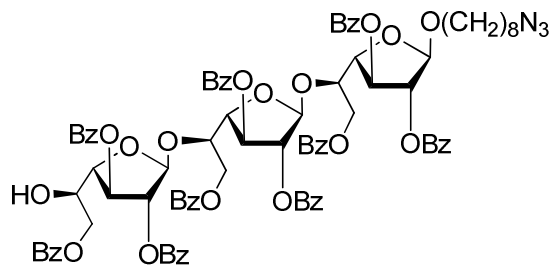
10 H, Ar), 7.86 (dd, 2 H, $J = 8.1, 1.0$ Hz, Ar), 7.60–7.28 (m, 16 H, Ar), 7.22 (t, 2 H, $J = 7.9$ Hz, Ar), 5.81–5.78 (m, 1 H, H-5), 5.75 (s, 1 H, H-1'), 5.72 (d, 1 H, $J = 1.6$ Hz, H-2'), 5.65 (app dt, 1 H, $J = 7.2, 3.2$ Hz, H-5'), 5.45 (d, 1 H, $J = 1.3$ Hz, H-2), 5.17 (s, 1 H, H-1), 4.78–4.60 (m, 5 H, H-3, H-3', H-4', H-6a',b'), 4.49–4.38 (m, 3 H, H-4, H-6a,b), 4.38 (s, 1 H, OH), 3.67 (dt, 1 H, $J = 9.5, 6.6$ Hz, octyl OCH₂), 3.45 (dt, 1 H, $J = 9.6, 6.3$ Hz, octyl OCH₂), 3.20 (t, 2 H, $J = 7.0$ Hz, octyl CH₂N₃), 1.55–1.48 (m, 4 H, octyl CH₂), 1.39–1.19 (m, 8 H, octyl CH₂); ¹³C NMR (125 MHz, CDCl₃, δ_c) 166.4 (C=O), 166.1 (C=O), 165.9 (C=O), 165.8 (C=O), 165.5 (C=O), 165.2 (C=O), 133.5 (Ar), 133.5 (Ar), 133.3 (Ar), 133.1 (Ar), 132.9 (Ar), 129.9 (Ar), 129.8 (Ar), 129.8 (Ar), 129.7 (Ar), 129.1 (Ar), 129 (Ar), 128.9 (Ar), 128.9 (Ar), 128.6 (Ar), 128.5 (Ar), 128.4 (Ar), 128.3 (Ar), 128.2 (Ar), 105.6 (C-1'), 105.5 (C-1), 83.6 (C-2'), 81.8 (C-4), 81.7 (C-2), 78.0 (C-4'), 73.4 (C-3), 72.3 (C-5), 70.2 (C-5'), 69.4 (C-3'), 67.5 (octyl OCH₂), 66.2 (C-6), 64.6 (C-6'), 51.4 (octyl CH₂N₃), 29.3 (octyl OCH₂), 29.2 (octyl OCH₂), 29.0 (octyl OCH₂), 28.8 (octyl OCH₂), 26.6 (octyl OCH₂), 26.0 (octyl OCH₂); HR ESIMS: m/z [M+Na⁺] calcd for C₆₂H₆₁N₃NaO₁₇: 1142.3893. Found: 1142.3883.



3.50

8-Azido-octyl 2,3,6-tri-*O*-benzoyl-5-*O*-levulinoyl- β -D-galactofuranosyl-(1 \rightarrow 5)-2,3,6-tri-*O*-benzoyl- β -D-galactofuranosyl-(1 \rightarrow 5)-2,3,6-tri-*O*-benzoyl- β -D-galactofuranoside (3.50). Extension of the chain was achieved when acceptor **3.49** (100 mg, 0.09 mmol) was coupled with donor **3.32** (78 mg, 0.11 mmol) in the presence of NIS (25 mg, 0.11 mmol) and AgOTf (5 mg, 0.017 mmol) as described for 3.48. After purification by column chromatography (2:1 Hexane–EtOAc) **3.50** (129 mg, 85%) was obtained as a colorless syrup, R_f 0.29; $[\alpha]_D -3.1$ (c 1.3, CH₂Cl₂); ¹H NMR (500 MHz, CDCl₃, δ_H) 8.06–7.86 (m, 14 H, Ar), 7.78–7.71 (m, 4 H, Ar), 7.59–7.11 (m, 27 H, Ar), 5.81–5.76 (m, 1 H, H-3''), 5.74 (s, 1 H, H-1'), 5.73 (s, 1 H, H-1''), 5.71 (m, 1 H, H-3'), 5.68 (d, 1 H, $J = 1.9$ Hz, H-2'), 5.67 (d, 1 H, $J = 1.7$ Hz, H-2''), 5.49 (dd, 1 H, $J = 7.1, 3.3$ Hz, H-5''), 5.46 (d, 1 H, $J = 1.2$ Hz, H-2), 5.19 (s, 1 H, H-1), 4.89–4.78 (m, 2 H, H-4', H-4''), 4.77–4.58 (m, 8 H, H-3, H-5, H-5', H-6a, H-6a', b', H-6a'', b''), 4.52–4.41 (m, 2 H, H-4, H-6b), 3.68 (dt, 1 H, $J = 9.5, 6.7$ Hz, octyl OCH₂), 3.46 (dt, 1 H, $J = 9.6, 6.2$ Hz, octyl OCH₂), 3.19 (t, 2 H, $J = 7.0$ Hz, octyl CH₂N₃), 2.64–2.28 (m, 4 H, Lev-CH₂), 1.98 (s, 3 H, Lev-CH₃), 1.55–1.39 (m, 4 H, octyl CH₂), 1.38–1.24 (m, 8 H, octyl CH₂); ¹³C NMR (125 MHz, CDCl₃, δ_C) 205.5 (Lev-C=O), 171.5 (C=O), 166.2 (C=O), 165.9 (C=O), 165.9 (C=O), 165.7 (C=O), 165.6 (C=O), 165.5 (C=O), 165.4 (C=O), 165.3 (C=O), 165.1

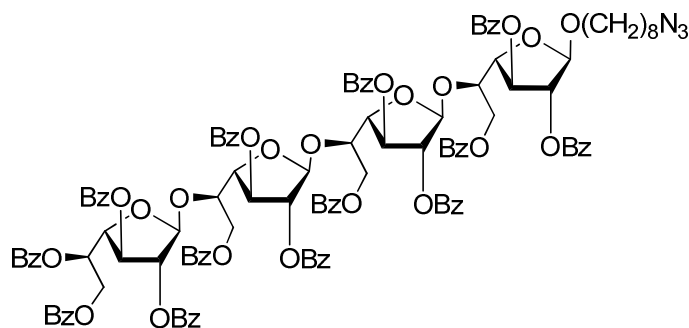
(C=O), 133.5 (Ar), 133.5 (Ar), 133.4 (Ar), 133.4 (Ar), 133.2 (Ar), 132.9 (Ar), 132.9 (Ar), 129.9 (Ar), 129.9 (Ar), 129.8 (Ar), 129.8 (Ar), 129.8 (Ar), 129.7 (Ar), 129.6 (Ar), 129.1 (Ar), 129.1 (Ar), 129.0 (Ar), 128.9 (Ar), 128.8 (Ar), 128.8 (Ar), 128.6 (Ar), 128.6 (Ar), 128.5 (Ar), 128.4 (Ar), 128.3 (Ar), 128.3 (Ar), 128.2 (Ar), 128.1 (Ar), 105.4 (C-1', C-1''), 105.3 (C-1), 83.2 (C-4', C-4''), 82.6 (C-2'), 81.9 (C-2), 81.8 (C-2''), 81.7 (C-4), 77.2 (C-5), 77.1 (C-5''), 73.2 (C-3), 73.1 (C-3'), 72.9 (C-3''), 70.1 (C-5'), 67.4 (octyl OCH₂), 65.0 (C-6), 64.4 (C-6'), 63.7 (C-6''), 51.4 (octyl CH₂N₃), 37.8 (Lev-CH₂), 29.6 (Lev-CH₃), 29.4 (Lev-CH₂), 29.3 (octyl CH₂), 29.1 (octyl CH₂), 28.8 (octyl CH₂), 27.9 (octyl CH₂), 26.7 (octyl CH₂), 26.0 (octyl CH₂); HR ESIMS: *m/z* [M+Na⁺] calcd for C₉₄H₈₉N₃NaO₂₇: 1714.5576. Found: 1714.5564.



3.51

8-Azido-octyl 2,3,6-tri-*O*-benzoyl- β -D-galactofuranosyl-(1 \rightarrow 5)-2,3,6-tri-*O*-benzoyl- β -D-galactofuranosyl-(1 \rightarrow 5)-2,3,6-tri-*O*-benzoyl- β -D-galactofuranoside (3.51). Trisaccharide acceptor **3.51** was obtained from **3.50** (80 mg, 0.047 mmol) according to the general deprotection procedure for the removal of the levulinoyl group above. Crude **3.51** was purified using column chromatography (2:1 Hexane–EtOAc) to give **3.51** (67 mg, 90%) as a colourless

symp, R_f 0.29 (2:1 Hexane–EtOAc); $[\alpha]_D -1.2$ (c 0.5, CH_2Cl_2); ^1H NMR (500 MHz, CDCl_3 , δ_{H}) 8.04–7.99 (m, 3 H, Ar), 7.96–7.81 (m, 12 H, Ar), 7.56 (dd, 1 H, $J = 14.7, 7.1$ Hz, Ar), 7.33–7.10 (m, 29 H, Ar), 5.82–5.80 (m, 2 H, H-2, H-2'), 5.73 (d, 2 H, $J = 2.8$ Hz, H-3, H-3'), 5.72 (s, 1 H, H-2',') 5.67 (s, 1 H, H-1''), 5.64–5.59 (m, 1 H, H-3''), 5.47 (s, 1 H, H-1'), 5.20 (s, 1 H, H-1), 4.87 (dd, 1 H, $J = 5.0, 3.1$ Hz, H-5''), 4.77–4.60 (m, 7 H, H-4, H-4', H-6a,b, H-6'a,b, H-6''a), 4.50–4.48 (m, 1 H, H-4''), 4.45 (d, 2 H, $J = 5.4$ Hz, H-5, H-5'), 4.39–4.32 (m, 2 H, H-6''b, OH), 3.76–3.63 (m, 1 H, octyl OCH_2), 3.47 (td, 1 H, $J = 9.6, 6.3$ Hz, octyl OCH_2), 3.19 (t, 2 H, $J = 6.9$ Hz, octyl CH_2N_3), 1.55–1.38 (m, 4 H, octyl CH_2), 1.41–1.22 (m, 8 H, octyl CH_2); ^{13}C NMR (125 MHz, CDCl_3 , δ_{C}) 166.3 (C=O), 166.1 (C=O), 165.9 (C=O), 165.8 (C=O), 165.7 (C=O), 165.6 (C=O), 165.4 (C=O), 165.2 (C=O), 165.1 (C=O), 133.7 (Ar), 133.4 (Ar), 133.4 (Ar), 133.4 (Ar), 133.3 (Ar), 133.2 (Ar), 133.2 (Ar), 132.9 (Ar), 132.9 (Ar), 132.8 (Ar), 129.9 (Ar), 129.8 (Ar), 129.8 (Ar), 129.8 (Ar), 129.7 (Ar), 129.7 (Ar), 129.6 (Ar), 129.6 (Ar), 129.6 (Ar), 129.0 (Ar), 129.0 (Ar), 128.9 (Ar), 128.9 (Ar), 128.7 (Ar), 128.6 (Ar), 128.6 (Ar), 128.5 (Ar), 128.4 (Ar), 128.3 (Ar), 128.3 (Ar), 128.2 (Ar), 128.2 (Ar), 128.1 (Ar), 105.6 (C-1''), 105.4 (C-1'), 105.2 (C-1), 83.5 (C-4'), 82.8 (C-4''), 82.5 (C-2'), 81.9 (C-2), 81.0 (C-2''), 81.6 (C-4), 77.9 (C-5), 77.1 (C-5''), 73.1 (C-3, C-3''), 73.0 (C-3'), 69.5 (C-5'), 67.4 (octyl OCH_2), 66.2 (C-6), 65.0 (C-6'), 64.4 (C-6''), 51.4 (octyl CH_2N_3), 29.4 (octyl CH_2), 29.2 (octyl CH_2), 29.0 (octyl CH_2), 28.7 (octyl CH_2), 26.6 (octyl CH_2), 26.0 (octyl CH_2); HR ESIMS: m/z $[\text{M}+\text{Na}^+]$ calcd for $\text{C}_{89}\text{H}_{83}\text{N}_3\text{NaO}_{25}$: 1616.5208. Found: 1616.5195.

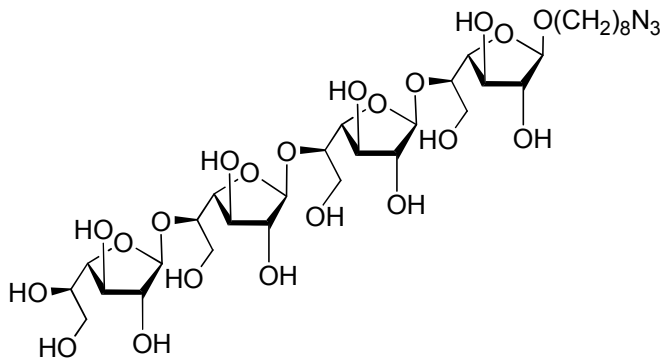


3.52

8-Azido-octyl 2,3,5,6-tetra-*O*-benzoyl- β -D-galactofuranosyl-(1 \rightarrow 5)-2,3,6-tri-*O*-benzoyl- β -D-galactofuranosyl-(1 \rightarrow 5)-2,3,6-tri-*O*-benzoyl- β -D-galactofuranosyl-(1 \rightarrow 5)-2,3,6-tri-*O*-benzoyl β -D-galactofuranoside (3.52).

Tetrasaccharide **3.52** was obtained when trisaccharide acceptor **3.51** (60 mg, 0.038 mmol) was coupled with thioglycoside donor **3.26** (33 mg, 0.047 mmol) in CH₂Cl₂ (20 mL). The reaction mixture was stirred for 15 min before the addition of NIS (10 mg, 0.038 mmol) and AgOTf (2 mg, 0.006 mmol). After 30 min, Et₃N was added. The mixture was diluted with CH₂Cl₂ and filtered through Celite. The organic layer was washed with a saturated solution of Na₂S₂O₃ then brine, dried over Na₂SO₄, filtered, and concentrated. Tetrasaccharide **3.52** was purified using column chromatography (2:1 Hexane–EtOAc) to give **3.52** (70.5 mg, 84%) as a colorless syrup. *R_f* 0.35 (2:1 Hexane–EtOAc); [α]_D –8.8 (*c* 0.3, CH₂Cl₂); ¹H NMR (500 MHz, CDCl₃, δ _H) 8.05–7.87 (m, 22 H, Ar), 7.76–7.70 (m, 6 H, Ar), 7.51–7.06 (m, 37 H, Ar), 6.01 (m, 1 H, *J* = 6.3, 3.5 Hz, H-3''), 5.85 (ddd, 2 H, *J* = 8.8, 5.0, 1.1 Hz, H-3, H-3'), 5.80 (d, 1 H, *J* = 4.9 Hz, H-3'''), 5.78 (d, 1 H, *J* = 3.7 Hz, H-2'), 5.74 (s, 2 H, H-1'', H-1'''), 5.70 (dd, 2 H, *J* = 5.1, 1.5 Hz, H-2, H-5'''), 5.66 (d, 1 H, *J* = 1.4 Hz, H-2'''), 5.63–5.60 (m, 2 H, H-3, H-5'''), 5.59 (dd, 1 H, *J* = 5.2, 1.2 Hz, H-2''), 5.45 (d, 1 H, *J* = 1.2 Hz, H-1'), 5.19 (s, 1 H, H-1), 5.00 (dd, 1 H, *J* = 5.1, 3.5

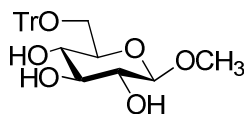
Hz, H-6a), 4.90–4.83 (m, 4 H, H-5, H-5', H-5'', H-6b), 4.77–4.59 (m, 9 H, H-4, H-4', H-4'', H-6'a,b, H-6''a,b, H-6'''a,b), 4.47 (dd, 1 H, $J = 4.8, 3.6$ Hz, H-4''), 3.67 (td, 1 H, $J = 9.6, 6.7$ Hz, octyl OCH₂), 3.45 (td, 1 H, $J = 9.6, 6.2$ Hz, octyl CH₂N₃), 3.19 (dd, 2 H, $J = 9.2, 4.8$ Hz, octyl OCH₂), 1.59–1.49 (m, 4 H, octyl CH₂), 1.33–1.23 (m, 8 H, octyl CH₂); ¹³C NMR (125 MHz, CDCl₃, δ_C) 166.1 (C=O), 165.9 (C=O), 165.9 (C=O), 165.8 (C=O), 165.6 (C=O), 165.6 (C=O), 165.5 (C=O), 165.4 (C=O), 165.2 (C=O), 165.2 (C=O), 165.1 (C=O), 133.4 (Ar), 133.4 (Ar), 133.3 (Ar), 133.2 (Ar), 133.1 (Ar), 133.0 (Ar), 132.9 (Ar), 132.9 (Ar), 132.8 (Ar), 132.7 (Ar), 129.9 (Ar), 129.8 (Ar), 129.7 (Ar), 129.6 (Ar), 129.6 (Ar), 129.0 (Ar), 128.9 (Ar), 128.9 (Ar), 128.7 (Ar), 128.6 (Ar), 128.6 (Ar), 128.4 (Ar), 128.3 (Ar), 128.2 (Ar), 128.2 (Ar), 128.1 (Ar), 128.0 (Ar), 105.4 (C-1'''), C-1''), 105.2 (C-1'), 105.2 (C-1), 83.5 (C-4'), 83.2 (C-4'''), 82.6 (C-4''), 82.0 (C-2'), 82.0 (C-2''), 81.8 (C-2), 81.8 (C-2'''), 81.6 (C-4), 77.8 (C-5), 77.7 (C-5''), 77.0, (C-5'''), 76.9 (C-5'), 73.1 (C-3), 72.9 (C-3'), 72.7 (C-3'''), 70.5 (C-3''), 67.3 (octyl OCH₂), 65.3 (C-6), 64.9 (C-6'''), 64.5 (C-6'), 63.9 (C-6''), 51.4 (octyl CH₂N₃), 29.4 (octyl CH₂), 29.2 (octyl CH₂), 29.0 (octyl CH₂), 28.7 (octyl CH₂), 26.6 (octyl CH₂), 26.0 (octyl CH₂); HR ESIMS: m/z [M+Na⁺] calcd for C₁₂₃H₁₀₉N₃NaO₃₄: 2194.6785. Found: 2194.6767.



3.4

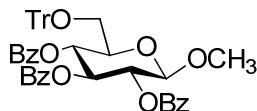
8-Azido octyl β -D-galactofuranosyl-(1 \rightarrow 5)- β -D-galactofuranosyl-(1 \rightarrow 5)- β -D-galactofuranosyl-(1 \rightarrow 5)- β -D-galactofuranoside (3.4). Tetrasaccharide **3.4** was produced using the general deprotection procedure under Zémlen conditions on **3.52** (30 mg, 0.013 mmol). Initially, compound **3.4** was purified by column chromatography (3:1 CH₂Cl₂-MeOH). The solvent was evaporated and the residue was dissolved in water and was filtered through C18 silica gel using H₂O-MeOH as eluent to give **3.4** (9 mg, 87%) as a colourless syrup, R_f 0.42 (3:1 CH₂Cl₂-MeOH); $[\alpha]_D -35.6$ (c 0.5, MeOH); ¹H NMR (500 MHz, CD₃OD, δ_H) 5.20 (d, 1 H, $J = 2.0$ Hz, H-1'''), 5.17 (s, 2 H, H-1', H-1''), 4.94 (d, 1 H, $J = 2.3$ Hz, H-1), 4.15–4.00 (m, 10 H), 3.97–3.88 (m, 4 H), 3.85–3.80 (m, 2 H), 3.80–3.74 (m, 8 H), 3.73–3.63 (m, 1 H, octyl OCH₂), 3.55 (d, 1 H, $J = 9.9$ Hz, octyl OCH₂), 3.30 (t, 2 H, $J = 6.9$ Hz, octyl CH₂N₃), 1.62–1.55 (m, 4 H, octyl CH₂), 1.35–1.30 (m, 8 H, octyl CH₂); ¹³C NMR (125 MHz, CD₃OD, δ_C) 109.2 (C-1'''), 109.0 (C-1), 108.9 (C-1''), 108.7 (C-1'''), 85.1 (C), 84.5 (C), 83.6 (C), 83.5 (C), 83.1 (C), 83.0 (C), 82.7 (C), 78.8 (C), 78.7 (C), 78.6 (C), 78.6 (C), 77.2 (C), 71.0 (C), 70.6 (C), 68.9 (octyl OCH₂), 64.2 (C), 63.5 (C), 62.7 (C), 52.4 (octyl CH₂N₃), 30.6 (octyl CH₂), 30.4 (octyl CH₂),

30.2 (octyl CH₂), 29.9 (octyl CH₂), 27.8 (octyl CH₂), 27.1 (octyl CH₂); HR ESIMS: m/z [M+Na⁺] calcd for C₃₂H₅₇N₃NaO₂₁: 842.3377. Found: 842.3374.



3.64

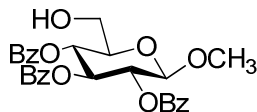
Methyl 6-*O*-trityl- β -D-glucopyranoside (3.64). Methyl β -glucopyranoside **3.63** (3 g, 15.5 mmol) was dissolved in pyridine (50 mL) and trityl chloride (6.6 g, 23.3 mmol) was added. The reaction mixture was stirred at 50 °C for 24 h. After cooling the solvent was evaporated; co-evaporation with toluene was done to ensure removal of all pyridine. The residue was then purified using column chromatography (19:1 CH₂Cl₂-MeOH) to give compound **3.64** (4.8 g, 75%) as a white powder. The ¹H NMR spectrum as well as ESI-MS data for **3.64** agreed with those reported previously.⁴⁵



3.65

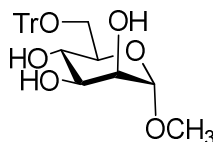
Methyl 2,3,4-tri-*O*-benzoyl-6-*O*-trityl- β -D-glucopyranoside (3.65). A solution of compound **3.64** (2.1 g, 4.8 mmol) in pyridine (50 mL) was cooled to 0 °C followed by the addition of benzoyl chloride (4.1 g, 28.8 mmol) dropwise. The reaction mixture was stirred for 6 h then poured over an ice water mixture and extracted with CH₂Cl₂. The combined organic layers were washed with brine, dried over anhydrous Na₂SO₄, filtered and concentrated to give a crude residue that was purified using column chromatography (3:1 Hexane-EtOAc) to give **3.65** (3.2 g,

89%) as a white solid. The ^1H NMR spectrum obtained for **3.65** matched those previously reported.⁴⁵



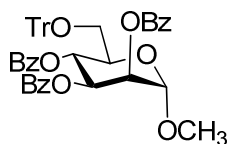
3.66

Methyl 2,3,4-tri-O-benzoyl- β -D-glucopyranoside (3.66).^{46, 47} A solution of compound **3.65** (1.5 g, 2.1 mmol) in CH_2Cl_2 (30 mL) was cooled to 0 °C and 5% HCl in MeOH (10 mL) was added dropwise. The reaction mixture was stirred for 8 h, The residue was purified using column chromatography (4:1 Hexane–EtOAc) to give **3.66** (0.86 g, 85%) as a white solid. The ^1H NMR data obtained for **3.66** matched that previously reported.⁴⁶



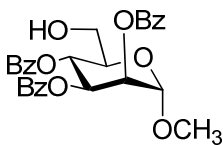
3.68

Methyl 6-O-trityl- α -D-mannopyranoside (3.68).⁴⁸ The same tritylation procedure which was done to obtain compound **3.64**, was followed here, where compound **3.67** (450 mg, 2.3 mmol) was tritylated to obtain the mannoside analog **3.68** (730 mg, 76%) as white powder.⁴⁸ ^1H NMR data of **3.68** matched the reported data.⁴⁸



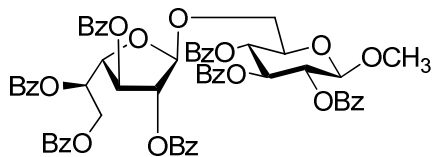
3.69

Methyl 2,3,4-tri-*O*-benzoyl-6-*O*-trityl- α -D-mannopyranoside (3.69). Compound **3.68** (500 mg, 1.1 mmol) was subjected to the same benzylation reaction as was done to obtain compound **3.65**, where the benzyolated mannoside derivative **3.69** (660 mg, 87%) was produced as a white solid. The ^1H NMR data of **3.69** matched that previously reported.⁴⁸



3.70

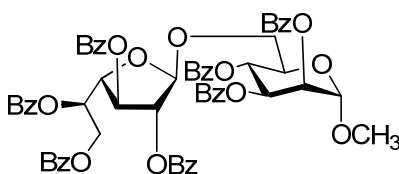
Methyl 2,3,4-tri-*O*-benzoyl- α -D-mannopyranoside (3.70).⁴⁹ The same detritylation conditions done to obtain compound **3.66** was applied here, starting with **3.69** (400 mg, 0.56 mmol). Compound **3.70** (223 mg, 83%) was obtained as a white solid. The ^1H NMR data of **3.70** matched that previously reported.⁴⁵



3.71

Methyl 2,3,5,6-tetra-*O*-benzoyl- β -D-galactofuranosyl-(1 \rightarrow 6)-2,3,4-tri-*O*-benzoyl- β -D-glucopyranoside (3.71). Donor **3.26** (1.1 g, 1.56 mmol) and acceptor **3.64** (522 mg, 1.04 mmol), were dissolved in dry CH_2Cl_2 (25 mL) in the presence of activated, powdered 4 Å molecular sieves (250 mg) and the solution was cooled

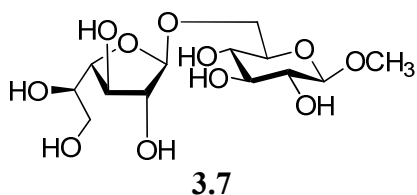
to 0 °C. The reaction mixture was stirred for 15 min followed by the addition of NIS (350 mg, 1.56 mmol) and AgOTf (66 mg, 0.26 mmol). The solution was stirred for another 30 min and then Et₃N was added. The reaction mixture was diluted with CH₂Cl₂ and filtered through Celite. The filtrate was washed with saturated Na₂S₂O₃ solution followed by water then brine, and then dried over Na₂SO₄ anhydrous and filtered. The solvent was then concentrated and the obtained residue was purified using column chromatography (4:1 hexanes–EtOAc) to give disaccharide **3.71** (990 mg, 88%) as a white semi-solid product, *R_f* 0.38 (4:1 hexanes–EtOAc); [α]_D –0.1 (*c* 0.5, CH₂Cl₂); ¹H NMR (500 MHz, CDCl₃, δ_H) 8.08–8.04 (m, 4 H, Ar), 7.98–7.96 (m, 4 H, Ar), 7.94–7.92 (m, 2 H, Ar), 7.89–7.85 (m, 2 H, Ar), 7.82–7.78 (m, 2 H, Ar), 7.52–7.24 (m, 20 H, Ar), 7.56–7.54 (m, 1 H, Ar), 6.03 (app dt, 1 H, *J* = 7.6, 3.9 Hz, H-5'), 5.89 (t, 1 H, *J* = 9.6 Hz, H-3), 5.66–5.63 (m, 1 H, H-2'), 5.57–5.44 (m, 4 H, H-1', H-2, H-3', H-4'), 4.77–4.72 (m, 3 H, H-1, H-6a,b), 4.71–4.68 (m, 1 H, H-4), 4.15–4.10 (m, 1 H, H-6a'), 4.05–3.90 (m, 1 H, H-5), 3.91 (dd, 1 H, *J* = 11.9, 6.2 Hz, H-6'b), 3.46 (s, 3 H, OCH₃); ¹³C NMR (125 MHz, CDCl₃, δ_C) 166.0 (C=O), 165.8 (C=O), 165.7 (C=O), 165.6 (C=O), 165.2 (C=O), 165.1 (C=O), 165.0 (C=O), 133.4 (Ar), 133.3 (Ar), 133.3 (Ar), 133.2 (Ar), 133.1 (Ar), 133.0 (Ar), 129.9 (Ar), 129.9 (Ar), 129.8 (Ar), 129.7 (Ar), 129.7 (Ar), 129.5 (Ar), 129.4 (Ar), 129.3 (Ar), 129.0 (Ar), 128.9 (Ar), 128.4 (Ar), 128.4 (Ar), 128.3 (Ar), 128.3 (Ar), 128.3 (Ar), 128.2 (Ar), 106.3 (C-1'), 102.0 (C-1), 81.8 (C-2'), 81.5 (C-4'), 77.4 (C-3'), 74.0 (C-2), 73.0 (C-4), 71.9 (C-3), 70.3 (C-5), 69.8 (C-5'), 66.4 (C-6), 63.5 (C-6'), 57.0 (OCH₃); HR ESIMS: *m/z* [M+Na⁺] calcd for C₆₂H₅₂NaO₁₈: 1107.3046. Found: 1107.3040.



3.72

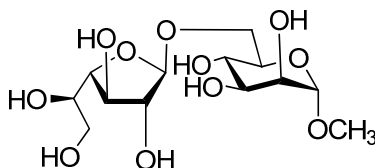
Methyl 2,3,5,6-tetra-*O*-benzoyl- β -D-galactofuranosyl-(1 \rightarrow 6)-2,3,4-tri-*O*-benzoyl- α -D-mannopyranoside (3.72). Donor **3.26** (1.5 g, 2.13 mmol) and acceptor **3.70** (714 mg, 1.42 mmol) were dissolved in dry CH₂Cl₂ (25 mL) in the presence of powdered 4 Å molecular sieves (250 mg) and the solution was cooled to 0°C. The reaction mixture was stirred for 15 min followed by the addition of NIS (476 mg, 2.13 mmol), and AgOTf (90 mg, 0.35 mmol). The solution was stirred for another 30 min then Et₃N was added. The reaction mixture was diluted with CH₂Cl₂ and filtered through Celite. The filtrate was washed with saturated Na₂S₂O₃ solution followed by water then brine, and dried over Na₂SO₄ anhydrous and filtered. The solvent was evaporated and the residue was purified using column chromatography (4:1 hexane–EtOAc) to give disaccharide **3.72** (1.34 g, 87%) as a white powder *R_f* 0.4 (4:1 hexanes–EtOAc); [α]_D –0.2 (*c* 0.4, CH₂Cl₂); ¹H NMR (500 MHz, CDCl₃, δ _H) 8.09 (d, 3 H, *J* = 8.3 Hz, Ar), 8.04 (d, 2 H, *J* = 8.3 Hz, Ar), 8.01–7.93 (m, 6 H, Ar), 7.89 (d, 2 H, *J* = 8.3 Hz, Ar), 7.82 (d, 2 H, *J* = 8.4 Hz, Ar), 7.54–7.39 (m, 10 H, Ar), 7.37–7.22 (m, 10 H, Ar), 6.04–5.98 (m, 1 H, H-5'), 5.91–5.87 (m, 2 H, H-3, H-3'), 5.68 (s, 1 H, H-2'), 5.64 (d, 1 H, *J* = 5.2 Hz, H-4), 5.58 (s, 1 H, H-2), 5.48 (s, 1 H, H-1'), 4.98 (br s, 1 H, H-1), 4.74–4.65 (m, 3 H, H-4', H-6'a, H-6'b), 4.36–4.26 (m, 1 H, H-5), 4.01 (dd, 1 H, *J* = 11.7, 1.55 Hz, H-6a), 3.92 (dd, 1 H, *J* = 11.6, 6.5 Hz, H-6b), 3.50 (s, 3 H, OCH₃); ¹³C NMR (125 MHz, CDCl₃, δ _C) 166.0 (C=O), 165.7 (C=O), 165.6 (C=O), 165.6 (C=O), 165.5 (C=O), 165.4 (C=O), 165.2 (C=O),

133.5 (Ar), 133.4 (Ar), 133.4 (Ar), 133.3 (Ar), 133.2 (Ar), 133.1 (Ar), 133.0 (Ar), 129.9 (Ar), 129.8 (Ar), 129.8 (Ar), 129.8 (Ar), 129.7 (Ar), 129.7 (Ar), 129.5 (Ar), 129.4 (Ar), 129.2 (Ar), 129.1 (Ar), 129.0 (Ar), 129.0 (Ar), 129.0 (Ar), 128.6 (Ar), 128.4 (Ar), 128.4 (Ar), 128.3 (Ar), 128.3 (Ar), 128.3 (Ar), 128.2 (Ar), 106.5 (C-1'), 98.5 (C-1), 81.8 (C-2'), 81.6 (C-4'), 77.6 (C-3'), 70.4 (C-2), 70.3 (C-4), 70.3 (C-3), 70.0 (C-5), 67.4 (C-5'), 66.7 (C-6), 63.5 (C-6'), 55.4 (OCH₃); HR ESIMS: m/z [M+Na⁺] calcd for C₆₂H₅₂NaO₁₈: 1107.3046. Found: 1107.3048.



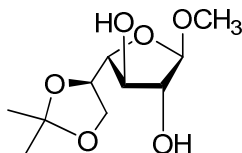
Methyl β -D-galactofuranosyl-(1 \rightarrow 6)- β -D-glucopyranoside (3.7). Disaccharide **3.7** was synthesized from compound **3.71** (20 mg, 0.018 mmol) by applying the general deprotection procedure using NaOMe in MeOH. The reaction mixture was stirred for 8 h and neutralized by the addition of glacial acetic acid. The crude residue obtained after evaporation of the solvent was purified using column chromatography (9:1 CH₂Cl₂-MeOH) to give **3.7** (5.7 mg, 89%) as a white powder, R_f 0.39 (9:1 CH₂Cl₂-MeOH); $[\alpha]_D -132.2$ (c 0.5, MeOH); ¹H NMR (500 MHz, D₂O, δ_H) 5.03 (d, 1 H, J = 1.8 Hz, H-1'), 4.35 (d, 1 H, J = 8.0 Hz, H-1), 4.09 (app dt, 1 H, J = 4.0, 2.0 Hz, H-5'), 4.06-4.01 (m, 2 H, H-2', H-3'), 3.97 (dd, 1 H, J = 6.4, 4.2 Hz, H-4'), 3.81-3.79 (m, 1 H, H-4), 3.72-3.67 (m, 2 H, H-6a', b'), 3.65-3.61 (m, 1 H, H-3), 3.58-3.54 (m, 1 H, H-2), 3.47-3.43 (m, 1 H, H-5), 3.54 (s, 3 H, OCH₃), 3.40 (dd, 1 H, J = 10.8, 8.1 Hz, H-6a), 3.23 (dd, 1 H, J = 9.3, 8.0 Hz, H-

6b); ^{13}C NMR (125 MHz, D_2O , δ_{C}) 108.8 (C-1'), 104.1 (C-1), 83.7 (C-2'), 81.8 (C-4'), 77.6 (C-3'), 76.5 (C-2), 75.6 (C-4), 73.9 (C-3), 71.6 (C-5), 70.4 (C-5'), 67.6 (C-6), 63.5 (C-6'), 58.1 (OCH_3); HR ESIMS: m/z [$\text{M}+\text{Na}^+$] calcd for $\text{C}_{13}\text{H}_{24}\text{NaO}_{11}$: 379.1211. Found: 379.1208.



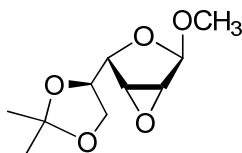
3.8

Methyl β -D-galactofuranosyl-(1 \rightarrow 6)- α -D-mannopyranoside (3.8). Disaccharide **3.8** was synthesized from compound **3.72** (20 mg, 0.018 mmol) by applying the general deprotection procedure using NaOMe in MeOH. The crude residue was purified using column chromatography (9:1 CH_2Cl_2 -MeOH) to give **3.8** (6 mg, 89%) as a white powder, R_f 0.41 (9:1 CH_2Cl_2 -MeOH); $[\alpha]_{\text{D}} -78.5$ (c 0.4, MeOH); ^1H NMR (500 MHz, CD_3OD , δ_{H}) 4.97 (d, 1 H, $J = 1.5$ Hz, H-1'), 4.62 (d, 1 H, $J = 1.7$ Hz, H-1), 4.01–3.97 (m, 3 H, H-2', H-3', H-4'), 3.77–3.59 (m, 4 H, H-5, H-5', 6a,b), 3.75–3.67 (m, 2 H, H-6'a,b), 3.67–3.59 (m, 3 H, H-2, H-3, H-4), 3.36 (s, 3 H, OCH_3); ^{13}C NMR (125 MHz, D_2O , δ_{C}) 109.9 (C-1'), 102.8 (C-1), 85.1 (C-2'), 82.7 (C-4'), 78.9 (C-3'), 74.4 (C-2), 73.2 (C-4), 72.5 (C-3), 71.9 (C-5), 68.8 (C-6), 64.4 (C-6'), 55.3 (OCH_3); HR ESIMS: m/z [$\text{M}+\text{Na}^+$] calcd for $\text{C}_{13}\text{H}_{24}\text{NaO}_{11}$: 379.1211. Found: 379.1212.



3.53

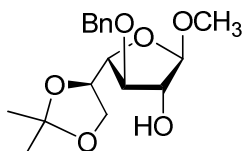
Methyl 5,6-*O*-isopropylidene- β -D-galactofuranoside (3.53). To a solution of methyl β -galactofuranoside **3.24** (1.1 g, 5.67 mmol) in acetone (25 mL), 2,2-dimethoxypropane (8 mL, 61 mmol) and catalytic (1*S*)-(+)-camphorsulfonic acid (10 mg, 0.04 mmol) were added. The solution was stirred for 4 h and then neutralized by the addition of Et₃N. Concentration of the reaction mixture gave a crude residue that was dissolved in CH₂Cl₂ and then washed with brine followed by water. The solution was dried over anhydrous Na₂SO₄, filtered and then concentrated. The crude mixture was purified using column chromatography (5:1 hexanes–EtOAc) to give **3.45** (796 mg, 90%) as a white powder. *R_f* 0.38 (1:1 hexanes–EtOAc). The ¹H NMR and ¹³C NMR spectra obtained for compound **3.45** matched those reported previously.³⁰



3.54

Methyl 2,3-anhydro-5,6-*O*-isopropylidene- β -D-galactofuranoside (3.54). Compound **3.53** (0.5 g, 2.13 mmol) was dissolved in THF followed by the addition of PPh₃ (0.71 g, 2.77 mmol). The solution was cooled to 0 °C and then DIAD (0.5 mL, 2.77 mmol) was added dropwise. The solution was stirred for 30 min while

warming to room temperature. The resulting reaction mixture was concentrated and the crude residue was carried to the next reaction.

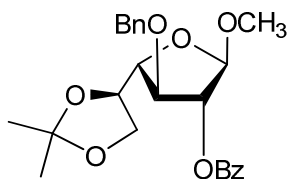


3.55

Methyl 3-O-benzyl-5,6-O-isopropylidene- β -D-galactofuranoside (3.55).

Following the same procedure for epoxide ring opening reported by Bai *et al.*,³⁰ compound **3.55** was obtained. Lithium metal (18 mg, 6 mmol) was added to a solution of benzyl alcohol (6 mL) and the solution was stirred at 65 °C until all the lithium metal was dissolved. The solution was cooled to room temperature. Using a syringe, the mixture (140 μ L, 1.2 mmol) was added to a solution of compound **3.54** (220 mg, 1.1 mmol) in benzyl alcohol (2 mL). The mixture was stirred for 5 h at 75 °C. The reaction mixture was cooled to room temperature and then neutralized by the addition of glacial acetic acid. After dilution with CH_2Cl_2 , the organic layer was washed with water, dried over anhydrous Na_2SO_4 and filtered. The concentrated crude residue was purified by column chromatography (4:1 hexanes–EtOAc) to give compound **3.55** (277 mg, 78%) as a colorless syrup. R_f 0.28 (4:1 hexanes–EtOAc); $[\alpha]_D -105.2$ (c 0.5, CH_2Cl_2); $^1\text{H NMR}$ (500 MHz, CDCl_3 , δ_{H}) 7.38–7.30 (m, 4 H, Ar), 7.32–7.27 (m, 1 H, Ar), 4.91 (s, 1 H, H-1), 4.72 (d, 1 H, $J = 12.3$ Hz, OCH_2Ph), 4.54 (d, 1 H, $J = 12.3$ Hz, OCH_2Ph), 4.11–3.98 (m, 3 H, H-2, H-4, H-5), 3.98 (dt, 2 H, $J = 12.2, 7.3$ Hz, H-6a,b), 3.83 (d, 1 H, $J = 2.6$ Hz, H-3), 3.44 (s, 3 H, OCH_3), 1.35 (s, 3 H, isopropylidene CH_3), 1.41 (s, 3 H, isopropylidene CH_3); $^{13}\text{C NMR}$ (125 MHz, CDCl_3 , δ_{C}) 137.5 (Ar), 128.4 (Ar),

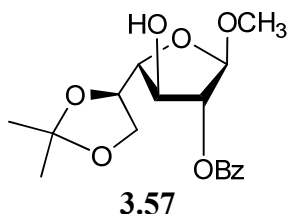
127.9 (Ar), 110.6 (isopropylidene C), 109.8 (C-1), 85.6 (OCH₂Ph), 82.8 (OCH₃), 77.0 (C-4), 76.3 (C-5), 72.1 (C-2), 65.6 (C-6), 55.4 (C-3), 25.7 (isopropylidene CH₃), 25.6 (isopropylidene CH₃); HR ESIMS: m/z [M+Na⁺] calcd for C₁₇H₂₄NaO₆: 347.1632. Found: 347.1621.



3.56

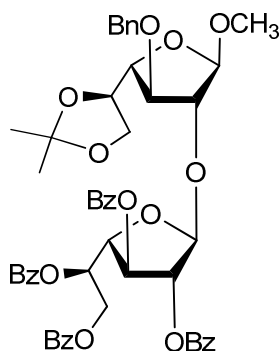
Methyl 2-*O*-benzoyl-3-*O*-benzyl-5,6-*O*-isopropylidene-β-D-galactofuranoside (3.56). To a solution of compound **3.55** (300 mg, 0.92 mmol) in pyridine cooled to 0 °C, benzoyl chloride (0.2 mL, 1.38 mmol) was added and the reaction mixture was stirred for 6 h. The solution was then poured into an ice water mixture and the organic layer was separated, diluted with CH₂Cl₂ and concentrated to dryness. The crude residue was dissolved in CH₂Cl₂, washed with a saturated solution of NaHCO₃, brine and then dried over anhydrous Na₂SO₄ and filtered. Concentration of the organic layer gave a crude product that was purified using column chromatography (4:1 hexanes–EtOAc) to give compound **3.56** (354 mg, 90%) as a colourless syrup. R_f 0.3 (5:1 hexanes–EtOAc); $[\alpha]_D$ –124.3 (c 0.4, CH₂Cl₂); ¹H NMR (500 MHz, CDCl₃, δ_H) 8.19–8.13 (m, 1 H, Ar), 7.35–7.25 (m, 6 H, Ar), 7.70–7.66 (m, 1 H, Ar), 7.48–7.45 (m, 2 H, Ar), 5.37 (d, 1 H, J = 0.9 Hz, H-1), 5.09 (s, 1 H, H-2), 4.81 (d, 1 H, J = 12.0 Hz, OCH₂Ph), 4.61 (d, 1 H, J = 12.2 Hz, OCH₂Ph), 4.15–4.10 (m, 1 H, H-3), 3.83–3.79 (m, 1 H, H-4), 3.79–3.74 (m, 3 H, H-5, H-6a,b), 3.46 (s, 3 H, OCH₃), 1.34 (s, 3 H, isopropylidene CH₃), 1.42 (s, 3 H, isopropylidene CH₃); ¹³C NMR (125 MHz, CDCl₃, δ_C); 165.4 (C=O), 134.5 (Ar), 133.5 (Ar), 130.6

(Ar), 129.8 (Ar), 128.9 (Ar), 128.6 (Ar), 128.1 (Ar), 109.9 (isopropylidene C), 107.2 (C-1), 83.5 (C-4), 81.4 (C-2), 77.3 (C-5), 72.4 (OCH₂Ph), 65.4 (C-6), 55.1 (C-3), 26.5 (isopropylidene CH₃), 25.4 (isopropylidene CH₃); HR ESIMS: *m/z* [M+Na⁺] calcd for C₂₄H₂₈NaO₇: 451.1727. Found: 451.1721.



Methyl 2-O-benzoyl-5,6-isopropylidene-β-D-galactofuranoside (3.57).

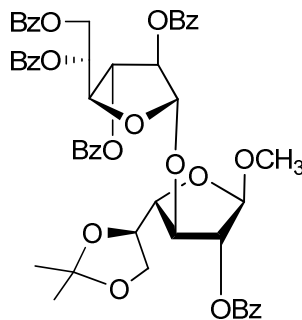
Compound **3.56** (220 mg, 0.51 mmol) was dissolved in EtOAc and then 20 wt. % Pd(OH)₂-C (35 mg) was added. The reaction mixture was stirred overnight under a hydrogen atmosphere. The solution was filtered through Celite and the filtrate was concentrated to give a crude product that was purified using column chromatography (3:1 hexanes–EtOAc) to give **3.57** (153 mg, 89%) as a colourless syrup. *R_f* 0.28 (3:1 hexanes–EtOAc); [α]_D -75.2 (*c* 0.5, CH₂Cl₂); ¹H NMR (400 MHz, CDCl₃, δ_H) 8.02 (td, 2 H, *J* = 8.4, 1.5 Hz, Ar), 7.63–7.55 (m, 1 H, Ar), 7.48–7.40 (m, 2 H, Ar), 5.16 (s, 1 H, H-1), 5.06 (dd, 1 H, *J* = 2.4, 0.9 Hz, H-2), 4.28 (app q, 1 H, *J* = 6.6 Hz, H-4), 4.11–4.02 (m, 3 H, H-3, H-5, H-6a), 3.97 (dd, 1 H, *J* = 8.5, 6.8 Hz, H-6b), 3.46 (s, 3 H, OCH₃), 1.46 (s, 3 H, isopropylidene CH₃), 1.38 (s, 3 H, isopropylidene CH₃); ¹³C NMR (125 MHz, CDCl₃, δ_C); 166.7 (C=O), 133.6 (Ar), 129.8 (Ar), 129.0 (Ar), 128.5 (Ar), 109.8 (isopropylidene C), 106.3 (C-1), 83.9 (C-4), 77.5 (C-5), 76.0 (C-2), 65.4 (C-6), 55.1 (C-3), 53.0 (OCH₃), 26.4 (isopropylidene CH₃), 25.4 (isopropylidene CH₃); HR ESIMS: *m/z* [M+Na⁺] calcd for C₁₇H₂₂NaO₇: 361.1258. Found: 361.1253.



3.58

Methyl 2,3,5,6-tetra-*O*-benzoyl- β -D-galactofuranosyl-(1 \rightarrow 2)-3-*O*-benzyl-5,6-isopropylidene- β -D-galactofuranoside (3.58). Donor **3.26** (120 mg, 0.17 mmol), acceptor **3.55** (44 mg, 0.14 mmol) and activated powdered 4 Å molecular sieves (425 mg) were added to CH₂Cl₂ (25 mL) and the solution was cooled to 0 °C. The solution was stirred for 15 min before the addition of NIS (37 mg, 0.15 mmol), and AgOTf (6 mg, 0.025 mmol). After 30 min Et₃N was added. The mixture was diluted with CH₂Cl₂ and filtered through Celite. The organic layer was washed with a saturated solution of Na₂S₂O₃ then brine, dried over Na₂SO₄, filtered, concentrated and purified by column chromatography (2:1 hexanes–EtOAc) afforded disaccharide **3.58** (111 mg, 89%) as a white semi-solid, *R_f* 0.31 (2:1 hexanes–EtOAc); [α]_D –80.2 (*c* 0.5, CH₂Cl₂); ¹H NMR (500 MHz, CDCl₃, δ _H) 8.13–8.08 (m, 2 H, Ar), 8.07–7.93 (m, 6 H, Ar), 7.62–7.51 (m, 3 H, Ar), 7.46–7.34 (m, 9 H, Ar), 7.31–7.20 (m, 5 H, Ar), 6.08 (app dt, 1 H, *J* = 6.8, 4.3 Hz, H-5'), 5.71 (dd, 1 H, *J* = 5.1, 1.0 Hz, H-3'), 5.45 (d, 1 H, *J* = 1.3 Hz, H-1'), 5.30 (d, 1 H, *J* = 3.7 Hz, H-2'), 5.09 (s, 1 H, H-1), 4.85–4.71 (m, 4 H, H-4', H-6'a,b, OCH₂Ph), 4.58 (d, 1 H, *J* = 12.1 Hz, OCH₂Ph), 4.28–4.22 (m, 2 H, H-2, H-5), 4.08 (dd, 1 H, *J* = 6.9, 5.9 Hz,

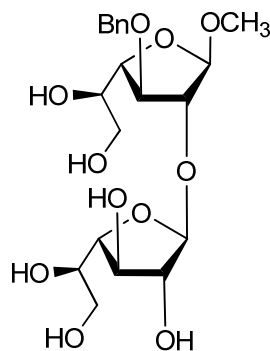
H-3), 3.92–3.89 (m, 1 H, H-6a), 3.85–3.79 (m, 2 H, H-4, H-6b), 3.39 (s, 3 H, OCH₃), 1.46 (s, 3 H, isopropylidene CH₃), 1.38 (s, 3 H, isopropylidene CH₃); ¹³C NMR (125 MHz, CDCl₃, δ_C) 166.1 (C=O), 165.7 (C=O), 165.6 (C=O), 165.5 (C=O), 137.2 (Ar), 133.6 (Ar), 133.6 (Ar), 133.3 (Ar), 133.1 (Ar), 129.9 (Ar), 129.9 (Ar), 129.9 (Ar), 129.8 (Ar), 129.5 (Ar), 129.5 (Ar), 128.9 (Ar), 128.8 (Ar), 128.5 (Ar), 128.5 (Ar), 128.4 (Ar), 128.4 (Ar), 128.1 (Ar), 109.8 (isopropylidene C), 107.8 (C-1), 105.9 (C-1'), 86.4 (C-2), 83.4 (C-2'), 82.7 (C-3), 82.6 (C-3'), 81.9 (C-4), 77.2 (C-4'), 76.4 (C-5), 72.5 (OCH₂Ph), 70.4 (C-5'), 65.5 (C-6), 63.4 (C-6'), 55.1 (OCH₃), 26.6 (isopropylidene CH₃), 25.5 (isopropylidene CH₃); HR ESIMS: *m/z* [M+Na⁺] calcd for C₅₁H₅₀NaO₁₅: 925.3042. Found: 925.3032.



3.59

Methyl 2,3,5,6-tetra-*O*-benzoyl-β-D-galactofuranosyl-(1→3)-2-*O*-benzoyl-5,6-isopropylidene-β-D-galactofuranoside (3.59). Acceptor **3.57** (246 mg, 0.73 mmol) and donor **3.26** (0.72 g, 1.09 mmol) were dissolved in dry CH₂Cl₂ at 0 °C in the presence of activated powdered 4 Å molecular sieves (250 mg). The reaction mixture was stirred for 15 min followed by the addition of NIS (365 mg, 1.63 mmol) and AgOTf (69 mg, 0.27 mmol). After 1 h Et₃N was added. The solution was diluted with CH₂Cl₂ and filtered through Celite. The filtrate was washed with a saturated solution of Na₂S₂O₃ then brine, dried over anhydrous Na₂SO₄, filtered,

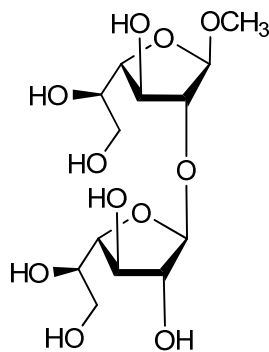
concentrated and purified by column chromatography (2:1 Hexane–EtOAc) to give **3.59** (878 mg, 88%) as a white powder. R_f 0.27 (2:1 Hexanes–EtOAc); $[\alpha]_D -45.3$ (c 0.6, CH_2Cl_2); $^1\text{H NMR}$ (500 MHz, CDCl_3 , δ_{H}) 8.04–7.96 (m, 6 H, Ar), 7.93–7.88 (m, 4 H, Ar), 7.47–7.40 (m, 9 H, Ar), 7.57–7.49 (m, 6 H, Ar), 6.03–5.96 (m, 1 H, H-5'), 5.75 (s, 1 H, H-1), 5.65 (d, 1 H, $J = 5.2$ Hz, H-3'), 5.59 (s, 1 H, H-2) 5.38 (s, 1 H, H-2'), 5.12 (s, 1 H, H-1'), 4.77–4.74 (m, 1 H, H-4), 4.72–4.62 (m, 2 H, H-6a,b), 4.30–4.26 (m, 2 H, H-4', H-5), 4.17 (app t, 1 H, $J = 5.6$ Hz, H-3), 3.97 (td, 2 H, $J = 12.2, 7.8$ Hz, H-6a,b), 3.45 (s, 3 H, OCH_3), 1.42 (s, 3 H, isopropylidene CH_3), 1.31 (s, 3 H, isopropylidene CH_3); $^{13}\text{C NMR}$ (125 MHz, CDCl_3 , δ_{C}); 165.9 (C=O), 165.6 (C=O), 165.5 (C=O), 165.4 (C=O), 165.2 (C=O), 133.5 (Ar), 133.4 (Ar), 133.3 (Ar), 133.2 (Ar), 133.0 (Ar), 129.9 (Ar), 129.9 (Ar), 129.9 (Ar), 129.8 (Ar), 129.6 (Ar), 129.4 (Ar), 129.3 (Ar), 129.3 (Ar), 128.9 (Ar), 128.8 (Ar), 128.4 (Ar), 128.3 (Ar), 109.9 (isopropylidene C), 107.0 (C-1'), 105.2 (C-1), 82.2 (C-2'), 81.9 (C-2), 81.9 (C-4), 81.2 (C-4'), 77.3 (C-3'), 75.6 (C-5), 70.4 (C-5'), 65.5 (C-6), 63.3 (C-6'), 54.9 (C-3), 53.2 (OCH_3), 26.4 (isopropylidene CH_3), 25.3 (isopropylidene CH_3); HR ESIMS: m/z $[\text{M}+\text{Na}^+]$ calcd for $\text{C}_{51}\text{H}_{48}\text{NaO}_{16}$: 939.2835. Found: 939.2825.



3.61

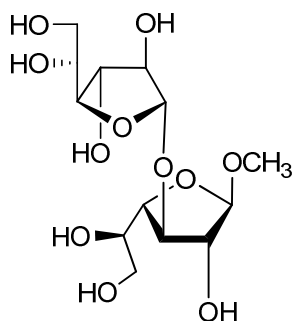
Methyl β -D-galactofuranosyl-(1 \rightarrow 2)-3-O-benzyl- β -D-galactofuranoside (3.61).

The general debenzoylation procedure was applied to disaccharide **3.60** (60 mg, 0.069 mmol) to synthesize **3.61**, which was purified using column chromatography (6:1 CH₂Cl₂–MeOH). Compound **3.61** (28 mg, 91%) was obtained as a colourless syrup, *R_f* 0.35 (3:1 CH₂Cl₂–MeOH); [α]_D –35.2 (*c* 0.4, CH₂Cl₂); ¹H NMR (500 MHz, CD₃OD, δ _H) 7.39–7.31 (m, 5 H, Ar), 4.99 (s, 1 H, H-1), 4.98 (s, 1 H, H-1'), 4.09–4.02 (m, 3 H, H-4', H-6a,b), 4.01–3.93 (m, 3 H, H-2, H-2', H-3'), 3.71–3.68 (m, 2 H, H-4, H-5), 3.65–3.56 (m, 4 H, H-3, H-5', H-6'a,b), 3.36 (s, 3 H, OCH₃); ¹³C NMR (125 MHz, CD₃OD, δ _C) 137.9 (Ar), 128.0 (Ar), 127.9 (Ar), 127.6 (Ar), 127.3 (Ar), 108.1 (C-1), 107.9 (C-1'), 86.9 (C-4), 83.6 (C-3'), 83.1 (C-3), 82.2 (C-5), 80.7 (OCH₂Ph), 77.2 (C-4'), 71.9 (C-5'), 71.1 (C-2'), 70.7 (C-2), 63.2 (C-6'), 63.1 (C-6), 53.6 (OCH₃); HR ESIMS: *m/z* [M+Na⁺] calcd for C₂₀H₃₀NaO₁₁: 469.1680. Found: 469.1675.



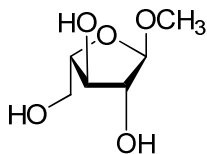
3.5

Methyl β -D-galactofuranosyl-(1 \rightarrow 2)- β -D-galactofuranoside (3.5). Compound **3.61** (50 mg, 0.1 mmol) was dissolved in MeOH (7 mL) and then 20 wt. % Pd(OH)₂-C (10 mg) was added. The solution was stirred overnight under a hydrogen atmosphere and then filtered through Celite. The filtrate was concentrated and the crude residue obtained was purified using column chromatography (5:1 CH₂Cl₂-MeOH) to produce compound **3.5** (31 mg, 87%) as a colourless syrup, *R_f* 0.35 (3:1 CH₂Cl₂-MeOH); [α]_D -105.2 (*c* 0.4, MeOH); ¹H NMR (500 MHz, CD₃OD, δ _H) 5.04 (s, 1 H, H-1'), 4.90 (d, 1 H, *J* = 1.0 Hz, H-1), 4.11 (app dt, 1 H, *J* = 7.5, 4.1 Hz, H-5'), 4.01 (app dt, 1 H, *J* = 6.6, 4.2 Hz, H-5), 3.93 (dd, 1 H, *J* = 6.6, 4.0 Hz, H-4), 3.96-3.90 (m, 2 H, H-2', H-4'), 3.83-3.80 (m, 1 H, H-3'), 3.73-3.66 (m, 2 H, H-2, H-3), 3.61-3.57 (m, 4 H, H-6a,b, H-6'a,b), 3.34 (s, 3 H, OCH₃); ¹³C NMR (125 MHz, CD₃OD, δ _C) 108.2 (C-1), 107.7 (C-1'), 86.8 (C-4), 83.7 (C-3'), 83.5 (C-3), 82.3 (C-4'), 77.4 (C-5), 71.6 (C-5'), 71.1 (C-2'), 70.9 (C-2), 63.6 (C-6'), 63.5 (C-6), 53.8 (OCH₃); HR ESIMS: *m/z* [M+Na⁺] calcd for C₁₃H₂₄NaO₁₁: 379.1211. Found: 379.1214.



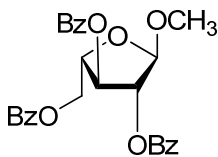
3.6

Methyl β -D-galactofuranosyl-(1 \rightarrow 3)- β -D-galactofuranoside (3.6). Disaccharide **3.62** (45 mg, 0.058 mmol) was subjected to Zémlen debenzoylation conditions to give disaccharide **3.6** (17 mg, 87%) as a colourless syrup. R_f 0.4 (5:1 CH₂Cl₂–MeOH); $[\alpha]_D -42.2$ (c 0.5, MeOH); ¹H NMR (500 MHz, CD₃OD, δ_H) 5.06 (d, 1 H, $J = 1.8$ Hz, H-1'), 4.76 (br s, 1 H, H-1), 4.14 (app dt, 1 H, $J = 6.4, 3.1$ Hz, H-5'), 4.06 (d, 1 H, $J = 1.5$ Hz, H-2), 4.04–3.92 (m, 3 H, H-2', H-3, H-3'), 3.82 (dt, 1 H, $J = 6.1, 5.7, 3.2$ Hz, H-5), 3.70 (ddd, 1 H, $J = 6.9, 5.8, 3.1$ Hz, H-6'a), 3.64–3.59 (m, 4 H, H-4, H-4', H-6a,b), 3.35 (s, 3 H, OCH₃); ¹³C NMR (125 MHz, CD₃OD, δ_C) 109.0 (C-1), 107.7 (C-1'), 86.5 (C-4), 83.5 (C-3'), 83.5 (C-3), 82.5 (C-5), 77.5 (C-4'), 71.9 (C-5'), 71.8 (C-2'), 72.8 (C-2), 63.5 (C-6'), 63.5 (C-6), 53.8 (OCH₃); HR ESIMS: m/z [M+Na⁺] calcd for C₁₃H₂₄NaO₁₁: 379.1211. Found: 379.1208.



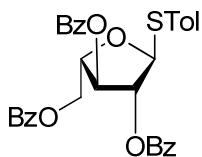
3.75

Methyl α -L-arabinofuranoside (3.75).¹³ L-Arabinose (5.3 g, 36.6 mmol) was dissolved in methanol (110 mL) and then treated with a solution of acetyl chloride (2.7 mL) in methanol (30 mL). The solution was stirred for 3 h and then pyridine was added dropwise until pH 7 was reached which as determined by pH universal indicator. The solvent was evaporated and the methyl glycoside **3.75** was produced. The crude product was taken forward to the next step.



3.76

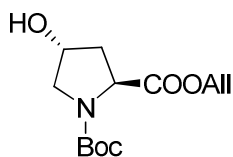
Methyl 2,3,5-tri-O-benzoyl- α -L-arabinofuranoside (3.76).¹³ The crude methyl glycoside **3.75** (250 mg, 1.52 mmol) was dissolved in pyridine (50 mL) and the solution was cooled to 0 °C. Benzoyl chloride (1.1 mL, 7.6 mmol) was added and the reaction mixture was stirred overnight. The solvent was evaporated and the crude residue was diluted with CH₂Cl₂. The organic layer was then washed with water 1 M HCl (150 mL), saturated NaHCO₃ and brine. The organic layer was dried over anhydrous Na₂SO₄ then concentrated and the crude mixture was purified using column chromatography (3:1 hexanes–EtOAc) to give **3.76** (506 mg, 70% from L-arabinose, α/β ratio 8:1) as a white solid. The ¹H NMR and ¹³C NMR spectra obtained for **3.76** matched those reported previously.¹³



3.77

***p*-Tolyl 2,3,5-tri-*O*-benzoyl-1-thio- α -L-arabinofuranoside (3.77).**

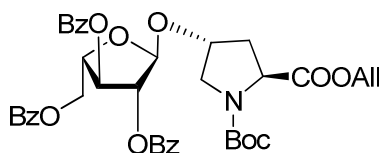
Arabinofuranoside **3.76** (2.2 g, 4.62 mmol) was dissolved in dry CH₂Cl₂ (50 mL) and the solution was cooled down to 0 °C followed by the addition of *p*-thiocresol (0.75 g, 6.2 mmol). The reaction mixture was stirred for 15 min and then BF₃·OEt₂ (2.9 mL, 23.1 mmol) was added dropwise. The solution was stirred for 7 h and then neutralized by the addition of Et₃N. The same work up procedure used to obtain **3.26** was done here to give the crude thioglycoside **3.77**, which was purified using column chromatography (4:1 hexanes–EtOAc) to give **3.77** (2.3 g, 88%) as a white solid. The ¹H NMR and ¹³C NMR spectra obtained for **3.77** matched those reported previously.¹³



3.79

***N*-tert-butoxycarbonyl-*trans*-4-hydroxy-L-proline allyl ester (3.79).**⁴⁰ *N*-Boc protected hydroxy proline **3.79** (1.5 g, 6.52 mmol) was dissolved in dry MeOH (15 mL) followed by the addition of cesium carbonate (1.2 g, 3.56 mmol). The reaction mixture was stirred for 2 h until a homogenous solution was formed. The solution was then evaporated and DMF (12 mL) was added to dissolve the residue. Allyl bromide (0.73 mL, 8.4 mmol) was added and the reaction mixture was stirred

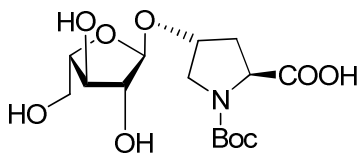
overnight. The reaction mixture was diluted with CH₂Cl₂ followed by washing with water and brine. The organic layer was then dried over anhydrous Na₂SO₄, filtered, concentrated and then purified using column chromatography (1:2 hexanes–EtOAc) to give compound **3.71** (1.58 g, 88%) as a colourless oil. The ¹H NMR and ¹³C NMR spectra obtained for **3.71** those reported previously.⁴⁰



3.80

Na-tert-butylloxycarbonyl-trans-4-hydroxy-4-O-[2,3,5-O-benzoyl-α-L-arabinofuranosyl]-L-proline allyl ester (3.80). Compound **3.79** (300 mg, 1.1 mmol) was dissolved in dry CH₂Cl₂ (25 mL) and activated 4 Å molecular sieves (15 mg) were added. The solution was cooled to 0 °C and then **3.77** (0.91 g, 1.65 mmol) was added. The solution was stirred for 15 min before the addition of NIS (630 mg, 2.48 mmol) and AgOTf (103 mg, 0.4 mmol). The solution was stirred for 1 h while warming to room temperature before being neutralized by the addition of Et₃N. The solution was then filtered, concentrated and the residue was redissolved in CH₂Cl₂, washed with a saturated Na₂S₂O₃ solution, and brine. The organic layer was dried over anhydrous Na₂SO₄, filtered, concentrated and the obtained residue was purified by column chromatography (5:1 Hexanes–EtOAc) to give **3.80** (692 mg, 88%) as a white solid, *R_f* 0.29 (2:1 hexanes–EtOAc); [α]_D –31.2 (*c* 0.5, CH₂Cl₂); ¹H NMR (500 MHz, CDCl₃, δ_H) 8.12–7.92 (m, 6 H, Ar), 7.47–7.44 (m, 9 H, Ar), 5.96–5.85 (m, 1 H, H-4, proline), 5.61–5.56 (m, 1 H, H-4), 5.47 (d, 1 H, *J*

= 1.3 Hz, H-2), 5.35 (s, 1 H, H-1), 5.33–5.21 (m, 1 H, allylic =CH), 4.61–4.44 (m, 9 H, H-3a,b-proline, allylic CH₂, allylic CH, H-3, H-5a,b), 3.76 (d, 2 H, *J* = 3.8 Hz, H-2, proline), 2.58–2.35 (m, 1 H, H-5a, proline), 2.22–2.06 (m, 1 H, H-5b, proline), 1.43 (s, 3 H, Boc-CH₃), 1.42 (s, 6 H, Boc-CH₃ x 2); ¹³C NMR (125 MHz, CDCl₃, δ_C); 182.9 (C=O, acid), 165.9 (C=O), 165.6 (C=O), 165.5 (C=O), 158.7 (C=O, amide), 140.1 (C=C), 133.8 (Ar), 131.4 (Ar), 130.9 (Ar), 115 (C=C), 109.0 (C-1), 86.1 (C-3), 84.2 (C-2), 83.8 (C-4 proline), 78.2 (C-4), 63.6 (C-2 proline), 62.9 (C-3 proline), 62.3 (C-5 proline), 58.4 (allylic CH₂), 55.1 (C-5), 38.3 (Boc-C), 30.4 (Boc-CH₃ x 2), 30.2 (Boc-CH₃); HR ESIMS: *m/z* [M+Na⁺] calcd for C₃₉H₄₁NNaO₁₂: 738.2657. Found: 738.2654.



3.82

Na-tert-butylloxycarbonyl-trans-4-hydroxy-4-O-[α-L-arabinofuranosyl]-L-proline (3.82). Compound **3.81** (20 mg, 0.03 mmol) was debenzoylated using the general debenzoylation procedure. The crude compound was purified using column chromatography (3:1 CH₂Cl₂–MeOH) to give pure compound **3.82** (18 mg, 90%) as a colourless syrup (80% over two steps). *R_f* 0.32 (5:1 CH₂Cl₂–MeOH); [α]_D –112.2 (*c* 0.5, MeOH); ¹H NMR (500 MHz, D₂O, δ_H) 5.19 (s, 1 H, H-1), 4.50 (s, 1 H, H-2), 4.23–4.19 (m, 1 H, H-4), 4.14 (dd, 1 H, *J* = 2.4, 1.3 Hz, H-3), 4.10 (dt, 1 H, *J* = 6.4, 6.0, 3.8 Hz, H-4, proline), 4.05–3.90 (m, 2 H, H-3a,b, proline), 3.80–3.63 (m, 3 H, H-5a,b, H-2, proline); 2.52–2.49 (m, 1 H, H-5b, proline), 2.07–2.02

(m, 1 H, H-5a, proline), 1.53 (s, 3 H, Boc-CH₃), 1.48 (s, 6 H, Boc-CH₃ x 2); ¹³C NMR (125 MHz, CDCl₃, δ_C); 182.9 (C=O, acid), 158.7 (C=O, amide), 109.0 (C-1), 86.1 (C-5), 84.2 (C-2), 83.8 (C-4 proline), 78.8 (C-3), 78.2 (C-4), 63.8 (C-2 proline), 63.6 (C-5 proline), 62.9 (C-3 proline), 38.6 (Boc-C), 32.3 (Boc-CH₃), 30.4 (Boc-CH₃ x 2); HR ESIMS: *m/z* [M-H] calcd for C₁₅H₂₄NO₉: 362.1457. Found: 362.1454.

3.6. References

1. Tsuji, S.; Uehori, J.; Matsumoto, M.; Suzuki, Y.; Matsuhisa, A.; Toyoshima, K.; Seya, T., Human intelectin is a novel soluble lectin that recognizes galactofuranose in carbohydrate chains of bacterial cell wall. *J. Biol. Chem.* **2001**, *276*, 23456-23463.
2. Fischer, E., The structure of both methyl-glucosides and a third methyl-glucoside. *Ber. Dtsch. Chem. Ges.* **1914**, *47*, 1980-1989.
3. Haworth, W. N.; Porter, C. R., Isolation of crystalline alpha- and beta-ethylglucofuranosides (gamma-ethylglucosides) and other crystalline derivatives of glucofuranose. *J. Chem. Soc.* **1929**, 2796-2806.
4. Arasappan, A.; Fraserreid, B., N-pentenyl furanosides - synthesis and glycosidation reactions of some galacto derivatives. *Tetrahedron Lett.* **1995**, *36*, 7967-7970.
5. Velly, R.; Benvegnu, T.; Gelin, M.; Privat, E.; Plusquellec, D., A convenient synthesis of disaccharides containing furanoside units. *Carbohydr. Res.* **1997**, *299*, 7-14.
6. Green, J. W., The glycofuranosides. *Adv. Carbohydr. Chem. Biochem.* **1966**, *21*, 95-142.
7. Ferrieres, V.; Bertho, J. N.; Plusquellec, D., A convenient synthesis of alkyl D-glycofuranosiduronic acids and alkyl D-glycofuranosides from unprotected carbohydrates. *Carbohydr. Res.* **1998**, *311*, 25-35.

8. Velty, R.; Benvegna, T.; Plusquellec, D., n-pentenyl furanosides and related glycosyl donors for the synthesis of archaeol glycolipid analogues. *Synlett* **1996**, 817-&.
9. Daccorso, N. B.; Thiel, I. M. E.; Schuller, M., Proton and C13 nuclear magnetic resonance spectra of some benzoylated aldohexoses. *Carbohydr. Res.* **1983**, *124*, 177-184.
10. Klotz, W.; Schmidt, R. R., Anomeric O-alkylation, .11. Anomeric O-alkylation of O-unprotected hexoses and pentoses - convenient synthesis of decyl, benzyl, and allyl glycosides. *Liebigs Ann. Chem.* **1993**, 683-690.
11. Green, J. W.; Pacsu, E., Glycofuranosides and thioglycofuranosides. I. A method of preparation and its application to galactose and glucose. *J. Am. Chem. Soc.* **1937**, *59*, 1205-1210.
12. McAuliffe, J. C.; Hindsgaul, O., Use of acyclic glycosyl donors for furanoside synthesis. *J. Org. Chem.* **1997**, *62*, 1234-1239.
13. Completo, G. C.; Lowary, T. L., Synthesis of galactofuranose-containing acceptor substrates for mycobacterial galactofuranosyltransferases. *J. Org. Chem.* **2008**, *73*, 4513-4525.
14. Szarek, W. A.; Zamojski, A.; Tiwari, K. N.; Ison, E. R., A new, facile method for cleavage of acetals and dithioacetals in carbohydrate derivatives. *Tetrahedron Lett.* **1986**, *27*, 3827-3830.
15. Imamura, A.; Lowary, T., Chemical Synthesis of Furanose Glycosides. *Trends Glycosci. Glyc.* **2011**, *23*, 134-152.

16. Kohn, P.; Samarita, R. H.; Lerner, L. M., A new method for synthesis of furanose derivatives of aldohexoses. *J. Am. Chem. Soc.* **1965**, *87*, 5475-5480.
17. Kartha, K. P. R.; Aloui, M.; Field, R. A., Iodine: A versatile reagent in carbohydrate chemistry .2. Efficient chemospecific activation of thiomethylglycosides. *Tetrahedron Lett.* **1996**, *37*, 5175-5178.
18. Veeneman, G. H.; Vanleeuwen, S. H.; Vanboom, J. H., Iodonium ion promoted reactions at the anomeric center .2. An efficient thioglycoside mediated approach toward the formation of 1,2-trans linked glycosides and glycosidic esters. *Tetrahedron Lett.* **1990**, *31*, 1331-1334.
19. Konradsson, P.; Udodong, U. E.; Fraser-Reid, B., Iodonium promoted reactions of disarmed thioglycosides. *Tetrahedron Lett.* **1990**, *31*, 4313-4316.
20. Crich, D.; Smith, M., 1-Benzenesulfonyl piperidine/trifluoromethanesulfonic anhydride: A potent combination of shelf-stable reagents for the low-temperature conversion of thioglycosides to glycosyl triflates and for the formation of diverse glycosidic linkages. *J. Am. Chem. Soc.* **2001**, *123*, 9015-9020.
21. Codee, J. D. C.; Litjens, R.; den Heeten, R.; Overkleeft, H. S.; van Boom, J. H.; van der Marel, G. A., Ph₂SO/Tf₂O: a powerful promoter system in chemoselective glycosylations using thioglycosides. *Org. Lett.* **2003**, *5*, 1519-1522.
22. Kang, Y.; Lou, C.; Ahmed, K. B. R.; Huang, P.; Jin, Z., Synthesis of biotinylated OSW-1. *Bioorg. Med. Chem. Lett.* **2009**, *19*, 5166-5168.

23. Komachi, Y.; Hatakeyama, S.; Motomatsu, H.; Futagami, T.; Kizjakina, K.; Sobrado, P.; Ekino, K.; Takegawa, K.; Goto, M.; Nomura, Y.; Oka, T., gfsA encodes a novel galactofuranosyltransferase involved in biosynthesis of galactofuranose antigen of O-glycan in *Aspergillus nidulans* and *Aspergillus fumigatus*. *Mol. Microbiol.* **2013**, *90*, 1054-1073.
24. Leal, J. A.; GomezMiranda, B.; Prieto, A.; Domenech, J.; Ahrazem, O.; Bernabe, M., Possible chemotypes from cell wall polysaccharides, as an aid in the systematics of *Penicillium* and its teleomorphic states *Eupenicillium* and *Talaromyces*. *Mycol. Res.* **1997**, *101*, 1259-1264.
25. Prieto, A.; Bernabe, M.; Leal, J. A., Isolation, purification and chemical characterization of alkali extractable polysaccharides from the cell walls of *Talaromyces* species. *Mycol. Res.* **1995**, *99*, 69-75.
26. Jones, C.; Todeschini, A. R.; Agrellos, O. A.; Previato, J. O.; Mendonca-Previato, L., Heterogeneity in the biosynthesis of mucin O-glycans from *Trypanosoma cruzi* Tulahuen strain with the expression of novel galactofuranosyl-containing oligosaccharides. *Biochemistry* **2004**, *43*, 11889-11897.
27. Leitao, E. A.; Bittencourt, V. C. B.; Haido, R. M. T.; Valente, A. P.; Peter-Katalinic, J.; Letzel, M.; de Souza, L. M.; Barreto-Bergter, E., beta-Galactofuranose-containing O-linked oligosaccharides present in the cell wall peptidogalactomannan of *Aspergillus fumigatus* contain immunodominant epitopes. *Glycobiology* **2003**, *13*, 681-692.

28. Peltier, P.; Euzen, R.; Daniellou, R.; Nugier-Chauvin, C.; Ferrieres, V., Recent knowledge and innovations related to hexofuranosides: structure, synthesis and applications. *Carbohydr. Res.* **2008**, *343*, 1897-1923.
29. Sorum, U.; Robertsen, B.; Kenne, L., Structural studies of the major polysaccharide in the cell wall of *Renibacterium salmoninarum*. *Carbohydr. Res.* **1998**, *306*, 305-314.
30. Bai, Y.; Lowary, T. L., 2,3-Anhydrosugars in glycoside bond synthesis. Application to alpha-D-galactofuranosides. *J. Org. Chem.* **2006**, *71*, 9658-9671.
31. Stevenson, G.; Neal, B.; Liu, D.; Hobbs, M.; Packer, N. H.; Batley, M.; Redmond, J. W.; Lindquist, L.; Reeves, P., Structure of the O-antigen of *Escherichia coli*-K12 and the sequence of its RFB gene cluster. *J. Bacteriol.* **1994**, *176*, 4144-4156.
32. Bernabe, M.; Ahrazem, O.; Prieto, A.; Leal, J. A., Evolution of fungal polysaccharides F1SS and proposal of their utilisation as antigens for rapid detection of fungal contaminants. *Electronic Journal of Environmental, Agricultural and Food Chemistry* **2002**, *1*, 1-3.
33. Levery, S. B.; Toledo, M. S.; Suzuki, E.; Salyan, M. E. K.; Hakomori, S. I.; Straus, A. H.; Takahashi, H. K., Structural characterization of a new galactofuranose-containing glycolipid antigen of *Paracoccidioides brasiliensis*. *Biochem. Biophys. Res. Commun.* **1996**, *222*, 639-645.
34. Latge, J. P.; Kobayashi, H.; Debeaupuis, J. P.; Diaquin, M.; Sarfati, J.; Wieruszkeski, J. M.; Parra, E.; Bouchara, J. P.; Fournet, B., Chemical and

- immunological characterization of the extracellular galactomannan of *Aspergillus fumigatus*. *Infect. Immun.* **1994**, *62*, 5424-5433.
35. Barretobergter, E.; Gorin, P. A. J.; Travassos, L. R., Cell constituents of mycelia and conidia of *Aspergillus fumigatus*. *Carbohydr. Res.* **1981**, *95*, 205-217.
36. Barretobergter, E. M.; Travassos, L. R., Chemical-structure of the D-galacto-D-mannan component from hyphae of *Aspergillus niger* and other *Aspergillus* spp. *Carbohydr. Res.* **1980**, *86*, 273-285.
37. Himly, M.; Jahn-Schmid, B.; Dedic, A.; Kelemen, P.; Wopfner, N.; Altmann, F.; van Ree, R.; Briza, P.; Richter, K.; Ebner, C.; Ferreira, F., Art v 1, the major allergen of mugwort pollen, is a modular glycoprotein with a defensin-like and a hydroxyproline-rich domain. *FASEB J.* **2003**, *17*, 106-107.
38. Leonard, R.; Petersen, B. O.; Himly, M.; Kaar, W.; Wopfner, N.; Kolarich, D.; van Ree, R.; Ebner, C.; Duus, J. O.; Ferreira, F.; Altmann, F., Two novel types of O-glycans on the mugwort pollen allergen Art v 1 and their role in antibody binding. *J. Biol. Chem.* **2005**, *280*, 7932-7940.
39. Jahn-Schmid, B.; Fischer, G. F.; Bohle, B.; Fae, I.; Gadermaier, G.; Dedic, A.; Ferreira, F.; Ebner, C., Antigen presentation of the immunodominant T-cell epitope of the major mugwort pollen allergen, Art v 1, is associated with the expression of HLA-DRB1*01. *J. Allergy Clin. Immun.* **2005**, *115*, 399-404.

40. Xie, N.; Taylor, C. M., Synthesis of a Dimer of beta-(1,4)-L-Arabinosyl-(2S,4R)-4-hydroxyproline Inspired by Art v 1, the Major Allergen of Mugwort. *Org. Lett.* **2010**, *12*, 4968-4971.
41. Peebles, R. S., Jr., The intelectins: a new link between the immune response to parasitic infections and allergic inflammation? *Am. J. Physiol-Lung C.* **2010**, *298*, L288-L289.
42. Gu, N. B.; Kang, G. N.; Jin, C. E.; Xu, Y. J.; Zhang, Z. X.; Erle, D. J.; Zhen, G. H., Intelectin is required for IL-13-induced monocyte chemotactic protein-1 and-3 expression in lung epithelial cells and promotes allergic airway inflammation. *Am. J. Physiol-Lung C.* **2010**, *298*, L290-L296.
43. Kerr, S. C.; Carrington, S. D.; Oscarson, S.; Gallagher, M. E.; Solon, M.; Yuan, S.; Ahn, J. N.; Dougherty, R. H.; Finkbeiner, W. E.; Peters, M. C.; Fahy, J. V., Intelectin-1 Is a Prominent Protein Constituent of Pathologic Mucus Associated with Eosinophilic Airway Inflammation in Asthma. *Am. J. Respir. Crit. Care Med.* **2014**, *189*, 1005-1007.
44. Szurmai, Z.; Liptak, A.; Snatzke, G., Anomalous zemplen deacylation reactions of 2-O-acyl-3-O-alkyl or 2-o-acyl-3-O-glycosyl derivatives of D-galactose and D-glucose - synthesis of O-alpha-D-mannopyranosyl-(1-4)-O-alpha-L-rhamnopyranosyl-(1-3)-D-galactose and an intermediate for the preparation of 2-O-glycosyl-3-O-(alpha-d-mannopyranosyl)-D-glucoses. *Carbohydr. Res.* **1990**, *200*, 201-208.
45. Komiotis, D.; Agelis, G.; Manta, S.; Tzioumaki, N.; Tsoukala, E.; Antonakis, K., A facile, one-step conversion of 6-O-trityl and 6-O-TBDMS

- monosaccharides into the corresponding formate esters. *J. Carbohydr. Chem.* **2006**, *25*, 441-450.
46. Ziegler, T.; Kovac, P.; Glaudemans, C. P. J., Selective bromoacetylation of alkyl hexopyranosides - a facile preparation of intermediates for the synthesis of (1- 6)-linked oligosaccharides. *Carbohydr. Res.* **1989**, *194*, 185-198.
47. Esmurziev, A. M.; Simic, N.; Hoff, B. H.; Sundby, E., Synthesis and Structure Elucidation of Benzoylated Deoxyfluoropyranosides. *J. Carbohydr. Chem.* **2010**, *29*, 348-367.
48. Ding, X. L.; Wang, W.; Kong, F. Z., Detritylation of mono- and disaccharide derivatives using ferric chloride hydrate. *Carbohydr. Res.* **1997**, *303*, 445-448.
49. Kumar, G. D. K.; Baskaran, S., A facile, catalytic, and environmentally benign method for selective deprotection of tert-butyldimethylsilyl ether mediated by phosphomolybdic acid supported on silica gel. *J. Org. Chem.* **2005**, *70*, 4520-4523.

4. Binding Specificity of Intelectins Using Surface Plasmon Resonance

4.1. Introduction

Carbohydrates and their conjugates (glycoconjugates) are well known for their importance in different physiological processes including cellular communication,¹ proliferation, adhesion² and apoptosis.³ In particular, carbohydrate-specific lectins play a very important role in different biological events.⁴ Lectins are carbohydrate-binding proteins that are found in microorganisms, plants, and animals.⁵ A characteristic feature of lectins is their ability to bind carbohydrates with a notable degree of specificity.^{5, 6} Lectins recognize carbohydrate epitopes through different types of interactions including hydrogen bonds, van der Waals forces, as well as hydrophobic interactions.⁷ Divalent cations (Ca^{2+} , Mg^{2+} , and Mn^{2+}) are also important partners in many in lectin–carbohydrate binding events.^{7, 8}

In general, the measurement of lectin–carbohydrate interactions is not an easy task. There are various analytical techniques and methods that have been used extensively to study and measure these interactions. The most common techniques are isothermal titration calorimetry (ITC),⁹ fluorescence spectroscopy,¹⁰ surface plasmon resonance (SPR) spectroscopy,¹¹ high-performance liquid chromatography (HPLC),¹² mass spectrometry,^{13, 14} and microarrays.^{15, 16} SPR spectroscopy has gained attention in the past two decades and has become one of the most important techniques for studying biomolecular interactions.^{17, 18} SPR spectroscopy monitors real time interactions¹⁹ between lectins and ligands and offers many advantages over fluorescence or calorimetric methods.²⁰ Among the

advantages of SPR spectroscopy is its ability to characterize different biomolecular interactions in a label-free manner.²¹

The detection method in SPR spectroscopy involves changes in the refractive index or mass at the biosensor surface upon complex formation between an immobilized ligand on the SPR surface chip and an analyte (e.g., a protein) in the running buffer^{22, 23}(**Figure 4.1**). The changes in the refractive index near the surface (within 300 nm) are detected and recorded in real time.²⁴ The results are plotted as response units (RU) versus time as shown in **Figure 4.2**. One RU equals approximately the binding of 1 pg protein/mm² of the chip surface.²⁵

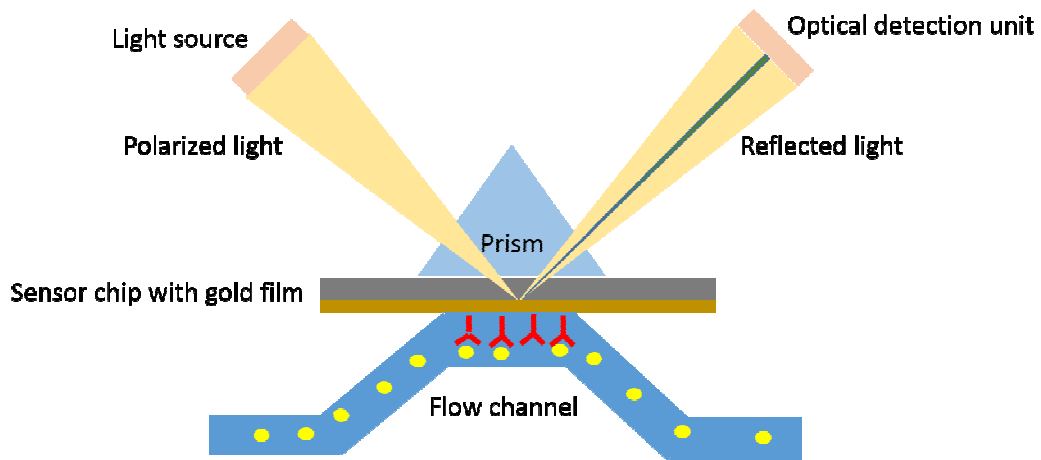


Figure 4.1: Schematic diagram illustrating SPR spectroscopy (modified from BIAcore website).

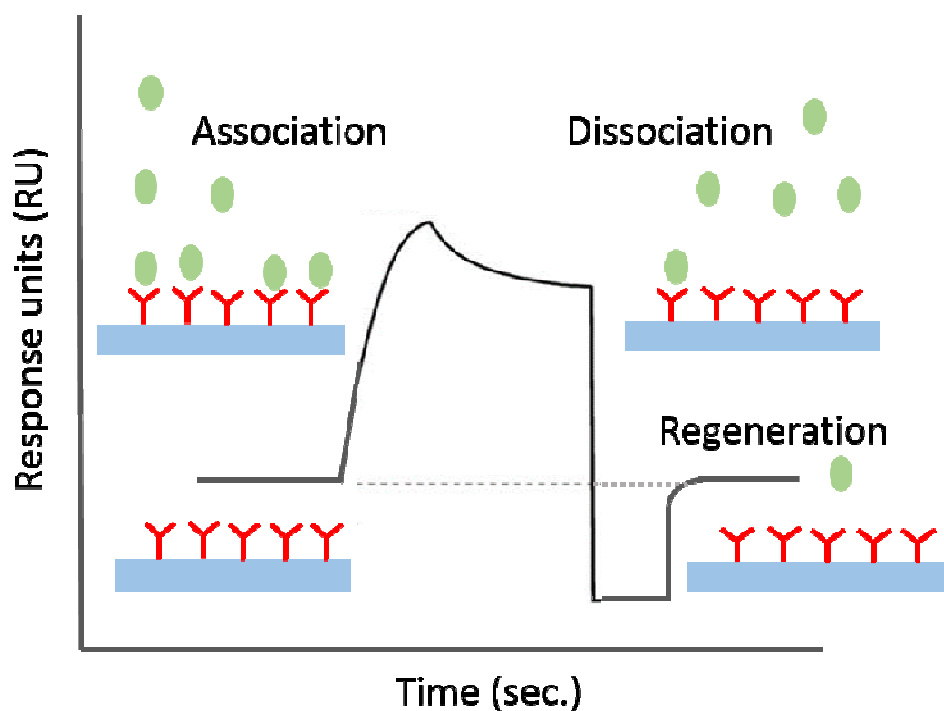


Figure 4.2: SPR sensogram showing the association, dissociation and regeneration phases (modified from BIAcore website).

SPR spectroscopy is a powerful method for studying the thermodynamics and kinetics of bimolecular interactions.²⁶ There are three main phases in any SPR experiment— association, dissociation, and regeneration – as illustrated in **Figure 4.2**. The association phase takes place while the analyte (protein) is being injected; the period that follows the end of the injection is known as the dissociation phase. There is simultaneous association and dissociation of the analyte during the association phase. At a certain point, equilibrium is reached, where the association rate equals the dissociation rate. During the association phase, the association rate constant (k_{on}) can be determined while the dissociation rate constant (k_{off}) is determined during the dissociation phase.¹¹ After the dissociation of the analyte it is important to elute any noncovalently bound

analyte without disrupting the immobilized ligand. This last step is known as the regeneration phase, where the SPR surface is regenerated for future use.

SPR spectroscopy has been used extensively in studying lectin–carbohydrate interactions.²⁷⁻²⁹ The most commonly-used SPR spectroscopic instrument today is the BIAcore system.²⁴ BIAcore surface chips are high quality glass plates coated with a thin (45–50 nm) layer of gold. Some SPR chips (e.g., CM5) are modified by having a carboxymethyl dextran layer covalently bonded to the gold surface.²⁴ Either the lectin or the carbohydrate can be immobilized on the biosensor surface. There are different immobilization strategies that can be used for surface derivatization. These strategies include carboxylate/amine coupling,³⁰ biotin–streptavidin interaction,³¹ and thiol–gold coupling.²⁵ More recently, bioorthogonal chemistry has been used to provide new techniques for protein or ligand immobilization.³² Important examples of bioorthogonal coupling processes are click chemistry reactions.³³ Bertozzi and coworkers³⁴ introduced chemoselective reaction called the Staudinger ligation. A typical Staudinger ligation occurs between an azide and a phosphine to yield an aza-ylide intermediate that hydrolyzes in the presence of water to produce an amide linkage and phosphine oxide.³⁵

In this chapter, I will discuss the binding studies that I did using hIntL-1 and hIntL-2 as well as other lectins. All of the binding experiments were done using SPR spectroscopy. In addition to the SPR experiments, the results of a

fluorescently labelled hIntL-1 screening against a bacterial glycan array will be discussed.

4.2. Results and discussion

4.2.1. Choice of the biosensor chip and surface functionalization method

My main aim in this study was to provide a better understanding about the binding specificity of intelectins. To obtain this information, I decided to measure the binding interactions between the lectins and the synthesized carbohydrate epitopes using SPR spectroscopy.

The first step to reach my goal was to design an effective protocol to immobilize the carbohydrate epitopes on the biosensor chip. I chose to immobilize the sugars, not the lectins, to obtain a better signal to noise ratio. Taking this into consideration, I designed the carbohydrate ligands such that they contained an octylamine linker at the reducing end, which will facilitate their immobilization onto the SPR chip. When I first started the immobilization procedure, I used the CM5 biosensor chip. The CM5 chip is the most commonly used chip for SPR spectroscopic investigations. Its surface is composed of carboxymethylated dextran (CMD) covalently attached to the gold surface. Initially, CM5 was functionalized. However, due to the presence of dextran on its surface I could not avoid a huge background signal that occurred upon lectin binding to the dextran. Therefore, I decided to use to a C1 biosensor chip, the surface of which is matrix free. C1 chips do not contain dextran, instead they contain alkyl chains with terminal carboxymethylated groups.

4.2.1.1. Amine coupling

Amine coupling was used as my first approach to immobilize the carbohydrate epitopes of interest (4.1, 4.2, and 4.4, Figure 4.3) on the biosensor chip. The steps used for the amine coupling are shown in Figure 4.4. First, the carboxylic acid groups of the C1 chip were activated with *N*-hydroxysuccinimide (NHS) in the presence of *N*-ethyl-*N'*-(3-diethylaminopropyl)-carbodiimide (EDC). The second step was reaction of the NHS-activated esters with the amine-containing carbohydrate ligands 4.1, 4.2, and 4.4. Unfortunately, when using this protocol the degree of surface functionalization was poor and there was not sufficient derivatization to detect lectin binding. Failure of the amine coupling was surprising and forced me to think about an alternative method to immobilize the desired carbohydrate ligands. The immobilization technique I chose was Staudinger ligation.

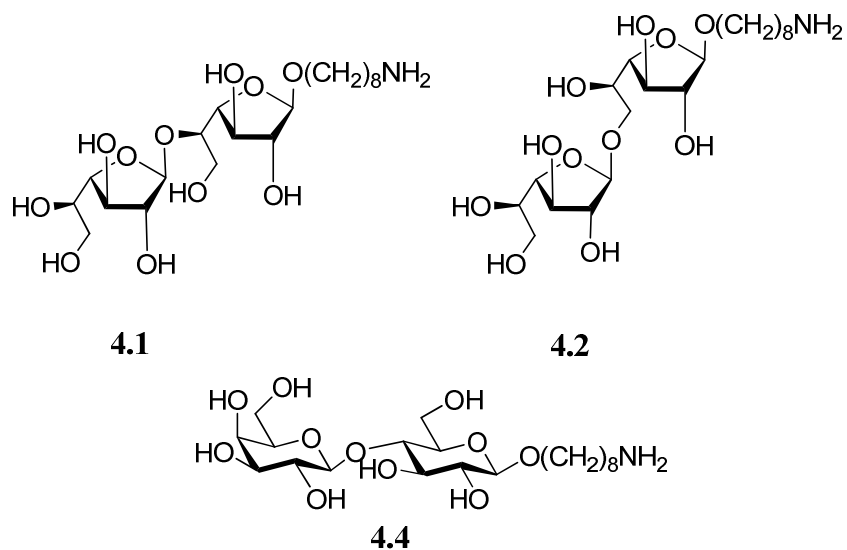


Figure 4.3: *The structures of amine-containing carbohydrate epitopes 4.1, 4.2 and 4.4.*

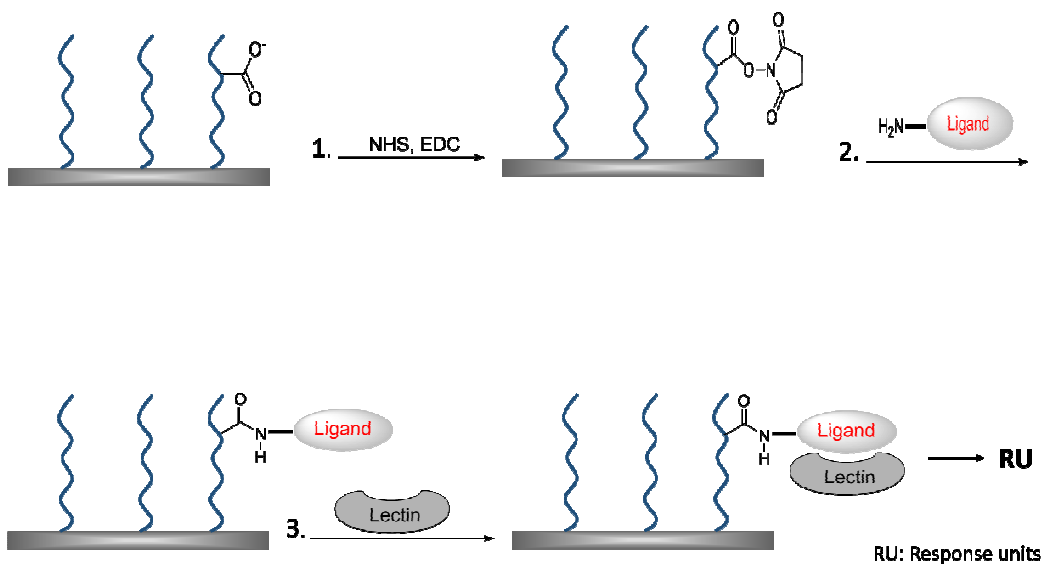


Figure 4.4: Immobilization of the amine carbohydrate epitopes to the CMD surface using amine coupling.

4.2.2. Staudinger ligation

My strategy for using Staudinger ligation was based on an immobilization technique developed by Loka and coworkers,³⁶ where they functionalized the CMD surface with azides followed by reaction with a phosphine-functionalized carbohydrate ligand.³⁶ I was fortunate that I had the azido carbohydrate precursors (3.1 and 3.2) in hand, which encouraged me to think about using Staudinger ligation as the immobilization method. To use this approach, it was necessary to synthesize the phosphine reagent 4.8, which will be discussed later in this chapter.

As outlined in **Figure 4.5**, the carboxylic groups on the C1 chip surface were activated by the addition of NHS/EDC, and then modified by the addition of ethylenediamine. The amines on the chip surface were then allowed to react with the phosphine reagent 4.8 under the continuous flow of HEPES buffer.

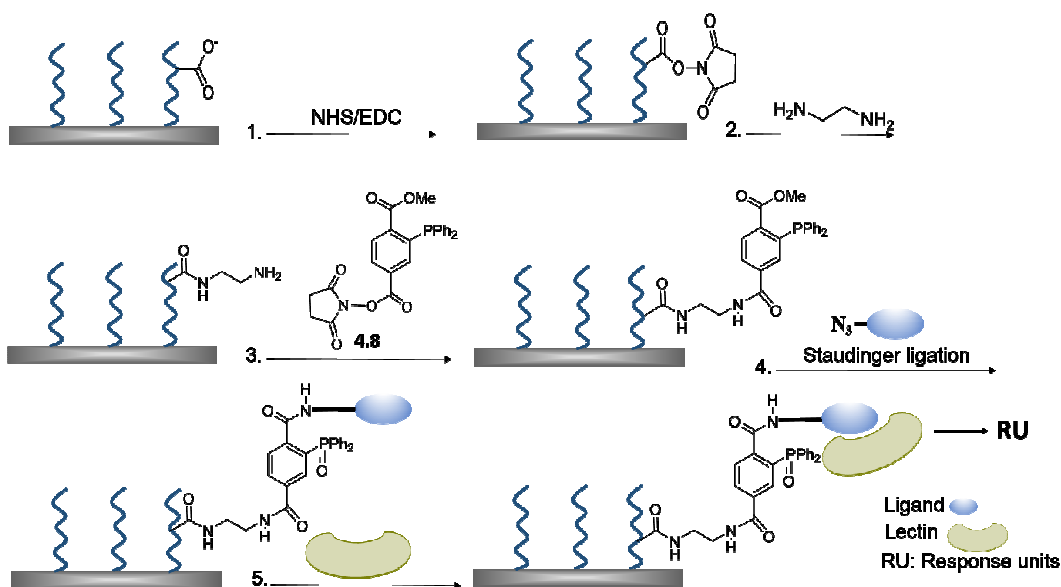
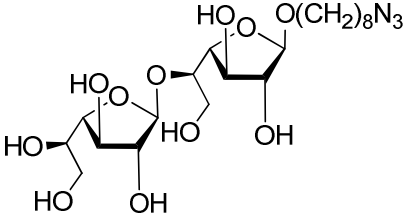
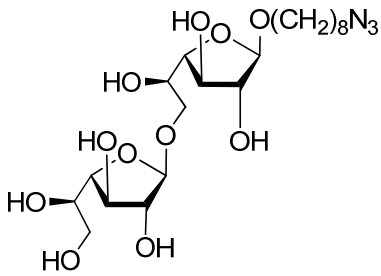
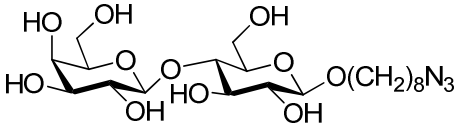


Figure 4.5: Biosensor surface modification using Staudinger ligation.

Each SPR chip is composed of four channels known as flow channels (FC). Each FC was functionalized with different ligands to generate the carbohydrate surfaces. This was achieved by injecting the corresponding azido sugar over the FCs. FC-1, 2 and 3 were derivatized with ligands **3.1**, **3.2** and **4.3**, respectively (**Table 4.1**). It was important to derivatize one flow channel, in this case FC-3, with a carbohydrate epitope that contains Galp (compound **4.3**) to compare the binding affinity of the studied lectins towards galactose in both the furanose and the pyranose forms. Injection of ethanolamine over FC-4 generated a negative control surface. In generating the surfaces, it was important to ensure that the injection of the azido sugars was done immediately after the addition of the phosphine reagent to minimize any possible oxidation of the reagent and to maximize the degree of surface functionalization. The change in RU before and after surface derivatization usually reflects the degree and success of the

immobilization step. The degree of surface derivatization (average for the four FC) was in the range of 1250–4194 RU. Thus, the surface was robust, sensitive and provided reproducible sensograms.

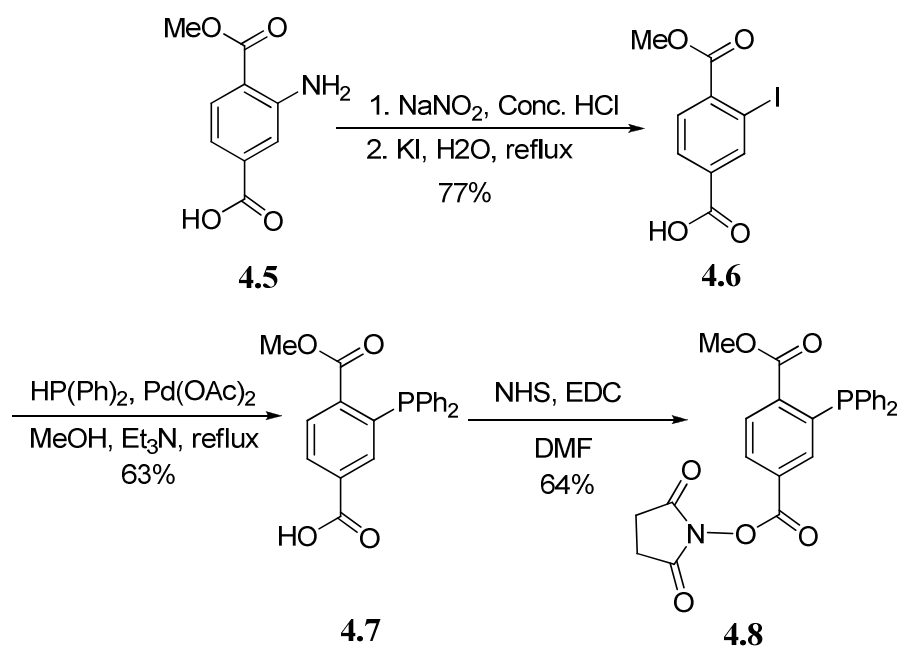
Table 4.1: Structure of the carbohydrate ligands immobilized on the corresponding flow channels using Staudinger ligation.

Flow Channel (FC)	Carbohydrate ligand
1	 <p style="text-align: center;">3.1</p>
2	 <p style="text-align: center;">3.2</p>
3	 <p style="text-align: center;">4.3¹</p>
4	Ethanolamine

¹ Compound **4.3** was synthesized by Dr. Li Xia (Lowary group).

4.2.3. Synthesis of NHS-activated phosphine reagent 4.8

Phosphine reagent **4.8** was the key compound to enable immobilization of the target azido sugars using the Staudinger ligation. To achieve the synthesis of the phosphine reagent **4.8**, I followed protocols reported in literature.^{37, 38} As shown in **Scheme 4.1**, the synthesis started with the aminoterephthalate derivative **4.5**, which was reacted with sodium nitrite and HCl to form the corresponding diazonium salt. The diazonium salt was not isolated but instead was, in the same pot, immediately converted to iodo derivative **4.6** (77% yield) upon treatment with potassium iodide under reflux in water. Subsequently, iodo derivative **4.6** was reacted with diphenylphosphine in a reaction catalyzed by palladium, which produced the Staudinger reagent **4.7** in 63% yield. Compound **4.7** must be handled cautiously during the reaction and workup because it is susceptible to air oxidation forming the corresponding diphenylphosphine oxide, which is inactive in the Staudinger reaction. The purity of **4.7** was confirmed using ³¹P NMR spectroscopy where it showed only a peak for the phosphine at ~ -3 ppm while there was no peak at ~ 30 ppm indicating absence of phosphine oxide. To obtain the final NHS-activated phosphine reagent **4.8**, compound **4.7** was reacted with NHS in the presence of 1-ethyl-3-(3-dimethylaminopropyl)-carbodiimide (EDC), which provided a 64% yield of the desired product.



Scheme 4.1: Synthesis of NHS-activated phosphine reagent 4.8.

Compound **4.8** was stored in the freezer under argon and protected from air, moisture and light to minimize undesired oxidation to the phosphine oxide. With **4.8** in hand, I could run the subsequent SPR biosensor surface modification mentioned above (**Figure 4.5**).

4.2.4. Lectin binding

4.2.4.1. Screening of concanavalin A (ConA), wheat germ agglutinin (WGA), peanut agglutinin (PNA) and soybean agglutinin (SBA)

There are number of reports in the literature showing that ConA exhibit binding affinity towards some furanosyl-containing molecules, e.g. carbohydrates with D-fructofuranosyl and D-arabinofuranosyl residues.³⁹⁻⁴² However, ConA is better known for binding to oligosaccharide containing α -D-Manp residues with high specificity.⁴⁰

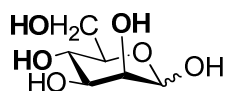


Figure 4.6: Structure of α -D-Manp. Hydroxyl groups that are essential for binding to ConA are shown in bold.

Figure 4.6 shows the structural features of α -D-Manp essential for the high binding affinity to ConA.⁴³ The disposition of the hydroxyl groups (the adjacent trans hydroxyl groups and the hydroxymethyl group on the carbon adjacent to that) in case of D-fructofuranosyl residue⁴⁰ (**Figure 4.7a**) as well as D-arabinofuranosyl⁴¹ (**Figure 4.7b**) is similar to α -D-Manp.

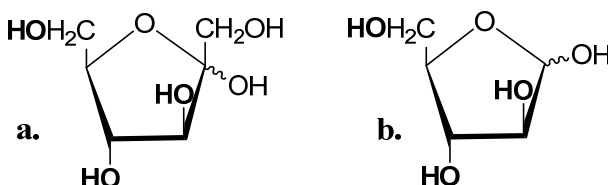


Figure 4.7: Structural features of furanosyl sugars that interact with ConA. Hydroxyl groups that are essential for binding to ConA are shown in bold.

Screening of the lectins listed in **Table 4.2** would provide insight into the binding affinity of these lectins towards Gal β -containing oligosaccharides, which has not been previously investigated. **Table 4.2** shows the names, sources and the known optimal ligands of the lectins used in these SPR experiments. All SPR experiments were done using BIAcore 3000 system in HEPES running buffer. To test the binding affinities of these lectins to the carbohydrate-derivatized surfaces, I injected serial dilutions of ConA, WGA, PNA and SBA (Sigma Aldrich) over the four flow channels of the biosensor chip at a flow rate 10 μ L/min.

Table 4.2: Lectins used in the study of binding specificities towards Gal β -containing oligosaccharides using SPR.

Lectin		Preferred oligosaccharide	Ref.
Name	Source		
Concanavalin A (ConA)	Jackbean	α -D-Man β and α -D-Glc β	44
Wheat germ agglutinin (WGA)	Wheat germ	Glc β NAc, Neu β NAc	45
Peanut agglutinin (PNA)	Peanut	Gal β - β -(1 \rightarrow 3)-Gal β NAc, Man β and Fuc β	46
Soybean agglutinin (SBA)	Soybean	Glucose, galactose/ Gal β NAc	47

BIAevaluation software was used for the analysis of the binding sensograms. It started with alignment of the sensograms of each lectin (in serial concentrations) for each flow channel. The responses from the reference channel (FC-4) were subtracted from the responses obtained from the other flow channels.

The responses obtained from the sensograms (after reference subtraction) were used to fit the data into the chosen binding model as will be discussed later.

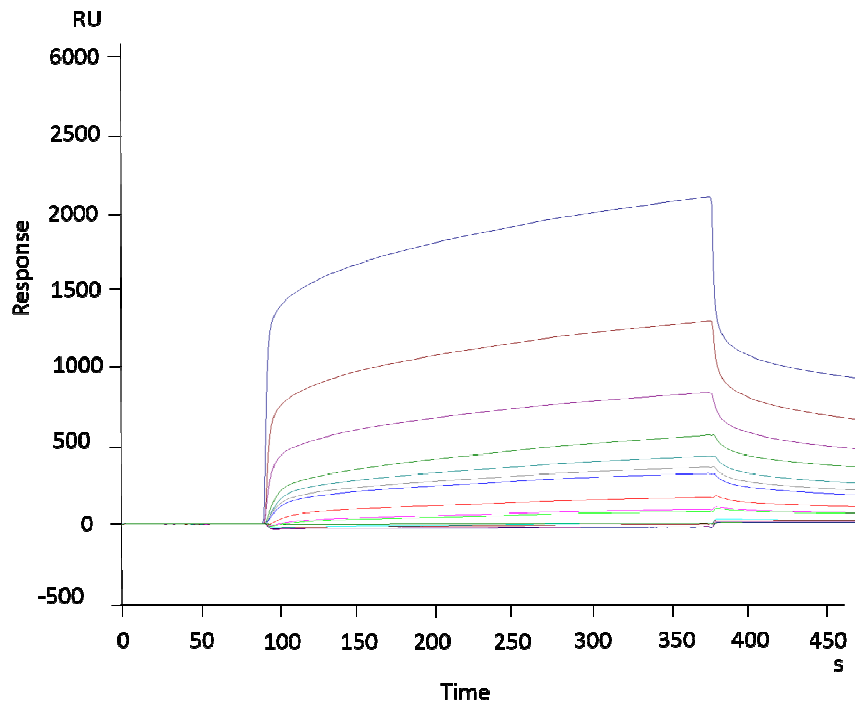


Figure 4.8: ConA (serial concentrations) over FC-1.

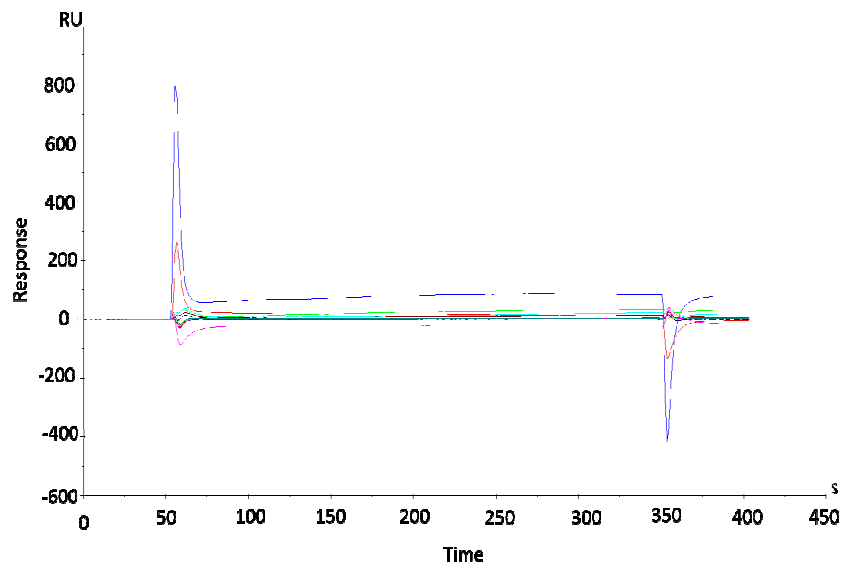


Figure 4.9: SPR sensogram of ConA after subtraction RU of FC-1 from the RU of the reference (FC-4).

For ConA, **Figures 4.8** and **4.9** showed the alignment of the sensograms obtained for serial concentrations of ConA over FC-1, and the responses after subtraction from FC-4, respectively. To obtain information about the binding affinity of ConA towards the ligands which are immobilized on the biosensor chip, I tried to fit the obtained data from the SPR sensograms into a single site binding model (**Equation 4.1**).

$$RU = \frac{B_{max}F}{K_D + F} \dots\dots\dots \text{Equation 4.1}$$

B_{max} : maximum binding,

K_D : affinity constant,

F : lectin concentration

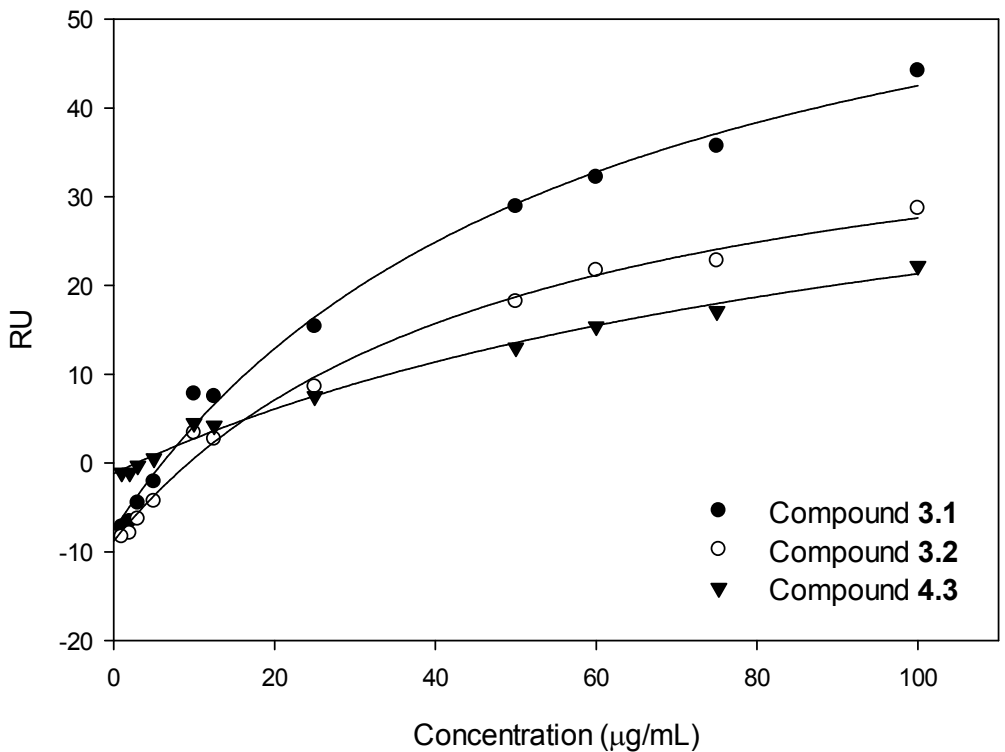


Figure 4.10: Binding isotherm of ConA (0-100 µg/mL) using C1 carbohydrate-derivatized biosensor chip.

The concentration range used to fit the data was from 0–100 $\mu\text{g}/\text{mL}$ ConA, (Figure 4.10). From the fitted data (Figure 4.10), I was able to determine the binding affinities (K_D) of ConA towards ligands 3.1, 3.2 and 4.4 as shown in Table 4.3. K_D values reflected that ConA showed highest binding preference towards compound 3.2 (1 \rightarrow 6 Galf disaccharide), followed by compounds 4.3 and 3.1 (1 \rightarrow 5 Galf disaccharide).

Table 4.3: Binding affinities (K_D) of ConA towards compounds 3.1, 3.2, and 4.4.

FC	Ligand	K_D (μM)	r^2
1	3.1	110 ± 30	0.992
2	3.2	50 ± 10	0.992
3	4.3	60 ± 10	0.993

The alignment of the different sensograms obtained for WGA (when serial dilutions were injected over FC-1 which was derivatized with compound 3.1) is shown in Figure 4.11.

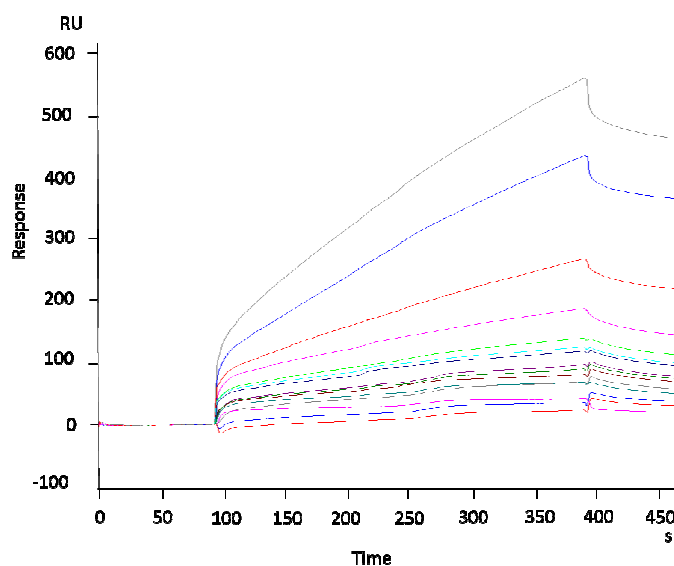


Figure 4.11: WGA (serial concentrations) over FC-1 (compound 3.1: (1 \rightarrow 5)-linked-Galf disaccharide).

The subtracted responses are shown in **Figure 4.12**. WGA sensograms with FC-2 and FC-3 are illustrated in the Appendix (**Figure 6.3** and **6.4**). Similarly, single site model (**Equation 4.1**) was applied to fit the data obtained from the WGA sensograms which resulted in the binding isotherm shown in **Figure 4.13**.

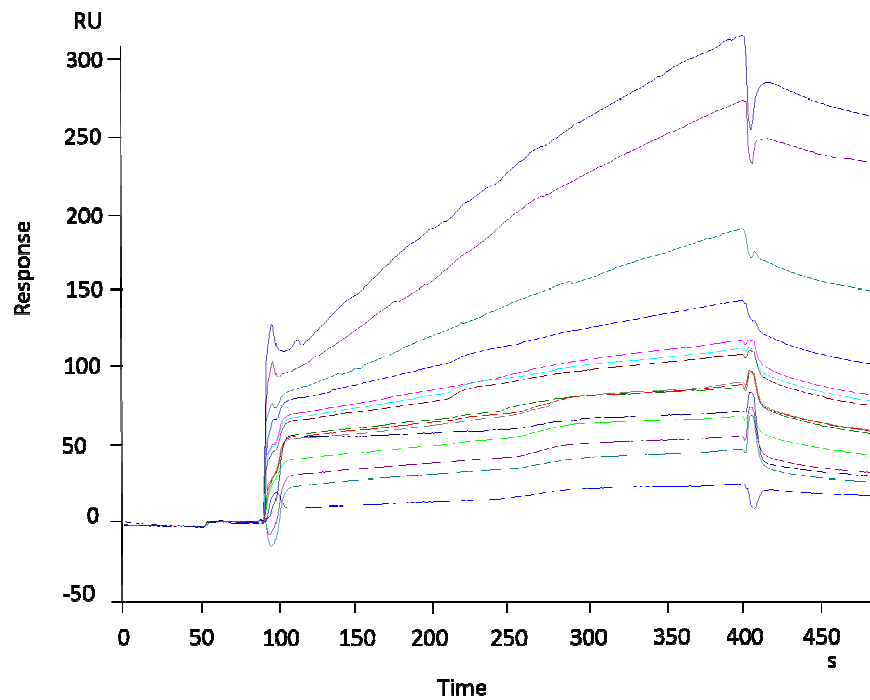


Figure 4.12: SPR sensogram of WGA after subtraction RU of FC-1 from the RU of the reference (FC-4).

The K_D values extracted from **Figure 4.13** are summarized in **Table 4.4**. There are certain binding preferences of WGA towards the furanosyl ligands **3.1** and **3.2**, with the best affinity towards ligand **3.2** (1→5)-linked-Galf disaccharide, (K_D , 4 μ M).

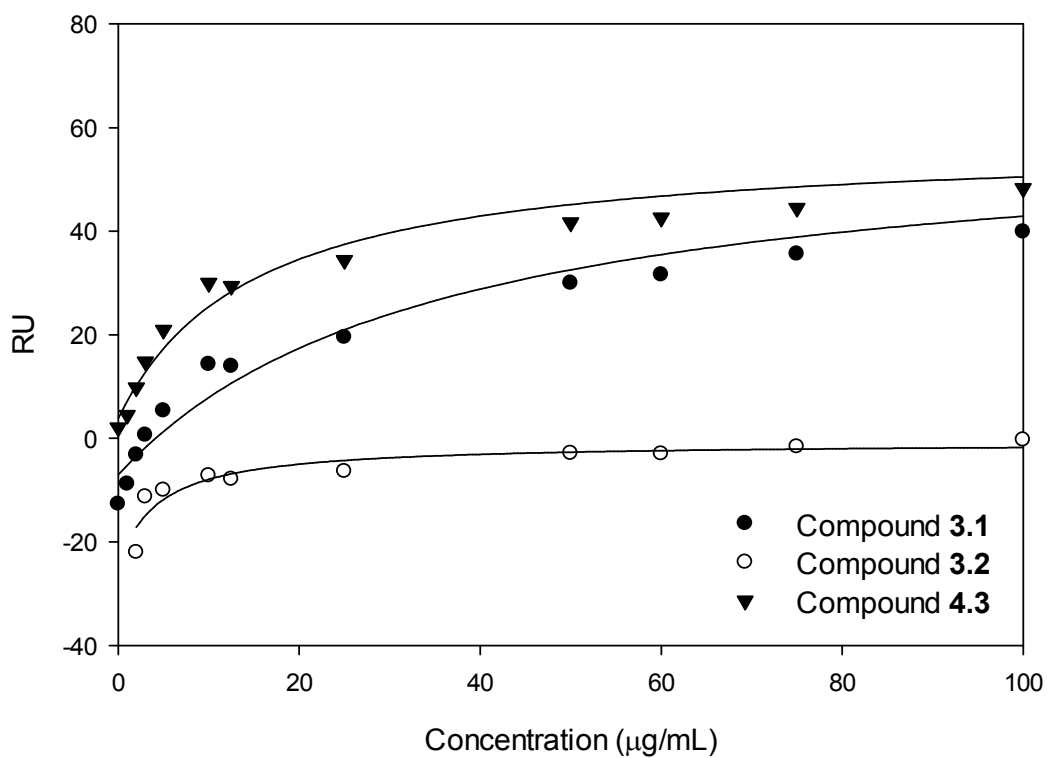


Figure 4.13: Binding isotherm of WGA using C1 carbohydrate-derivatized biosensor chip.

Table 4.4: Binding affinities (K_D) of WGA towards compounds 3.1, 3.2, and 4.4.

FC	Ligand	K_D (μ M)	r^2
1	3.1	40 ± 10	0.960
2	3.2	4 ± 1	0.930
3	4.3	15 ± 5	0.947

Furthermore, **Figure 4.14** shows the sensograms obtained for PNA (serial concentrations) when injected over FC-3, which was derivatized with lactose. PNA sensograms with FC-1 and 2 are illustrated in the Appendix (**Figure 6.9** and **6.10**). When I tried to fit the data obtained from the PNA using the single binding model as done for ConA and WGA, unfortunately I could not obtain good fitting. This could be attributed to the weak binding of PNA towards the immobilized ligands **3.1**, **3.2** and **4.4**.

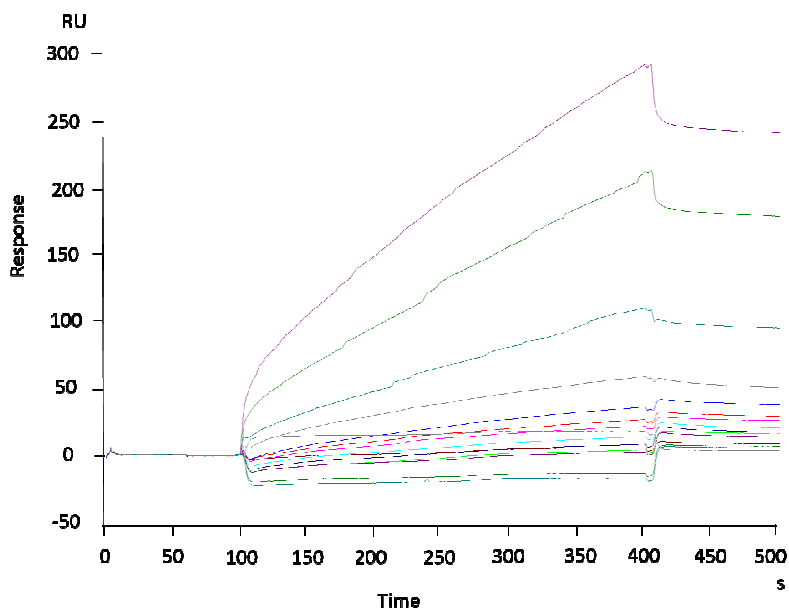


Figure 4.14: PNA (serial concentrations) over FC-3 (4.4 lactose).

SBA did not show any binding to the biosensor chip, where no change in RU upon lectin injection was observed.

As a conclusion, both ConA and WGA exhibited certain binding preferences towards the (1→5)-linked-Galf disaccharide (**3.1**) as well as the (1→6)-linked-Galf disaccharide (**3.2**). On the other hand, due to the poor fitting of PNA to the

single site binding model, I could not determine the binding affinities of this lectin towards the ligands on the chip. Finally, SBA did not show any binding to the derivatized biosensor chip.

It was an important piece of information, which showed that both ConA and WGA could bind to Gal β -containing oligosaccharides. I intended to determine the binding affinities of these two lectins before I started running the binding assays with hIntL.

4.2.4.2. Determining the binding specificity of hIntL-1 and hIntL-2

After studying the binding of ConA, WGA, PNA, and SBA to the SPR chip I had prepared, I moved to investigate the binding of hIntL-1 and hIntL-2. This work involved direct binding of the proteins to the chip and some competitive binding assays.

i) Direct measurement of binding affinity using SPR spectroscopy

A series of dilutions of hIntL-1 and hIntL-2 was injected over the biosensor surface and the response at equilibrium was recorded. In the case of hIntL-2, the SPR sensograms did not show any binding. With hIntL-2, the bulk responses obtained from the control channel FC-4 were always higher than the responses obtained from the other carbohydrate-derivatized channels (FC-1–FC-3). Therefore, I focused the rest of my efforts on hIntL-1.

For hIntL-1, the RU obtained from the reference channel (FC-4) was subtracted from the resulting RU_{\max} (from triplicate runs) from the SPR sensogram (**Figure**

6.11, Appendix) to obtain the sensogram showed in **Figure 4.15**. hIntL-1 sensograms with FC-2 and FC-3 are shown in the Appendix (**Figure 6.12** and **6.13**). The RU_{max} illustrated in **Figure 4.15** were plotted versus the lectin concentrations to provide the binding isotherm of hIntL-1 (**Figure 4.15**).

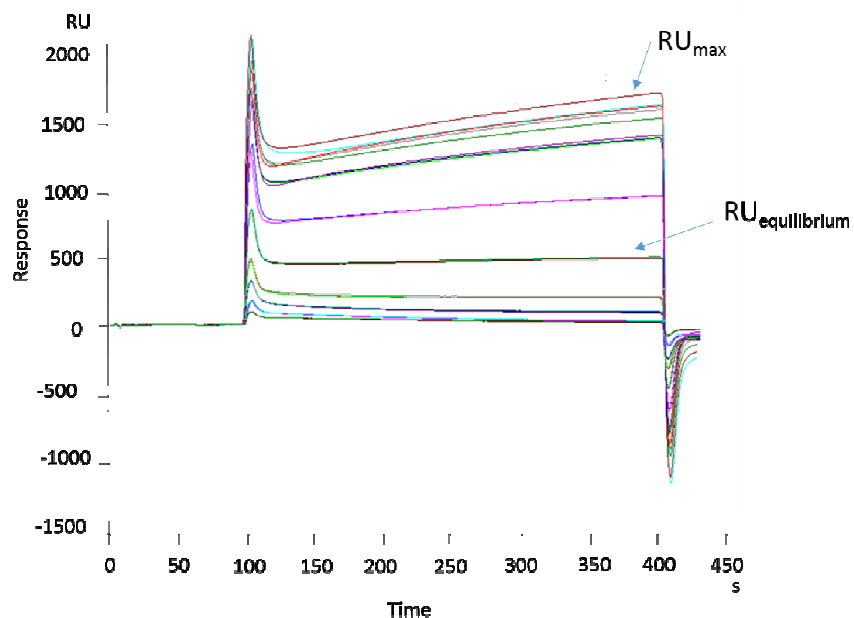


Figure 4.15: SPR sensogram of hIntL-1 after subtraction RU of FC-1 from the RU of the reference (FC-4), showing maximum response units (RU_{max}) and response units at equilibrium ($RU_{equilibrium}$).

Figure 4.15 illustrates that upon higher concentrations of hIntL-1, equilibration could not be reached, instead the response units are increasing as shown by the RU_{max} . As highlighted above, C1 chip composed of alkyl chains coated on the gold surface, which could result in certain hydrophobic interactions between the chip and the protein which increases the probability of non-specific binding to the surface.

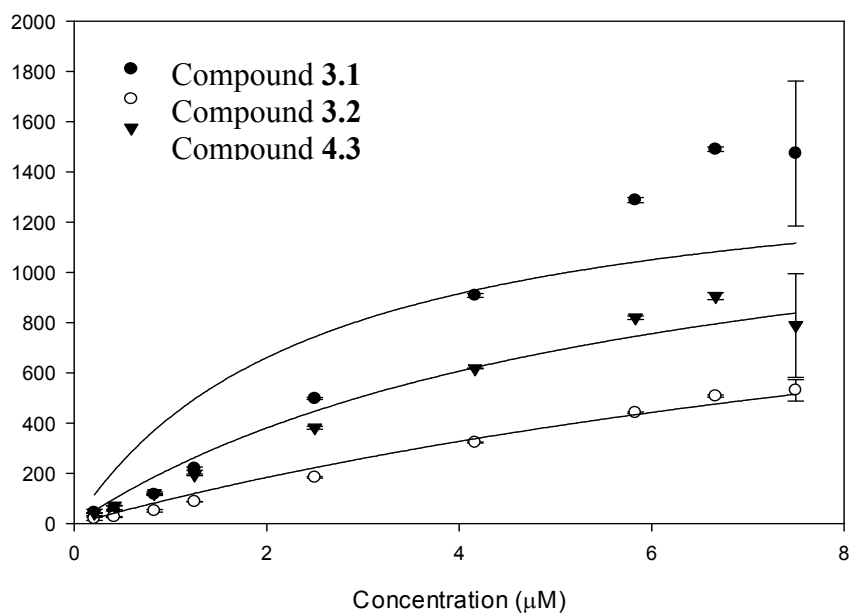


Figure 4.16: Binding isotherm of hIntL-1 using C1 chip when single site binding model was applied (Equation 4.1).

First, I tried to fit the data obtained from hIntL-1 sensograms into the single site binding model (Equation 4.1), but, as shown in Figure 4.16 it resulted in poor fitting, which encouraged me to try to fit the data using alternative binding model (Equation 4.2). This is a single site binding model but it also takes in consideration the non-specific interactions.

$$RU = \frac{B_{max} F}{K_D + F} + K_{ns} F \dots\dots\dots \text{Equation 4.2}$$

B_{max} : maximum binding, K_D : affinity constant

K_{ns} : Non-specific binding constant, F : lectin concentration

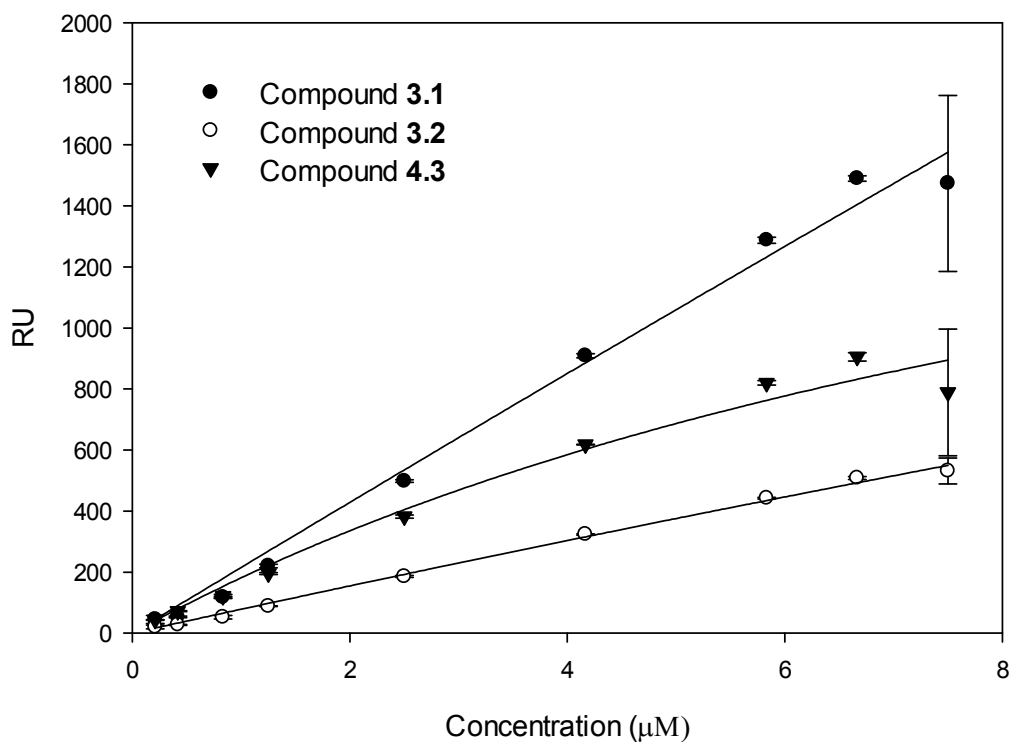


Figure 4.17: Binding isotherm of hIntL-1 using C1 chip when equation 4.2 was applied.

The binding data obtained from applying **Equation 4.2** was used to generate the binding curve shown in **Figure 4.17**. As illustrated in **Figure 4.17**, hIntL-1 did not reach to the saturation level using the concentration range (0–7.6 μM). Furthermore, single site binding model (**Equation 4.2**) suggested that the estimated K_D values are highly beyond the used hIntL-1 concentrations. Therefore, I could assume that the binding affinities of hInt-1 towards the immobilized ligands are higher than 10 μM.

ii) Indirect binding affinity measurement using competitive binding experiment

As described in Chapter 3, I was able to produce a panel of Gal β -containing oligosaccharides via chemical synthesis. One challenge I faced was how to determine the binding affinity of hIntL towards all the compounds. The cost effectiveness of getting all them immobilized on SPR biosensor chips was not ideal, which made a competition binding experiment a more viable choice.

There are different ways to perform the competition binding experiment. Both of the two common techniques for the competitive experiment involve immobilizing the ligand (with known binding affinity to the analyte protein) on the biosensor chip. They differ in the manner in which the protein is added with the competing ligand. One is to choose the competitive binding mode program from the BIAcore system, where the protein (at fixed concentration) is being mixed with the competing ligand (at serial dilutions) and injected over the biosensor chip. On the other hand, a pre-incubation method can be used.⁴⁹ In this method, pre-incubation of the competing ligand together with the analyte takes place before the injection over the biosensor chip.⁴⁹ In my studies, I applied the pre-incubation method using the C1 sensor chip that was previously modified by carbohydrate epitopes **3.1**, **3.2**, and **4.3** using the Staudinger ligation. I chose the pre-incubation method, which allowed me to maximize the mixing time between the protein and the competing ligand.

I started the competitive binding experiment with commercially available ligands i.e., D-ribose and 2-deoxy-D-ribose, and then tried my synthetic oligosaccharides as potential competitive inhibitors. It is known in literature⁴⁸ that hIntL-1 can be completely eluted from a galactose–Sepharose column when the elution buffer contained D-ribose or 2-deoxy-D-ribose. This result showed that hIntL-1 exhibited binding preferences towards these two compounds. Thus, I wanted to quantitate this affinity in terms of an IC_{50} values through competition experiments using SPR spectroscopy.

From the IC_{50} curves of both D-ribose and 2-deoxy-D-ribose (**Figures 4.18** and **4.19**), the IC_{50} values for both of D-ribose and 2-deoxy-D-ribose were calculated and are shown in **Table 4.5**. The IC_{50} values were found to be in the low millimolar range and the binding pattern of hIntL-1 with the sugar epitopes on the chip was similar to what was shown in the direct binding experiment.

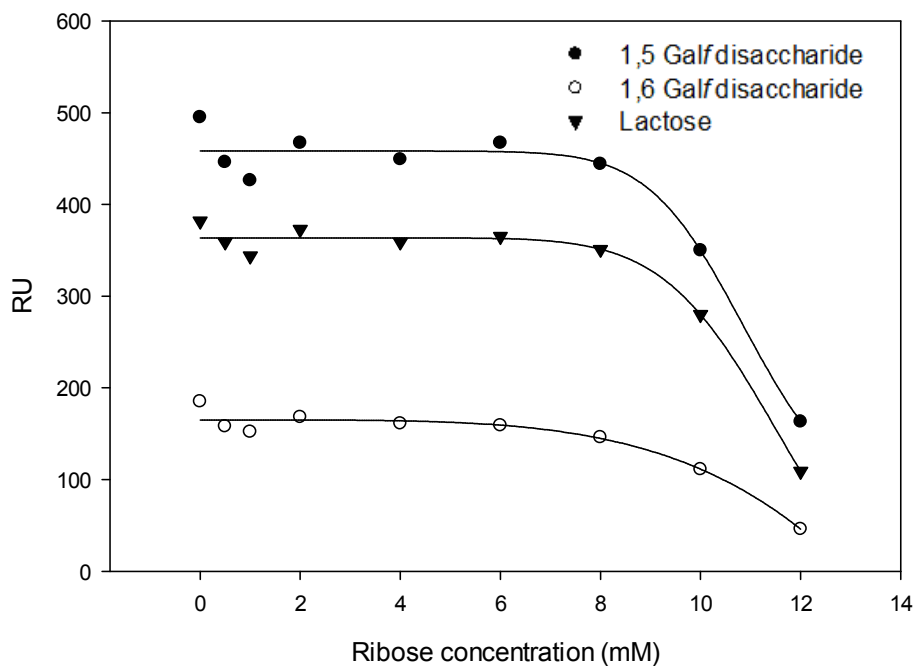


Figure 4.18: IC_{50} curve of D-ribose (0–12 mM).

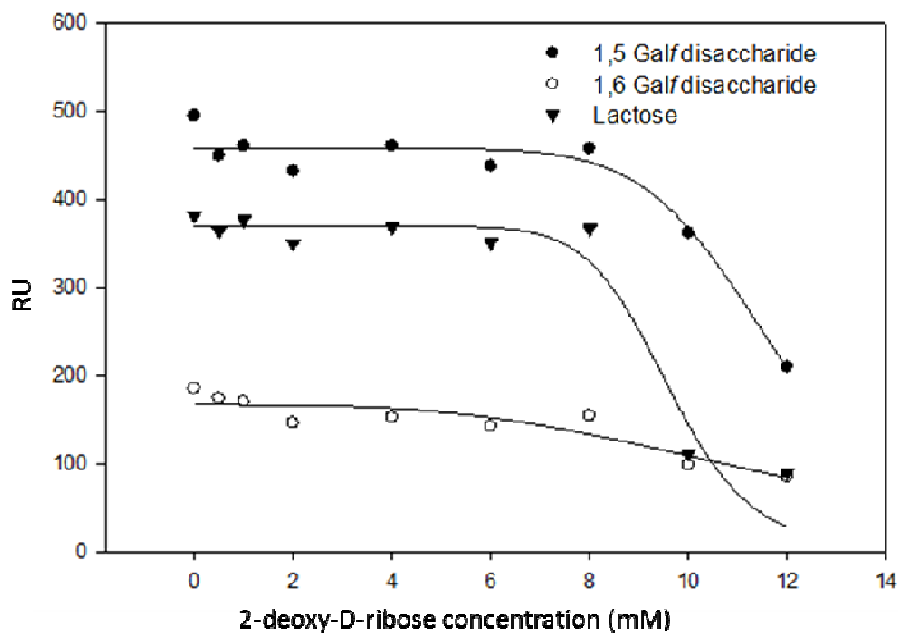


Figure 4.19: IC_{50} curve of 2-deoxy-D-ribose (0–12 mM).

Table 4.5: IC_{50} of D-ribose and 2-deoxy-D-ribose.

Ligand	Flow channel (FC)	IC_{50} (mM)
D-ribose	FC-1 (1→5 Gal f Disaccharide)	11 ± 2
	FC-2 (1→6 Gal f Disaccharide)	10.8 ± 0.3
	FC-3 (lactose)	12 ± 3
2-deoxy-D-ribose	FC-1 (1→5 Gal f Disaccharide)	11.7 ± 0.2
	FC-2 (1→6 Gal f Disaccharide)	12.0 ± 1
	FC-3 (lactose)	9.6 ± 0.3

Using the same competitive experiment protocol, I decided to test the synthesized compounds as potential competing ligands. I chose to start with compounds **3.4** and **3.7** (**Figure 4.20**). Using the same concentration range used for D-ribose (0–12 mM), I was not able to generate IC_{50} curves for compounds **3.4** and **3.7**. Due to the limited quantities of the synthesized compounds, I could not use higher concentrations (> 12 mM) of those compounds. Optimization of the competitive binding experiments using the synthesized compounds will be revisited in the future. One of the proposed approaches is the immobilization of the synthesized compounds e.g., compound **3.4** on the chip surface and to run the SPR binding experiment directly instead of using the competitive binding mode.

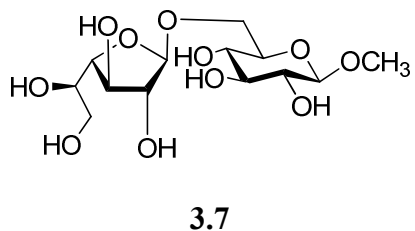
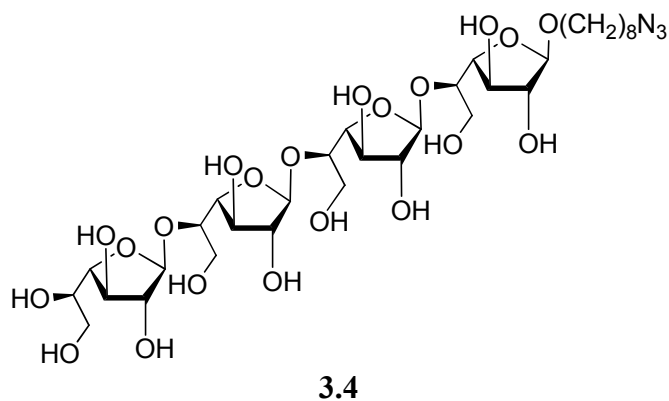


Figure 4.20: Structures of compounds 3.4 and 3.7.

4.2.5. hIntL-1 binding data from Consortium for Functional Glycomics (CFG)

The results I obtained from the SPR experiments with hIntL-1 showed that hIntL-1 exhibited binding preferences towards the synthesized Gal β -containing disaccharides. This agreed with the data were reported previously⁵⁰ on the binding affinity of hIntL-1 towards heat-killed *Mycobacterium bovis* bacillus Calmette–Guerin. This work inspired me to further investigate the binding affinity of hIntL-1 towards a number of glycans isolated from other bacteria. This work was done in collaboration with the CFG.

The main aim of this work was to screen a fluorescently-labelled sample of hIntL-1 against a bacterial glycan array. Cyanine (Cy5-NHS dye, **Figure 4.21**) was chosen for the fluorescent-labelling of hIntL-1.

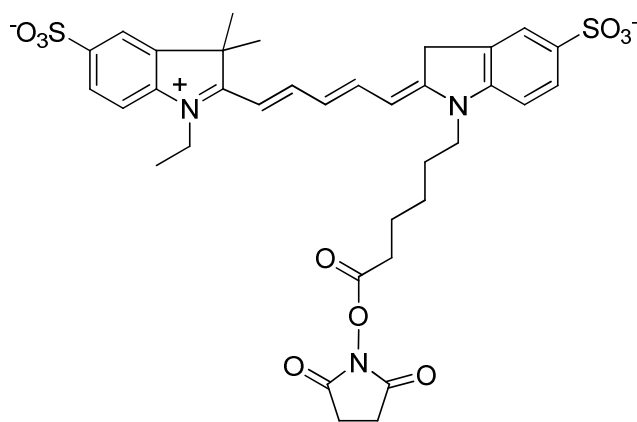


Figure 4.21: Structure of Cy5-NHS dye.

This fluorescently-labelled hIntL-1 was sent to the CFG where it was screened against their “pathogen” glycan array. The printed array contains 48 bacterial lipopolysaccharide (LPS) antigens.⁵¹ The results obtained from scanning the array showed weak binding of hIntL-1 with LPS from *Proteus mirabilis* O3a,3c, *Proteus mirabilis* O54a, *Proteus mirabilis* 54b, *Providencia alcalifaciens* O21, *Providencia rustigianni* O14 and *Pseudomonas aeruginosa* O6a,6c (**Figure 4.22**). When I examined the structures of the LPS from these bacteria (**Table 4.6**), interestingly, I found that none of these glycan structures contain Gal f residues, or any other furanose moieties. However, all the five LPS have at least one *N*-acetyl galactosamine (Gal p NAc) unit in their structures.

It is worth mentioning here that the proposed affinity of intelectins towards Gal f -containing molecules came from the selective elution of the protein from a galactose–Sepharose column.⁴⁸ The column contains galactose in the pyranose form (Gal p), which means that intelectins must bind Gal p with some affinity. The next step will be studying the structure activity relationship (SAR) among these

LPS, which requires conducting more binding experiments with these LPS. Samples of all of these LPS have been obtained for competitive binding measurements using SPR.

Table 4.6: Names and structures from a 48-member glycan array of bacterial LPS molecules that exhibited binding with hIntL-1.

Name	LPS Structure
<i>P. mirabilis</i> O3a,3c ⁵²	$\begin{array}{c} \alpha\text{-D-GalpA6(L-Lys)} * \\ \downarrow 1 \\ 4 \\ \rightarrow 3\text{-}\beta\text{-D-GalpNAc-(1}\rightarrow 6\text{)-}\beta\text{-D-GalpNAc-(1}\rightarrow 4\text{)-}\beta\text{-D-GlcA-(1}\rightarrow \end{array}$ <p>* N-α-(D-galacturonoyl)-L-lysine</p>
<i>P. mirabilis</i> O54a,54b ⁵³	-6)- α -D-GlcNAc-(1 \rightarrow 3)- β -D-Galp-(1 \rightarrow 3)- α -D-GalpNAc-(1-
<i>P. alcalifaciens</i> O21 ⁵⁴	$\begin{array}{c} \rightarrow 4\text{-}\alpha\text{-D-GalpNAc-(1}\rightarrow 4\text{-}\alpha\text{-D-GalpNAc-(1}\rightarrow 3\text{-}\beta\text{-D-GalpNAc-(1}\rightarrow 3\text{-}\alpha\text{-D-GalpA-(1}\rightarrow \\ \uparrow 4 \\ 1 \\ \alpha\text{-D-Fucp3NFo} \end{array}$
<i>P. rustigianni</i> O14 ⁵⁵	(2S,8S)-cetLys-(2 \rightarrow 6)- -3)- α -D-GalpA-(1 \rightarrow 4)- α -D-GalpNAc-(1 \rightarrow 3)- α -D-GlcNAc-(1-
<i>P. aeruginosa</i> O6a,6c ⁵⁶	-3)- α -L-Rhap-(1 \rightarrow 4)- α -D-GalpNAcA-(1 \rightarrow 4)- α -D-GalpNFoA- (1 \rightarrow 3)- α -D-QuipNAc-(1-

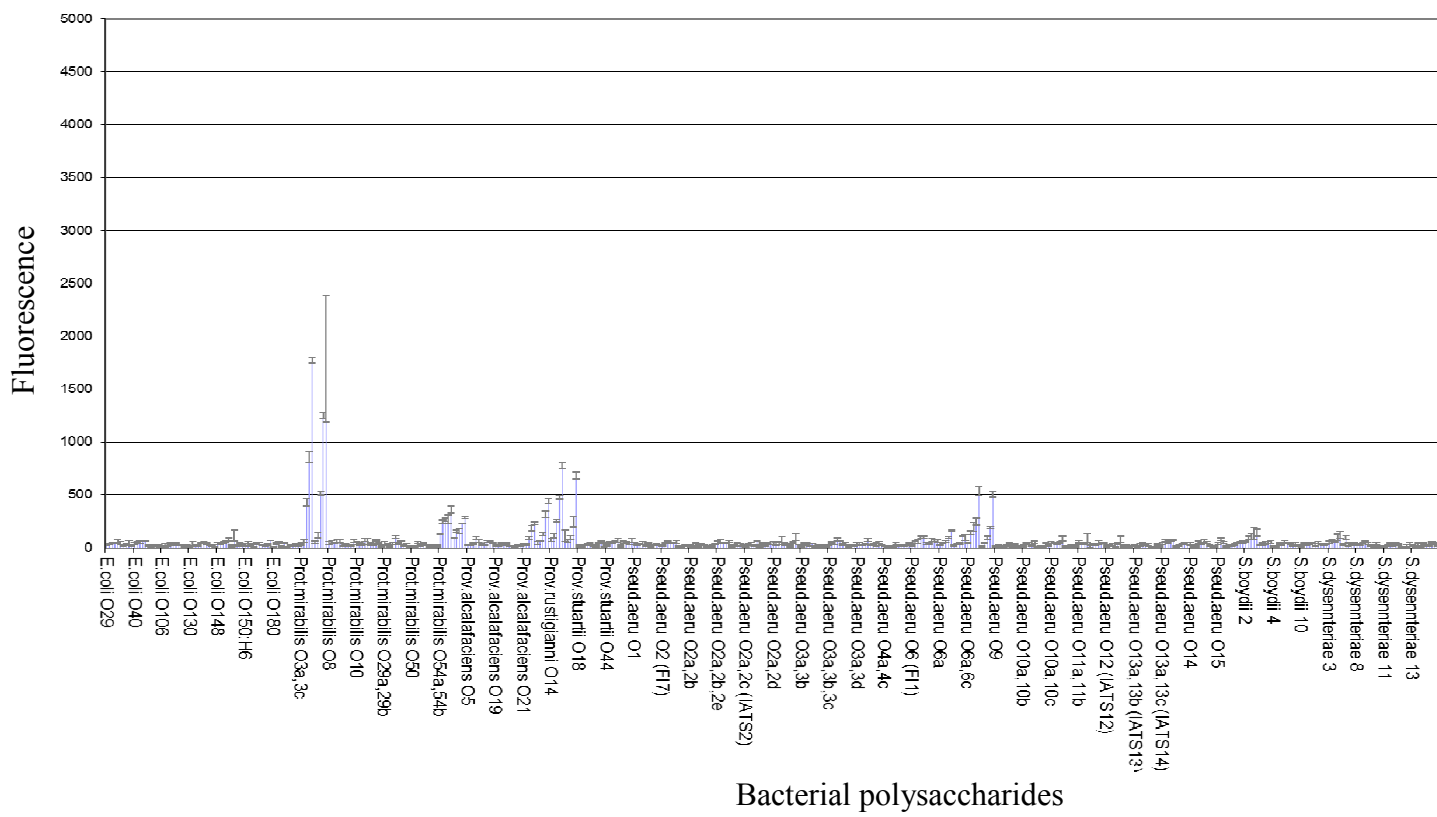


Figure 4.22: Binding between fluorescently labelled IntL-1 (72 µg/mL) and the corresponding bacterial LPS printed on CFG pathogen array.

4.2.6. Conclusion

The binding interactions between different lectins and certain carbohydrate epitopes were studied using SPR spectroscopy. For surface immobilization of the carbohydrate epitopes on the SPR biosensor chip, Staudinger ligation was more effective than carbodiimide coupling, as derivatization using amine-containing carbohydrate epitopes did not enable the detection of binding with hIntL. I used a C1 chip instead of CM5 chip to avoid the presence of high background due to binding to the dextran layer on the CM5 chip. Among the screened lectins, the binding results showed that ConA and WGA bound to the Gal*f* disaccharides as well as lactose. On the other hand, I was not able to quantitate the binding affinities of PNA due to poor fitting. SBA did not show any binding with the derivatized chip.

The data obtained by Tsuji and co-workers⁴⁸, reported the better binding preferences of hIntL towards Gal*f* compared to Gal*p*. Through my binding experiments using hIntL-1, I could not confirm this hypothesis, as I showed that hIntL-1 exhibited comparable binding preferences towards both Gal*f* and Gal*p* residues.

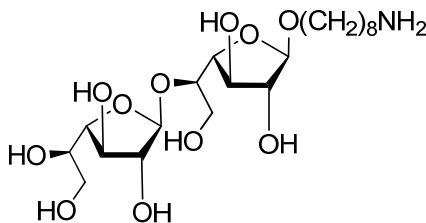
Using competitive binding experiments I was able to calculate the IC₅₀ values of two potential competing ligands (D-ribose and 2-deoxy-D-ribose), which were in the low millimolar range. Unfortunately, I was not able to determine the IC₅₀ of compounds **3.4** and **3.7** due to limitation of the available quantities for both.

A sample of pure hIntL-1 was fluorescently-labelled using the Cy5 dye and was sent to the CFG where it was screened against a small pathogen glycan microarray consisting of a series of 48 bacterial LPS molecules. Five of these structures showed weak binding with hIntL-1 and samples of their LPS will be used in future binding experiments with hIntL-1 using SPR. None of those LPS has Galf in its structure instead they share at least one GalpNac unit. CFG data suggested that hIntL-1 could have binding preferences towards galactose in the pyranose form.

4.3. General Methods

All reagents were purchased from commercial sources and used without further purification. Oven-dried glassware was used for all reactions. Reaction solvents were dried by passage through columns of alumina and copper under nitrogen. All reactions, unless stated otherwise, were carried out at room temperature under positive pressure of argon. Organic solutions were concentrated under vacuum below 40 °C. Reaction progress was monitored by TLC on Silica Gel 60 F₂₅₄ (0.25 mm, E. Merck). Visualization of the TLC spots was done either under UV light or charring the TLC plates with acidified *p*-anisaldehyde solution in ethanol or phosphomolybdic acid stain. Most of the purification methods were done using column chromatography (Silica Gel 40–60 μM). ¹H NMR spectra were recorded using 500 MHz or 400 MHz instruments, and the data are reported as if they were first order. ¹³C NMR (APT) spectra were recorded at 125 MHz. Assignments of data were made using ¹H–¹H COSY and HMQC experiments. Electrospray mass spectra were recorded on samples suspended in THF/MeOH mixture with added NaCl.

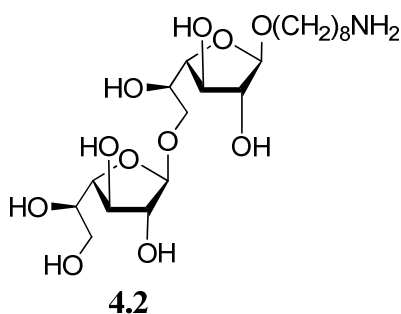
4.3.1. Synthetic procedures



4.1

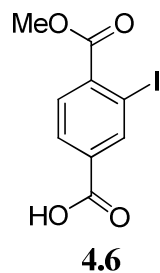
8-Amino-octyl β-D-galactofuranosyl-(1→5)-β-D-galactofuranoside (4.1).

Compound **3.1** (8.0 mg, 0.02 mmol) was dissolved in MeOH and then 20 wt. % Pd(OH)₂-C (3 mg) was added. The reaction mixture was stirred overnight under a hydrogen atmosphere. The solution was filtered through Celite and the filtrate was concentrated to give a crude product that was purified using column chromatography (2:1 CH₂Cl₂-MeOH) followed by further purification using C18 silica gel using H₂O-MeOH as the eluent, to give disaccharide **4.1** (8.4 mg, 90%) as a colourless syrup. *R_f* 0.28 (2:1 CH₂Cl₂-MeOH); [α]_D -102.1 (*c* 0.3, MeOH); ¹H NMR (500 MHz, CD₃OD, δ _H) 5.16 (br s, 1 H, H-1'), 4.85 (br s, 1 H, H-1), 4.10 (dd, 1 H, *J* = 5.9, 3.7 Hz, H-3'), 4.13-3.95 (m, 3 H, H-2, H-2', H-3), 3.94-3.85 (m, 1 H, H-4'), 3.85-3.79 (m, 2 H, H-4', H-5'), 3.75-3.69 (m, 3 H, H-5, H-6a, H-6b), 3.73-3.63 (m, 3 H, H-6'a, H-6'b, octyl OCH₂), 3.40 (td, 1 H, *J* = 9.6, 6.5 Hz, octyl OCH₂), 3.05 (t, 2 H, *J* = 6.9 Hz, octyl CH₂NH₂), 1.54-1.45 (m, 4 H, octyl CH₂), 1.41-1.34 (m, 8 H, octyl CH₂); ¹³C NMR (125 MHz, CD₃OD, δ _C) 109.4 (C-1'), 109.2 (C-1), 84.7 (C-2'), 83.5 (C-2), 83.7 (C-4'), 82.7 (C-4), 78.7 (C-3), 78.6 (C-3'), 77.1 (C-5), 72.2 (C-5'), 68.9 (C-6), 64.2 (octyl OCH₂), 62.8 (C-6'), 56.1 (octyl CH₂NH₂), 30.6 (octyl CH₂), 30.3 (octyl CH₂), 30.4 (octyl CH₂), 29.7 (octyl CH₂), 27.9 (octyl CH₂), 27.5 (octyl CH₂); HR ESIMS: *m/z* [M+Na⁺] calcd. for C₂₀H₃₉NNaO₁₁: 492.2340. Found: 492.2337.

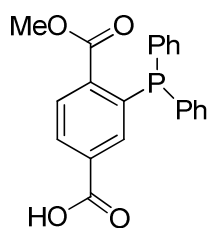


8-Amino-octyl β -D-galactofuranosyl-(1 \rightarrow 6)- β -D-galactofuranoside (4.2).

Compound **3.2** (6 mg, 0.01 mmol) was subjected to the same hydrogenation and purification conditions used to obtain **4.1**, where compound **4.2** (4.2 mg, 90%) was obtained as a colourless syrup. R_f 0.21 (2:1 CH_2Cl_2 -MeOH); $[\alpha]_D -62.4$ (c 2, MeOH); ^1H NMR (500 MHz, CD_3OD , δ_{H}) 4.92 (d, 1 H, $J = 1.1$ Hz, H-1'), 4.85 (br s, 1 H, H-1), 4.12–3.94 (m, 1 H, H-3'), 3.97–3.98 (m, 3 H, H-2, H-2', H-3), 3.95 (dd, 1 H, $J = 3.8, 1.86$ Hz, H-4'), 3.84–3.85 (m, 2 H, H-4', H-5'), 3.84 (dd, 1 H, $J = 10.3, 4.33$ Hz, H-6a'), 3.74–3.69 (m, 3 H, H-6'b, H-6a,b), 3.67–3.58 (m, 1 H, H-5), 3.57–3.58 (m, 1 H, octyl OCH_2), 3.47 (td, 1 H, $J = 9.6, 6.6$ Hz, octyl OCH_2), 3.01 (t, 2 H, $J = 6.9$ Hz, octyl CH_2NH_2), 1.53–1.47 (m, 4 H, octyl CH_2), 1.35–1.22 (m, 8 H, octyl CH_2); ^{13}C NMR (125 MHz, CD_3OD , δ_{C}) 110.1 (C-1'), 109.5 (C-1), 84.4 (C-2'), 84.5 (C-2), 83.5 (C-4'), 82.7 (C-4), 78.4 (C-3), 72.7 (C-3'), 71.7 (C-5), 70.8 (C-5'), 68.4 (C-6), 64.8 (C-6'), 62.8 (octyl OCH_2), 56.5 (octyl CH_2NH_2), 30.5 (octyl CH_2), 30.7 (octyl CH_2), 30.3 (octyl CH_2), 29.9 (octyl CH_2), 27.4 (octyl CH_2), 27.4 (octyl CH_2); HR ESIMS: m/z $[\text{M}+\text{Na}^+]$ calcd. for $\text{C}_{20}\text{H}_{39}\text{NNaO}_{11}$: 492.2320. Found: 492.2340.

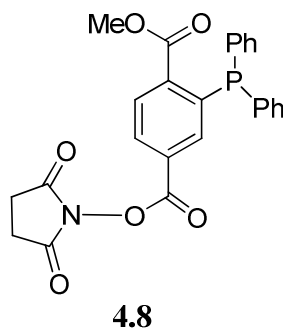


2-Iodo-terephthalic acid 1-methyl ester (4.6). The synthetic procedure for compound **4.6** was adapted from the literature.^{37, 57} In an ice-water bath, concentrated HCl (10 mL) was cooled for 30 min before the addition of 1-methyl-2-aminoterephthalate (1.0 g, 5.10 mmol). The mixture was stirred for further 10 min and then a NaNO₂ (0.35 g, 5.21 mmol) solution in water (2.5 mL) was added slowly while stirring was continued for 5 min. The reaction mixture was then allowed to stir at room temperature for 25 min, before it was transferred using a pipette to a solution of potassium iodide (8.6 g, 51.7 mmol) in water (15 mL). The colour of the reaction mixture turned dark red with the formation of reddish brown precipitate. The reaction was stirred for 1 h, diluted with CH₂Cl₂ (50 mL) and the organic layers was washed with saturated Na₂S₂O₃ solution (30 mL). Finally, the organic layer was washed with brine and dried over anhydrous Na₂SO₄. The solvent was removed leaving behind a yellow solid precipitate, which was recrystallized from MeOH to give **4.6** (1.2 g, 77%) as a yellow amorphous solid. The acquired data for **4.6** were consistent with the literature.⁵⁷



4.7

2-(Diphenylphosphinyl)-terephthalic acid 1-methyl ester (4.7). Compound **4.6** (500 mg, 1.63 mmol), dry CH₃OH (2.5 mL), palladium acetate (3.6 mg, 0.016 mmol) and triethylamine (244 μL, 4.6 mmol) were loaded into a flame-dried flask. The reaction mixture was degassed *in vacuo* and allowed to stir under an argon atmosphere for 30 min. Using a syringe, diphenylphosphine (0.28 mL, 1.67 mmol) was added and the resulting solution was stirred overnight under reflux. The reaction mixture was then cooled to room temperature and the solvent was removed. The crude residue was re-dissolved in a 1:1 mixture of CH₂Cl₂-H₂O (300 mL). The CH₂Cl₂ layer was then washed with (10 mL) 1 N HCl and then concentrated. The obtained crude residue was dissolved in CH₃OH (4 mL) and then cold water (5 mL) was added upon which a yellow solid precipitated. The precipitated solid was dissolved in water and then freeze-dried to give **4.7** (373 mg, 63%) as orange-yellow solid. The data for **4.7** matched that reported previously in literature.³⁶



Succinimidyl 3-diphenylphosphino-4-methoxy-carbonylbenzoate (4.8). To a solution of diphenylphosphine derivative **4.7** (0.989 g, 0.5 mmol) in DMF (7 mL), EDC (0.622 g, 0.6 mmol) and NHS (0.342 g, 0.55 mmol) were added. The solution was stirred at room temperature for 5 h and then concentrated. The obtained residue was poured into CH₂Cl₂-H₂O (50 mL), gently mixed and the CH₂Cl₂ layer was separated and dried over anhydrous Na₂SO₄. Removal of the solvent afforded **4.8** (150 mg, 64%) as yellow amorphous solid. The data for **4.8** matched that reported previously in literature.³⁶

4.3.2. Biosensor surface preparation using amine coupling

SPR binding studies were done using BIAcore 3000 SPR spectrometer. Both CM5 (carboxymethyl dextran) and C1 sensor chips were derivatized using the following protocol. The biosensor surface derivatization reactions were performed at a flow rate 5 μL/min to give sufficient contact time between the surface and the reagents. First, the chip was equilibrated overnight with HEPES running buffer (10 mM HEPES, 1 mM CaCl₂, 150 mM NaCl, 0.005% surfactant P20, pH 7.4), and then was allowed to react with the following solutions as shown in **Figure 4.4**: 1) 200 μL of 1:1 solution of *N*-hydroxy-succinimide (NHS) (0.1 M in water) and *N*-ethyl-*N'*-(3-diethylaminopropyl)-carbodiimide (EDC) (0.1 M in water).

This first step was done for the four flow channels. 2) The surface was then allowed to react with the amine carbohydrate epitopes **4.1**, **4.2** and **4.3** (200 μ L, 1.25 mM solution in HEPES buffer, pH 7.6). Compounds **4.1**, **4.2** and **4.3** were injected over flow channels (FC) 1, 2 and 3, respectively. 3) 200 μ L ethanolamine (EA) (1 M in water, pH 8.5) were injected over all the FC, including FC-4.

4.3.3. Biosensor surface preparation using Staudinger ligation

First, C1 chip was equilibrated overnight with HEPES running buffer (10 mM HEPES, 1 mM CaCl_2 , 150 mM NaCl, 0.005% surfactant P20, pH 7.4) and then the C1 biosensor chip surface was derivatized as illustrated in **Figure 4.5** according to the following steps: 1) 200 μ L of 1:1 solution of *N*-hydroxysuccinimide (NHS) (0.1 M in water) and *N*-ethyl-*N'*-(3-diethylaminopropyl)-carbodiimide (EDC) (0.1 M in water). 2) 325 μ L of ethylenediamine (EDA) (1 M in water, pH 8.5) were injected over the four Fc. 3) 300 μ L of the NHS-activated phosphine reagent **4.8** (50 mM, 6% DMSO in HEPES, pH 8) were injected at flow rate 8 μ L/min over FC 1–3. The chip surface was allowed to react with the azido carbohydrate epitopes **3.1**, **3.2** and **4.4** via Staudinger ligation, where 300 μ L of compounds **3.1**, **3.2** and **4.4** (1.25 mM in HEPES buffer, pH 7.5) were injected at flow rate 8 μ L/min over FC-1, 2 and 3, respectively.

4.3.4. Detection of lectin binding specificity

SPR binding studies were done using BIAcore 3000 SPR spectrometer and the analysis of the data was done using BIAevaluation software supplied by BIAcore. The binding studies was done using a C1 chip derivatized with ligands **3.1**, **3.2**

and 4.4. The same HEPES buffer used in the biosensor surface preparation was used in the lectin binding experiments. Kinject injection mode was used at a flow rate of 10 $\mu\text{L}/\text{min}$. Serial dilutions of each lectin in HEPES buffer were prepared and the exact final concentration of each solution was determined by measuring A_{280} (using UV-spectrophotometer) of the lectin solution. Lectins solutions were injected over the four FC and data correction was performed by subtracting the response obtained from the carbohydrate-derivatized surfaces (FC 1–3) from control lane (FC-4). RU_{max} from each sensogram was used to fit the following single site binding mode (**Equation 4.1**).

4.3.5. Competitive binding experiment with hIntL-1 using SPR

In these experiments the C1 biosensor chip was used. The following concentrations of the competing ligand (D-ribose, 2-deoxy-D-ribose, **3.4**, and **3.7** at 12, 10, 8, 6, 4, 2, 1, 0.5, 0 mM) were prepared in HEPES running buffer (10 mM HEPES, 1 mM CaCl_2 , 150 mM NaCl, 0.005% surfactant P20, pH 7.4). Serial dilutions of the ligand were pre-incubated with 300 mg/mL of hIntL-1 for 1 h at room temperature, then the SPR experiment was started. Kinject injection mode was used at a flow rate of 10 $\mu\text{L}/\text{min}$ and the RU_{max} from each concentration was used to create the IC_{50} curves for the competing ligands.

4.3.6. Surface regeneration

Surface regeneration was achieved by injecting 400 μL 10 mM glycine (pH 1.5) after each lectin concentration. Similar regeneration outcomes were obtained when 400 μL 10 mM glycine (pH 2) was used.

4.3.7. Fluorescent labelling of hIntL-1

The protocol for the fluorescent-labelling of hIntL-1 was adapted from the literature.⁵⁸ A solution of pure hIntL-1 (1mg/mL) in 0.1 M sodium carbonate (pH 8.4) was prepared. In the experiments a freshly prepared solution of the dye was prepared by dissolving cyanine dye (Life Technologies, Cy5 in dry dimethylsulfoxide, DMSO) at a concentration 1mg/mL. Preparation of the dye solution should be done in a darkened lab and the dye solution should be protected from light either by using amber vials or wrapping the vial with aluminum foil. In a darkened lab, the Cy5 dye solution (25 μ L) was added slowly to 1 mL of the hIntL-1 solution. The protein/dye mixture was left in the dark for 7 h. The excess dye was quenched by the addition of 0.1 M aminoethanol at pH 8 followed by dialysis of the protein solution using a spin column (MWCO 10 kDa) for 2 h. The protein was dialyzed in 10 mM HEPES, 150 mM NaCl and 1 mM CaCl₂ buffer. After fluorescent-labelling of the protein, it was necessary to determine the fluorophore–protein (FP) ratio, which reflects the degree of the protein labelling. The FP ratio is the number of mol of dye per mol of protein. To calculate the FP ratio, both A_{280} and A_{\max} (A_{\max} is the absorbance at 650 nm for Cy5 dye) were measured using a UV-Vis spectrophotometer. The A_{280} and A_{650} values were 0.082 and 0.029 mg/mL, respectively. The following two equations were used to calculate the FP ratio of hIntL-1:

$$\begin{aligned} 1. M &= A_{280} - \left[(A_{\max} \cdot CF) \cdot \epsilon^{-1} \cdot b^{-1} \right] \\ &= 0.082 - \left[\frac{(0.029 \times 0.05)}{79,925 \text{ M}^{-1} \text{ cm}^{-1} \times 1 \text{ cm}} \right] \\ &= 1.008 \times 10^{-6} \text{ M} \end{aligned}$$

M: molar protein concentration (M), **CF**: correction factor (dilution factor), **ε**: hIntL-1 extinction coefficient ($M^{-1} \text{ cm}^{-1}$) calculated using ProtParam tool on ExPASy⁵⁹, **b**: path length (1 cm)

$$\begin{aligned}
 2. \text{ FP ratio} &= \frac{A_{\text{max}} \text{ of the labelled protein}}{\epsilon' \cdot b \cdot M} \\
 &= \frac{0.029}{25000 \text{ M}^{-1} \text{ cm}^{-1} \times 1 \text{ cm} \times 1.008 \times 10^{-6} \text{ M}} \\
 &= 0.1 \text{ mol dye/moles protein}
 \end{aligned}$$

ε': Cy5 molar extinction coefficient ($M^{-1} \text{ cm}^{-1}$), **b**: pathlength (1 cm), **M**: molar protein concentration (M)

4.3.8. hIntL-1 screening against pathogen glycan array through CFG

The printed pathogen array consists of the polysaccharides derived from 48 different Gram-negative bacteria. Each polysaccharide was printed in 2 forms: the native form and the native plus a spacer group (aliphatic amine linker). Each form was printed at 5 concentrations for a total of 10 polysaccharide spots corresponding to each bacterial species. Each of the 10 polysaccharides was printed in replicates of 6.⁵¹

The average relative fluorescent units (RFU) from the replicates, the standard deviation, the standard error of the mean (used for the error bars) and percentage coefficient of variation (%CV, %CV=100 X Std. Dev/Mean) were calculated and the graph shown in Figure 4.19 was plotted. The graph shows bacterial polysaccharide name vs. average fluorescence (RFU). The highest and lowest point from each set of six replicates has been removed so that the average RFU is

of 4 values rather than 6. This eliminates some of the false hits that contain a single very high or low point. Thus, points with high %CV should be considered suspect. The scanner response is linear to a maximum RFU value of about 50,000.

4.4. References

1. Dube, D. H.; Bertozzi, C. R., Glycans in cancer and inflammation. Potential for therapeutics and diagnostics. *Nat. Rev. Drug Discov.* **2005**, *4*, 477-488.
2. Kasamatsu, A.; Uzawa, K.; Nakashima, D.; Koike, H.; Shiiba, M.; Bukawa, H.; Yokoe, H.; Tanzawa, H., Galectin-9 as a regulator of cellular adhesion in human oral squamous cell carcinoma cell lines. *Int. J. Mol. Med.* **2005**, *16*, 269-273.
3. Nakahara, S.; Oka, N.; Raz, A., On the role of galectin-3 in cancer apoptosis. *Apoptosis* **2005**, *10*, 267-275.
4. Vasta, G. R.; Ahmed, H.; Tasumi, S.; Odom, E. W.; Saito, K., Biological roles of lectins in innate immunity: Molecular and structural basis for diversity in self/non-self recognition. In *Current Topics in Innate Immunity*, Lambris, J. D., Ed. 2007; Vol. 598, pp 389-406.
5. Sharon, N., Lectin carbohydrate complexes of plants and animals - an atomic view. *Trends Biochem. Sci* **1993**, *18*, 221-226.
6. Drickamer, K., Multiplicity of lectin carbohydrate interactions. *Nat. Struct. Biol.* **1995**, *2*, 437-439.
7. Safina, G., Application of surface plasmon resonance for the detection of carbohydrates, glycoconjugates, and measurement of the carbohydrate-specific interactions: A comparison with conventional analytical techniques. A critical review. *Analytica Chimica Acta* **2012**, *712*, 9-29.

8. Holmskov, U.; Malhotra, R.; Sim, R. B.; Jensenius, J. C., Collectins - collagenous C-type lectins of the innate immune defense system. *Immunology Today* **1994**, *15*, 67-74.
9. Dam, T. K.; Brewer, C. F., Thermodynamic studies of lectin-carbohydrate interactions by isothermal titration calorimetry. *Chem. Rev.* **2002**, *102*, 387-429.
10. Lee, Y. C., Fluorescence spectrometry in studies of carbohydrate-protein interactions. *J Biochem* **1997**, *121*, 818-825.
11. Safina, G.; Duran, I. B.; Alasel, M.; Danielsson, B., Surface plasmon resonance for real-time study of lectin-carbohydrate interactions for the differentiation and identification of glycoproteins. *Talanta* **2011**, *84*, 1284-1290.
12. Royle, L.; Campbell, M. P.; Radcliffe, C. M.; White, D. M.; Harvey, D. J.; Abrahams, J. L.; Kim, Y.-G.; Henry, G. W.; Shadick, N. A.; Weinblatt, M. E.; Lee, D. M.; Rudd, P. M.; Dwek, R. A., HPLC-based analysis of serum N-glycans on a 96-well plate platform with dedicated database software. *Anal. Biochem.* **2008**, *376*, 1-12.
13. Patwa, T.; Li, C.; Simeone, D. M.; Lubman, D. M., Glycoprotein analysis using protein microarrays and mass spectrometry. *Mass Spectrom. Rev.* **2010**, *29*, 830-844.
14. Budnik, B. A.; Lee, R. S.; Steen, J. A. J., Global methods for protein glycosylation analysis by mass spectrometry. *Biochim. Biophys. Acta-Proteins and Proteomics* **2006**, *1764*, 1870-1880.

15. Carroll, G. T.; Wang, D.; Turro, N. J.; Koberstein, J. T., *Photo-Generation of Carbohydrate Microarrays*. 2009; p 191-210.
16. Fais, M.; Karamanska, R.; Russell, D. A.; Field, R. A., Lectin and carbohydrate microarrays: New high-throughput methods for glycoprotein, carbohydrate-binding protein and carbohydrate-active enzyme analysis. *J. Cereal Sci.* **2009**, *50*, 306-311.
17. Cho, W. W.; Bittova, L.; Stahelin, R. V., Membrane binding assays for peripheral proteins. *Anal. Biochem.* **2001**, *296*, 153-161.
18. Lakey, J. H.; Raggett, E. M., Measuring protein-protein interactions. *Curr. Opin. Struct. Biol.* **1998**, *8*, 119-123.
19. Jonsson, U.; Fagerstam, L.; Ivarsson, B.; Johnsson, B.; Karlsson, R.; Lundh, K.; Lofas, S.; Persson, B.; Roos, H.; Ronnberg, I.; Sjolander, S.; Stenberg, E.; Stahlberg, R.; Urbaniczky, C.; Ostlin, H.; Malmqvist, M., Real-time biospecific interaction analysis using surface plasmon resonance and a sensor chip technology. *Biotechniques* **1991**, *11*, 620-&.
20. Tanious, F. A.; Nguyen, B.; Wilson, W. D., Biosensor-surface plasmon resonance methods for quantitative analysis of biomolecular interactions. In *Method Cell Biol*, Correia, J. J.; Detrich, H. W., Eds. 2008; Vol. 84, pp 53-77.
21. Van Regenmortel, M. H. V., Improving the quality of BIACORE-based affinity measurements. *Dev. Biol. (Basel)* **2003**, *112*, 141-51.
22. Karlsson, R., Affinity analysis of non-steady-state data obtained under mass transport limited conditions using BIACore technology. *J. Mol. Recognit.* **1999**, *12*, 285-292.

23. Myszka, D. G., Kinetic, equilibrium, and thermodynamic analysis of macromolecular interactions with BIACORE. *Method Enzymol.* **2000**, *323*, 325-+.
24. Rich, R. L.; Myszka, D. G., BIACORE J: a new platform for routine biomolecular interaction analysis. *J. Mol. Recognit.* **2001**, *14*, 223-228.
25. Smith, E. A.; Thomas, W. D.; Kiessling, L. L.; Corn, R. M., Surface plasmon resonance imaging studies of protein-carbohydrate interactions. *J. Am. Chem. Soc.* **2003**, *125*, 6140-6148.
26. Karlsson, R.; Larsson, A., Affinity measurement using surface plasmon resonance. *Methods Mol. Biol.* **2004**, *248*, 389-415.
27. Mann, D. A.; Kanai, M.; Maly, D. J.; Kiessling, L. L., Probing low affinity and multivalent interactions with surface plasmon resonance: Ligands for concanavalin A. *J. Am. Chem. Soc.* **1998**, *120*, 10575-10582.
28. Nakamura, K.; Sakagami, H.; Asanuma-Date, K.; Nagasawa, N.; Nakahara, Y.; Akiyama, H.; Ogawa, H., Immobilized glycosylated Fmoc-amino acid for SPR: comparative studies of lectin-binding to linear or biantennary diLacNAc structures. *Carbohydr. Res.* **2013**, *382*, 77-85.
29. Penezic, A.; Deokar, G.; Vignaud, D.; Pichonat, E.; Happy, H.; Subramanian, P.; Gasparovic, B.; Boukherroub, R.; Szunerits, S., Carbohydrate-Lectin Interaction on Graphene-Coated Surface Plasmon Resonance (SPR) Interfaces. *Plasmonics* **2014**, *9*, 677-683.
30. Hutchinson, A. M., Characterization of glycoprotein oligosaccharides using surface plasmon resonance. *Anal. Biochem.* **1994**, *220*, 303-307.

31. Linman, M. J.; Taylor, J. D.; Yu, H.; Chen, X.; Cheng, Q., Surface plasmon resonance study of protein-carbohydrate interactions using biotinylated sialosides. *Anal. Chem.* **2008**, *80*, 4007-4013.
32. Sletten, E. M.; Bertozzi, C. R., Bioorthogonal Chemistry: Fishing for Selectivity in a Sea of Functionality. *Angew. Chem. Int. Ed.* **2009**, *48*, 6974-6998.
33. Kolb, H. C.; Finn, M. G.; Sharpless, K. B., Click chemistry: Diverse chemical function from a few good reactions. *Angew. Chem. Int. Ed.* **2001**, *40*, 2004-+.
34. Saxon, E.; Bertozzi, C. R., Cell surface engineering by a modified Staudinger reaction. *Science* **2000**, *287*, 2007-2010.
35. Gololobov, Y. G.; Kasukhin, L. F., Recent advances in the staudinger reaction. *Tetrahedron* **1992**, *48*, 1353-1406.
36. Loka, R. S.; Cairo, C. W., Immobilization of carbohydrate epitopes for surface plasmon resonance using the Staudinger ligation. *Carbohydr. Res.* **2010**, *345*, 2641-2647.
37. Kiick, K. L.; Saxon, E.; Tirrell, D. A.; Bertozzi, C. R., Incorporation of azides into recombinant proteins for chemoselective modification by the Staudinger ligation. *Proc. Natl. Acad. Sci. U. S. A.* **2002**, *99*, 19-24.
38. Wang, C. C. Y.; Seo, T. S.; Li, Z. M.; Ruparel, H.; Ju, J. Y., Site-specific fluorescent labeling of DNA using Staudinger ligation. *Bioconj. Chem.* **2003**, *14*, 697-701.
39. Goldstei.Ij; So, L. L., PROTEIN-CARBOHYDRATE INTERACTION .3. Agar gel-diffusion studies on interaction of concanavalin a a lectin

- isolated from jack bean with polysaccharides. *Arch. Biochem. Biophys.* **1965**, *111*, 407
40. So, L. L.; Goldstein, I. J., Protein-carbohydrate interaction .21. interaction of concanavalin A with D-fructans. *Carbohydr. Res.* **1969**, *10*, 231
41. Goldstein, I. J.; Misaki, A., Interaction of concanavalin-A with an arabinogalactan from cell wall of *Mycobacterium-bovis*. *Journal of Bacteriology* **1970**, *103*, 422
42. Daniel, T. M.; Wisniewski, J., REACTION OF CONCAVALIN-A WITH MYCOBACTERIAL CULTURE FILTRATES. *Am. Rev. Respir. Dis.* **1970**, *101*, 762
43. Goldstein, I. J.; Reichert, C. M.; Misaki, A.; Gorin, P. A. J., EXTENSION OF CARBOHYDRATE BINDING SPECIFICITY OF CONCAVALIN-A. *Biochimica Et Biophysica Acta* **1973**, *317*, 500-504.
44. Mandal, D. K.; Kishore, N.; Brewer, C. F., Thermodynamics of lectin-carbohydrate interactions - titration microcalorimetry measurements of the binding of N-linked carbohydrates and ovalbumin to concanavalin-A. *Biochemistry* **1994**, *33*, 1149-1156.
45. Bains, G.; Lee, R. T.; Lee, Y. C.; Freire, E., Microcalorimetric study of wheat-germ-agglutinin binding to N-acetylglucosamine and its oligomers. *Biochemistry* **1992**, *31*, 12624-12628.
46. Lotan, R.; Skutelsky, E.; Danon, D.; Sharon, N., Purification, composition, and specificity of anti-T lectin from peanut (*arachis-hypogaea*). *J. Biol. Chem.* **1975**, *250*, 8518-8523.

47. Olsen, L. R.; Dessen, A.; Gupta, D.; Sabesan, S.; Sacchettini, J. C.; Brewer, C. F., X-ray crystallographic studies of unique cross-linked lattices between four isomeric biantennary oligosaccharides and soybean agglutinin. *Biochemistry* **1997**, *36*, 15073-15080.
48. Tsuji, S.; Uehori, J.; Matsumoto, M.; Suzuki, Y.; Matsuhisa, A.; Toyoshima, K.; Seya, T., Human intelectin is a novel soluble lectin that recognizes galactofuranose in carbohydrate chains of bacterial cell wall. *J. Biol. Chem.* **2001**, *276*, 23456-23463.
49. de Mol, N. J., Affinity Constants for Small Molecules from SPR Competition Experiments. In *Surface Plasmon Resonance: Methods and Protocols*, DeMol, N. J.; Fischer, M. J. E., Eds. 2010; Vol. 627, pp 101-111.
50. Tsuji, S.; Yamashita, M.; Hoffman, D. R.; Nishiyama, A.; Shinohara, T.; Ohtsu, T.; Shibata, Y., Capture of heat-killed *Mycobacterium bovis* bacillus Calmette-Guerin by intelectin-1 deposited on cell surfaces. *Glycobiology* **2009**, *19*, 518-526.
51. www.functionalglycomics.org, Accessed on August 28, 2012.
52. Sidorchuk, Z.; Zych, K.; Toukach, F. V.; Arbatsky, N. P.; Zablotti, A.; Shashkov, A. S.; Knirel, Y. A., Structure of the O-polysaccharide and classification of *Proteus mirabilis* strain G1 in *Proteus* serogroup O3. *Eur. J. Biochem.* **2002**, *269*, 1406-1412.
53. Kolodziejska, K.; Perepelov, A. V.; Zablotti, A.; Drzewiecka, D.; Senchenkova, S. N.; Zych, K.; Shashkov, A. S.; Knirel, Y. A.; Sidorchuk, Z., Structure of the glycerol phosphate-containing O-polysaccharides and

- serological studies of the lipopolysaccharides of *Proteus mirabilis* CCUG 10704 (OE) and *Proteus vulgaris* TG 103 classified into a new *Proteus* serogroup, O54. *Fems Immunology and Medical Microbiology* **2006**, *47*, 267-274.
54. Kocharova, N. A.; Maszewska, A.; Zatonsky, G. V.; Bystrova, O. V.; Ziolkowski, A.; Torzewska, A.; Shashkov, A. S.; Knirel, Y. A.; Rozalski, A., Structure of the O-polysaccharide of *Providencia alcalifaciens* O21 containing 3-formamido-3,6-dideoxy-D-galactose. *Carbohydr. Res.* **2003**, *338*, 1425-1430.
55. Kocharova, N. A.; Zatonsky, G. V.; Torzewska, A.; Macieja, Z.; Bystrova, O. V.; Shashkov, A. S.; Knirel, Y. A.; Rozalski, A., Structure of the O-specific polysaccharide of *Providencia rustigianii* O14 containing N-epsilon-(S)-1-carboxyethyl-N-alpha-(D-galacturonoyl)-L-lysine. *Carbohydr. Res.* **2003**, *338*, 1009-1016.
56. King, J. D.; Kocincova, D.; Westman, E. L.; Lam, J. S., Lipopolysaccharide biosynthesis in *Pseudomonas aeruginosa*. *Innate Immunity* **2009**, *15*, 261-312.
57. Kho, Y.; Kim, S. C.; Jiang, C.; Barma, D.; Kwon, S. W.; Cheng, J. K.; Jaunbergs, J.; Weinbaum, C.; Tamanoi, F.; Falck, J.; Zhao, Y. M., A tagging-via-substrate technology for detection and proteomics of farnesylated proteins. *Proc. Natl. Acad. Sci. U. S. A.* **2004**, *101*, 12479-12484.
58. Hermanson, G. T., *Bioconjugate Techniques*, 2nd Edition. 2008.
59. <http://web.expasy.org/protparam/>, Accessed on November 25, 2012.

5. Summary and Future Directions

5.1. Summary

My goal in this project was to study human intelectins (hIntL) and gain more detailed knowledge about their binding preferences and affinity. This would provide a better understanding about the possible role of this protein in the host innate immune system. This project is interdisciplinary; its goals were achieved using a variety of synthetic chemistry approaches as well as molecular biology techniques.

I succeeded in gaining access to a panel of oligosaccharides (**3.1–3.8**) through synthetic chemistry approaches. Compound **3.9** precursor was obtained successfully. In the design of the synthesized target oligosaccharides, I took into consideration naturally occurring molecules found in a variety of microorganisms including bacteria and fungi. Eight of the synthesized oligosaccharides (**3.1–3.8**) contain D-galactofuranose (*Galf*) in their structures while one, compound **3.9**, has an L-arabinofuranosyl moiety (**Figure 5.1**).

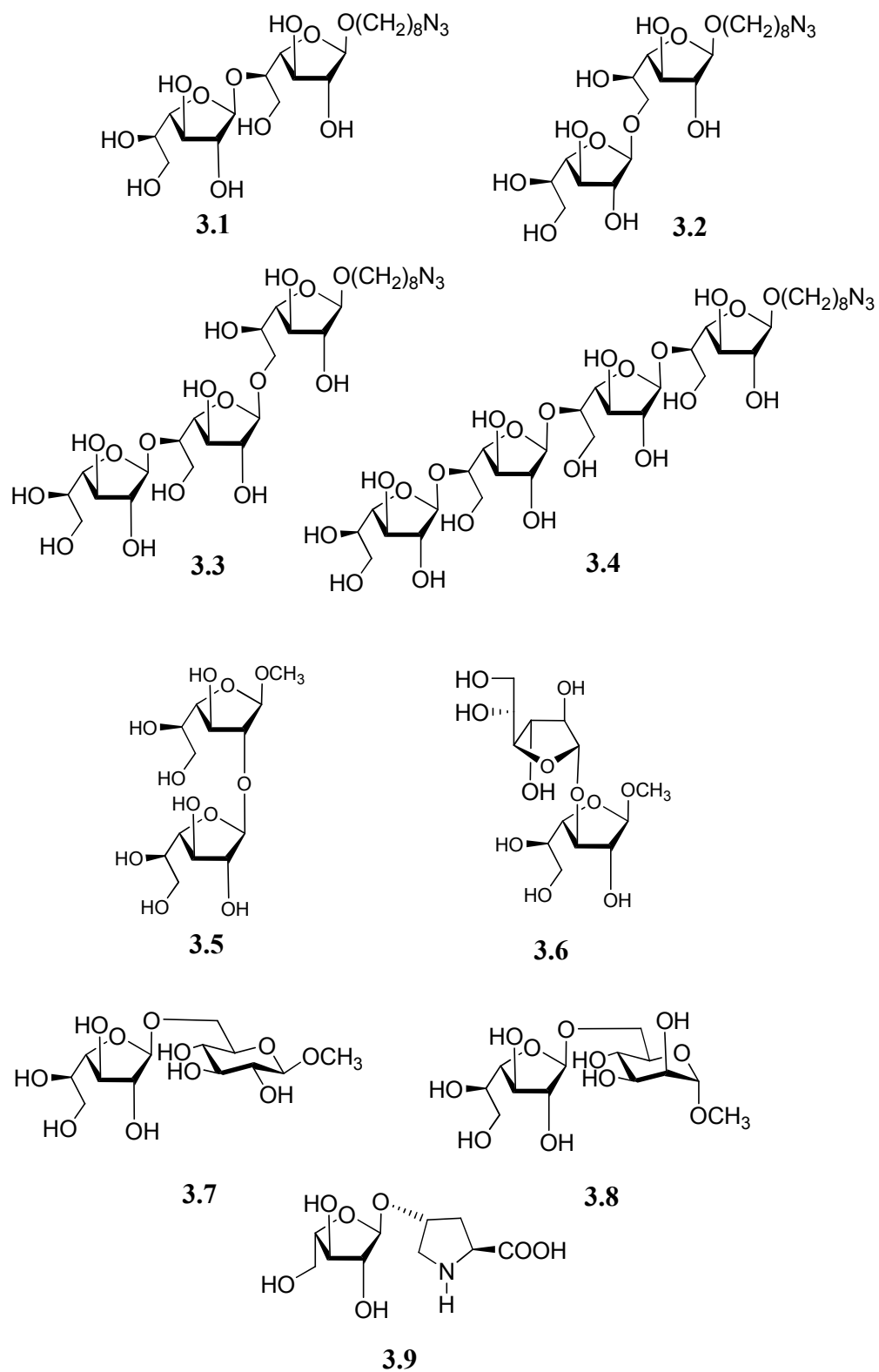


Figure 5.1: The structures of the synthesized compounds (3.1–3.9).

The main building blocks in our synthetic approach were the thioglycoside donor **3.26**, 2,3-anhydro Gal β derivative **3.54**, (Figure 5.2), as well as the azido-octyl acceptors **3.41** and **3.42**, (Figure 5.3).

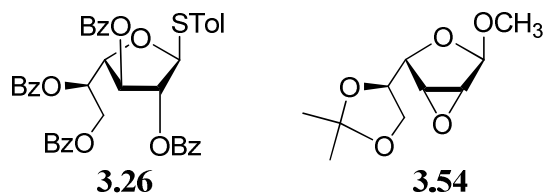


Figure 5.2: Structures of essential building blocks 3.26 and 3.54.

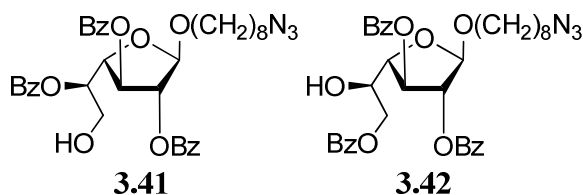


Figure 5.3: Azido-octyl acceptors 3.41 and 3.42.

The next step in achieving my project goals after having this library in hand was the recombinant expression of hIntL. This was the most challenging part in my project and took from me the longest time and effort to achieve it. The factors that contributed to the difficulty in achieving this goal arose from the intrinsic characteristics of hIntL. The protein was not easy to express and characterize due to many reasons briefly summarized here. The trimeric glycosylated structure of hIntL forced me to exclude the use of *E. coli* as a potential expression system. After several unsuccessful attempts to clone the desired gene in the pPIC9 vector, I could not use yeast (*Pachia pastoris*) as expression system for IntL and hence I decided

to search for another alternative host. Low yield and problems in protein purification were the main disadvantages of hIntL expression in HeLa cells. However, after discussions with our collaborators, I was able to repeat their success in expressing hIntL in H5V cells. Thus, H5V cells are the expression system of choice for hIntL.

Having obtained a good yield of pure and stable hIntL-1 and hIntL-2, I explored the binding preferences of the protein towards our synthesized library. SPR was the analytical technique I chose to study the binding interactions of hIntL and my carbohydrate epitopes. Staudinger ligation proved to be an effective immobilization method of the synthesized azido sugars onto the SPR chip. The C1 biosensor chip was better than the CM5 chip as it avoided the background effect caused by the presence of the dextran layer on the CM5 chip.

I was able to estimate the binding affinities (K_D) of hIntL-1 towards the immobilized sugar epitopes (**3.1**, **3.2** and **4.4**) to be higher than 10 μ M. Using competitive binding experiments IC_{50} values of both D-ribose and 2-D-deoxyribose were calculated. The main limitation I faced when I started the competitive experiments using the synthesized compounds **3.4** and **3.7** was the limited quantity of these compounds and thus inability to calculate their IC_{50} values. I was not able to study the binding activity of hIntL-2 as it did not exhibit any binding preferences towards the same derivatized chip used with hIntL-1.

Finally, fluorescent-labelling of hIntL-1 using the Cy5 dye enabled its screening against an array of LPS molecules from 48 different bacteria, in collaboration with the Consortium for Functional Glycomics (CFG). Five hits (*Proteus mirabilis* O3a, 3c, *Proteus mirabilis* O54a, *Proteus mirabilis* 54b, *Providencia alcalifaciens* O21, *Providencia rustigianni* O14 and *Pseudomonas aeruginosa* O6a, 6c) showed weak binding with hIntL-1. Interestingly, none of these LPS contain Gal β residues.

5.2. Future directions

5.2.1. Completion of the binding experiments

As discussed in the summary section, I was not able to determine the IC₅₀ of the synthesized oligosaccharides (3.4 and 3.7) due to limited quantities of material. Looking for an alternative method other than the competitive binding technique will be necessary. One of the solutions to overcome this limitation is to immobilize number of the synthesized compounds (3.3, 3.4, and 3.7) on the biosensor chips and run the binding experiment directly with hIntL instead of using the competitive method.

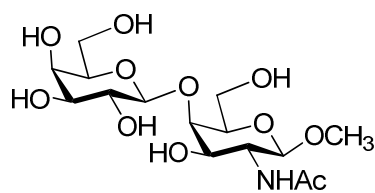
5.2.2. Studying the binding interactions using other analytical methods

Among the potential analytical methods which could be used to study the binding affinity of hIntL is isothermal titration calorimetry (ITC). ITC provides information about the thermodynamics of binding of a carbohydrate to a lectin.¹

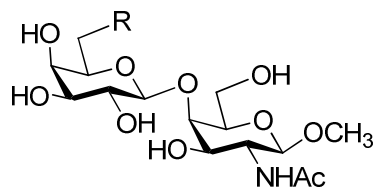
Furthermore, mass spectrometry could be another technique for measuring the thermodynamics of hIntL for the synthesized compounds (3.3–3.9). Electron spray ionization-mass spectrometry (ESI–MS) has emerged as a very useful and sensitive tool for both identifying and quantifying different carbohydrate–protein interactions.² The main advantage of this method that it requires very small amounts of both the protein and the ligand.

5.2.3. Expansion of the carbohydrate library and synthesis of more ligands

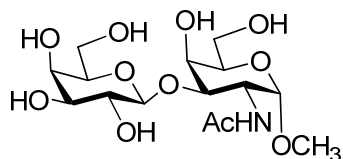
To obtain better idea about the binding preferences and specificity of hIntL, access to more ligands will be required. The design of these ligands will be guided by the results we obtained from the CFG. As discussed in Chapter 4, the screening of hIntL-1 against a CFG pathogen array showed the binding to five bacterial LPS. When examining these LPS structures, I found that they share at least one Gal p NAc motif. Therefore, designing ligands analogues to those LPS structures could be a good start. **Figure 5.4** shows the structure of the proposed ligands (5.1–5.6) to be synthesized in the future.



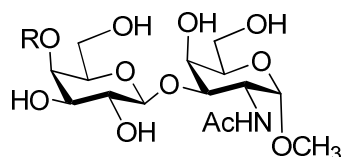
5.1



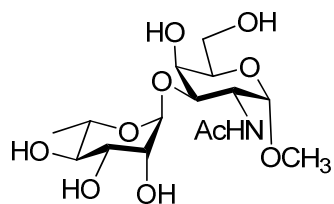
5.2, R = β -D-Galp



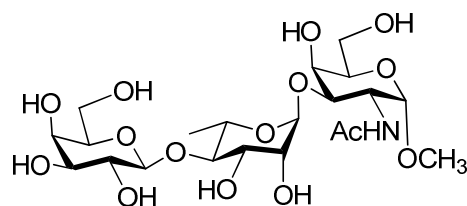
5.3



5.4, R = β -D-Galp



5.5



5.6

Figure 5.4: Structure of the proposed compounds 5.1–5.6.

5.2.4. Study structure–activity relationships (SAR) between ligands with high affinity and intelectins

Developing the SAR for these ligands could be useful in designing more ligands with higher binding affinity.³ SAR studies would start by choosing the ligands which showed highest binding affinity to hIntL and then design new ligands based on structural modification e.g. methylation at selected position. Synthesis of these designed ligands followed by testing their binding affinities towards hIntL would provide useful information about the structural features which are essential for hIntL binding.

Another potential way to study the SAR for these ligands is to obtain a crystal structure of hIntL-1 bound to one of the ligands. X-ray crystallography could provide us with detailed information about the binding site of the protein and the amino acids which are crucial for binding activity and hence we could then design more ligands with potential binding affinity.

5.2.5. Conducting *in vitro* assays with live bacteria

The results we got from screening hIntL-1 against a pathogen CFG array (as discussed in Chapter 4) could be the starting point towards running *in vitro* assays with live bacteria. One or more of the strains (*Proteus mirabilis* O3a,3c, *Proteus mirabilis* O54a, *Proteus mirabilis* 54b, *Providencia alcalifaciens* O21, *Providencia rustigianni* O14 and *Pseudomonas aeruginosa* O6a,6c) whose LPS showed binding with hIntL-1 could be obtained and subjected to *in vitro* assays in the presence of pure hIntL.

5.3. References

1. Dam, T. K.; Brewer, C. F., Multivalent protein-carbohydrate interactions: Isothermal titration microcalorimetry studies. *Energetics of Biological Macromolecules, Pt D* **2004**, *379*, 107-128.
2. El-Hawiet, A.; Kitova, E. N.; Klassen, J. S., Quantifying Carbohydrate-Protein Interactions by Electrospray Ionization Mass Spectrometry Analysis. *Biochemistry* **2012**, *51*, 4244-4253.
3. Kulkarni, S. A.; Barton-Maclaren, T. S., Performance of (Q)SAR Models for Predicting Ames Mutagenicity of Aryl Azo and Benzidine Based Compounds. *Environ Carcin Eco R* **2014**, *32*, 46-82.

6. Appendix

6.1. SPR sensograms for ConA, WGA, PNA and hIntL-1

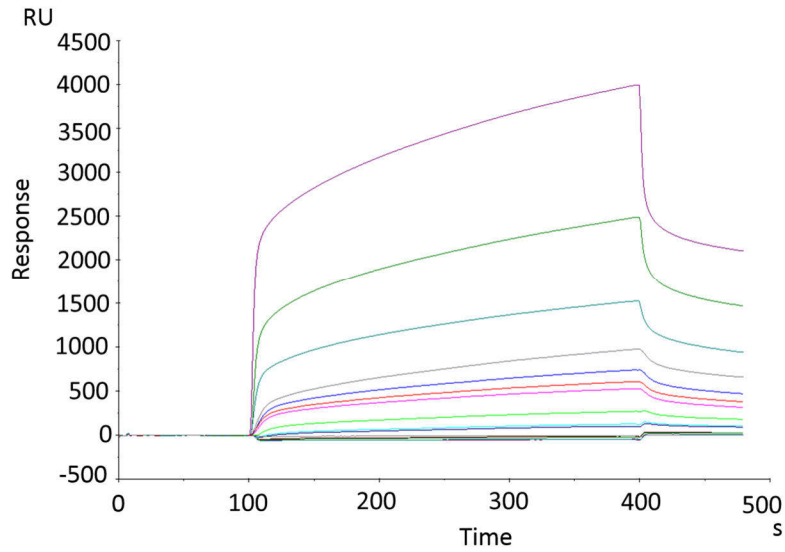


Figure 6.1: SPR sensogram of ConA (serial dilutions) injected over FC-2 of C1 carbohydrate-derivatized biosensor chip.

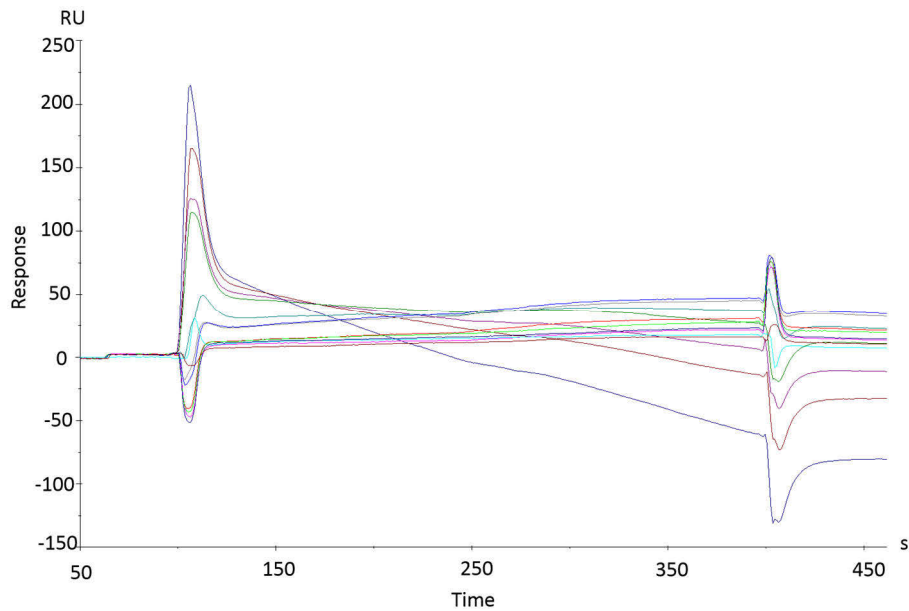


Figure 6.2: SPR sensogram of ConA after subtraction RU of FC-2 from the RU of the reference (FC-4).

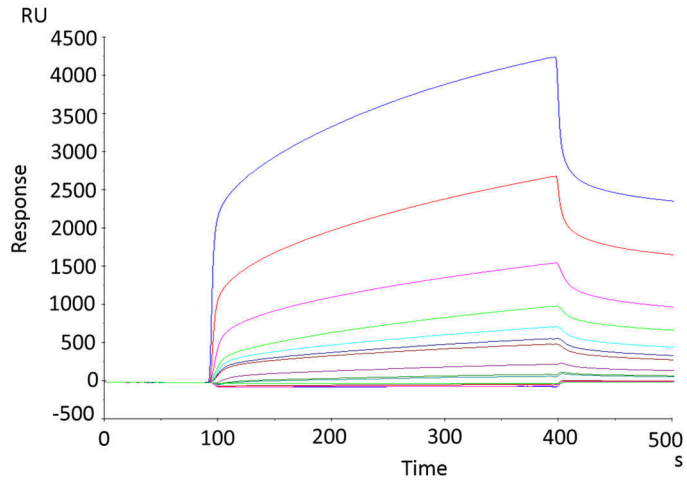


Figure 6.3: SPR sensogram of ConA (serial dilutions) injected over FC-3 of C1 carbohydrate-derivatized biosensor chip.

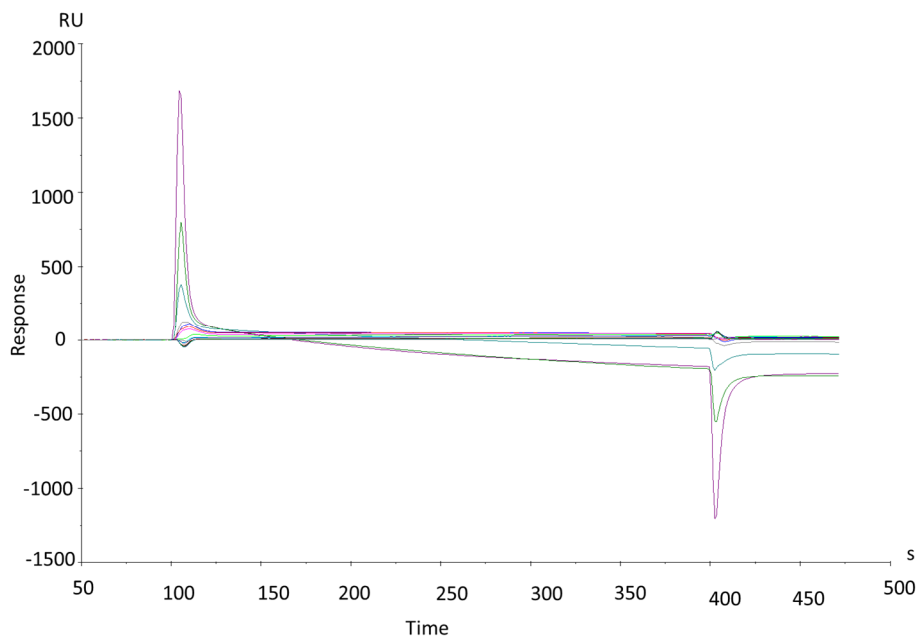


Figure 6.4: SPR sensogram of ConA after subtraction RU of FC-3 from the RU of the reference (FC-4).

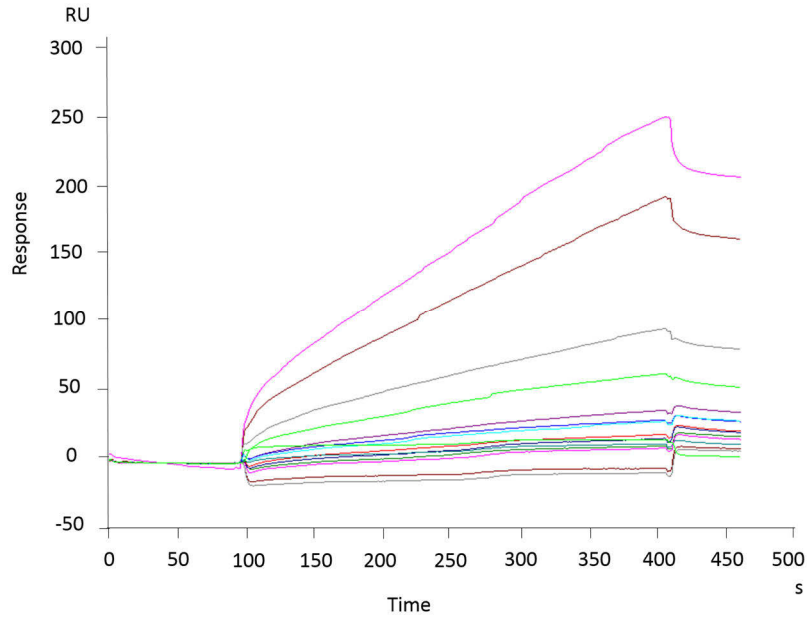


Figure 6.5: SPR sensogram of WGA (serial dilutions) injected over FC-2 of C1 carbohydrate-derivatized biosensor chip.

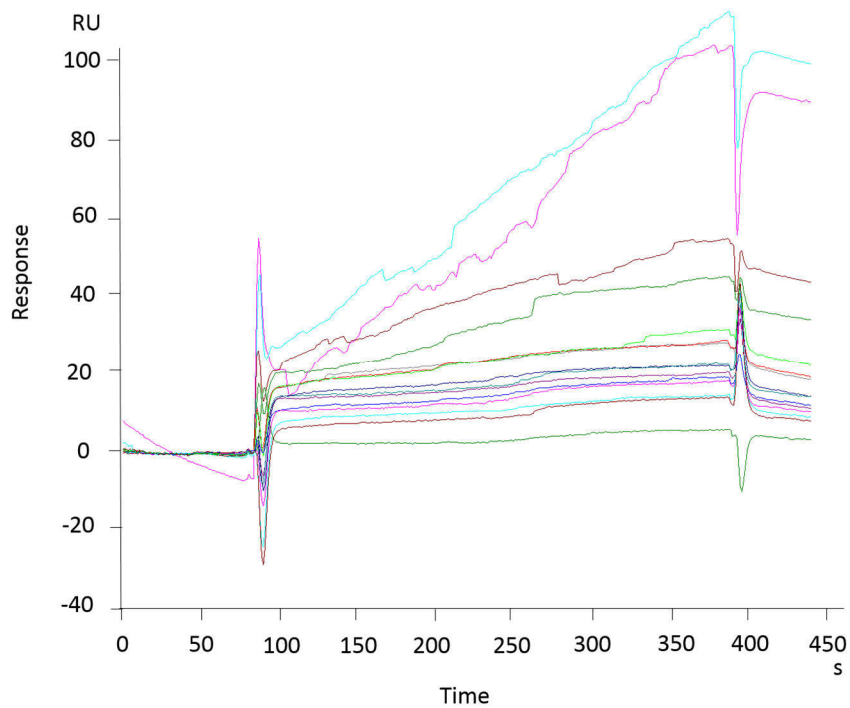


Figure 6.6: SPR sensogram of WGA after subtraction RU of FC-2 from the RU of the reference (FC-4).

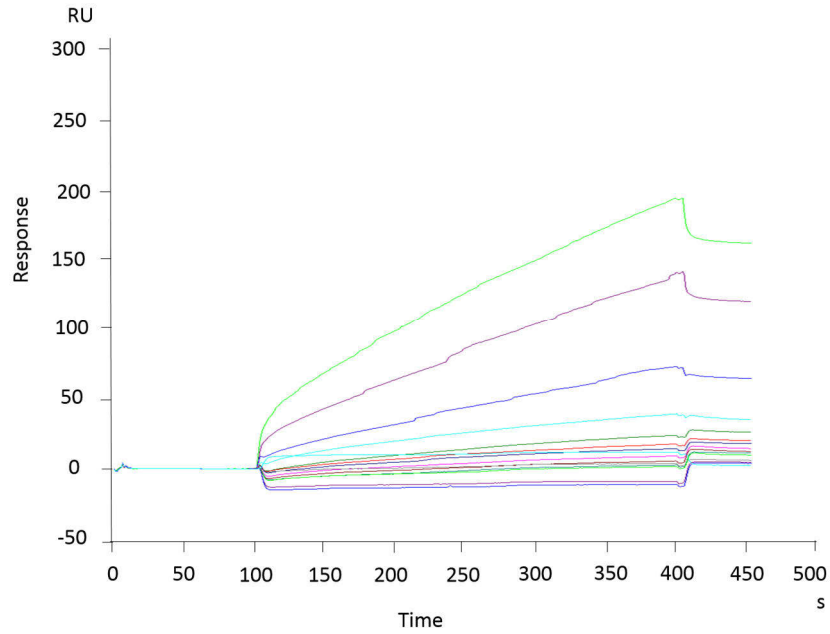


Figure 6.7: SPR sensogram of WGA (serial dilutions) injected over FC-3 of C1 carbohydrate-derivatized biosensor chip.

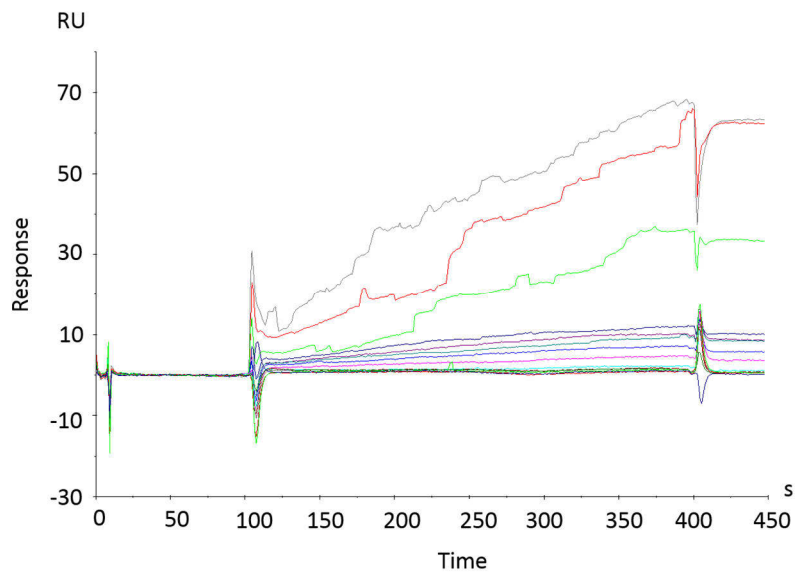


Figure 6.8: SPR sensogram of WGA after subtraction RU of FC-3 from the RU of the reference (FC-4).

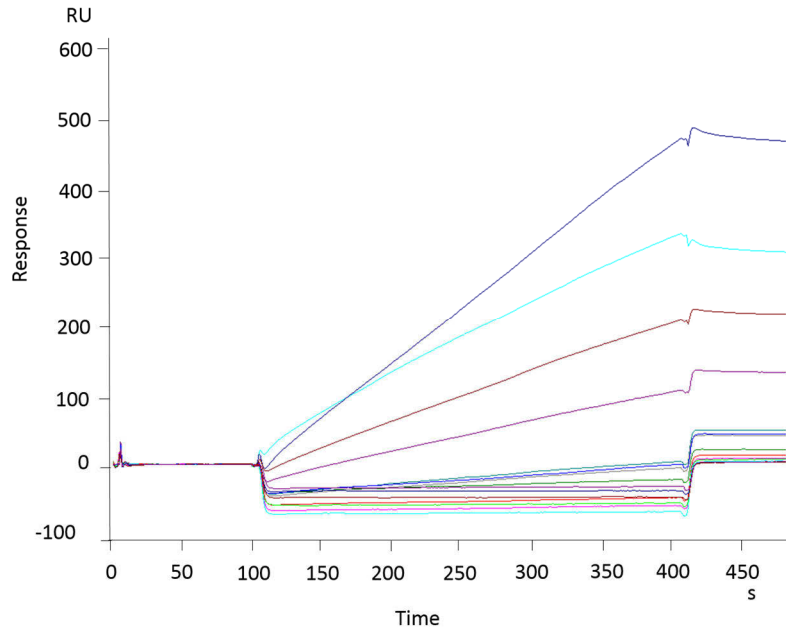


Figure 6.9: SPR sensogram of PNA (serial dilutions) injected over FC-1 of C1 carbohydrate-derivatized biosensor chip.

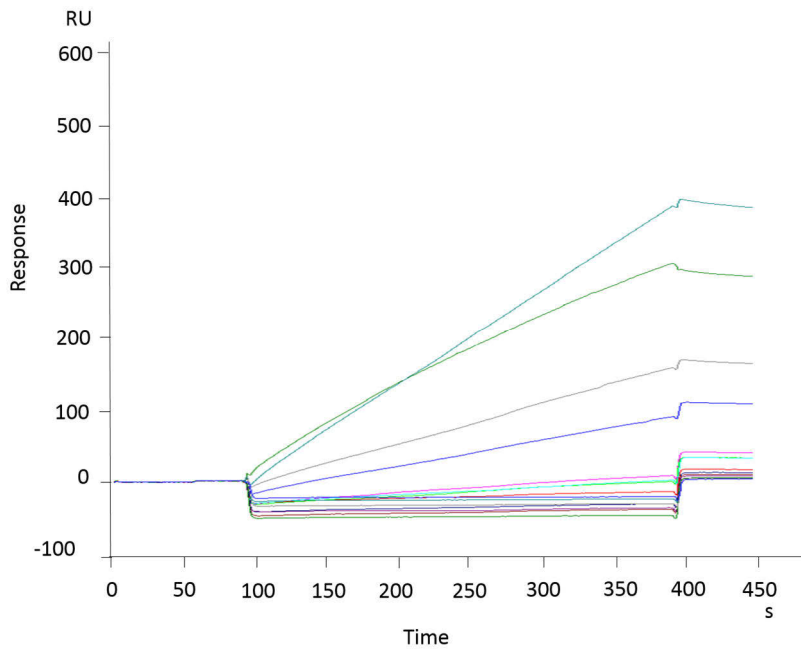


Figure 6.10: SPR sensogram of PNA (serial dilutions) injected over FC-2 of C1 carbohydrate-derivatized biosensor chip.

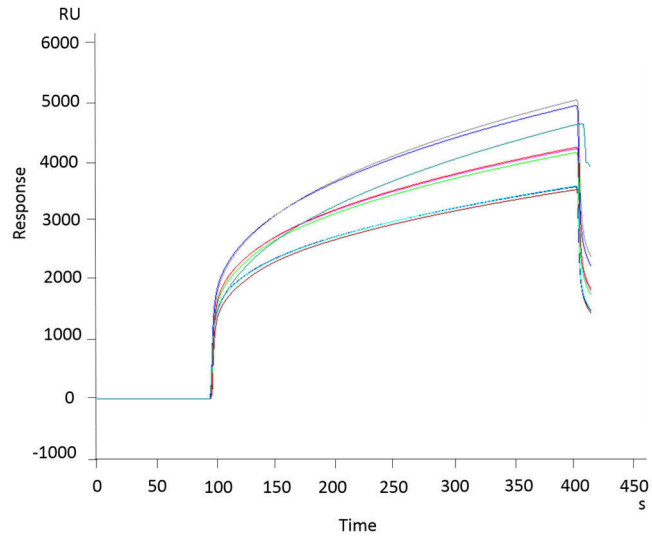


Figure 6.11: SPR sensogram of hIntL-1 (serial dilutions) injected over FC-1 of C1 carbohydrate-derivatized biosensor chip.

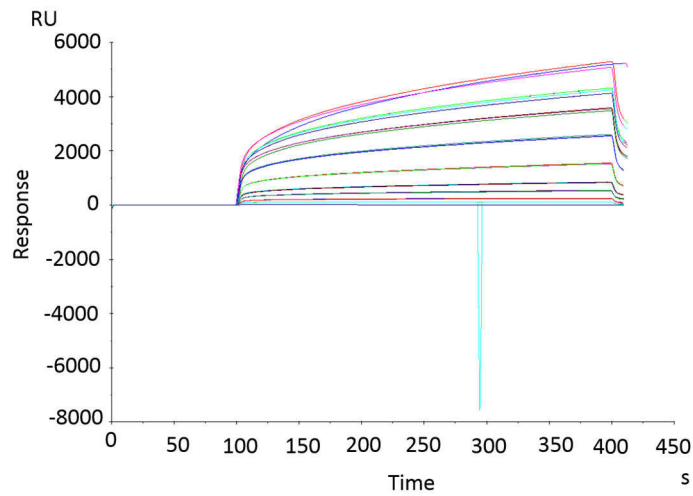


Figure 6.12: SPR sensogram of hIntL-1 (serial dilutions) injected over FC-2 of C1 carbohydrate-derivatized biosensor chip.

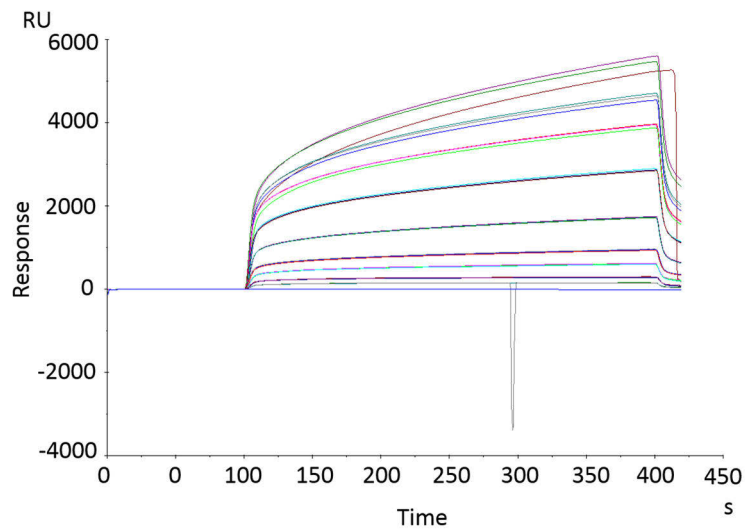


Figure 6.13: SPR sensogram of hIntL-1 (serial dilutions) injected over FC-3 of C1 carbohydrate-derivatized biosensor chip.

Bibliography

Abe, Y.; Tokuda, M.; Ishimoto, R.; Azumi, K.; Yokosawa, H., A unique primary structure, cDNA cloning and function of a galactose-specific lectin from ascidian plasma. *Eur. J. Biochem.* **1999**, 261, 33-39.

Abeygunawardana, C.; Bush, C. A.; Cisar, J. O., Complete structure of the cell surface polysaccharide of *Streptococcus oralis*-C104 - a 600-MHz NMR-study. *Biochemistry* **1991**, 30, 8568-8577.

Ahmad, M.; Hirz, M.; Pichler, H.; Schwab, H., Protein expression in *Pichia pastoris*: recent achievements and perspectives for heterologous protein production. *Appl. Microbiol. Biotechnol.* **2014**, 98, 5301-5317.

Ahrazem, O.; Prieto, A.; Leal, J. A.; Jimenez-Barbero, J.; Bernabe, M., Fungal cell wall galactomannan isolated from *Apodus deciduus*. *Carbohydr. Res.* **2002**, 337, 1503-1506.

Arasappan, A.; Fraserreid, B., N-pentenyl furanosides - synthesis and glycosidation reactions of some galacto derivatives. *Tetrahedron Lett.* **1995**, 36, 7967-7970.

Arranz-Plaza, E.; Tracy, A. S.; Siriwardena, A.; Pierce, J. M.; Boons, G. J., High-avidity, low-affinity multivalent interactions and the block to polyspermy in *Xenopus laevis*. *J. Am. Chem. Soc.* **2002**, 124, 13035-13046.

Bai, Y.; Lowary, T. L., 2,3-Anhydrosugars in glycoside bond synthesis. Application to alpha-D-galactofuranosides. *J. Org. Chem.* **2006**, 71, 9658-9671.

Banchereau, J.; Briere, F.; Caux, C.; Davoust, J.; Lebecque, S.; Liu, Y.-J.; Pulendran, B.; Palucka, K., Immunobiology of dendritic cells. In *Annu. Rev.*

Immunol., Paul, W. E.; Fathman, C. G.; Glimcher, L. H., Eds. **2000**; Vol. 18, pp 767-811.

Baneyx, F., Recombinant protein expression in *Escherichia coli*. *Curr. Opin. Biotech.* **1999**, 10, 411-421.

Barretobergter, E. M.; Travassos, L. R., Chemical-structure of the D-galacto-D-mannan component from hyphae of *Aspergillus niger* and other *Aspergillus* spp. *Carbohydr. Res.* **1980**, 86, 273-285.

Barretobergter, E.; Gorin, P. A. J.; Travassos, L. R., Cell constituents of mycelia and conidia of *Aspergillus fumigatus*. *Carbohydr. Res.* **1981**, 95, 205-217.

Batista, C. M. d. S.; Yang, R.-Z.; Lee, M.-J.; Glynn, N. M.; Yu, D.-Z.; Pray, J.; Ndubuizu, K.; Patil, S.; Schwartz, A.; Kligman, M.; Fried, S. K.; Gong, D.-W.; Shuldiner, A. R.; Pollin, T. I.; McLenithan, J. C., Omentin plasma levels and gene expression are decreased in obesity. *Diabetes* **2007**, 56, 1655-1661.

Bayne, C. J.; Gerwick, L.; Fujiki, K.; Nakao, M.; Yano, T., Immune-relevant (including acute phase) genes identified in the livers of rainbow trout, *Oncorhynchus mykiss*, by means of suppression subtractive hybridization. *Dev. Comp. Immunol.* **2001**, 25, 205-217.

Berlec, A.; Strukelj, B., Current state and recent advances in biopharmaceutical production in *Escherichia coli*, yeasts and mammalian cells. *J. Ind. Microbiology & Biotechnology* **2013**, 40, 257-274.

Bernabe, M.; Ahrazem, O.; Prieto, A.; Leal, J. A., Evolution of fungal polysaccharides F1SS and proposal of their utilisation as antigens for rapid

detection of fungal contaminants. *Electronic Journal of Environmental, Agricultural and Food Chemistry* **2002**, 1, 1-3.

Besra, G. S.; Khoo, K. H.; McNeil, M. R.; Dell, A.; Morris, H. R.; Brennan, P. J., A new interpretation of the structure of the mycolyl arabinogalactan complex of *Mycobacterium tuberculosis* as revealed through characterization of oligoglycosylalditol fragments by fast-atom-bombardment mass-spectrometry and H1 nuclear magnetic resonance spectroscopy. *Biochemistry* **1995**, 34, 4257-4266.

Bill, R. M., Yeast - a panacea for the structure-function analysis of membrane proteins? *Current Genetics* **2001**, 40, 157-171.

Bloom, B. R.; Murray, C. J. L., Tuberculosis - commentary on a reemergent killer. *Science* **1992**, 257, 1055-1064.

Bornstein, P.; Sage, E. H., Matricellular proteins: extracellular modulators of cell function. *Curr. Opin. Cell Biol.* **2002**, 14, 608-616.

Braccia, A.; Villani, M.; Immerdal, L.; Niels-Christiansen, L. L.; Nystrom, B. T.; Hansen, G. H.; Danielsen, E. M., Microvillar membrane Microdomains exist at physiological temperature - Role of galectin-4 as lipid raft stabilizer revealed by "superrafts". *J. Biol. Chem.* **2003**, 278, 15679-15684.

Brennan, P. J.; Nikaido, H., The envelope of *Mycobacteria*. *Annu. Rev. Biochem.* **1995**, 64, 29-63.

Brewer, C. F., Binding and cross-linking properties of galectins. *BBA-Gen. Subjects* **2002**, 1572, 255-262.

Brock, J. H., The physiology of lactoferrin. *Biochem. Cell Biol.* **2002**, 80, 1-6.

Brock, J., Lactoferrin - a multifunctional immunoregulatory protein. *Immunol. Today* **1995**, 16, 417-419.

Calixto, R.; Mattos, B.; Bittencourt, V.; Lopes, L.; Souza, L.; Sasaki, G.; Cipriani, T.; Silva, M.; Barreto-Bergter, E., beta-Galactofuranose-containing structures present in the cell wall of the saprophytic fungus *Cladosporium (Hormoconis) resinae*. *Res. Microbiol.* **2010**, 161, 720-728.

Cao, R. H.; Farnebo, J.; Kurimoto, M.; Cao, Y. H., Interleukin-18 acts as an angiogenesis and tumor suppressor. *FASEB J.* **1999**, 13, 2195-2202.

Carolan, B. J.; Harvey, B. G.; De, B. P.; Vanni, H.; Crystal, R. G., Decreased expression of intelectin 1 in the human airway epithelium of smokers compared to nonsmokers. *J. Immunol.* **2008**, 181, 5760-5767.

Cereghino, G. P. L.; Cereghino, J. L.; Ilgen, C.; Cregg, J. M., Production of recombinant proteins in fermenter cultures of the yeast *Pichia pastoris*. *Current Opinion in Biotechnology* **2002**, 13, 329-332.

Cereghino, G. P. L.; Cereghino, J. L.; Sunga, A. J.; Johnson, M. A.; Lim, M.; Gleeson, M. A. G.; Cregg, J. M., New selectable marker/auxotrophic host strain combinations for molecular genetic manipulation of *Pichia pastoris*. *Gene* **2001**, 263, 159-169.

Cereghino, J. L.; Cregg, J. M., Heterologous protein expression in the methylotrophic yeast *Pichia pastoris*. *Fems Microbiology Reviews* **2000**, 24, 45-66.

Cerliani, J. P.; Stowell, S. R.; Mascanfroni, I. D.; Arthur, C. M.; Cummings, R. D.; Rabinovich, G. A., Expanding the Universe of Cytokines and Pattern Recognition

Receptors: Galectins and Glycans in Innate Immunity. *J. Clin. Immunol.* **2011**, 31, 10-21.

Chadd, H. E.; Chamow, S. M., Therapeutic antibody expression technology. *Current Opinion in Biotechnology* **2001**, 12, 188-194.

Chiodo, F.; Marradi, M.; Park, J.; Ram, A. F. J.; Penades, S.; van Die, I.; Tefsen, B., Galactofuranose-Coated Gold Nanoparticles Elicit a Pro-inflammatory Response in Human Monocyte-Derived Dendritic Cells and Are Recognized by DC-SIGN. *ACS Chem. Biol.* **2014**, 9, 383-389.

Chu, L.; Robinson, D. K., Industrial choices for protein production by large-scale cell culture. *Current Opinion in Biotechnology* **2001**, 12, 180-187.

Clarke, B. R.; Bronner, D.; Keenleyside, W. J.; Severn, W. B.; Richards, J. C.; Whitfield, C., Role of RFE and RFBF in the initiation of biosynthesis of D-galactan-I, the lipopolysaccharide O-antigen from *Klebsiella pneumoniae* serotype-O1. *J. Bacteriol.* **1995**, 177, 5411-5418.

Codee, J. D. C.; Litjens, R.; den Heeten, R.; Overkleeft, H. S.; van Boom, J. H.; van der Marel, G. A., Ph2SO/Tf2O: a powerful promotor system in chemoselective glycosylations using thioglycosides. *Org. Lett.* **2003**, 5, 1519-1522.

Completo, G. C.; Lowary, T. L., Synthesis of galactofuranose-containing acceptor substrates for mycobacterial galactofuranosyltransferases. *J. Org. Chem.* **2008**, 73, 4513-4525.

Cooper, D. N. W., Galectinomics: finding themes in complexity. *BBA-Gen. Subjects* **2002**, 1572, 209-231.

Crich, D.; Smith, M., 1-Benzenesulfinyl piperidine/trifluoromethanesulfonic anhydride: A potent combination of shelf-stable reagents for the low-temperature conversion of thioglycosides to glycosyl triflates and for the formation of diverse glycosidic linkages. *J. Am. Chem. Soc.* **2001**, 123, 9015-9020.

Daccorso, N. B.; Thiel, I. M. E.; Schuller, M., Proton and C13 nuclear magnetic resonance spectra of some benzoylated aldohexoses. *Carbohydr. Res.* **1983**, 124, 177-184.

Daffe, M.; McNeil, M.; Brennan, P. J., Major structural features of the cell-wall arabinogalactans of Mycobacterium, Rhodococcus, and Nocardia spp. *Carbohydr. Res.* **1993**, 249, 383-398.

Dam, T. K.; Brewer, C. F., Multivalent protein-carbohydrate interactions: Isothermal titration microcalorimetry studies. *Energetics of Biological Macromolecules, Pt D* **2004**, 379, 107-128.

Dann, S. M.; Eckmann, L., Innate immune defenses in the intestinal tract. *Curr. Opin. Gastroen.* **2007**, 23, 115-120.

Darville, L. N. F.; Merchant, M. E.; Maccha, V.; Siddavarapu, V. R.; Hasan, A.; Murray, K. K., Isolation and determination of the primary structure of a lectin protein from the serum of the American alligator (*Alligator mississippiensis*). *Comp. Biochem. Phys. B* **2012**, 161, 161-169.

Dashti, Y.; Grkovic, T.; Quinn, R. J., Predicting natural product value, an exploration of anti-TB drug space. *Nat. Prod. Rep.* **2014**, 31.

Datta, R.; deSchoolmeester, M. L.; Hedeler, C.; Paton, N. W.; Brass, A. M.; Else, K. J., Identification of novel genes in intestinal tissue that are regulated after infection with an intestinal nematode parasite. *Infect. Immun.* **2005**, *73*, 4025-4033.

Dawson, H.; Andre, S.; Karamitopoulou, E.; Zlobec, I.; Gabius, H.-J., The Growing Galectin Network in Colon Cancer and Clinical Relevance of Cytoplasmic Galectin-3 Reactivity. *Anticancer Res.* **2013**, *33*, 3053-3059.

de Jong, L. A. A.; Grunewald, S.; Franke, J. P.; Uges, D. R. A.; Bischoff, R., Purification and characterization of the recombinant human dopamine D2S receptor from *Pichia pastoris*. *Protein Expression and Purification* **2004**, *33*, 176-184.

Delederkremer, R. M.; Colli, W., Galactofuranose-containing glycoconjugates in trypanosomatids. *Glycobiology* **1995**, *5*, 547-552.

Demain, A. L., Small bugs, big business: The economic power of the microbe. *Biotechnology Advances* **2000**, *18*, 499-514.

Demetter, P.; Nagy, N.; Martin, B.; Mathieu, A.; Dumont, P.; Decaestecker, C.; Salmon, I., The galectin family and digestive disease. *J. Pathol.* **2008**, *215*, 1-12.

Ding, X. L.; Wang, W.; Kong, F. Z., Detritylation of mono- and di-saccharide derivatives using ferric chloride hydrate. *Carbohydr. Res.* **1997**, *303*, 445-448.

Dube, D. H.; Bertozzi, C. R., Glycans in cancer and inflammation. Potential for therapeutics and diagnostics. *Nat. Rev. Drug Discov.* **2005**, *4*, 477-488.

Duthie, M. S.; Raychaudhuri, R.; Tutterrow, Y. L.; Misquith, A.; Bowman, J.; Casey, A.; Balagon, M. F.; Maghanoy, A.; Beltran-Alzate, J. C.; Romero-Alzate, M.; Cardona-Castro, N.; Reed, S. G., A rapid ELISA for the diagnosis of MB

leprosy based on complementary detection of antibodies against a novel protein-glycolipid conjugate. *Diagn. Micr. Infec. Dis.* **2014**, 79, 233-239.

Dwek, R. A., Glycobiology: Toward understanding the function of sugars. *Chem. Rev.* **1996**, 96, 683-720.

El-Hawiet, A.; Kitova, E. N.; Klassen, J. S., Quantifying Carbohydrate-Protein Interactions by Electrospray Ionization Mass Spectrometry Analysis. *Biochemistry* **2012**, 51, 4244-4253.

Elola, M. T.; Wolfenstein-Todel, C.; Troncoso, M. F.; Vasta, G. R.; Rabinovich, G. A., Galectins: matricellular glycan-binding proteins linking cell adhesion, migration, and survival. *Cell Mol. Life Sci.* **2007**, 64, 1679-1700.

Endo, Y.; Takahashi, M.; Fujita, T., Lectin complement system and pattern recognition. *Immunobiology* **2006**, 211, 283-293.

Esmurziev, A. M.; Simic, N.; Hoff, B. H.; Sundby, E., Synthesis and Structure Elucidation of Benzoylated Deoxyfluoropyranosides. *J. Carbohydr. Chem.* **2010**, 29, 348-367.

Feinberg, H.; Mitchell, D. A.; Drickamer, K.; Weis, W. I., Structural basis for selective recognition of oligosaccharides by DC-SIGN and DC-SIGNR. *Science* **2001**, 294, 2163-2166.

Ferrieres, V.; Bertho, J. N.; Plusquellec, D., A convenient synthesis of alkyl D-glycofuranosiduronic acids and alkyl D-glycofuranosides from unprotected carbohydrates. *Carbohydr. Res.* **1998**, 311, 25-35.

Figdor, C. G.; van Kooyk, Y.; Adema, G. J., C-type lectin receptors on dendritic cells and Langerhans cells (vol 2, pg 77, 2002). *Nat. Rev. Immunol.* **2002**, 2, 377-377.

Fischer, E., The structure of both methyl-glucosides and a third methyl-glucoside. *Ber. Dtsch. Chem. Ges.* **1914**, 47, 1980-1989.

Freigassner, M.; Pichler, H.; Glieder, A., Tuning microbial hosts for membrane protein production. *Microbial Cell Factories* **2009**, 8.

French, A. T.; Bethune, J. A.; Knight, P. A.; McNeilly, T. N.; Wattedgedera, S.; Rhind, S.; Miller, H. R. P.; Pemberton, A. D., The expression of intelectin in sheep goblet cells and upregulation by interleukin-4. *Vet. Immunol. Immunop.* **2007**, 120, 41-46.

French, A. T.; Knight, P. A.; Smith, W. D.; Brown, J. K.; Craig, N. M.; Pate, J. A.; Miller, H. R. P.; Pemberton, A. D., Up-regulation of intelectin in sheep after infection with *Teladorsagia circumcincta*. *Int. J. Parasitol.* **2008**, 38, 467-475.

French, A. T.; Knight, P. A.; Smith, W. D.; Pate, J. A.; Miller, H. R. P.; Pemberton, A. D., Expression of three intelectins in sheep and response to a Th2 environment. *Vet. Res.* **2009**, 40.

Fujita, T.; Matsushita, M.; Endo, Y., The lectin-complement pathway - its role in innate immunity and evolution. *Immunol. Rev.* **2004**, 198, 185-202.

Geijtenbeek, T. B. H.; Kwon, D. S.; Torensma, R.; van Vliet, S. J.; van Duijnhoven, G. C. F.; Middel, J.; Cornelissen, I.; Nottet, H.; KewalRamani, V. N.; Littman, D. R.; Figdor, C. G.; van Kooyk, Y., DC-SIGN, a dendritic cell-specific HIV-1-binding protein that enhances trans-infection of T cells. *Cell* **2000**, 100, 587-597.

Geijtenbeek, T. B. H.; Torensma, R.; van Vliet, S. J.; van Duijnhoven, G. C. F.; Adema, G. J.; van Kooyk, Y.; Figdor, C. G., Identification of DC-SIGN, a novel dendritic cell-specific ICAM-3 receptor that supports primary immune responses. *Cell* **2000**, 100, 575-585.

Gelperin, D. M.; White, M. A.; Wilkinson, M. L.; Kon, Y.; Kung, L. A.; Wise, K. J.; Lopez-Hoyo, N.; Jiang, L. X.; Piccirillo, S.; Yu, H. Y.; Gerstein, M.; Dumont, M. E.; Phizicky, E. M.; Snyder, M.; Grayhack, E. J., Biochemical and genetic analysis of the yeast proteome with a movable ORF collection. *Genes & Development* **2005**, 19, 2816-2826.

Goodman, M., MARKET WATCH Sales of biologics to show robust growth through to 2013. *Nature Reviews Drug Discovery* **2009**, 8, 837-837.

Green, J. W., The glycofuranosides. *Adv. Carbohydr. Chem. Biochem.* **1966**, 21, 95-142.

Green, J. W.; Pacsu, E., Glycofuranosides and thioglycofuranosides. I. A method of preparation and its application to galactose and glucose. *J. Am. Chem. Soc.* **1937**, 59, 1205-1210.

Gringhuis, S. I.; van der Vlist, M.; van den Berg, L. M.; den Dunnen, J.; Litjens, M.; Geijtenbeek, T. B. H., HIV-1 exploits innate signaling by TLR8 and DC-SIGN for productive infection of dendritic cells. *Nat. Immunol.* **2010**, 11, 419-U81.

Gu, N. B.; Kang, G. N.; Jin, C. E.; Xu, Y. J.; Zhang, Z. X.; Erle, D. J.; Zhen, G. H., Intelectin is required for IL-13-induced monocyte chemotactic protein-1 and-3 expression in lung epithelial cells and promotes allergic airway inflammation. *Am. J. Physiol-Lung C.* 2010, 298, L290-L296.

Guo, Y.; Feinberg, H.; Conroy, E.; Mitchell, D. A.; Alvarez, R.; Blixt, O.; Taylor, M. E.; Weis, W. I.; Drickamer, K., Structural basis for distinct ligand-binding and targeting properties of the receptors DC-SIGN and DC-SIGNR. *Nat. Struct. Mol. Biol.* **2004**, 11, 591-598.

Hansen, G. H.; Niels-Christiansen, L. L.; Immerdal, L.; Danielsen, E. M., Antibodies in the small intestine: mucosal synthesis and deposition of anti-glycosyl IgA, IgM, and IgG in the enterocyte brush border. *Am. J. Physiol-Gastr. L.* **2006**, 291, G82-G90.

Haworth, W. N.; Porter, C. R., Isolation of crystalline alpha- and beta-ethylglucofuranosides (gamma-ethylglucosides) and other crystalline derivatives of glucofuranose. *J. Chem. Soc.* **1929**, 2796-2806.

He, J. L.; Furmanski, P., Sequence specificity and transcriptional activation in the binding of lactoferrin to DNA. *Nature* **1995**, 373, 721-724.

Hernandez, J. D.; Baum, L. G., Ah, sweet mystery of death! Galectins and control of cell fate. *Glycobiology* **2002**, 12, 127R-136R.

Higgins, D. R.; Cregg, J. M., Introduction to *Pichia pastoris*. In *Methods in Molecular Biology*; Pichia protocols, Higgins, D. R.; Cregg, J. M., Eds. **1998**; Vol. 103, pp 1-15.

Himly, M.; Jahn-Schmid, B.; Dedic, A.; Kelemen, P.; Wopfner, N.; Altmann, F.; van Ree, R.; Briza, P.; Richter, K.; Ebner, C.; Ferreira, F., Art v 1, the major allergen of mugwort pollen, is a modular glycoprotein with a defensin-like and a hydroxyproline-rich domain. *FASEB J.* **2003**, 17, 106-107.

Hirabayashi, J.; Kasai, K., The family of metazoan metal-independent beta galactoside binding lectins - structure, function and molecular evolution. *Glycobiology* **1993**, 3, 297-304.

Hirsch, C.; Blom, D.; Ploegh, H. L., A role for N-glycanase in the cytosolic turnover of glycoproteins. *EMBO J.* **2003**, 22, 1036-1046.

Holeman, A.; Seeberger, P. H., Carbohydrate diversity: synthesis of glycoconjugates and complex carbohydrates. *Curr. Opin. Biotech.* **2004**, 15, 615-622.

Holmskov, U.; Malhotra, R.; Sim, R. B.; Jensenius, J. C., Collectins - collagenous C-type lectins of the innate immune defense system. *Immunol. Today* **1994**, 15, 67-74.

http://tools.lifetechnologies.com/content/sfs/manuals/pich_man.pdf, Accessed on October 5, 2011.

<http://www.bio-rad.com/>, Accessed on April 5, 2014.

<http://www.piercenet.com/instructions/>, Accessed on April 28, 2014.

<http://www.thermoscientificbio.com/>, Accessed on May 10, 2014.

<http://www.thermoscientificbio.com/fermentas/>, Accessed on April 7, 2014.

Iigo, M.; Kuhara, T.; Ushida, Y.; Sekine, K.; Moore, M. A.; Tsuda, H., Inhibitory effects of bovine lactoferrin on colon carcinoma 26 lung metastasis in mice. *Clin. Exp. Metastas.* **1999**, 17, 35-40.

Imamura, A.; Lowary, T., Chemical Synthesis of Furanose Glycosides. *Trends Glycosci. Glyc.* **2011**, 23, 134-152.

Inoue, K.; Korenaga, H.; Tanaka, N. G.; Sakamoto, N.; Kadoya, S., The sulfated polysaccharide-peptidoglycan complex potently inhibits embryonic angiogenesis and tumor growth in the presence of cortisone acetate. *Carbohydr. Res.* **1988**, 181, 135-142.

Izumi, S.; Hirai, O.; Hayashi, K.; Konishi, Y.; Okuhara, M.; Kohsaka, M.; Aoki, H.; Yamamura, Y., Induction of a tumor necrosis factor-like activity by *Nocardia rubra* cell-wall skeleton. *Cancer Res.* **1987**, 47, 1785-1792.

Jahn-Schmid, B.; Fischer, G. F.; Bohle, B.; Fae, I.; Gadermaier, G.; Dedic, A.; Ferreira, F.; Ebner, C., Antigen presentation of the immunodominant T-cell epitope of the major mugwort pollen allergen, Art v 1, is associated with the expression of HLA-DRB1*01. *J. Allergy Clin. Immun.* **2005**, 115, 399-404.

Jann, B.; Shashkov, A. A.; Kochanowski, H.; Jann, K., Structural comparison of the O6 specific polysaccharides from *Escherichia coli* O6-K2-H1, *Escherichia coli* O6-K13-H1, and *Escherichia coli* O6-K54-H10. *Carbohydr. Res.* **1994**, 263, 217-225.

Jones, C.; Todeschini, A. R.; Agrellos, O. A.; Previato, J. O.; Mendonca-Previato, L., Heterogeneity in the biosynthesis of mucin O-glycans from *Trypanosoma cruzi* Tulahuen strain with the expression of novel galactofuranosyl-containing oligosaccharides. *Biochemistry* **2004**, 43, 11889-11897.

Kang, Y.; Lou, C.; Ahmed, K. B. R.; Huang, P.; Jin, Z., Synthesis of biotinylated OSW-1. *Bioorg. Med. Chem. Lett.* **2009**, 19, 5166-5168.

Kartha, K. P. R.; Aloui, M.; Field, R. A., Iodine: A versatile reagent in carbohydrate chemistry .2. Efficient chemospecific activation of thiomethylglycosides. *Tetrahedron Lett.* **1996**, 37, 5175-5178.

Kasamatsu, A.; Uzawa, K.; Nakashima, D.; Koike, H.; Shiiba, M.; Bukawa, H.; Yokoe, H.; Tanzawa, H., Galectin-9 as a regulator of cellular adhesion in human oral squamous cell carcinoma cell lines. *Int. J. Mol. Med.* **2005**, 16, 269-273.

Kerr, S. C.; Carrington, S. D.; Oscarson, S.; Gallagher, M. E.; Solon, M.; Yuan, S.; Ahn, J. N.; Dougherty, R. H.; Finkbeiner, W. E.; Peters, M. C.; Fahy, J. V., Intelectin-1 Is a Prominent Protein Constituent of Pathologic Mucus Associated with Eosinophilic Airway Inflammation in Asthma. *Am. J. Respir. Crit. Care Med.* **2014**, 189, 1005-1007.

Kilpatrick, D. C.; Fujita, T.; Matsushita, M., P35, an opsonic lectin of the ficolin family, in human blood from neonates, normal adults, and recurrent miscarriage patients. *Immunol. Lett.* **1999**, 67, 109-112.

Klotz, W.; Schmidt, R. R., Anomeric O-alkylation, .11. Anomeric O-alkylation of O-unprotected hexoses and pentoses - convenient synthesis of decyl, benzyl, and allyl glycosides. *Liebigs Ann. Chem.* **1993**, 683-690.

Knappskog, S.; Ravneberg, H.; Gjerdrum, C.; Trosse, C.; Stern, B.; Pryme, I. F., The level of synthesis and secretion of *Gaussia princeps* luciferase in transfected CHO cells is heavily dependent on the choice of signal peptide. *Journal of Biotechnology* **2007**, 128, 705-715.

Kohn, P.; Samarita, R.; Lerner, L. M., A new method for synthesis of furanose derivatives of aldohexoses. *J. Am. Chem. Soc.* **1965**, 87, 5475-&.

Kol, O.; Wieruszeski, J. M.; Strecker, G.; Montreuil, J.; Fournet, B.; Zalisz, R.; Smets, P., Structure of the O-specific polysaccharide chain from *Klebsiella pneumoniae* O1K2 (NCTC-5055) lipopolysaccharide. *Carbohydr. Res.* **1991**, 217, 117-125.

Komachi, Y.; Hatakeyama, S.; Motomatsu, H.; Futagami, T.; Kizjakina, K.; Sobrado, P.; Ekino, K.; Takegawa, K.; Goto, M.; Nomura, Y.; Oka, T., gfsA encodes a novel galactofuranosyltransferase involved in biosynthesis of galactofuranose antigen of O-glycan in *Aspergillus nidulans* and *Aspergillus fumigatus*. *Mol. Microbiol.* **2013**, 90, 1054-1073.

Komiotis, D.; Agelis, G.; Manta, S.; Tzioumaki, N.; Tsoukala, E.; Antonakis, K., A facile, one-step conversion of 6-O-trityl and 6-O-TBDMS monosaccharides into the corresponding formate esters. *J. Carbohydr. Chem.* **2006**, 25, 441-450.

Komiya, T.; Tanigawa, Y.; Hirohashi, S., Cloning of the novel gene intelectin, which is expressed in intestinal paneth cells in mice. *Biochem. Biophys. Res. Commun.* **1998**, 251, 759-762.

Konradsson, P.; Udodong, U. E.; Fraserreid, B., Iodonium promoted reactions of disarmed thioglycosides. *Tetrahedron Lett.* **1990**, 31, 4313-4316.

Kuhara, T.; Iigo, M.; Itoh, T.; Ushida, Y.; Sekine, K.; Terada, N.; Okamura, H.; Tsuda, H., Orally administered lactoferrin exerts an antimetastatic effect and enhances production of IL-18 in the intestinal epithelium. *Nutr. Cancer* **2000**, 38, 192-199.

Kuhara, T.; Yamauchi, K.; Tamura, Y.; Okamura, H., Oral administration of lactoferrin increases NK cell activity in mice via increased production of IL-18 and type IIFN in the small intestine. *J. Interf. Cytok. Res.* **2006**, 26, 489-499.

Kulkarni, S. A.; Barton-Maclaren, T. S., Performance of (Q)SAR Models for Predicting Ames Mutagenicity of Aryl Azo and Benzidine Based Compounds. *Environ Carcin Eco R* **2014**, 32, 46-82.

Kumar, G. D. K.; Baskaran, S., A facile, catalytic, and environmentally benign method for selective deprotection of tert-butyldimethylsilyl ether mediated by phosphomolybdic acid supported on silica gel. *J. Org. Chem.* **2005**, 70, 4520-4523.

Kuperman, D. A.; Lewis, C. C.; Woodruff, P. G.; Rodriguez, M. W.; Yang, Y. H.; Dolganov, G. M.; Fahy, J. V.; Erle, D. J., Dissecting asthma using focused transgenic modeling and functional genomics. *J. Allergy Clin. Immun.* **2005**, 116, 305-311.

Lash, J. A.; Coates, T. D.; Baehner, R. L.; Boxer, L. A., Plasma lactoferrin reflects granulocyte activation in-vivo. *Pediatr. Res.* **1982**, 16, 208A-208A.

Latge, J. P.; Kobayashi, H.; Debeaupuis, J. P.; Diaquin, M.; Sarfati, J.; Wieruszkeski, J. M.; Parra, E.; Bouchara, J. P.; Fournet, B., Chemical and immunological characterization of the extracellular galactomannan of *Aspergillus fumigatus*. *Infect. Immun.* **1994**, 62, 5424-5433.

Law, S. K.; Lichtenberg, N. A.; Levine, R. P., Covalent binding and hemolytic activity of complement proteins. *Proc. Natl. Acad. Sci-Biol.* **1980**, 77, 7194-7198.

Leal, J. A.; GomezMiranda, B.; Prieto, A.; Domenech, J.; Ahrazem, O.; Bernabe, M., Possible chemotypes from cell wall polysaccharides, as an aid in the

systematics of *Penicillium* and its teleomorphic states *Eupenicillium* and *Talaromyces*. *Mycol. Res.* **1997**, 101, 1259-1264.

Lee, J. K.; Baum, L. G.; Moremen, K.; Pierce, M., The X-lectins: A new family with homology to the *Xenopus laevis* oocyte lectin XL-35. *Glycoconjugate J.* **2004**, 21, 443-450.

Lee, J. K.; Buckhaults, P.; Wilkes, C.; Teilhet, M.; King, M. L.; Moremen, K. W.; Pierce, M., Cloning and expression of a *Xenopus laevis* oocyte lectin and characterization of its mRNA levels during early development. *Glycobiology* **1997**, 7, 367-372.

Lee, J. K.; Schnee, J.; Pang, M.; Wolfert, M.; Baum, L. G.; Moremen, K. W.; Pierce, M., Human homologs of the *Xenopus* oocyte cortical granule lectin XL35. *Glycobiology* **2001**, 11, 65-73.

Leitao, E. A.; Bittencourt, V. C. B.; Haido, R. M. T.; Valente, A. P.; Peter-Katalinic, J.; Letzel, M.; de Souza, L. M.; Barreto-Bergter, E., beta-Galactofuranose-containing O-linked oligosaccharides present in the cell wall peptidogalactomannan of *Aspergillus fumigatus* contain immunodominant epitopes. *Glycobiology* **2003**, 13, 681-692.

Leonard, R.; Petersen, B. O.; Himly, M.; Kaar, W.; Wopfner, N.; Kolarich, D.; van Ree, R.; Ebner, C.; Duus, J. O.; Ferreira, F.; Altmann, F., Two novel types of O-glycans on the mugwort pollen allergen Art v 1 and their role in antibody binding. *J. Biol. Chem.* **2005**, 280, 7932-7940.

Leverly, S. B.; Toledo, M. S.; Straus, A. H.; Takahashi, H. K., Structure elucidation of sphingolipids from the mycopathogen *Paracoccidioides brasiliensis*: An

immunodominant beta-galactofuranose residue is carried by a novel glycosylinositol phosphorylceramide antigen. *Biochemistry* **1998**, 37, 8764-8775.

Leverly, S. B.; Toledo, M. S.; Suzuki, E.; Salyan, M. E. K.; Hakomori, S. I.; Straus, A. H.; Takahashi, H. K., Structural characterization of a new galactofuranose-containing glycolipid antigen of *Paracoccidioides brasiliensis*. *Biochem. Biophys. Res. Commun.* 1996, 222, 639-645.

Lichtenstein, R. G.; Rabinovich, G. A., Glycobiology of cell death: when glycans and lectins govern cell fate. *Cell Death Differ.* **2013**, 20, 976-986.

Lin Cereghino, G. P.; Sunga, A. J.; Lin Cereghino, J.; Cregg, J. M., Expression of foreign genes in the yeast *Pichia pastoris*. *Genetic engineering* **2001**, 23, 157-69.

Liu, F. T.; Patterson, R. J.; Wang, J. L., Intracellular functions of galectins. *BBA-Gen. Subjects* **2002**, 1572, 263-273.

Lonnerdal, B.; Iyer, S., Lactoferrin - molecular structure and biological function. *Annu. Rev. Nutr.* **1995**, 15, 93-110.

Macauley-Patrick, S.; Fazenda, M. L.; McNeil, B.; Harvey, L. M., Heterologous protein production using the *Pichia pastoris* expression system. *Yeast* **2005**, 22, 249-270.

Maeda, N.; Nigou, J.; Herrmann, J. L.; Jackson, M.; Amara, A.; Lagrange, P. H.; Puzo, G.; Gicquel, B.; Neyrolles, O., The cell surface receptor DC-SIGN discriminates between *Mycobacterium* species through selective recognition of the mannose caps on lipoarabinomannan. *J. Biol. Chem.* **2003**, 278, 5513-5516.

McAuliffe, J. C.; Hindsgaul, O., Use of acyclic glycosyl donors for furanoside synthesis. *J. Org. Chem.* **1997**, 62, 1234-1239.

- McConville, M. J.; Ferguson, M. A. J., The structure, biosynthesis and function of glycosylated phosphatidylinositols in the parasitic protozoa and higher eukaryotes. *Biochem. J.* **1993**, 294, 305-324.
- McConville, M. J.; Homans, S. W.; Thomasoates, J. E.; Dell, A.; Bacic, A., Structures of the glycoinositolphospholipids from *Leishmania major* - a family of novel galactofuranose-containing glycolipids. *J. Biol. Chem.* **1990**, 265, 7385-7394.
- Mikogami, T.; Marianne, T.; Spik, G., Effect of intracellular iron depletion by picolinic acid on expression of the lactoferrin receptor in the human colon carcinoma cell subclone HT29-18-C-1. *Biochem. J.* **1995**, 308, 391-397.
- Mitchell, D. A.; Fadden, A. J.; Drickamer, K., A novel mechanism of carbohydrate recognition by the C-type lectins DC-SIGN and DC-SIGNR - Subunit organization and binding to multivalent ligands. *J. Biol. Chem.* **2001**, 276, 28939-28945.
- Moody, S. F.; Handman, E.; McConville, M. J.; Bacic, A., The structure of *Leishmania major* amastigote lipophosphoglycan. *J. Biol. Chem.* **1993**, 268, 18457-18466.
- Murphy-Ullrich, J. E., The de-adhesive activity of matricellular proteins: is intermediate cell adhesion an adaptive state? *J. Clin. Invest.* **2001**, 107, 785-790.
- Nakahara, S.; Oka, N.; Raz, A., On the role of galectin-3 in cancer apoptosis. *Apoptosis* **2005**, 10, 267-275.
- Okamoto, I.; Kohno, K.; Tanimoto, T.; Ikegami, H.; Kurimoto, M., Development of CD8(+) effector T cells is differentially regulated by IL-18 and IL-12. *J. Immunol.* **1999**, 162, 3202-3211.

Outenreath, R. L.; Roberson, M. M.; Barondes, S. H., Endogenous lectin secretion into the extracellular matrix of early embryos of *Xenopus laevis*. *Dev. Biol.* **1988**, 125, 187-194.

Pan, F.; Jackson, M.; Ma, Y. F.; McNeil, M., Cell wall core galactofuran synthesis is essential for growth of mycobacteria (vol 183, pg 3991, 2001). *J. Bacteriol.* **2001**, 183, 6971-6971.

Park, I.-H.; Park, S.-J.; Cho, J.-S.; Moon, Y.-M.; Kim, T. H.; Lee, S. H.; Lee, H.-M., Increased expression of intelectin-1 in nasal polyps. *Am. J. Rhinol. Allergy* **2012**, 26, 274-277.

Pathak, A. K.; Pathak, V.; Seitz, L.; Maddry, J. A.; Gurcha, S. S.; Besra, G. S.; Suling, W. J.; Reynolds, R. C., Studies on (beta,1 -> 5) and (beta,1 -> 6) linked octyl Gal(f) disaccharides as substrates for mycobacterial galactosyltransferase activity. *Bioorg. Med. Chem.* **2001**, 9, 3129-3143.

Pedersen, L. L.; Turco, S. J., Galactofuranose metabolism: a potential target for antimicrobial chemotherapy. *Cell Mol. Life Sci.* **2003**, 60, 259-266.

Peebles, R. S., Jr., The intelectins: a new link between the immune response to parasitic infections and allergic inflammation? *Am. J. Physiol-Lung C.* **2010**, 298, L288-L289.

Peltier, P.; Euzen, R.; Daniellou, R.; Nugier-Chauvin, C.; Ferrieres, V., Recent knowledge and innovations related to hexofuranosides: structure, synthesis and applications. *Carbohydr. Res.* **2008**, 343, 1897-1923.

Pemberton, A. D.; Knight, P. A.; Wright, S. H.; Miller, H. R. P., Proteomic analysis of mouse jejunal epithelium and its response to infection with the intestinal nematode, *Trichinella spiralis*. *Proteomics* **2004**, 4, 1101-1108.

Prazeres, D. M. F.; Ferreira, G. N. M.; Monteiro, G. A.; Cooney, C. L.; Cabral, J. M. S., Large-scale production of pharmaceutical-grade plasmid DNA for gene therapy: problems and bottlenecks. *Trends in Biotechnology* **1999**, 17, 169-174.

Prieto, A.; Bernabe, M.; Leal, J. A., Isolation, purification and chemical characterization of alkali extractable polysaccharides from the cell walls of *Talaromyces* species. *Mycol. Res.* **1995**, 99, 69-75.

Puren, A. J.; Razeghi, P.; Fantuzzi, G.; Dinarello, C. A., Interleukin-18 enhances lipopolysaccharide-induced interferon-gamma production in human whole blood cultures. *J. Infect. Dis.* **1998**, 178, 1830-1834.

Reilander, H.; Weiss, H. M., Production of G-protein-coupled receptors in yeast. *Current Opinion in Biotechnology* **1998**, 9, 510-517.

Ren, Y.; Ding, Q.; Zhang, X., Ficolins and infectious diseases. *Virologica Sinica* 2014, 29, 25-32.

Richards, M. R.; Lowary, T. L., Chemistry and Biology of Galactofuranose-Containing Polysaccharides. *Chembiochem* **2009**, 10, 1920-1938.

Roberson, M. M.; Barondes, S. H., Lectin from embryos and oocytes of *Xenopus laevis* - purification and properties. *J. Biol. Chem.* **1982**, 257, 7520-7524.

Ruffie, P.; Feld, R.; Minkin, S.; Cormier, Y.; Boutanlaroze, A.; Ginsberg, R.; Ayoub, J.; Shepherd, F. A.; Evans, W. K.; Figueredo, A.; Pater, J. L.; Pringle, J. F.;

Kreisman, H., Diffuse malignant mesothelioma of the pleura in Ontario and Quebec - a retrospective study of 332 patients. *J. Clin. Oncol.* **1989**, 7, 1157-1168.

Sacchettini, J. C.; Baum, L. G.; Brewer, C. F., Multivalent protein-carbohydrate interactions. A new paradigm for supermolecular assembly and signal transduction. *Biochemistry* **2001**, 40, 3009-3015.

Sarramegna, V.; Talmont, R.; Demange, P.; Milon, A., Heterologous expression of G-protein-coupled receptors: comparison of expression systems from the standpoint of large-scale production and purification. *Cellular and Molecular Life Sciences* **2003**, 60, 1529-1546.

Schaffler, A.; Herfarth, H., Creeping fat in Crohn's disease: travelling in a creeper lane of research? *Gut* **2005**, 54, 742-744.

Schaffler, A.; Neumeier, A.; Herfarth, H.; Furst, A.; Scholmerich, J.; Buchler, C., Genomic structure of human omentin, a new adipocytokine expressed in omental adipose tissue. *BBA-Gene struct. Expr.* **2005**, 1732, 96-102.

Seki, M.; Sakata, K.-m.; Oomizu, S.; Arikawa, T.; Sakata, A.; Ueno, M.; Nobumoto, A.; Niki, T.; Saita, N.; Ito, K.; Dai, S.-Y.; Katoh, S.; Nishi, N.; Tsukano, M.; Ishikawa, K.; Yamauchi, A.; Kuchroo, V.; Hirashima, M., Beneficial effect of galectin 9 on rheumatoid arthritis by induction of apoptosis of synovial fibroblasts. *Arthritis Rheum.* **2007**, 56, 3968-3976.

Shah, M. A.; Kelsen, D. P., Gastric Cancer: A Primer on the Epidemiology and Biology of the Disease and an Overview of the Medical Management of Advanced Disease. *Journal of the National Comprehensive Cancer Network* **2010**, 8, 437-447.

Sharon, N., Lectins: past, present and future. *Biochem. Soc. T.* **2008**, 36, 1457-1460.

Shuger, S. L.; Sui, X.; Church, T. S.; Meriwether, R. A.; Blair, S. N., Body mass index as a predictor of hypertension incidence among initially healthy normotensive women. *Am. J. Hypertens.* **2008**, 21, 613-619.

Simons, K.; Gerl, M. J., Revitalizing membrane rafts: new tools and insights. *Nat. Rev. Mol. Cell Bio.* **2010**, 11, 688-699.

Singh, S. M.; Panda, A. K., Solubilization and refolding of bacterial inclusion body proteins. *Journal of Bioscience and Bioengineering* **2005**, 99, 303-310.

Sorum, U.; Robertsen, B.; Kenne, L., Structural studies of the major polysaccharide in the cell wall of *Renibacterium salmoninarum*. *Carbohydr. Res.* **1998**, 306, 305-314.

Stevenson, G.; Neal, B.; Liu, D.; Hobbs, M.; Packer, N. H.; Batley, M.; Redmond, J. W.; Lindquist, L.; Reeves, P., Structure of the O-antigen of *Escherichia coli*-K12 and the sequence of its RFB gene cluster. *J. Bacteriol.* **1994**, 176, 4144-4156.

Suzuki, E.; Toledo, M. S.; Takahashi, H. K.; Straus, A. H., A monoclonal antibody directed to terminal residue of beta-galactofuranose of a glycolipid antigen isolated from *Paracoccidioides brasiliensis*; Cross-reactivity with *Leishmania major* and *Trypanosoma cruzi*. *Glycobiology* **1997**, 7, 463-468.

Suzuki, Y. A.; Lopez, V.; Lonnerdal, B., Mammalian lactoferrin receptors: structure and function. *Cell Mol. Life Sci.* **2005**, 62, 2560-2575.

Suzuki, Y. A.; Shin, K.; Lonnerdal, B., Molecular cloning and functional expression of a human intestinal lactoferrin receptor. *Biochemistry* **2001**, 40, 15771-15779.

Swartz, J. R., Advances in *Escherichia coli* production of therapeutic proteins. *Current Opinion in Biotechnology* **2001**, 12, 195-201.

Szarek, W. A.; Zamojski, A.; Tiwari, K. N.; Ison, E. R., A new, facile method for cleavage of acetals and dithioacetals in carbohydrate derivatives. *Tetrahedron Lett.* **1986**, 27, 3827-3830.

Szurmai, Z.; Liptak, A.; Snatzke, G., Anomalous zemplen deacylation reactions of 2-O-acyl-3-O-alkyl or 2-o-acyl-3-O-glycosyl derivatives of D-galactose and D-glucose- synthesis of O-alpha-D-mannopyranosyl-(1-4)-O-alpha-L-rhamnopyranosyl-(1-3)-D-galactose and an intermediate for the preparation of 2-O-glycosyl-3-O-(alpha-d-mannopyranosyl)-D-glucoses. *Carbohydr. Res.* **1990**, 200, 201-208.

Tefsen, B.; Ram, A. F. J.; van Die, I.; Routier, F. H., Galactofuranose in eukaryotes: aspects of biosynthesis and functional impact. *Glycobiology* **2012**, 22, 456-469.

Tsuji, S.; Matsumoto, M.; Takeuchi, O.; Akira, S.; Azuma, I.; Hayashi, A.; Toyoshima, K.; Seya, T., Maturation of human dendritic cells by cell wall skeleton of *Mycobacterium bovis* bacillus Calmette-Guerin: Involvement of Toll-like receptors. *Infect. Immun.* **2000**, 68, 6883-6890.

Tsuji, S.; Tsuura, Y.; Morohoshi, T.; Shinohara, T.; Oshita, F.; Yamada, K.; Kameda, Y.; Ohtsu, T.; Nakamura, Y.; Miyagi, Y., Secretion of intelectin-1 from malignant pleural mesothelioma into pleural effusion. *Brit. J. Cancer* **2010**, 103, 517-523.

Tsuji, S.; Uehori, J.; Matsumoto, M.; Suzuki, Y.; Matsuhisa, A.; Toyoshima, K.; Seya, T., Human intelectin is a novel soluble lectin that recognizes galactofuranose in carbohydrate chains of bacterial cell wall. *J. Biol. Chem.* **2001**, 276, 23456-23463.

Tsuji, S.; Yamashita, M.; Hoffman, D. R.; Nishiyama, A.; Shinohara, T.; Ohtsu, T.; Shibata, Y., Capture of heat-killed *Mycobacterium bovis* bacillus Calmette-Guerin by intelectin-1 deposited on cell surfaces. *Glycobiology* **2009**, *19*, 518-526.

Tsuji, S.; Yamashita, M.; Nishiyama, A.; Shinohara, T.; Zhongwei, U.; Myrvik, Q. N.; Hoffman, D. R.; Henriksen, R. A.; Shibata, Y., Differential structure and activity between human and mouse intelectin-1: Human intelectin-1 is a disulfide-linked trimer, whereas mouse homologue is a monomer. *Glycobiology* **2007**, *17*, 1045-1051.

Turco, S. J.; Descoteaux, A., The lipophosphoglycan of leishmania parasites. *Annu. Rev. Microbiol.* **1992**, *46*, 65-94.

Veeneman, G. H.; Vanleeuwen, S. H.; Vanboom, J. H., Iodonium ion promoted reactions at the anomeric center .2. An efficient thioglycoside mediated approach toward the formation of 1,2-trans linked glycosides and glycosidic esters. *Tetrahedron Lett.* **1990**, *31*, 1331-1334.

Velty, R.; Benvegna, T.; Gelin, M.; Privat, E.; Plusquellec, D., A convenient synthesis of disaccharides containing furanoside units. *Carbohydr. Res.* **1997**, *299*, 7-14.

Velty, R.; Benvegna, T.; Plusquellec, D., n-pentenyl furanosides and related glycosyl donors for the synthesis of archaeol glycolipid analogues. *Synlett* **1996**, 817-&.

Voehringer, D.; Stanley, S. A.; Cox, J. S.; Completo, G. C.; Lowary, T. L.; Locksley, R. M., *Nippostrongylus brasiliensis*: Identification of intelectin-1 and -2

as Stat6-dependent genes expressed in lung and intestine during infection. *Exp. Parasitol.* **2007**, 116, 458-466.

Wali, A.; Morin, P. J.; Hough, C. D.; Lonardo, F.; Seya, T.; Carbone, M.; Pass, H. I., Identification of intelectin overexpression in malignant pleural mesothelioma by serial analysis of gene expression (SAGE). *Lung Cancer-J* **2005**, 48, 19-29.

Walport, M. J., Advances in immunology: Complement (First of two parts). *New Engl. J. Med.* **2001**, 344, 1058-1066.

Walport, M. J., Advances in immunology: Complement (Second of two parts). *New Engl. J. Med.* **2001**, 344, 1140-1144.

Walsh, G., Biopharmaceutical benchmarks 2010. *Nature Biotechnology* 2010, 28, 917-924.

Wang, W. P., Activation of intestinal mucosal immunity in tumor-bearing mice by lactoferrin. *Jpn. J. Cancer Res.* **2000**, 91, 1359-1359.

Ward, P. P.; Uribe-Luna, S.; Conneely, O. M., Lactoferrin and host defense. *Biochem. Cell Biol.* **2002**, 80, 95-102.

Wegner, G. H., Emerging applications of the methylotrophic yeasts. *FEMS Microbiol. Lett.* **1990**, 87, 279-283.

Weis, W. I.; Taylor, M. E.; Drickamer, K., The C-type lectin superfamily in the immune system. *Immunol. Rev.* **1998**, 163, 19-34.

White, J. F.; Trinh, L. B.; Shiloach, J.; Grisshammer, R., Automated large-scale purification of a G protein-coupled receptor for neurotensin. *FEBS Lett.* **2004**, 564, 289-293.

- Whitfield, C., Biosynthesis of lipopolysaccharide O-antigens. *Trends Microbiol.* 1995, 3, 178-185.
- Wiederschain, G. Y., Glycobiology: Progress, problems, and perspectives. *Biochemistry-Moscow* **2013**, 78, 679-696.
- Wrackmeyer, U.; Hansen, G. H.; Seya, T.; Danielsen, E. M., Intelectin: A novel lipid raft-associated protein in the enterocyte brush border. *Biochemistry* **2006**, 45, 9188-9197.
- Xie, H.; Xie, P. L.; Luo, X. H.; Wu, X. P.; Zhou, H. D.; Tang, S. Y.; Liao, E. Y., Omentin-1 exerts bone-sparing effect in ovariectomized mice. *Osteoporosis Int.* **2012**, 23, 1425-1436.
- Xie, N.; Taylor, C. M., Synthesis of a Dimer of beta-(1,4)-L-Arabinosyl-(2S,4R)-4-hydroxyproline Inspired by Art v 1, the Major Allergen of Mugwort. *Org. Lett.* **2010**, 12, 4968-4971.
- Yamawaki, H.; Tsubaki, N.; Mukohda, M.; Okada, M.; Hara, Y., Omentin, a novel adipokine, induces vasodilation in rat isolated blood vessels. *Biochem. Biophys. Res. Commun.* **2010**, 393, 668-672.
- Yamazaki, K.; Suzuki, M.; Inukai, K.; Kuga, H.; Korenaga, H., Structural study on a sulfated polysaccharide-peptidoglycan complex produced by *Arthrobacter sp.* *Biosci. Biotech. Bioch.* **1998**, 62, 2138-2144.
- Yang, R. Z.; Lee, M. J.; Hu, H.; Pray, J.; Wu, H. B.; Hansen, B. C.; Shuldiner, A. R.; Fried, S. K.; McLenithan, J. C.; Gong, D. W., Identification of omentin as a novel depot-specific adipokine in human adipose tissue: possible role in modulating insulin action. *Am. J. Physiol-Endoc. M.* **2006**, 290, E1253-E1261.

Yang, R.-Y.; Rabinovich, G. A.; Liu, F.-T., Galectins: structure, function and therapeutic potential. *Expert Rev. Mol. Med.* **2008**, 10, 1-24.

Yokosawa, H.; Harada, K.; Igarashi, K.; Abe, Y.; Takahashi, K.; Ishii, S., Galactose-specific lectin in the hemolymph of solitary ascidian, *Halocynthia roretzi* - molecular, binding and functional properties. *Biochim. Biophys. Acta.* **1986**, 870, 242-247.

Zheng, L. D.; Weng, M. X.; Qi, M.; Qi, T.; Tong, L.; Hou, X. H.; Tong, Q. S., Aberrant expression of intelectin-1 in gastric cancer: its relationship with clinicopathological features and prognosis. *J. Cancer Res. Clin.* **2012**, 138, 163-172.

Ziegler, T.; Kovac, P.; Glaudemans, C. P. J., Selective bromoacetylation of alkyl hexopyranosides - a facile preparation of intermediates for the synthesis of (1- 6)-linked oligosaccharides. *Carbohydr. Res.* **1989**, 194, 185-198.

Zuberi, R. I.; Hsu, D. K.; Kalayci, O.; Chen, H. Y.; Sheldon, H. K.; Yu, L.; Apgar, J. R.; Kawakami, T.; Lilly, C. M.; Liu, F. T., Critical role for galectin-3 in airway inflammation and bronchial hyperresponsiveness in a murine model of asthma. *Am. J. Pathol.* **2004**, 165, 2045-2053.